

Supporting Information

Structurally Diverse Diketopiperazine Alkaloids from the Marine-Derived Fungus *Aspergillus versicolor* SCSIO 41016

Xiaowei Luo,^{a,b} Chunmei Chen,^{a,b} Huaming Tao,^c Xiuping Lin,^a Bin Yang,^a Xuefeng Zhou,^{*,a} and Yonghong Liu^{*,a,b}

^aCAS Key Laboratory of Tropical Marine Bio-resources and Ecology/Guangdong Key Laboratory of Marine Materia Medica, South China Sea Institute of Oceanology, Chinese Academy of Sciences, Guangzhou 510301, China

^bUniversity of Chinese Academy of Sciences, Beijing 100049, China

^cSchool of Traditional Chinese Medicine, Southern Medical University, Guangzhou 510515, China

Table of Contents

1. Experimental Procedures

1.1 General Experimental Procedures.....	9
1.2 Fungi Material.....	9
1.3 The 18S rRNA gene sequences data of <i>Aspergillus versicolor</i> SCSIO 41016.....	9-10
1.4 Fermentation and Extraction.....	10
1.5 Purification.....	10-12
1.6 Crystallographic Data of 10	12-13
1.7 Biological Assay	13-14

Table S1. Cytotoxicities of Compounds **1**, **3**, **7**, **10**, and **12** 14

2. Computational Methods

Table S2. Energies of 1 at MMFF94 force field.....	14-15
Table S3. Energies of 1 at B3LYP/6-31+G (d, p) level in methanol.....	15
Figure S1. The optimized conformers and equilibrium populations of pyranamide A (1).....	16-17
Figure S2. The possible diastereomers, 1A , 1B , 1C , and 1D , of 1 used for DP4+ analysis.....	18
Table S4. DP4+ analysis of calculated ^1H -NMR data of 1A , 1B , 1C , and 1D	18
Table S5. DP4+ analysis of calculated ^{13}C -NMR data of 1A , 1B , 1C , and 1D	18-19
Table S6. Calculated (calc.) and experimental (exp.) ^1H NMR chemical shift values of 1A , 1B , 1C , and 1D at the B3LYP/6-31+G (d, p) level in methanol and total absolute deviation (TAD) and mean absolute error (MAE).	19-20
Table S7. Calculated (calc.) and experimental (exp.) ^{13}C NMR chemical shift values of 1A , 1B , 1C , and 1D at the B3LYP/6-31+G(d, p) level in methanol and total absolute deviation (TAD) and mean absolute error (MAE).	20-21
Table S8. Energies of 2 at MMFF94 force field.....	21-22
Table S9. Energies of 2 at B3LYP/6-31+G (d) level in methanol.	23-26
Figure S3. The optimized conformers and equilibrium populations of pyranamide B (2).....	26
Figure S4. Total absolute deviation (TAD), mean absolute error (MAE), and DP4+ probability analyses for four candidate diastereomers of 2	26
Table S10. DP4+ analysis of calculated ^1H -NMR data of 2A , 2B , 2C , and 2D	26

Table S11. DP4+ analysis of calculated ^{13}C -NMR data of 2A , 2B , 2C , and 2D	26-27
Table S12. Calculated (calc.) and experimental (exp.) ^1H NMR chemical shift values of 2A , 2B , 2C , and 2D at the B3LYP/6-31+G (d, p) level in methanol and total absolute deviation (TAD) and mean absolute error (MAE).	27-28
Table S13. Calculated (calc.) and experimental (exp.) ^{13}C NMR chemical shift values of 2A , 2B , 2C , and 2D at the B3LYP/6-31+G(d, p) level in methanol and total absolute deviation (TAD) and mean absolute error (MAE).	28-29
Table S14. Energies of 3 at MMFF94 force field.	29
Table S15. Energies of 3 at B3LYP/6-31+G (d) level in methanol.....	30
Figure S5. The optimized conformers and equilibrium populations of pyranamide C (3).....	30-32
Figure S6. Total absolute deviation (TAD), mean absolute error (MAE), and DP4+ probability analyses for two candidate diastereomers of 3	32
Table S16. DP4+ analysis of calculated ^1H -NMR data of 3A and 3B	33
Table S17. DP4+ analysis of calculated ^{13}C -NMR data of 3A and 3B	33
Table S18. Calculated (calc.) and experimental (exp.) ^1H NMR chemical shift values of 3A and 3B at the B3LYP/6-31+G (d, p) level in methanol and total absolute deviation (TAD) and mean absolute error (MAE).	34
Table S19. Calculated (calc.) and experimental (exp.) ^{13}C NMR chemical shift values of 3A and 3B at the B3LYP/6-31+G(d, p) level in methanol and total absolute deviation (TAD) and mean absolute error (MAE).	34-36
Table S20. Energies of 4 at MMFF94 force field.	36
Table S21. Energies of 4 at B3LYP/6-31+G (d) level in methanol.....	36
Figure S7. The optimized conformers and equilibrium populations of pyranamide D (4).	37-38
Figure S8. Total absolute deviation (TAD), mean absolute error (MAE), and DP4+ probability analyses for two candidate diastereomers of 4	39
Table S22. DP4+ analysis of calculated ^1H -NMR data of 4A and 4B	39
Table S23. DP4+ analysis of calculated ^{13}C -NMR data of 4A and 4B	39-40
Table S24. Calculated (calc.) and experimental (exp.) ^1H NMR chemical shift values of 4A and 4B at the B3LYP/6-31+G (d, p) level in methanol and total absolute deviation (TAD) and mean absolute error (MAE).	40-41

Table S25. Calculated (calc.) and experimental (exp.) ^{13}C NMR chemical shift values of 4A and 4B at the B3LYP/6-31+G(d, p) level in methanol and total absolute deviation (TAD) and mean absolute error (MAE).....	41-42
Table S26. Energies of 6 at MMFF94 force field.....	42
Table S27. Energies of 6 at B3LYP/6-31+G (d, p) level in methanol.....	42
Figure S9. The optimized conformers and equilibrium populations of protuboxepin F (6).....	43
Table S28. Energies of 8 at MMFF94 force field.....	43
Table S29. Energies of 8 at B3LYP/6-31+G (d, p) level in methanol.....	43
Figure S10. The optimized conformers and equilibrium populations of protuboxepin H (8)	44
Table S30. Energies of 10 at MMFF94 force field.....	44
Table S31. Energies of 10 at B3LYP/6-31+G (d, p) level in methanol.....	44
Figure S11. The optimized conformers and equilibrium populations of protuboxepin J (10).....	45
3. Other Experimental Data	
Table S32. ^1H and ^{13}C NMR Spectroscopic Data of 1-5 in CD_3OD (δ ppm).....	46-47
Table S33. ^1H (700 MHz) and ^{13}C (175 MHz) NMR Spectroscopic Data of 6-10 in $\text{DMSO}-d_6$ (δ ppm).....	47-48
Table S34. ^1H (700 MHz) and ^{13}C (175 MHz) NMR Spectroscopic Data of 1 and 4 in $\text{DMSO}-d_6$ (δ ppm)	49
Figure S12. Key COSY, HMBC and NOESY correlations of 6 , 8 and 10	50
Figure S13. ^1H NMR spectrum of pyranamide A (1) (CD_3OD , 700 MHz).....	50
Figure S14. ^{13}C NMR and DEPT spectra of pyranamide A (1) (CD_3OD , 175 MHz)	51
Figure S15. HSQC spectrum of pyranamide A (1) (CD_3OD)	52
Figure S16. HMBC spectrum of pyranamide A (1) (CD_3OD)	52
Figure S17. ^1H - ^1H COSY spectrum of pyranamide A (1) (CD_3OD).....	53
Figure S18. NOESY spectrum of pyranamide A (1) (CD_3OD)	53
Figure S19. ^1H NMR spectrum of pyranamide A (1) ($\text{DMSO}-d_6$, 700 MHz)	54
Figure S20. ^{13}C NMR and DEPT spectra of pyranamide A (1) ($\text{DMSO}-d_6$, 175 MHz).....	54-55
Figure S21. HSQC spectrum of pyranamide A (1) ($\text{DMSO}-d_6$)	55
Figure S22. HMBC spectrum of pyranamide A (1) ($\text{DMSO}-d_6$)	56
Figure S23. ^1H - ^1H COSY spectrum of pyranamide A (1) ($\text{DMSO}-d_6$)	56

Figure S24. NOESY spectrum of pyranamide A (1) (DMSO- <i>d</i> ₆)	57
Figure S25. Positive HR-ESI-MS spectrum of pyranamide A (1).....	57
Figure S26. UV spectrum of pyranamide A (1).....	58
Figure S27. IR spectrum of pyranamide A (1)	58
Figure S28. ¹ H NMR spectrum of pyranamide B (2) (CD ₃ OD, 700 MHz).....	59
Figure S29. ¹³ C NMR and DEPT spectra of pyranamide B (2) (CD ₃ OD, 175 MHz)	59-60
Figure S30. HSQC spectrum of pyranamide B (2) (CD ₃ OD)	60
Figure S31. HMBC spectrum of pyranamide B (2) (CD ₃ OD)	61
Figure S32. ¹ H- ¹ H COSY spectrum of pyranamide B (2) (CD ₃ OD).....	61
Figure S33. NOESY spectrum of pyranamide B (2) (CD ₃ OD).....	62
Figure S34. Positive HR-ESI-MS spectrum of pyranamide B (2)	63
Figure S35. UV spectrum of pyranamide B (2)	63
Figure S36. IR spectrum of pyranamide B (2)	64
Figure S37. ¹ H NMR spectrum of pyranamide C (3) (CD ₃ OD, 700 MHz).....	64
Figure S38. ¹³ C NMR and DEPT spectra of pyranamide C (3) (CD ₃ OD, 175 MHz)	65
Figure S39. HSQC spectrum of pyranamide C (3) (CD ₃ OD)	66
Figure S40. HMBC spectrum of pyranamide C (3) (CD ₃ OD)	66
Figure S41. ¹ H- ¹ H COSY spectrum of pyranamide C (3) (CD ₃ OD).....	67
Figure S42. NOESY spectrum of pyranamide C (3) (CD ₃ OD).....	67-68
Figure S43. Positive HR-ESI-MS spectrum of pyranamide C (3)	68
Figure S44. UV spectrum of pyranamide C (3)	69
Figure S45. IR spectrum of pyranamide C (3)	69
Figure S46. ¹ H NMR spectrum of pyranamide D (4) (CD ₃ OD, 500 MHz)	70
Figure S47. ¹³ C NMR and DEPT spectra of pyranamide D (4) (CD ₃ OD, 125 MHz).....	70-71
Figure S48. HSQC spectrum of pyranamide D (4) (CD ₃ OD)	71
Figure S49. HMBC spectrum of pyranamide D (4) (CD ₃ OD)	72
Figure S50. ¹ H- ¹ H COSY spectrum of pyranamide D (4) (CD ₃ OD)	72
Figure S51. NOESY spectrum of pyranamide D (4) (CD ₃ OD).....	73
Figure S52. ¹ H NMR spectrum of pyranamide D (4) (DMSO- <i>d</i> ₆ , 700 MHz)	74
Figure S53. ¹³ C NMR and DEPT spectra of pyranamide D (4) (DMSO- <i>d</i> ₆ , 175 MHz)	74-75

Figure S54. HSQC spectrum of pyranamide D (4) (DMSO- <i>d</i> ₆).....	75
Figure S55. HMBC spectrum of pyranamide D (4) (DMSO- <i>d</i> ₆)	76
Figure S56. ¹ H- ¹ H COSY spectrum of pyranamide D (4) (DMSO- <i>d</i> ₆).....	76
Figure S57. NOESY spectrum of pyranamide D (4) (DMSO- <i>d</i> ₆)	77
Figure S58. Positive HR-ESI-MS spectrum of pyranamide D (4)	78
Figure S59. UV spectrum of pyranamide D (4)	78
Figure S60. IR spectrum of pyranamide D (4).....	79
Figure S61. ¹ H NMR spectrum of secopyranamide C (5) (CD ₃ OD, 700 MHz)	79
Figure S62. ¹³ C NMR and DEPT spectra of secopyranamide C (5) (CD ₃ OD, 175 MHz).....	80
Figure S63. HSQC spectrum of secopyranamide C (5) (CD ₃ OD)	81
Figure S64. HMBC spectrum of secopyranamide C (5) (CD ₃ OD)	81
Figure S65. ¹ H- ¹ H COSY spectrum of secopyranamide C (5) (CD ₃ OD).....	82
Figure S66. NOESY spectrum of secopyranamide C (5) (CD ₃ OD).....	82
Figure S67. Positive HR-ESI-MS spectrum of secopyranamide C (5)	83
Figure S68. UV spectrum of secopyranamide C (5)	83
Figure S69. IR spectrum of secopyranamide C (5)	84
Figure S70. ¹ H NMR spectrum of protuboxepin F (6) (DMSO- <i>d</i> ₆ , 700 MHz).....	84
Figure S71. ¹³ C NMR and DEPT spectra of protuboxepin F (6) (DMSO- <i>d</i> ₆ , 175 MHz).....	85
Figure S72. HSQC spectrum of protuboxepin F (6) (DMSO- <i>d</i> ₆).....	86
Figure S73. HMBC spectrum of protuboxepin F (6) (DMSO- <i>d</i> ₆).....	86
Figure S74. ¹ H- ¹ H COSY spectrum of protuboxepin F (6) (DMSO- <i>d</i> ₆)	87
Figure S75. NOESY spectrum of protuboxepin F (6) (DMSO- <i>d</i> ₆)	87-88
Figure S76. Positive HR-ESI-MS spectrum of protuboxepin F (6)	88
Figure S77. UV spectrum of protuboxepin F (6)	89
Figure S78. IR spectrum of protuboxepin F (6)	89
Figure S79. ¹ H NMR spectrum of protuboxepin G (7) (DMSO- <i>d</i> ₆ , 700 MHz)	90
Figure S80. ¹³ C NMR and DEPT spectra of protuboxepin G (7) (DMSO- <i>d</i> ₆ , 175 MHz).....	90-91
Figure S81. HSQC spectrum of protuboxepin G (7) (DMSO- <i>d</i> ₆)	91
Figure S82. HMBC spectrum of protuboxepin G (7) (DMSO- <i>d</i> ₆)	92
Figure S83. ¹ H- ¹ H COSY spectrum of protuboxepin G (7) (DMSO- <i>d</i> ₆).....	92

Figure S84. NOESY spectrum of protuboxepin G (7) (DMSO- <i>d</i> ₆).....	93
Figure S85. Positive HR-ESI-MS spectrum of protuboxepin G (7).....	93
Figure S86. UV spectrum of protuboxepin G (7).....	94
Figure S87. IR spectrum of protuboxepin G (7)	94
Figure S88. ¹ H NMR spectrum of protuboxepin H (8) (DMSO- <i>d</i> ₆ , 700 MHz)	95
Figure S89. ¹³ C NMR and DEPT spectra of protuboxepin H (8) (DMSO- <i>d</i> ₆ , 175 MHz).....	95-96
Figure S90. HSQC spectrum of protuboxepin H (8) (DMSO- <i>d</i> ₆)	96
Figure S91. HMBC spectrum of protuboxepin H (8) (DMSO- <i>d</i> ₆)	97
Figure S92. ¹ H- ¹ H COSY spectrum of protuboxepin H (8) (DMSO- <i>d</i> ₆).....	97
Figure S93. NOESY spectrum of protuboxepin H (8) (DMSO- <i>d</i> ₆).....	98
Figure S94. Positive HR-ESI-MS spectrum of protuboxepin H (8).....	99
Figure S95. UV spectrum of protuboxepin H (8).....	99
Figure S96. IR spectrum of protuboxepin H (8)	100
Figure S97. ¹ H NMR spectrum of protuboxepin I (9) (DMSO- <i>d</i> ₆ , 700 MHz).....	100
Figure S98. ¹³ C NMR and DEPT spectra of protuboxepin I (9) (DMSO- <i>d</i> ₆ , 175 MHz)	101
Figure S99. HSQC spectrum of protuboxepin I (9) (DMSO- <i>d</i> ₆).....	102
Figure S100. HMBC spectrum of protuboxepin I (9) (DMSO- <i>d</i> ₆).....	102
Figure S101. ¹ H- ¹ H COSY spectrum of protuboxepin I (9) (DMSO- <i>d</i> ₆)	103
Figure S102. NOESY spectrum of protuboxepin I (9) (DMSO- <i>d</i> ₆)	103
Figure S103. Positive HR-ESI-MS spectrum of protuboxepin I (9)	104
Figure S104. UV spectrum of protuboxepin I (9)	104
Figure S105. IR spectrum of protuboxepin I (9)	105
Figure S106. ¹ H NMR spectrum of protuboxepin J (10) (DMSO- <i>d</i> ₆ , 700 MHz).....	105
Figure S107. ¹³ C NMR and DEPT spectra of protuboxepin J (10) (DMSO- <i>d</i> ₆ , 175 MHz)	106
Figure S108. HSQC spectrum of protuboxepin J (10) (DMSO- <i>d</i> ₆)	107
Figure S109. HMBC spectrum of protuboxepin J (10) (DMSO- <i>d</i> ₆)	107
Figure S110. ¹ H- ¹ H COSY spectrum of protuboxepin J (10) (DMSO- <i>d</i> ₆)	108
Figure S111. NOESY spectrum of protuboxepin J (10) (DMSO- <i>d</i> ₆)	108
Figure S112. Positive HR-ESI-MS spectrum of protuboxepin J (10)	109
Figure S113. UV spectrum of protuboxepin J (10)	109

Figure S114. IR spectrum of protuboxepin J (10)	110
Figure S115. ^1H NMR spectrum of protuboxepin E (11) (DMSO- d_6 , 700 MHz)	110
Figure S116. ^{13}C NMR and DEPT spectra of protuboxepin E (11) (DMSO- d_6 , 175 MHz).....	111
Figure S117. ^1H NMR spectrum of protuboxepin C (12) (DMSO- d_6 , 700 MHz).....	112
Figure S118. ^{13}C NMR and DEPT spectra of protuboxepin C (12) (DMSO- d_6 , 175 MHz) .	112-113
4. References	114

1. Experimental Procedures

1.1 General Experimental Procedures

Optical rotations were acquired using a Perkin Elmer MPC 500 (Waltham) polarimeter. UV spectra were recorded on a Shimadzu UV-2600 PC spectrometer (Shimadzu). ECD spectra were measured with a Chirascan circular dichroism spectrometer (Applied Photophysics). IR spectra were measured on an IR Affinity-1 spectrometer (Shimadzu). The NMR spectra were obtained on a Bruker Avance spectrometer (Bruker) operating at 500 MHz and 700 MHz for ¹H-NMR, 125 MHz and 175 MHz for ¹³C-NMR, using TMS as an internal standard. HRESIMS spectra were collected on a Bruker miXis TOF-QII mass spectrometer (Bruker). X-ray diffraction intensity data were collected on a CrysAlis PRO CCD area detector diffractometer with graphite-monochromated Cu K α radiation ($\lambda = 1.54178 \text{ \AA}$). TLC and column chromatography (CC) were performed on plates precoated with silica gel GF254 (10–40 μm) and over silica gel (200–300 mesh) (Qingdao Marine Chemical Factory), and Sephadex LH-20 (Amersham Biosciences), respectively. Spots were detected on TLC (Qingdao Marine Chemical Factory) under 254 nm UV light. All solvents employed were of analytical grade (Tianjin Fuyu Chemical and Industry Factory). Semi-preparative HPLC was carried out using an ODS column (YMC-pack ODS-A, YMC Co. Ltd., 10 \times 250 mm, 5 μm , 2.5 mL/min). The artificial sea salt was a commercial product (Guangzhou Haili Aquarium Technology Company).

1.2 Fungi Material

The fungal strain SCSIO 41016 was isolated from a sponge, *Callyspongia* sp., which was collected in Xuwen County, Guangdong Province, China. The isolates were stored on Müller Hinton broth (MB) agar (malt extract 15 g, artificial sea salt 15 g, and agar 15 g) slants at 4 °C, and a voucher specimen was deposited in the CAS Key Laboratory of Tropical Marine Bio-resources and Ecology, South China Sea Institute of Oceanology, Chinese Academy of Sciences, Guangzhou, China. It was identified as *Aspergillus versicolor* SCSIO 41016 by analysis of its ITS region of the rDNA, which has been deposited in the GenBank database (accession no. MH244341).

1.3 The ITS sequences data of *Aspergillus versicolor* SCSIO 41016

TTTGAAAGTAAAAAAATGTAACAAGGTTCCGTAGGTGAACCTGCGGAAGGGATCAT
TACTGAGTGCAGGCTGCCTCGGGCGCCAACCTCCCACCCGTGACTACCTAACACTG

TTGCTTCGGCGGGAGCCCTCTGGGGCGCGCCGGGACTACTGAACATTCATGC
CTGAGAGTGATGCAGTCTGAGTCTGAATATAAAATCAGTAAAACCAACAATGGAT
CTCTGGTCCGGCATCGATGAAGAACGCAGCGAAGTGCATAAGTAATGTGAATTGC
AGAATTCACTGAATCATCGAGTCTTGAACGCACATTGCGCCCCCTGGCATTCCGGG
GGCATGCCTGTCCGAGCGTCATTGCTGCCATCAAGCCGGCTTGTGTGTTGGTCGTC
GTCCCCCCCAGGGGACGGGCCGAAAGGCAGCGCGGCACCGTGTCCGGTCCTCGAG
CGTATGGGCTTGTCAACCGCTCGATTAGGGCCGGCCGGCGCCAGCCGACGTCCA
ACCATTTTCTTCAGGTTGACCTCGATCAGGTAGGGATACCCGCTGAACTTAACGATA
CAAAACCGGGAAAGGAA

1.4 Fermentation and Extraction

The strain *Aspergillus versicolor* SCSIO 41016 was cultured on MB-agar plates at 25 °C for 7 days. The seed medium (malt extract 15 g and artificial sea salt 2.5 g in 1.0 L tap distilled H₂O, pH 7.4–7.8) was inoculated with strain SCSIO 41016 and incubated at 25 °C for 3 days on a rotating shaker (180 rpm). Then, a large-scale fermentation of fungal isolate SCSIO 41016 was incubated for 40 days at room temperature in 1 L × 49 conical flasks with solid rice medium (each flask contained 100 g rice, 2.2 g artificial sea salt, 1.1 g bacteriological peptone and 110 mL H₂O). The whole fermented cultures were overlaid and extracted with EtOAc three times to afford a brown extract (100 g). The EtOAc extract was subjected to silica gel vacuum liquid chromatography (VLC) using step gradient elution with petroleum ether/CH₂Cl₂ (0~100%) to obtain ten fractions according to TLC profiles.

1.5 Purification

Fraction 10 was separated into seven subfractions (Fr.10-1~10-7) by Sephadex LH-20 chromatography eluting with MeOH/CH₂Cl₂ (1:1). Fr.10-1 was then separated by ODS silica gel chromatography eluting with MeOH/H₂O (10~100%) to obtain six subfractions (Fr.10-1-1~10-1-6). Fr.10-1-2 was separated by semipreparative HPLC (56% MeOH/H₂O, 2 mL/min, 220 nm) to provide **1** (9.5 mg, *t*_R 20 min) and **2** (6.5 mg, *t*_R 21 min), respectively. Fr.10-1-6 was separated by semipreparative HPLC (67% MeOH/H₂O, 2 mL/min, 220 nm) to yield **5** (3.8 mg, *t*_R 33 min) and a subfraction (Fr.10-1-6-7, 12 mg, *t*_R 39 min). And Fr.10-1-6-7 was further purified by semipreparative HPLC (47% MeCN/H₂O, 2 mL/min, 220 nm) to offer **3** (5.9 mg, *t*_R 39 min) and **4** (1.9 mg, *t*_R 34 min), respectively. Besides, Fr.10-2 was divided into four

subfractions (Fr.10-2-1~10-2-4) by ODS silica gel eluting with MeOH/H₂O (10~100%). Fr.10-2-2 was separated by semipreparative HPLC (60% MeCN/H₂O, 2 mL/min, 220 nm) to yield **7** (7.0 mg, *t*_R 24 min) and **9** (1.2 mg, *t*_R 25 min), respectively. Meanwhile, Fr.10-2-3 was separated by semipreparative HPLC (57% MeCN/H₂O, 2 mL/min, 220 nm) to yield **12** (14.0 mg, *t*_R 35 min) and a subfraction (Fr.10-2-3-4, 31 mg, *t*_R 26 min). Then Fr.10-2-3-4 was purified by semipreparative HPLC (75% MeOH/H₂O, 2.2 mL/min, 210 nm) to yield **11** (3.8 mg, *t*_R 26 min), **8** (2.7 mg, *t*_R 39 min), **10** (1.5 mg, *t*_R 44 min) and **6** (2.0 mg, *t*_R 47 min), respectively.

Pyranamide A (1): white solid; $[\alpha]_D^{25} -217$ (*c* 0.20, MeOH); UV (MeOH) λ_{\max} (log ε) 200 (3.58), 318 (3.14) nm; ECD (0.25 mg/mL, MeOH) λ_{\max} ($\Delta\varepsilon$) 200 (+28.2), 221 (-9.46), 248 (+57.3), 314 (-27.5) nm; IR (film) ν_{\max} 3234, 2931, 1666, 1660, 1396, 1336, 1062, 1031 cm⁻¹; ¹H and ¹³C NMR data, **Table S32**; HRESIMS *m/z* 448.1842 [M + Na]⁺ (calcd for C₂₃H₂₇N₃NaO₅, 448.1848).

Pyranamide B (2): white solid; $[\alpha]_D^{25} -153$ (*c* 0.18, MeOH); UV (MeOH) λ_{\max} (log ε) 200 (3.47), 314 (2.90) nm; ECD (0.30 mg/mL, MeOH) λ_{\max} ($\Delta\varepsilon$) 201 (+9.12), 222 (-4.64), 248 (+28.8), 312 (-12.4) nm; IR (film) ν_{\max} 3390, 2964, 1681, 1662, 1379, 1354, 1093, 1022 cm⁻¹; ¹H and ¹³C NMR data, **Table S32**; HRESIMS *m/z* 480.2102 [M + Na]⁺ (calcd for C₂₄H₃₁N₃NaO₆, 480.2111).

Pyranamide C (3): white solid; $[\alpha]_D^{25} -142$ (*c* 0.15, MeOH); UV (MeOH) λ_{\max} (log ε) 200 (3.51), 329 (3.22) nm; ECD (0.20 mg/mL, MeOH) λ_{\max} ($\Delta\varepsilon$) 200 (+13.7), 222 (-15.7), 250 (+41.8), 330 (-16.1) nm; IR (film) ν_{\max} 3361, 2943, 1681, 1668, 1456, 1394, 1321, 1093, 1022 cm⁻¹; ¹H and ¹³C NMR data, **Table S32**; HRESIMS *m/z* 494.2259 [M + Na]⁺ (calcd for C₂₅H₃₃N₃NaO₆, 494.2267).

Pyranamide D (4): white solid; $[\alpha]_D^{25} -145$ (*c* 0.10, MeOH); UV (MeOH) λ_{\max} (log ε) 200 (3.55), 331 (3.10) nm; ECD (0.20 mg/mL, MeOH) λ_{\max} ($\Delta\varepsilon$) 200 (+8.72), 226 (-5.94), 252 (+24.9), 333 (-9.09) nm; IR (film) ν_{\max} 3379, 2935, 1687, 1668, 1454, 1373, 1321, 1109, 1028 cm⁻¹; ¹H and ¹³C NMR data, **Table S32**; HRESIMS *m/z* 494.2250 [M + Na]⁺ (calcd for C₂₅H₃₃N₃NaO₆, 494.2267).

Secopyranamide C (5): white solid; $[\alpha]_D^{25} -118$ (*c* 0.35, MeOH); UV (MeOH) λ_{\max} (log ε) 200 (3.48), 325 (3.29) nm; ECD (0.20 mg/mL, MeOH) λ_{\max} ($\Delta\varepsilon$) 200 (+9.34), 226 (-6.35), 252 (+26.6), 333 (-9.73) nm; IR (film) ν_{\max} 3396, 2958, 1666, 1660, 1456, 1384, 1192, 1120, 1029 cm⁻¹; ¹H

and ^{13}C NMR data, **Table S32**; HRESIMS m/z 526.2533 [M + Na] $^+$ (calcd for C₂₆H₃₇N₃NaO₇, 526.2529).

Protuboxepin F (6): white solid; $[\alpha]_{\text{D}}^{25} -53.8$ (c 0.10, MeOH); UV (MeOH) λ_{\max} (log ε) 200 (3.45), 265 (2.70), 360 (2.62) nm; ECD (0.20 mg/mL, MeOH) λ_{\max} ($\Delta\varepsilon$) 200 (+15.1), 231 (−0.555), 244 (+1.34), 275 (−6.14) nm; IR (film) ν_{\max} 3350, 2927, 1681, 1653, 1521, 1435, 1203, 1134, 1020 cm^{−1}; ^1H and ^{13}C NMR data, **Table S33**; HRESIMS m/z 398.1486 [M + Na] $^+$ (calcd for C₂₂H₂₁N₃NaO₃, 398.1481).

Protuboxepin G (7): white solid; $[\alpha]_{\text{D}}^{25} -52.1$ (c 0.20, MeOH); UV (MeOH) λ_{\max} (log ε) 200 (3.40), 264 (2.77), 360 (2.63) nm; ECD (0.20 mg/mL, MeOH) λ_{\max} ($\Delta\varepsilon$) 200 (+18.2), 232 (−1.56), 245 (+0.878), 276 (−7.47) nm; IR (film) ν_{\max} 3334, 2929, 1681, 1670, 1521, 1435, 1228, 1101, 1022 cm^{−1}; ^1H and ^{13}C NMR data, **Table S33**; HRESIMS m/z 376.1665 [M + H] $^+$ (calcd for C₂₂H₂₂N₃O₃, 376.1661).

Protuboxepin H (8): white solid; $[\alpha]_{\text{D}}^{25} -30.0$ (c 0.10, MeOH); UV (MeOH) λ_{\max} (log ε) 200 (3.18), 239 (2.91), 337 (2.59) nm; ECD (0.25 mg/mL, MeOH) λ_{\max} ($\Delta\varepsilon$) 200 (+20.0), 229 (−9.45), 302 (+2.52), 343 (−1.35) nm; IR (film) ν_{\max} 3442, 2924, 1681, 1573, 1456, 1392, 1205, 1136, 1022 cm^{−1}; ^1H and ^{13}C NMR data, **Table S33**; HRESIMS m/z 398.1479 [M + Na] $^+$ (calcd for C₂₂H₂₁N₃NaO₃, 398.1481).

Protuboxepin I (9): white solid; $[\alpha]_{\text{D}}^{25} -58.3$ (c 0.12, MeOH); UV (MeOH) λ_{\max} (log ε) 200 (3.20), 235 (2.98), 338 (2.66) nm; ECD (0.30 mg/mL, MeOH) λ_{\max} ($\Delta\varepsilon$) 200 (+27.6), 228 (−15.3), 303 (+3.41), 346 (−1.98) nm; IR (film) ν_{\max} 3454, 2926, 1681, 1573, 1467, 1392, 1219, 1134 cm^{−1}; ^1H and ^{13}C NMR data, **Table S33**; HRESIMS m/z 398.1471 [M + Na] $^+$ (calcd for C₂₂H₂₁N₃NaO₃, 398.1481).

Protuboxepin J (10): colorless needle crystals; $[\alpha]_{\text{D}}^{25} -97.6$ (c 0.15, MeOH); UV (MeOH) λ_{\max} (log ε) 200 (3.34), 272 (2.38) nm; ECD (0.20 mg/mL, MeOH) λ_{\max} ($\Delta\varepsilon$) 213 (+2.51), 236 (−9.35), 275 (−1.59), 310 (−1.98) nm; IR (film) ν_{\max} 3363, 2927, 1683, 1635, 1386, 1205, 1141 cm^{−1}; ^1H and ^{13}C NMR data, **Table S33**; HRESIMS m/z 414.1795 [M + Na] $^+$ (calcd for C₂₃H₂₅N₃NaO₃, 414.1794).

1.6 Crystallographic Data of protuboxepin J (10)

Crystallographic data for protuboxepin J (10) was collected on an Agilent Xcalibur Nova single-crystal diffractometer using Cu K α radiation. The structures of these compounds were

solved by direct methods (SHELXS97), expanded using difference Fourier techniques, and refined by full-matrix least-squares calculation. The non-hydrogen atoms were refined anisotropically, and hydrogen atoms were fixed at calculated positions. Crystallographic data for protuboxepin J (**10**) has been deposited in the Cambridge Crystallographic Data Centre database (deposition number CCDC 1863377). Copies of the data can be obtained free of charge from the CCDC at www.ccdc.cam.ac.uk.

Crystal data: protuboxepin J (**10**) was crystallized from methanol to give colorless crystals. Crystal data: Orthorhombic, $a = 11.8106$ (4) Å, $b = 12.5767$ (4) Å, $c = 26.9924$ (10) Å, $\alpha = 90^\circ$, $\beta = 90^\circ$, $\gamma = 90^\circ$, $V = 4009.4$ (2) Å³, $T = 100.0$ (3) K, space group $P2_12_12_1$, $Z = 1$, μ (Cu K α) = 0.688 mm⁻¹, 18,067 reflections collected, 7112 independent reflections ($R_{\text{int}} = 0.0460$, $R_{\text{sigma}} = 0.0486$). The final R_1 values were 0.0501 ($I > 2\sigma(I)$). The final wR_2 (F2) values were 0.1414 (all data). The goodness of fit on F2 was 1.029. Flack parameter = -0.05 (12).

1.7 Biological Assay

Cytotoxic Assay. The obtained compounds (**1**, **3**, **7**, **10**, and **12**) were evaluated for their cytotoxic activities against three renal carcinoma cell lines, ACHN, OS-RC-2 and 786-O cells (Shanghai Cell Bank, Chinese Academy of Sciences). The cytotoxic activity was determined by the CCK-8 (Dojindo) method.¹ Briefly, ACHN, OS-RC-2 and 786-O cells were cultured in MEM, RPMI1640 and RPMI1640 media supplemented with 10% phosphate-buffered saline (FBS), respectively. The cells were seeded at a density of 400 to 800 cells/well in 384 well plates and then incubated with the compounds in a gradient concentration (50, 10.0, 2.0, 0.40, and 0.080 μM) or with a solvent control for 72 h, followed by the addition of CCK-8 reagent and the OD value of each well was measured at 450 nm using SpectraMax M5 Microplate Reader (Molecular Devices). Sorafenib functioned as the positive control. Dose response curves were plotted to determine IC₅₀ based upon the average values of three parallel experiments using Prism 5.0.

Kinase Inhibition Assay. The in vitro inhibitory activity of compounds **7** and **12** was further tested by Medicilon Co., Ltd., Shanghai, People's Republic of China. The mobility shift assay was performed for FLT1, FLT4, VEGFR2, PDGFR- α and PDGFR- β . Staurosporine was used as a positive control. The inhibition rates at single compound concentrations were tested in duplicate. For IC₅₀ estimations, 5 concentrations were measured for each compound, with the starting point of 80 nM and gradient 5-fold dilution.

Table S1. Cytotoxicities of Compounds 1, 3, 7, 10, and 12

Comp.	IC ₅₀ (μ M)		
	ACHN	786-O	OS-RC-2
1	>100	>100	>100
3	>100	>100	>100
7	27.0	34.9	47.1
10	>100	>100	>100
12	56.1	41.0	57.8
Sorafenib	3.4	4.9	7.0

2. Computational Methods

Conformational analysis of the isomers of **1–4**, **6**, **8**, and **10** were carried out by means of the Spartan 14 software using the Merck Molecular Force Field (MMFF) method¹. The conformers with Boltzmann-population of over 1% (the relative energy within 10 kcal/mol) were reoptimized using density functional theory (DFT) at the B3LYP/6-31+G (d) level under vacuum using the Gaussian 09 program². The overall theoretical calculation of ECD was conducted in MeOH using Time-dependent Density functional theory (TD-DFT) at the B3LYP/6-311+G (d, p) level for the stable conformers (the relative energy within 6 kcal/mol) of compounds **1**, **6**, **8**, and **10**. Rotatory strengths for a total of 50 excited states were calculated. The ECD spectra of different conformers were generated using the program SpecDis 1.6 (University of Würzburg) and Prism 5.0 (GraphPad Software Inc.) with a half-bandwidth of 0.2–0.4 eV, according to the Boltzmann-calculated contribution of each conformer after UV correction.

Meanwhile, the stable conformers of diastereomers of compounds **1–4** with Boltzmann-population of over 1% (the relative energy within 10 kcal/mol) were chosen for ¹H and ¹³C NMR chemical shift calculations using the gauge including atomic orbital (GIAO) method at the PCM//B3LYP/6-31+G (d,p) level of theory for DP4+ calculations. The calculations in solution were carried out using the polarizable continuum model, PCM, for methanol (the solvent used experimentally). The unscaled chemical shifts (δu) were computed using TMS as the reference standard using equation: $\delta u = \sigma 0 - \sigma x$, where σx is the Boltzmann averaged shielding tensor and $\sigma 0$ is the shielding tensor of TMS computed at the same level of theory employed for σx . For

methyl groups, averages of the computed values of the three hydrogens were used to compare with the experimental data. The DP4+ calculations were carried out using the Excel spreadsheet available for free at sarotti-NMR.weebly.com. These computed chemical shifts were compared with the experimental values utilizing total absolute deviation (TAD), mean absolute error (MAE) and DP4+ probability analyses.

Table S2. Energies of **1** at MMFF94 force field.

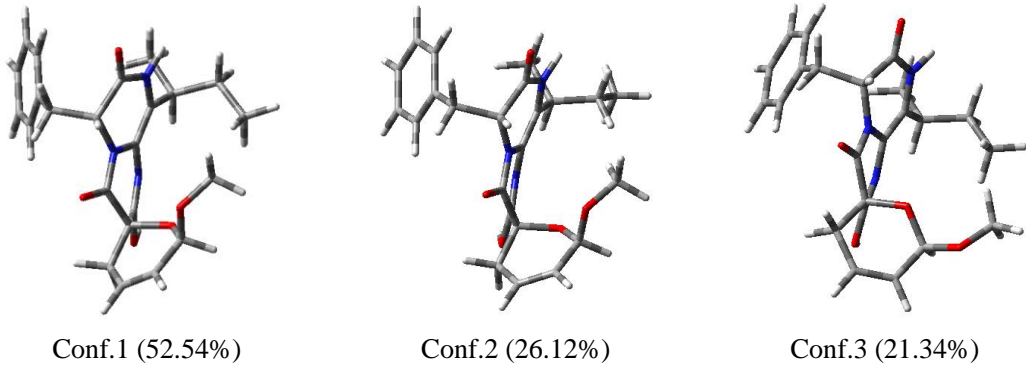
Configuration	Conformer	Energy (kJ/mol)	Population (%)
(8 <i>R</i> ,12 <i>R</i> ,15 <i>R</i> ,16 <i>S</i>)- 1A	1	184.89	79.9
(8 <i>R</i> ,12 <i>R</i> ,15 <i>R</i> ,16 <i>S</i>)- 1A	2	189.83	10.9
(8 <i>R</i> ,12 <i>R</i> ,15 <i>R</i> ,16 <i>S</i>)- 1A	3	193.47	2.5
(8 <i>S</i> ,12 <i>S</i> ,15 <i>R</i> ,16 <i>S</i>)- 1B	1	196.38	49.4
(8 <i>S</i> ,12 <i>S</i> ,15 <i>R</i> ,16 <i>S</i>)- 1B	2	199.08	16.6
(8 <i>S</i> ,12 <i>S</i> ,15 <i>R</i> ,16 <i>S</i>)- 1B	3	200.17	10.7
(8 <i>S</i> ,12 <i>S</i> ,15 <i>R</i> ,16 <i>S</i>)- 1B	4	200.83	8.2
(8 <i>S</i> ,12 <i>S</i> ,15 <i>R</i> ,16 <i>S</i>)- 1B	5	203.10	3.3
(8 <i>R</i> ,12 <i>S</i> ,15 <i>R</i> ,16 <i>S</i>)- 1C	1	181.21	69.3
(8 <i>R</i> ,12 <i>S</i> ,15 <i>R</i> ,16 <i>S</i>)- 1C	2	185.70	11.3
(8 <i>R</i> ,12 <i>S</i> ,15 <i>R</i> ,16 <i>S</i>)- 1C	3	186.46	8.3
(8 <i>R</i> ,12 <i>S</i> ,15 <i>R</i> ,16 <i>S</i>)- 1C	4	190.88	1.4
(8 <i>S</i> ,12 <i>R</i> ,15 <i>R</i> ,16 <i>S</i>)- 1D	1	185.15	57.7
(8 <i>S</i> ,12 <i>R</i> ,15 <i>R</i> ,16 <i>S</i>)- 1D	2	188.64	14.1
(8 <i>S</i> ,12 <i>R</i> ,15 <i>R</i> ,16 <i>S</i>)- 1D	3	189.65	9.4
(8 <i>S</i> ,12 <i>R</i> ,15 <i>R</i> ,16 <i>S</i>)- 1D	4	190.54	6.6
(8 <i>S</i> ,12 <i>R</i> ,15 <i>R</i> ,16 <i>S</i>)- 1D	5	193.61	1.9

Table S3. Energies of **1** at B3LYP/6–31+G(d, p) level in methanol.

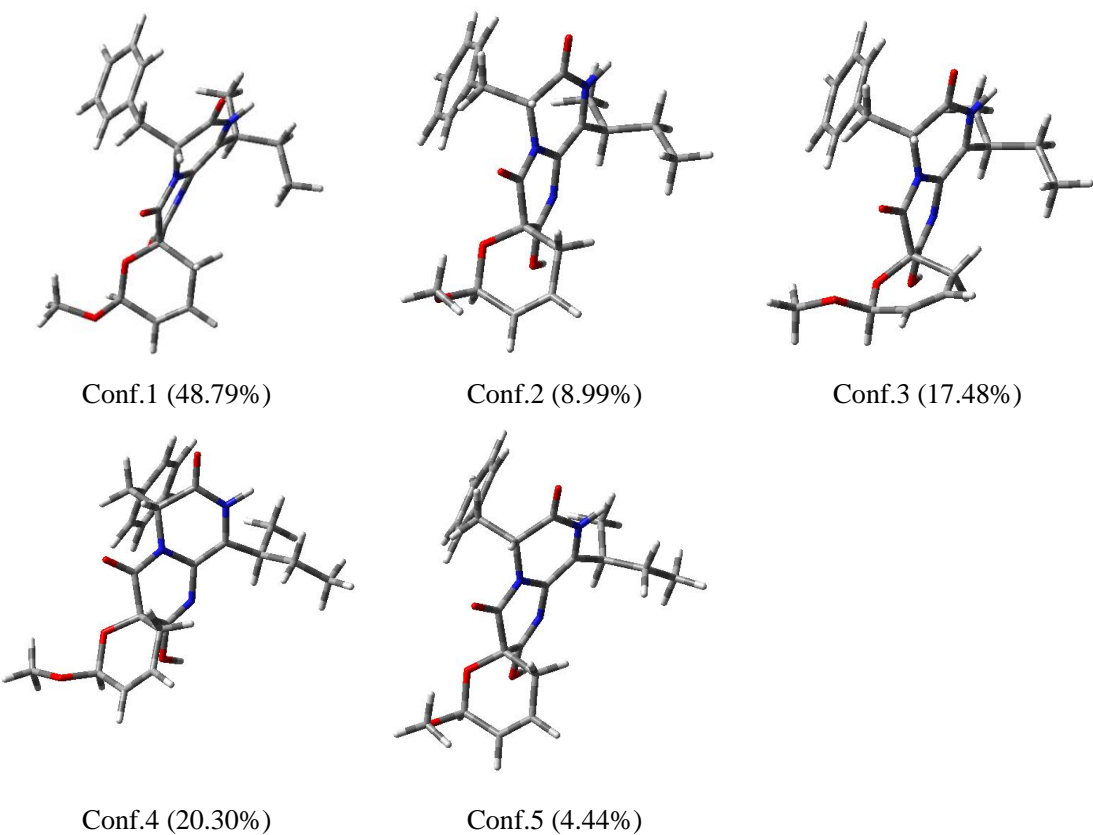
Configuration	Conformer	E (Hartree)	E (kcal/mol)	Population (%)
(8 <i>R</i> ,12 <i>R</i> ,15 <i>R</i> ,16 <i>S</i>)- 1A	1	-1433.4873126	-899527.623529626	52.54
(8 <i>R</i> ,12 <i>R</i> ,15 <i>R</i> ,16 <i>S</i>)- 1A	2	-1433.4866532	-899527.209749532	26.12
(8 <i>R</i> ,12 <i>R</i> ,15 <i>R</i> ,16 <i>S</i>)- 1A	3	-1433.4864626	-899527.090146126	21.34
(8 <i>S</i> ,12 <i>S</i> ,15 <i>R</i> ,16 <i>S</i>)- 1B	1	-1433.4855804	-899526.536556804	48.79
(8 <i>S</i> ,12 <i>S</i> ,15 <i>R</i> ,16 <i>S</i>)- 1B	2	-1433.4839845	-899525.535113595	8.99
(8 <i>S</i> ,12 <i>S</i> ,15 <i>R</i> ,16 <i>S</i>)- 1B	3	-1433.4846123	-899525.929064373	17.48
(8 <i>S</i> ,12 <i>S</i> ,15 <i>R</i> ,16 <i>S</i>)- 1B	4	-1433.4847532	-899526.017480532	20.30
(8 <i>S</i> ,12 <i>S</i> ,15 <i>R</i> ,16 <i>S</i>)- 1B	5	-1433.4833184	-899525.117129184	4.44
(8 <i>R</i> ,12 <i>S</i> ,15 <i>R</i> ,16 <i>S</i>)- 1C	1	-1433.4891495	-899528.776202745	65.79
(8 <i>R</i> ,12 <i>S</i> ,15 <i>R</i> ,16 <i>S</i>)- 1C	2	-1433.4883191	-899528.255118441	27.28
(8 <i>R</i> ,12 <i>S</i> ,15 <i>R</i> ,16 <i>S</i>)- 1C	3	-1433.4867148	-899527.248404148	4.98
(8 <i>R</i> ,12 <i>S</i> ,15 <i>R</i> ,16 <i>S</i>)- 1C	4	-1433.4858271	-899526.691363521	1.94

(8 <i>S</i> ,12 <i>R</i> ,15 <i>R</i> ,16 <i>S</i>)- 1D	1	-1433.487606	-899527.80764106	48.09
(8 <i>S</i> ,12 <i>R</i> ,15 <i>R</i> ,16 <i>S</i>)- 1D	2	-1433.487524	-899527.75618524	44.08
(8 <i>S</i> ,12 <i>R</i> ,15 <i>R</i> ,16 <i>S</i>)- 1D	3	-1433.4827076	-899524.733846076	0.27
(8 <i>S</i> ,12 <i>R</i> ,15 <i>R</i> ,16 <i>S</i>)- 1D	4	-1433.4858482	-899526.704603982	7.46
(8 <i>S</i> ,12 <i>R</i> ,15 <i>R</i> ,16 <i>S</i>)- 1D	5	-1433.4818174	-899524.175236674	0.10

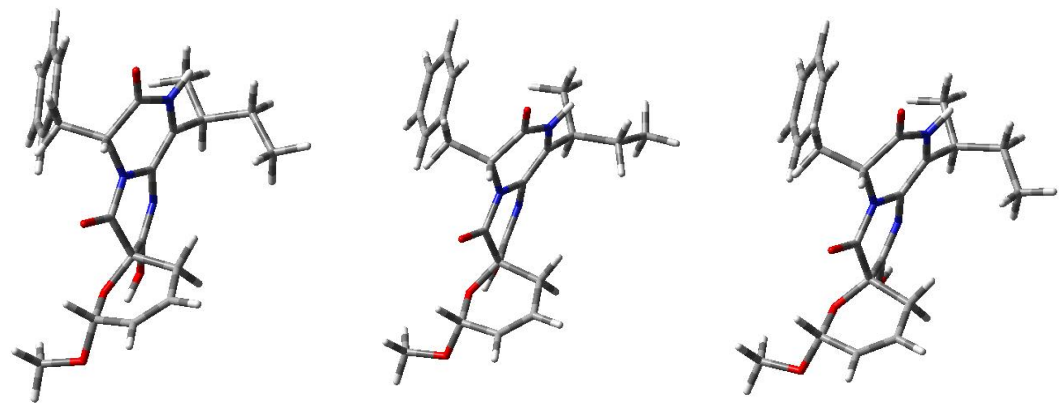
(8*R*,12*R*,15*R*,16*S*)-1A****



(8*S*,12*S*,15*R*,16*S*)-1B****



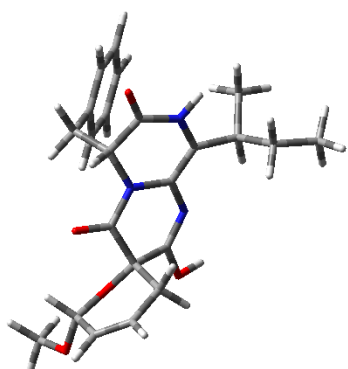
(8*R*,12*S*,15*R*,16*S*)-1C****



Conf.1 (65.79%)

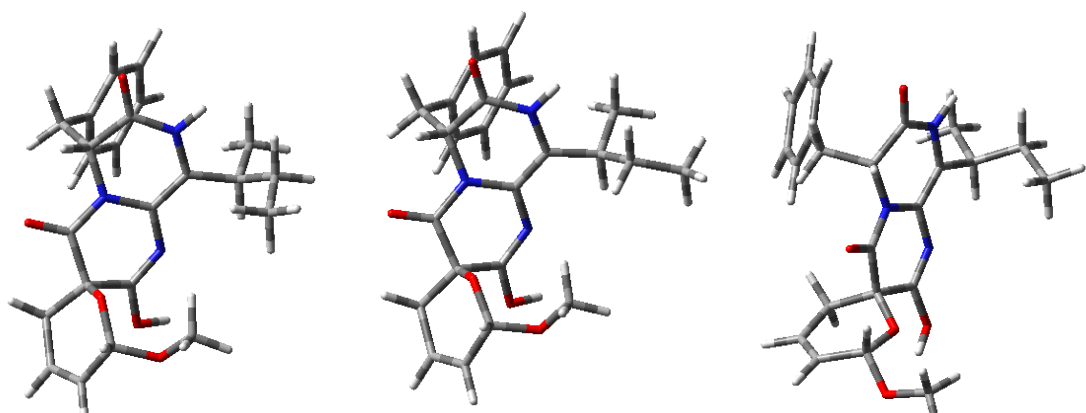
Conf.2 (27.28%)

Conf.3 (4.98%)



Conf.4 (1.94%)

(8*S*,12*R*,15*R*,16*S*)-1D



Conf.1 (48.09%)

Conf.2 (44.08%)

Conf.3 (0.27%)

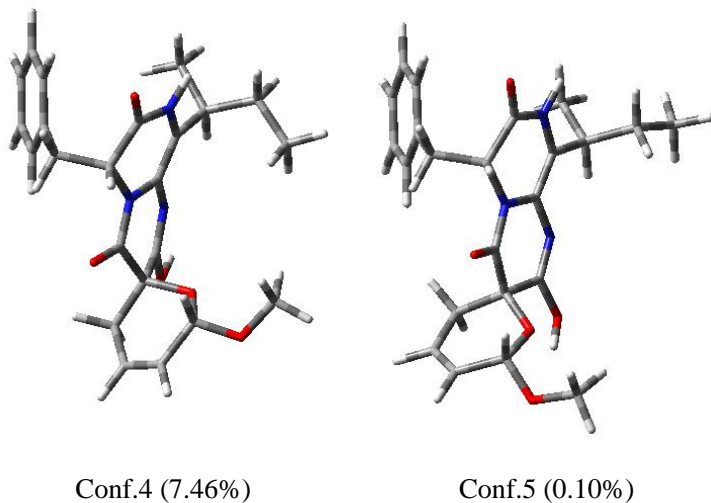


Figure S1. The optimized conformers and equilibrium populations of pyranamide A (**1**)

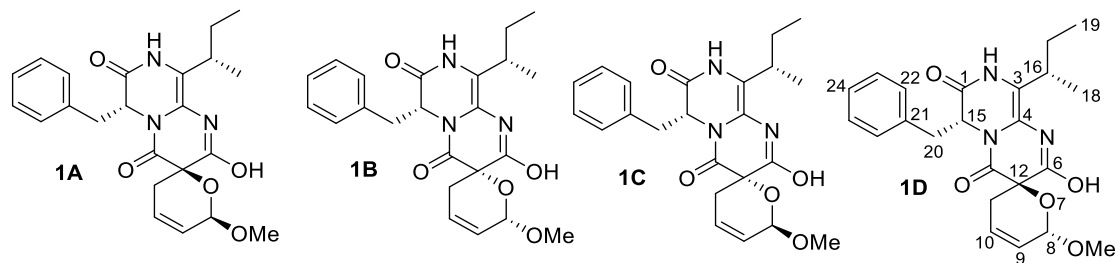


Figure S2. The possible diastereomers, **1A**, **1B**, **1C**, and **1D**, of **1** used for DP4+ analysis.

Table S4. DP4+ analysis of calculated ^1H -NMR data of **1A**, **1B**, **1C**, and **1D** (experimental for **1**, isomers **1–4** for **1A–1D**, respectively)

A	B	C	D	E	F	G	H
Functional		Solvent?		Basis Set		Type of Data	
B3LYP		PCM		6-31+G(d, p)		Unscaled Shifts	
		DP4+	0.00%	0.00%	0.00%	100.00%	-
Nuclei	sp2?	Experimental	Isomer 1	Isomer 2	Isomer 3	Isomer 4	Isomer 5
H		4.83	5.0	5.9	6.3	5.0	
H	x	5.61	6.0	6.1	6.0	6.1	
H	x	6.09	6.5	6.3	6.2	6.6	
H		2.87	3.5	2.6	2.4	3.3	
H		2.32	2.6	2.1	2.2	2.5	
H		4.93	5.0	5.1	5.1	5.1	
H		2.45	2.8	2.8	2.8	2.7	
H		1.42	1.3	1.3	1.2	1.4	
H		0.77	0.3	0.3	0.3	0.3	
H		0.89	0.8	0.7	0.7	0.8	
H		3.13	3.46	3.36	3.3	3.4	
H		3.05	3.07	3.21	3.19	3.13	
H	x	7.06	7.68	7.69	7.62	7.66	
H	x	7.23	7.63	7.62	7.61	7.63	
H	x	7.21	7.56	7.54	7.56	7.55	
H	x	7.22	7.38	7.47	7.52	7.50	
H	x	7.06	7.28	7.37	7.36	7.24	
H		3.32	3.40	3.72	3.79	3.39	

Table S5. DP4+ analysis of calculated ^{13}C -NMR data of **1A**, **1B**, **1C**, and **1D** (experimental for **1**,
18

isomers **1–4** for **1A–1D**, respectively)

	A	B	C	D	E	F	G	H
1	Functional		Solvent?		Basis Set		Type of Data	
2	B3LYP		PCP		6-31+G(d,p)		Unscaled Shifts	
3								
12		DP4+	19.02%	2.05%	0.93%	78.00%	-	
14	Nuclei	sp2?	Experimental	Isomer 1	Isomer 2	Isomer 3	Isomer 4	Isomer 5
15	C	x	168.3	163.6	163.1	163.6	163.3	
16	C	x	115.3	121.4	119.8	121.2	121.7	
17	C	x	113.7	118.5	118.1	118.7	117.3	
18	C	x	166.4	155.2	158.3	156.4	157.5	
19	C		98.2	100.7	100.7	101.7	99.9	
20	C	x	123.7	122.3	125.6	125.3	122.3	
21	C	x	127.7	128.2	125.4	124.3	128.2	
22	C		23.8	29.1	35.7	34.7	29.9	
23	C		74.7	73.6	77.0	78.7	71.9	
24	C	x	167	162.6	164.3	164.4	162.0	
25	C		58	63.92	63.30	62.9	64.0	
26	C		33.8	37.49	36.91	37.29	37.36	
27	C		27.9	32.49	31.54	32.19	31.51	
28	C		17.6	20.13	20.10	19.64	19.02	
29	C		12.5	14.53	14.13	14.51	14.66	
30	C		37.7	39.76	40.35	40.15	40.11	
31	C	x	136.7	135.55	135.03	135.39	135.94	
32	C	x	130.7	127.34	127.69	128.12	128.31	
33	C	x	129.5	126.32	125.89	126.25	126.58	
34	C	x	128.2	124.22	124.36	124.56	124.77	
35	C	x	129.5	125.79	125.89	126.06	126.20	
36	C	x	130.7	126.73	127.13	127.48	126.81	
37	C		56.3	57.71	57.33	58.83	57.78	
38								

Table S6. Calculated (calc.) and experimental (exp.) ^1H NMR chemical shift values of **1A**, **1B**, **1C**, and **1D** at the B3LYP/6-31+G (d,p) level in methanol and total absolute deviation (TAD^a) and mean absolute error (MAE).

^1H	exp.	calc. 1	calc. 1A –e	calc.1	calc. 1	calc. 1	calc. 1	calc.1	calc. 1D
	A	xp.	B	B–exp.	C	C–exp.	D	–exp.	
H-8	4.83	5.01	0.18	5.86	1.03	6.32	1.49	4.96	0.13
H-9	5.61	6.01	0.40	6.12	0.51	6.03	0.42	6.08	0.47
H-10	6.09	6.54	0.45	6.32	0.23	6.22	0.13	6.56	0.47
H-11a	2.87	3.54	0.67	2.55	0.32	2.4	0.47	3.29	0.42
H-11b	2.32	2.61	0.29	2.07	0.25	2.15	0.17	2.49	0.17
H-15	4.93	4.99	0.06	5.12	0.19	5.05	0.12	5.13	0.20
H-16	2.45	2.83	0.38	2.75	0.30	2.79	0.34	2.69	0.24
H-17	1.42	1.30	0.12	1.26	0.16	1.24	0.18	1.41	0.01
H-18	0.77	0.34	0.43	0.33	0.44	0.33	0.44	0.28	0.49
H-19	0.89	0.76	0.13	0.72	0.17	0.73	0.16	0.79	0.10

H-20a	3.13	3.46	0.33	3.36	0.23	3.34	0.21	3.39	0.26
H-20b	3.05	3.07	0.02	3.21	0.16	3.19	0.14	3.13	0.08
H-22	7.06	7.68	0.62	7.69	0.63	7.62	0.56	7.66	0.60
H-23	7.23	7.63	0.40	7.62	0.39	7.61	0.38	7.63	0.40
H-24	7.21	7.56	0.35	7.54	0.33	7.56	0.35	7.55	0.34
H-25	7.22	7.38	0.16	7.47	0.25	7.52	0.30	7.50	0.28
H-26	7.06	7.28	0.22	7.37	0.31	7.36	0.30	7.24	0.18
H-27	3.32	3.40	0.08	3.72	0.40	3.79	0.47	3.39	0.07
	TADc	5.29			6.3		6.63		4.91
	MAE	0.29			0.35		0.37		0.27

^aTAD = $\Sigma | \text{calc.} - \text{exp.} |$

Table S7. Calculated (calc.) and experimental (exp.) ¹³C NMR chemical shift values of **1A**, **1B**, **1C**, and **1D** at the B3LYP/6-31+G(d, p) level in methanol and total absolute deviation (TAD^a) and mean absolute error (MAE).

¹³ C	exp.	calc. 1	calc. 1A	calc. 1B	calc. 1B	calc. 1	calc. 1C	calc. 1	calc. 1D
		A	-exp.		-exp.	C	-exp.	D	-exp.
C-1	168.3	163.56	4.74	163.13	5.17	163.62	4.68	163.29	5.01
C-3	115.3	121.42	6.12	119.81	4.51	121.15	5.85	121.71	6.41
C4	113.7	118.48	4.78	118.06	4.36	118.67	4.97	117.32	3.62
C-6	166.4	155.24	11.16	158.26	8.14	156.35	10.05	157.45	8.95
C-8	98.2	100.69	2.49	100.66	2.46	101.73	3.53	99.89	1.69
C-9	123.7	122.27	1.43	125.59	1.89	125.32	1.62	122.26	1.44
C-10	127.7	128.24	0.54	125.43	2.27	124.32	3.38	128.24	0.54
C-11	23.8	29.06	5.26	35.69	11.89	34.68	10.88	29.86	6.06
C-12	74.7	73.56	1.14	77	2.3	78.69	3.99	71.88	2.82
C-13	167	162.63	4.37	164.25	2.75	164.35	2.65	161.97	5.03
C-15	58	63.92	5.92	63.3	5.3	62.9	4.9	63.98	5.98
C-16	33.8	37.49	3.69	36.91	3.11	37.29	3.49	37.36	3.56
C-17	27.9	32.49	4.59	31.54	3.64	32.19	4.29	31.51	3.61

C-18	17.6	20.13	2.53	20.1	2.5	19.64	2.04	19.02	1.42
C-19	12.5	14.53	2.03	14.13	1.63	14.51	2.01	14.66	2.16
C-20	37.7	39.76	2.06	40.35	2.65	40.15	2.45	40.11	2.41
C-21	136.7	135.55	1.15	135.03	1.67	135.39	1.31	135.94	0.76
C-22	130.7	127.34	3.36	127.69	3.01	128.12	2.58	128.31	2.39
C-23	129.5	126.32	3.18	125.89	3.61	126.25	3.25	126.58	2.92
C-24	128.2	124.22	3.98	124.36	3.84	124.56	3.64	124.77	3.43
C-25	129.5	125.79	3.71	125.89	3.61	126.06	3.44	126.2	3.3
C-26	130.7	126.73	3.97	127.13	3.57	127.48	3.22	126.81	3.89
C-27	56.3	57.71	1.41	57.33	1.03	58.83	2.53	57.78	1.48
	TADc	83.61			84.91		90.75		78.88
	MAE	3.64			3.69		3.94		3.43

^aTAD = $\Sigma|\text{calc.} - \text{exp.}|$

Table S8. Energies of **2** at MMFF94 force field.

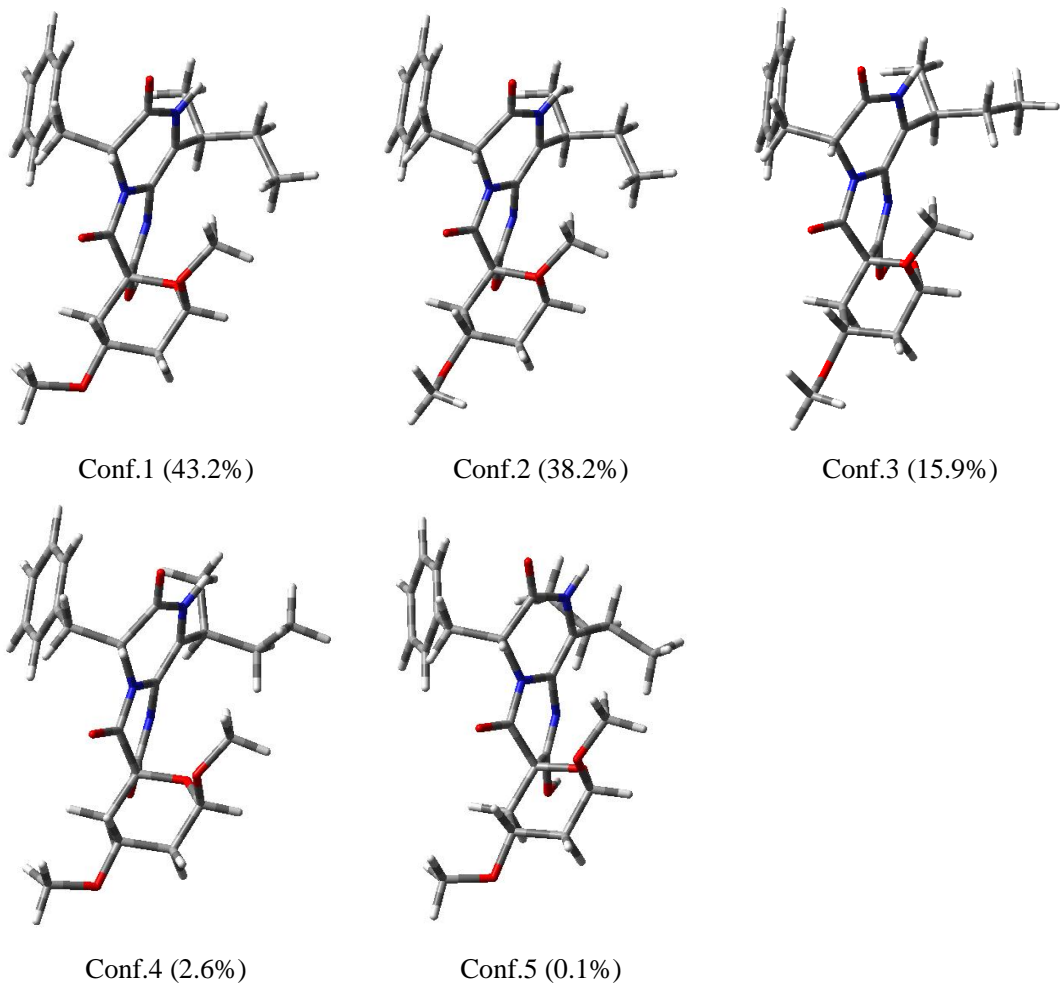
Configuration	Conformer	Energy (kJ/mol)	Population (%)
(8R,10R,12R,15R,16S)- 2A	1	155.92	52.4
(8R,10R,12R,15R,16S)- 2A	2	156.72	38.0
(8R,10R,12R,15R,16S)- 2A	3	161.47	5.6
(8R,10R,12R,15R,16S)- 2A	4	165.88	0.9
(8R,10R,12R,15R,16S)- 2A	5	166.26	0.8
(8S,10S,12R,15R,16S)- 2B	1	159.73	88.3
(8S,10S,12R,15R,16S)- 2B	2	168.95	2.1
(8S,10S,12R,15R,16S)- 2B	3	169.26	1.9
(8S,10S,12R,15R,16S)- 2B	4	169.76	1.5
(8S,10S,12R,15R,16S)- 2B	5	170.09	1.4
(8S,10S,12R,15R,16S)- 2B	6	170.29	1.2
(8S,10S,12R,15R,16S)- 2B	7	170.51	1.1
(8R,10R,12S,15R,16S)- 2C	1	160.11	55.2
(8R,10R,12S,15R,16S)- 2C	2	162.76	18.9
(8R,10R,12S,15R,16S)- 2C	3	163.77	12.6
(8R,10R,12S,15R,16S)- 2C	4	165.96	5.2
(8R,10R,12S,15R,16S)- 2C	5	167.29	3.0
(8R,10R,12S,15R,16S)- 2C	6	169.96	1.0
(8R,10R,12S,15R,16S)- 2C	7	170.77	0.7
(8S,10S,12S,15R,16S)- 2D	1	167.51	42.1
(8S,10S,12S,15R,16S)- 2D	2	169.17	21.5
(8S,10S,12S,15R,16S)- 2D	3	170.36	13.3

(8S,10S,12S,15R,16S)- 2D	4	171.68	7.8
(8S,10S,12S,15R,16S)- 2D	5	172.01	6.9
(8S,10S,12S,15R,16S)- 2D	6	174.95	2.1
(8S,10S,12S,15R,16S)- 2D	7	176.05	1.3
(8S,10S,12S,15R,16S)- 2D	8	176.66	1.1
(8S,10S,12S,15R,16S)- 2D	9	177.04	0.9

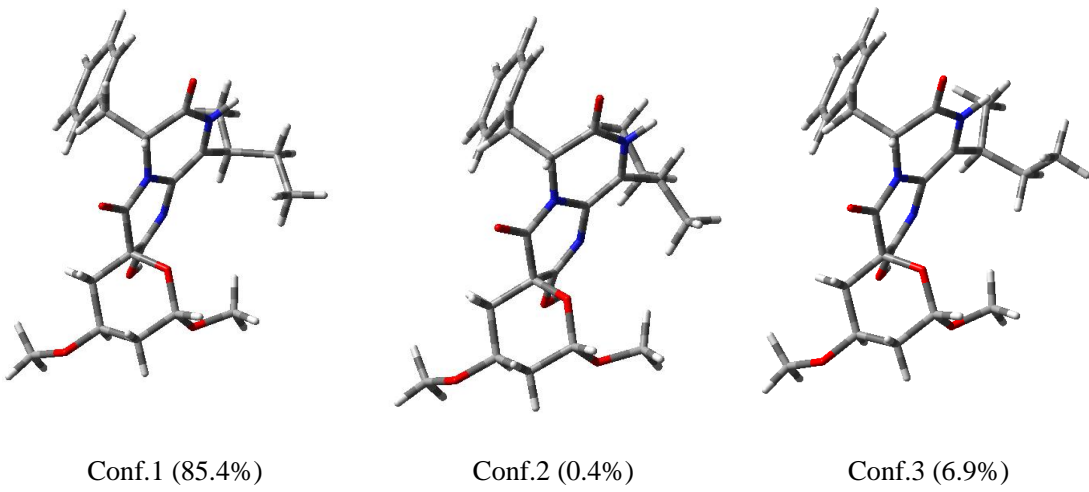
Table S9. Energies of **2** at B3LYP/6–31+G (d) level in methanol.

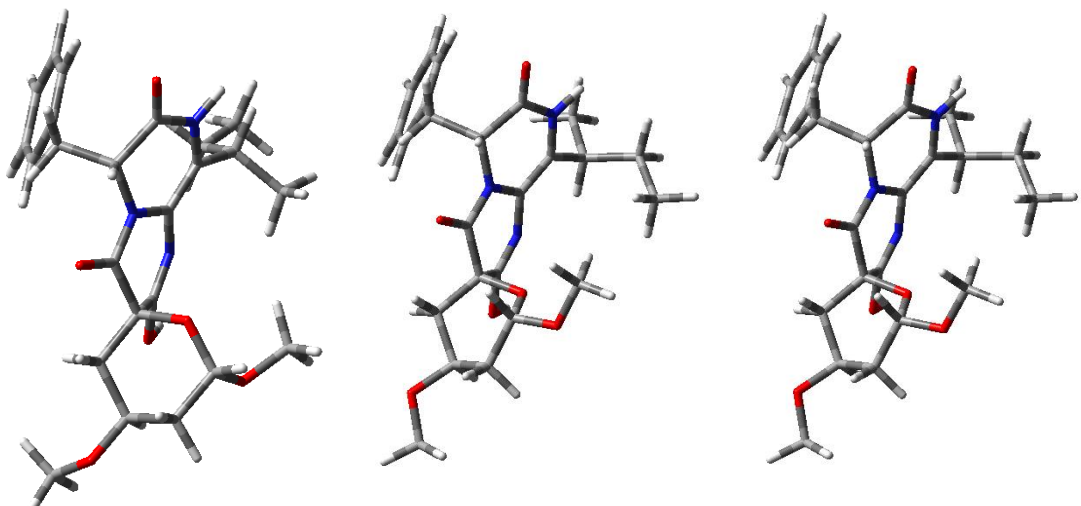
Configuration	Conformer	E (Hartree)	E (kcal/mol)	Population (%)
(8R,10R,12R,15R,16S)- 2A	1	-1548.8950125	-971947.109293875	43.2
(8R,10R,12R,15R,16S)- 2A	2	-1548.8948965	-971947.036502715	38.2
(8R,10R,12R,15R,16S)- 2A	3	-1548.8940691	-971946.517300941	15.9
(8R,10R,12R,15R,16S)- 2A	4	-1548.8923431	-971945.434218681	2.6
(8R,10R,12R,15R,16S)- 2A	5	-1548.8897528	-971943.808779528	0.1
(8S,10S,12R,15R,16S)- 2B	1	-1548.8953905	-971947.346492655	85.4
(8S,10S,12R,15R,16S)- 2B	2	-1548.8904014	-971944.215782514	0.4
(8S,10S,12R,15R,16S)- 2B	3	-1548.8930212	-971945.859733212	6.9
(8S,10S,12R,15R,16S)- 2B	4	-1548.8915347	-971944.926939597	1.4
(8S,10S,12R,15R,16S)- 2B	5	-1548.8919583	-971945.192752833	2.3
(8S,10S,12R,15R,16S)- 2B	6	-1548.8919583	-971945.192752833	2.3
(8S,10S,12R,15R,16S)- 2B	7	-1548.8914312	-971944.861992312	1.3
(8R,10R,12S,15R,16S)- 2C	1	-1548.8971341	-971948.440619091	47.2
(8R,10R,12S,15R,16S)- 2C	2	-1548.8971409	-971948.444886159	47.6
(8R,10R,12S,15R,16S)- 2C	3	-1548.8941217	-971946.550307967	1.9
(8R,10R,12S,15R,16S)- 2C	4	-1548.8926233	-971945.610046983	0.4
(8R,10R,12S,15R,16S)- 2C	5	-1548.8944526	-971946.757951026	2.8
(8R,10R,12S,15R,16S)- 2C	6	-1548.8917622	-971945.069698122	0.1
(8S,10S,12S,15R,16S)- 2D	1	-1548.8922153	-971945.354022903	2.3
(8S,10S,12S,15R,16S)- 2D	2	-1548.8924076	-971945.474693076	2.9
(8S,10S,12S,15R,16S)- 2D	3	-1548.8922398	-971945.369396898	2.4
(8S,10S,12S,15R,16S)- 2D	4	-1548.8913659	-971944.821015909	0.9
(8S,10S,12S,15R,16S)- 2D	5	-1548.8938741	-971946.394936491	13.6
(8S,10S,12S,15R,16S)- 2D	6	-1548.8947735	-971946.959318985	35.1
(8S,10S,12S,15R,16S)- 2D	7	-1548.8873773	-971942.318129523	0.0
(8S,10S,12S,15R,16S)- 2D	8	-1548.894958	-971947.07509458	42.8
(8S,10S,12S,15R,16S)- 2D	9	-1548.883246	-971939.72569746	0.0

(8*R*,10*R*,12*R*,15*R*,16*S*)-2A



(8*S*,10*S*,12*R*,15*R*,16*S*)-2B

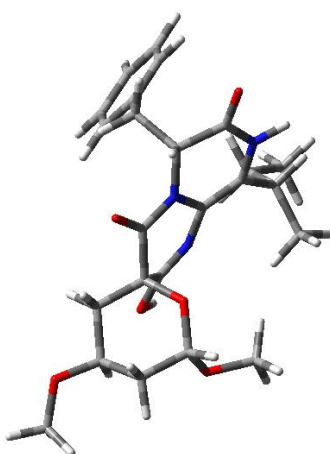




Conf.4 (1.4%)

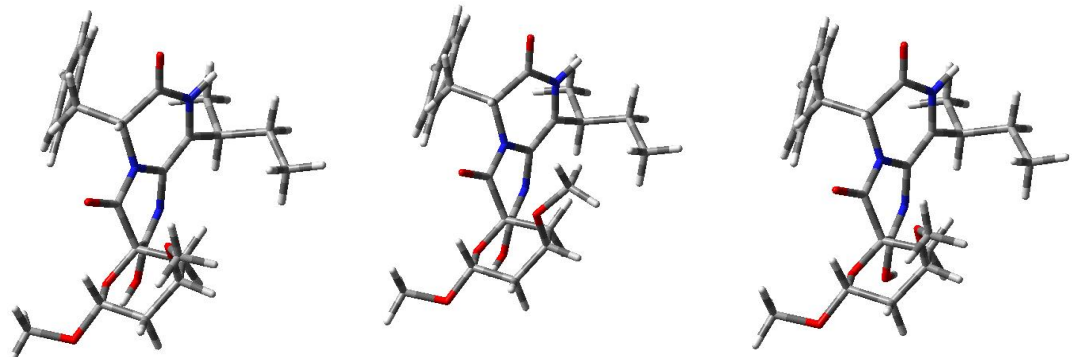
Conf.5 (2.3%)

Conf.6 (2.3%)



Conf.7 (1.3%)

(8*R*,10*R*,12*S*,15*R*,16*S*)-2C



Conf.1 (47.2%)

Conf.2 (47.6%)

Conf.3 (1.9%)

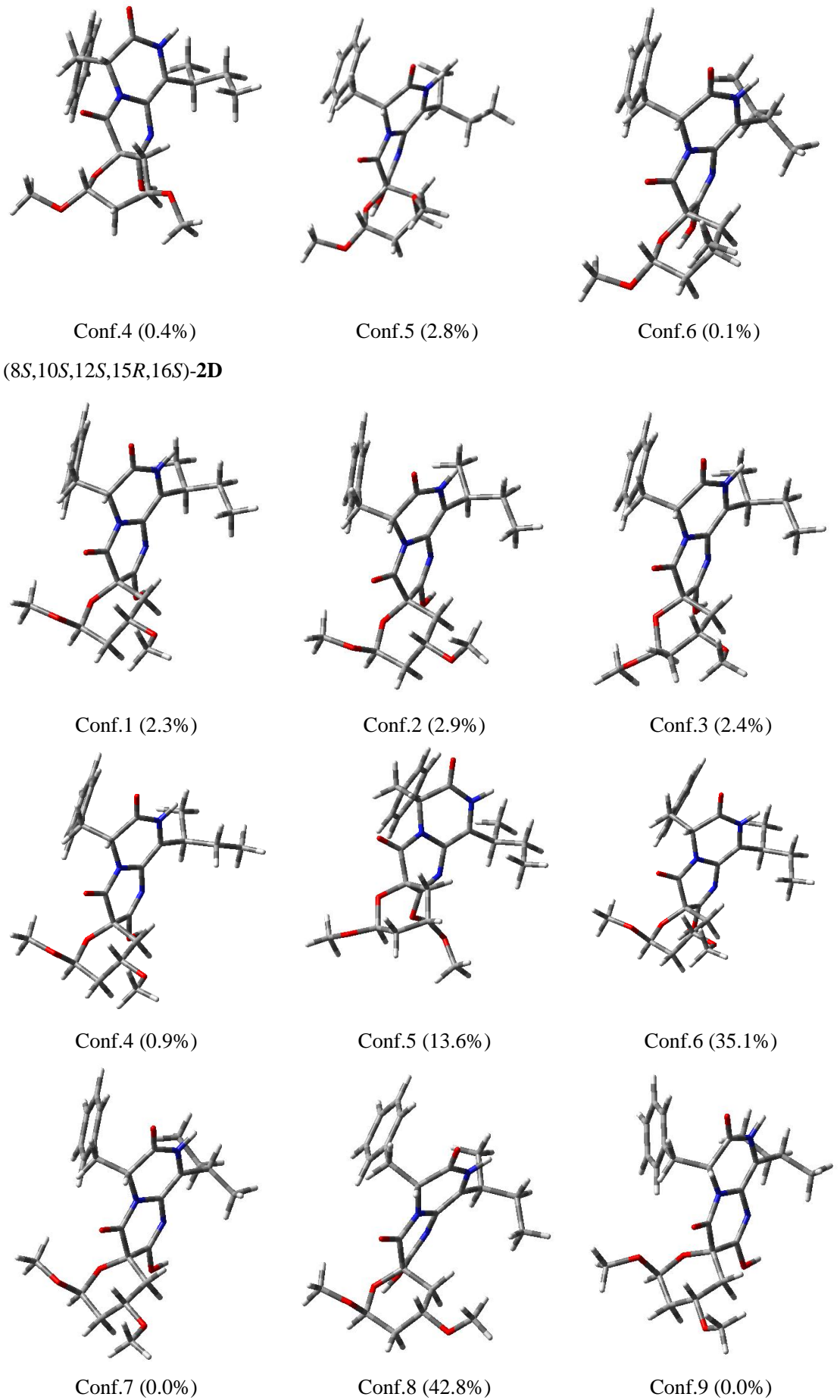
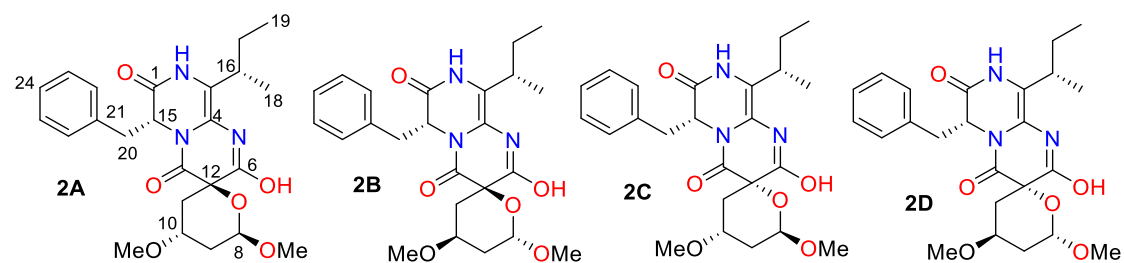


Figure S3. The optimized conformers and equilibrium populations of pyranamide B (**2**)



	DP4+	TAD	MAE		DP4+	TAD	MAE		DP4+	TAD	MAE		DP4+	TAD	MAE
H	100%	4.53	0.23		0.0%	5.42	0.27		0.0%	6.82	0.34		0.0%	6.09	0.30
C	93.62%	77.65	3.24		2.08%	83.52	3.48		0.99%	83.13	3.46		3.30%	87.77	3.66
Both	100%	82.18	3.47		0.0%	88.94	3.75		0.0%	89.95	3.80		0.0%	93.86	3.96

Figure S4. Total absolute deviation (TAD), mean absolute error (MAE), and DP4+ probability analyses (sarotti-nmr.weebly.com) for four candidate diastereomers of **2**.

Table S10. DP4+ analysis of calculated ¹H-NMR data of **2A**, **2B**, **2C**, and **2D** (experimental for **2**, isomers **1–4** for **2A–2D**, respectively)

Functional B3LYP		Solvent?	Basis Set		Type of Data			
		PCM	6-31+G(d,p)		Unscaled Shifts			
Nuclei	sp2?	Experimental	DP4+	100.00%	0.00%	0.00%	0.00%	-
H		4.81		4.8	4.9	6.2	5.5	
H		2.1		2.1	1.9	2.2	2.3	
H		1.42		1.4	1.6	1.5	1.5	
H		4.23		4.5	4.3	3.6	3.6	
H		2.26		2.5	2.7	2.0	2.2	
H		1.87		2.0	2.4	1.5	1.4	
H		4.94		4.9	5.1	4.9	5.0	
H		2.44		2.9	2.9	2.8	2.8	
H		1.43		1.4	1.4	1.4	1.4	
H		0.78		0.4	0.4	0.3	0.4	
H		0.87		0.76	0.71	0.7	0.7	
H		3.12		3.50	3.50	3.39	3.40	
H		3.06		3.13	3.20	3.20	3.13	
H	x	7.07		7.92	7.71	7.80	7.88	
H	x	7.23		7.61	7.51	7.66	7.59	
H	x	7.21		7.62	7.56	7.61	7.60	
H	x	7.23		7.38	7.50	7.48	7.38	
H	x	7.07		7.32	7.41	7.31	7.38	
H		3.23		3.35	3.35	3.79	3.74	
H		3.38		3.60	3.59	3.38	3.41	

Table S11. DP4+ analysis of calculated ¹³C-NMR data of **2A**, **2B**, **2C**, and **2D** (experimental for **2**, isomers **1–4** for **2A–2D**, respectively)

Functional		Solvent?	Basis Set		Type of Data		
B3LYP		PCII	6-31+G(d,p)		Unscaled Shifts		
Nuclei	sp2?	DP4+	93.62%	2.08%	0.99%	3.30%	-
C	x	168.4	163.6	163.0	163.3	163.5	
C	x	115.8	120.8	120.3	119.6	119.0	
C	x	113.8	118.4	118.5	119.7	119.0	
C	x	166.9	158.4	157.9	158.4	156.1	
C		103.4	105.5	105.9	101.4	104.6	
C		36.8	39.3	39.1	36.8	38.5	
C		70.2	72.6	72.8	77.6	73.0	
C		31.4	35.3	34.4	35.3	39.1	
C		77.4	76.2	75.5	80.2	80.7	
C	x	168	164.8	161.7	164.7	163.2	
C		58	63.34	63.77	63.4	63.4	
C		33.8	37.43	36.51	36.73	37.27	
C		27.9	31.69	31.36	31.71	31.41	
C		17.8	19.79	21.49	20.85	21.14	
C		12.3	14.45	14.21	14.44	14.63	
C		37.6	40.07	39.93	41.33	40.58	
C	x	136.6	137.08	135.86	137.41	136.25	
C	x	130.7	127.66	127.12	128.09	127.20	
C	x	129.5	127.10	126.52	126.89	126.79	
C	x	128.2	124.34	124.05	124.73	124.05	
C	x	129.5	125.75	126.29	125.84	125.96	
C	x	130.7	126.53	126.24	127.65	126.39	
C		56.4	57.63	57.46	58.38	58.04	
C		55.9	56.95	57.21	57.12	56.87	

Table S12. Calculated (calc.) and experimental (exp.) ¹H NMR chemical shift values of **2A**, **2B**, **2C**, and **2D** at the B3LYP/6-31+G(d, p) level in methanol and total absolute deviation (TAD^a) and mean absolute error (MAE).

¹ H	exp.	calc. 2	calc. 2A	calc.	calc. 2B	calc.	calc. 2C	calc. 2D	calc. 2D
			A	-exp.	2B	-exp.	2C	-exp.	-exp.
H-8	4.81	4.83	0.02	4.87	0.06	6.15	1.34	5.50	0.69
H-9a	2.10	2.13	0.03	1.93	0.17	2.16	0.06	2.25	0.15
H-9b	1.42	1.43	0.01	1.64	0.22	1.47	0.05	1.52	0.10
H-10	4.23	4.50	0.27	4.34	0.11	3.61	0.62	3.58	0.65
H-11a	2.26	2.49	0.23	2.69	0.43	2.04	0.22	2.19	0.07
H-11b	1.87	2.02	0.15	2.43	0.56	1.46	0.41	1.40	0.47
H-15	4.94	4.93	0.01	5.05	0.11	4.87	0.07	5.00	0.06
H-16	2.44	2.85	0.41	2.87	0.43	2.82	0.38	2.79	0.35
H-17	1.43	1.36	0.07	1.37	0.06	1.37	0.06	1.36	0.07

H-18	0.78	0.39	0.39	0.40	0.38	0.34	0.44	0.35	0.43
H-19	0.87	0.76	0.11	0.71	0.16	0.72	0.15	0.73	0.14
H-20a	3.12	3.50	0.38	3.50	0.38	3.39	0.27	3.40	0.28
H-20b	3.06	3.13	0.07	3.20	0.14	3.20	0.14	3.13	0.07
H-22	7.07	7.92	0.85	7.71	0.64	7.80	0.73	7.88	0.81
H-23	7.23	7.61	0.38	7.51	0.28	7.66	0.43	7.59	0.36
H-24	7.21	7.62	0.41	7.56	0.35	7.61	0.4	7.60	0.39
H-25	7.23	7.38	0.15	7.50	0.27	7.48	0.25	7.38	0.15
H-26	7.07	7.32	0.25	7.41	0.34	7.31	0.24	7.38	0.31
H-27	3.23	3.35	0.12	3.35	0.12	3.79	0.56	3.74	0.51
H-28	3.38	3.60	0.22	3.59	0.21	3.38	0.0	3.41	0.03
	TADc	4.53			5.42		6.82		6.09
	MAE	0.23			0.27		0.34		0.30

^aTAD = $\Sigma | \text{calc.} - \text{exp.} |$

Table S13. Calculated (calc.) and experimental (exp.) ¹³C NMR chemical shift values of **2A**, **2B**, **2C**, and **2D** at the B3LYP/6-31+G(d, p) level in methanol and total absolute deviation (TAD^a) and mean absolute error (MAE).

¹³ C	exp.	calc. 2	calc. 2A	calc. 2	calc. 2B	calc. 2	calc. 2C	calc. 2	calc. 2D
			A	-exp.	B	-exp.	C	-exp.	D
C-1	168.4	163.55	4.85	163.00	5.40	163.28	5.12	163.48	4.92
C-3	115.8	120.78	4.98	120.34	4.54	119.56	3.76	119	3.2
C-4	113.8	118.36	4.56	118.50	4.70	119.69	5.89	119	5.2
C-6	166.9	158.37	8.53	157.92	8.98	158.36	8.54	156.1	10.8
C-8	103.4	105.51	2.11	105.85	2.45	101.42	1.98	104.57	1.17
C-9	36.8	39.32	2.52	39.12	2.32	36.83	0.03	38.52	1.72
C-10	70.2	72.58	2.38	72.80	2.60	77.6	7.40	73.03	2.83
C-11	31.4	35.32	3.92	34.38	2.98	35.25	3.85	39.1	7.7
C-12	77.4	76.15	1.25	75.48	1.92	80.17	2.77	80.66	3.26

C-13	168	164.8	3.2	161.73	6.27	164.67	3.33	163.24	4.76
C-15	58.0	63.34	5.34	63.77	5.77	63.39	5.39	63.41	5.41
C-16	33.8	37.43	3.63	36.51	2.71	36.73	2.93	37.27	3.47
C-17	27.9	31.69	3.79	31.36	3.46	31.71	3.81	31.41	3.51
C-18	17.8	19.79	1.99	21.49	3.69	20.85	3.05	21.14	3.34
C-19	12.3	14.45	2.15	14.21	1.91	14.44	2.14	14.63	2.33
C-20	37.6	40.07	2.47	39.93	2.33	41.33	3.73	40.58	2.98
C-21	136.6	137.08	0.48	135.86	0.74	137.41	0.81	136.25	0.35
C-22	130.7	127.66	3.04	127.12	3.58	128.09	2.61	127.2	3.50
C-23	129.5	127.1	2.40	126.52	2.98	126.89	2.61	126.79	2.71
C-24	128.2	124.34	3.86	124.05	4.15	124.73	3.47	124.05	4.15
C-25	129.5	125.75	3.75	126.29	3.21	125.84	3.66	125.96	3.54
C-26	130.7	126.53	4.17	126.24	4.46	127.65	3.05	126.39	4.31
C-27	56.4	57.63	1.23	57.46	1.06	58.38	1.98	58.04	1.64
C-28	55.9	56.95	1.05	57.21	1.31	57.12	1.22	56.87	0.97
	TADc	77.65			83.52		83.13		87.77
	MAE	3.24		3.48		3.46		3.66	

^aTAD = $\Sigma |\text{calc.} - \text{exp.}|$

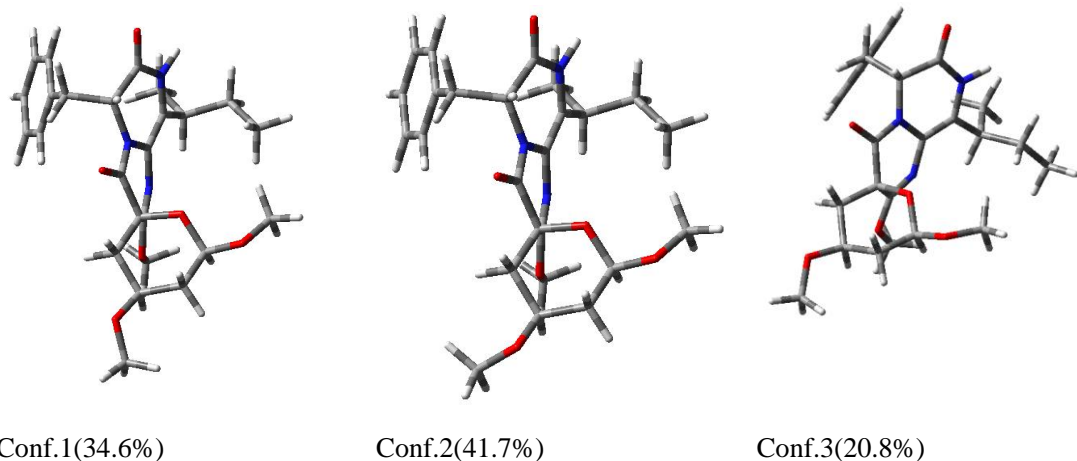
Table S14. Energies of **3** at MMFF94 force field.

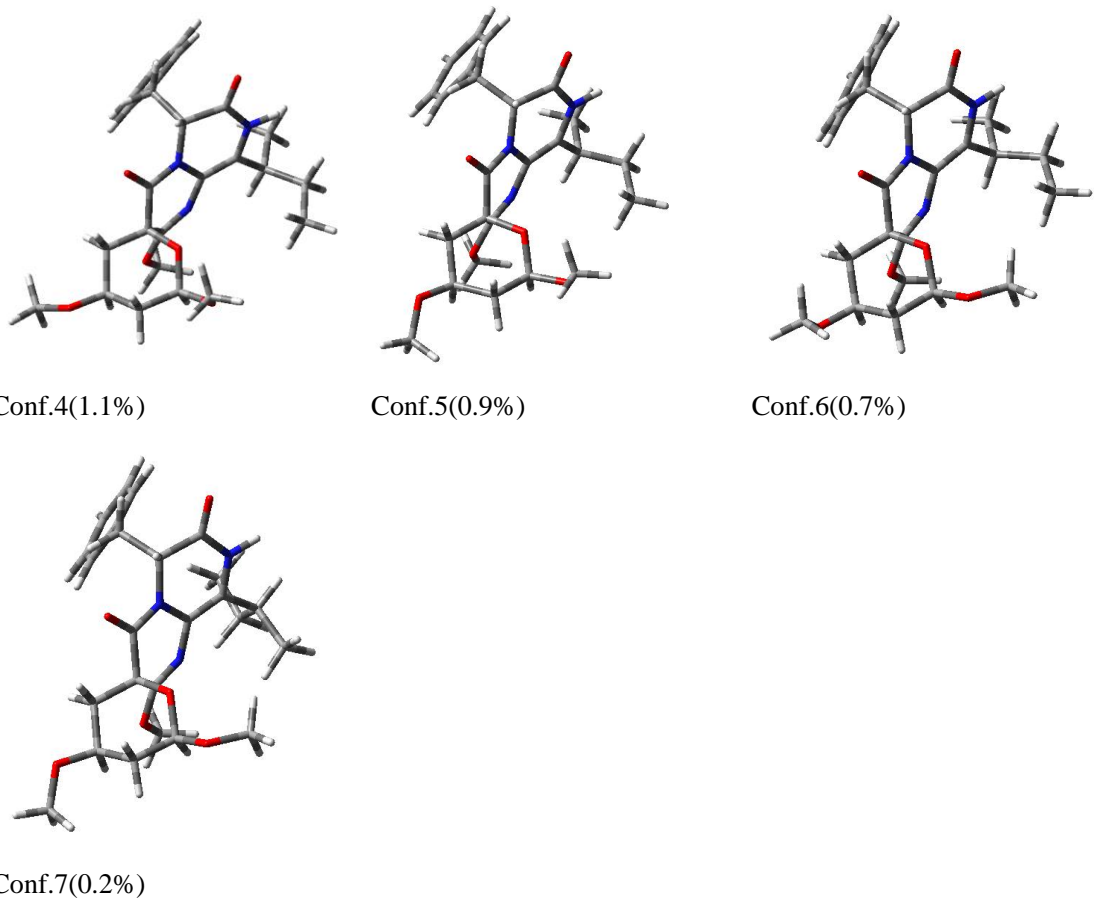
Configuration	Conformer	Energy (kJ/mol)	Population (%)
(8 <i>R</i> ,10 <i>S</i> ,12 <i>R</i> ,15 <i>R</i> ,16 <i>S</i>)- 3A	1	221.59	44.1
(8 <i>R</i> ,10 <i>S</i> ,12 <i>R</i> ,15 <i>R</i> ,16 <i>S</i>)- 3A	2	221.79	40.7
(8 <i>R</i> ,10 <i>S</i> ,12 <i>R</i> ,15 <i>R</i> ,16 <i>S</i>)- 3A	3	227.22	4.6
(8 <i>R</i> ,10 <i>S</i> ,12 <i>R</i> ,15 <i>R</i> ,16 <i>S</i>)- 3A	4	228.63	2.6
(8 <i>R</i> ,10 <i>S</i> ,12 <i>R</i> ,15 <i>R</i> ,16 <i>S</i>)- 3A	5	229.13	2.1
(8 <i>R</i> ,10 <i>S</i> ,12 <i>R</i> ,15 <i>R</i> ,16 <i>S</i>)- 3A	6	229.46	1.8
(8 <i>R</i> ,10 <i>S</i> ,12 <i>R</i> ,15 <i>R</i> ,16 <i>S</i>)- 3A	7	231.05	1.0
(8 <i>S</i> ,10 <i>R</i> ,12 <i>R</i> ,15 <i>R</i> ,16 <i>S</i>)- 3B	1	211.68	49.1
(8 <i>S</i> ,10 <i>R</i> ,12 <i>R</i> ,15 <i>R</i> ,16 <i>S</i>)- 3B	2	212.61	33.7
(8 <i>S</i> ,10 <i>R</i> ,12 <i>R</i> ,15 <i>R</i> ,16 <i>S</i>)- 3B	3	217.41	4.9
(8 <i>S</i> ,10 <i>R</i> ,12 <i>R</i> ,15 <i>R</i> ,16 <i>S</i>)- 3B	4	219.87	1.8
(8 <i>S</i> ,10 <i>R</i> ,12 <i>R</i> ,15 <i>R</i> ,16 <i>S</i>)- 3B	5	220.42	1.4
(8 <i>S</i> ,10 <i>R</i> ,12 <i>R</i> ,15 <i>R</i> ,16 <i>S</i>)- 3B	6	220.54	1.4
(8 <i>S</i> ,10 <i>R</i> ,12 <i>R</i> ,15 <i>R</i> ,16 <i>S</i>)- 3B	7	220.63	1.3

Table S15. Energies of **3** at B3LYP/6–31+G(d) level in methanol.

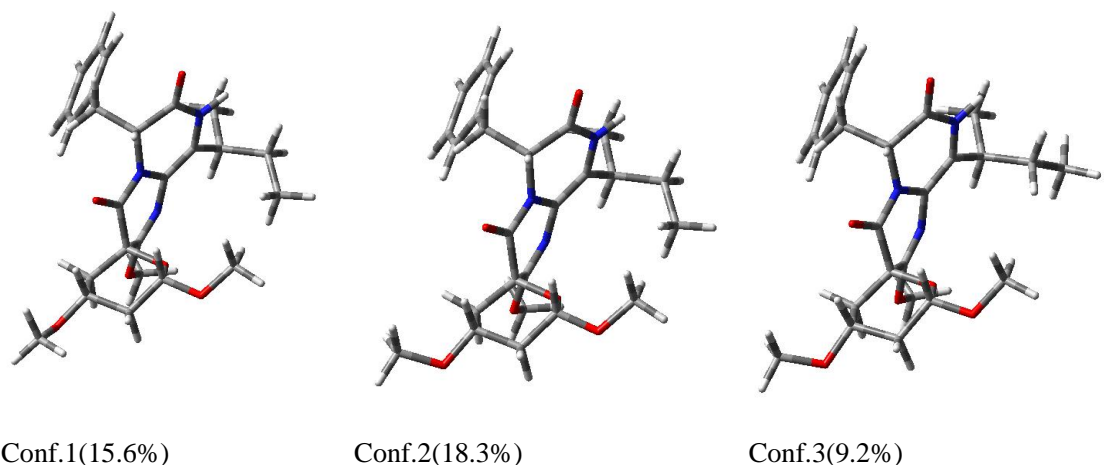
Configuration	Conformer	E (Hartree)	E (kcal/mol)	Population (%)
(8 <i>R</i> ,10 <i>S</i> ,12 <i>R</i> ,15 <i>R</i> ,16 <i>S</i>)- 3A	1	-1588.2003841	-996611.623026591	34.6
(8 <i>R</i> ,10 <i>S</i> ,12 <i>R</i> ,15 <i>R</i> ,16 <i>S</i>)- 3A	2	-1588.2005598	-996611.733280098	41.7
(8 <i>R</i> ,10 <i>S</i> ,12 <i>R</i> ,15 <i>R</i> ,16 <i>S</i>)- 3A	3	-1588.1999054	-996611.322637554	20.8
(8 <i>R</i> ,10 <i>S</i> ,12 <i>R</i> ,15 <i>R</i> ,16 <i>S</i>)- 3A	4	-1588.197125	-996609.57790875	1.1
(8 <i>R</i> ,10 <i>S</i> ,12 <i>R</i> ,15 <i>R</i> ,16 <i>S</i>)- 3A	5	-1588.1969616	-996609.475373616	0.9
(8 <i>R</i> ,10 <i>S</i> ,12 <i>R</i> ,15 <i>R</i> ,16 <i>S</i>)- 3A	6	-1588.1966972	-996609.309459972	0.7
(8 <i>R</i> ,10 <i>S</i> ,12 <i>R</i> ,15 <i>R</i> ,16 <i>S</i>)- 3A	7	-1588.1954852	-996608.548917852	0.2
(8 <i>S</i> ,10 <i>R</i> ,12 <i>R</i> ,15 <i>R</i> ,16 <i>S</i>)- 3B	1	-1588.2005552	-996611.730393552	15.6
(8 <i>S</i> ,10 <i>R</i> ,12 <i>R</i> ,15 <i>R</i> ,16 <i>S</i>)- 3B	2	-1588.2007054	-996611.824645554	18.3
(8 <i>S</i> ,10 <i>R</i> ,12 <i>R</i> ,15 <i>R</i> ,16 <i>S</i>)- 3B	3	-1588.2000544	-996611.416136544	9.2
(8 <i>S</i> ,10 <i>R</i> ,12 <i>R</i> ,15 <i>R</i> ,16 <i>S</i>)- 3B	4	-1588.1954364	-996608.518295364	0.0
(8 <i>S</i> ,10 <i>R</i> ,12 <i>R</i> ,15 <i>R</i> ,16 <i>S</i>)- 3B	5	-1588.1969032	-996609.438727032	0.3
(8 <i>S</i> ,10 <i>R</i> ,12 <i>R</i> ,15 <i>R</i> ,16 <i>S</i>)- 3B	6	-1588.2017665	-996612.490496415	56.2
(8 <i>S</i> ,10 <i>R</i> ,12 <i>R</i> ,15 <i>R</i> ,16 <i>S</i>)- 3B	7	-1588.1971196	-996609.574520196	0.4

(8*R*,10*S*,12*R*,15*R*,16*S*)-**3A**





(8*S*,10*R*,12*R*,15*R*,16*S*)-3B



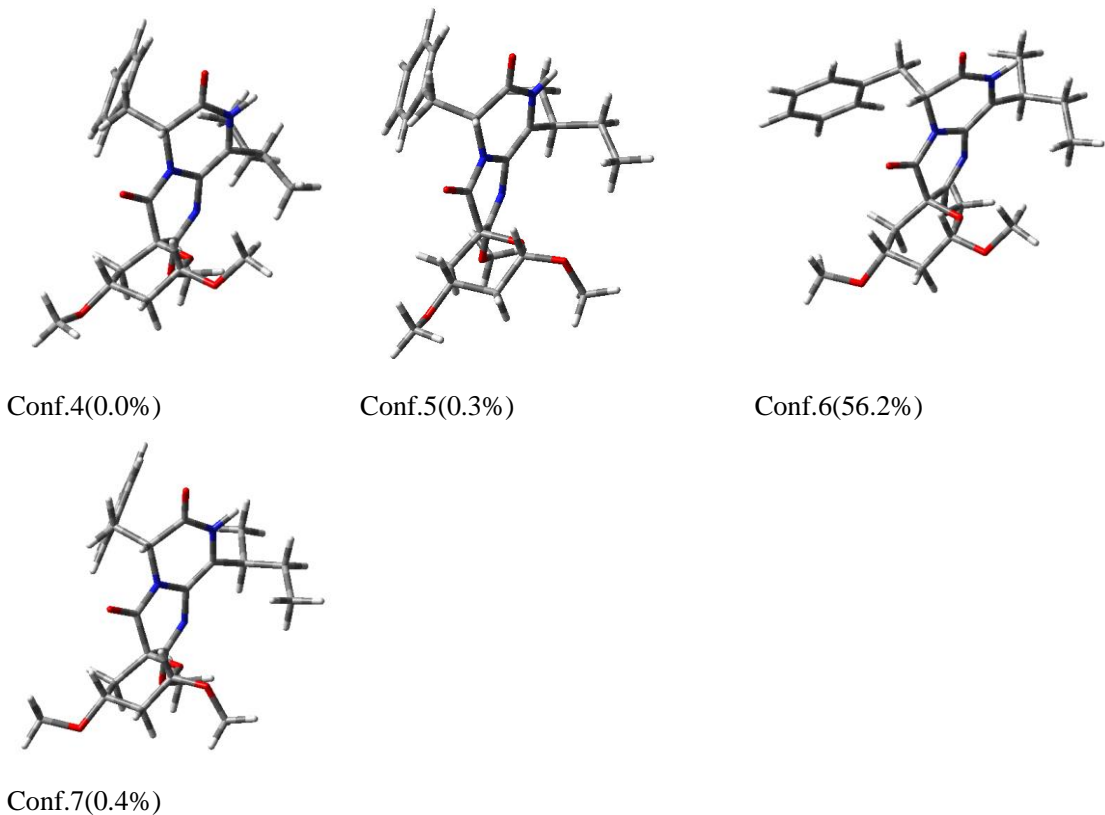


Figure S5. The optimized conformers and equilibrium populations of pyranamide C (**3**)

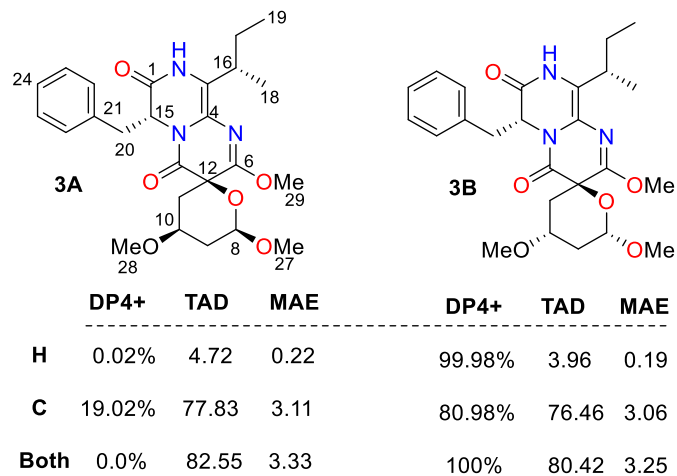


Figure S6. Total absolute deviation (TAD), mean absolute error (MAE), and DP4+ probability analyses (sarotti-nmr.weebly.com) for two candidate diastereomers of **3**.

Table S16. DP4+ analysis of calculated ¹H-NMR data of **3A** and **3B** (experimental for **3**, isomers 1–2 for **3A**–**3B**, respectively)

Functional		Solvent?	Basis Set		Type of Data		
B3LYP		PCM	6-31+G(d,p)		Unscaled Shifts		
		DP4+	0.02%	99.98%	-	-	-
Nuclei	sp2?	Experimental	Isomer 1	Isomer 2	Isomer 3	Isomer 4	Isomer 5
H		4.4	4.5	4.3			
H		2.24	2.3	2.0			
H		1.21	1.2	1.2			
H		4.06	4.3	4.3			
H		2.08	2.5	2.0			
H		1.97	2.2	1.8			
H		5.13	5.1	5.1			
H		3.08	3.0	3.3			
H		1.46	1.3	1.5			
H		0.89	0.4	0.9			
H		0.78	0.75	0.88			
H		3.16	3.45	3.21			
H		2.98	3.15	3.04			
H	x	7	7.81	7.88			
H	x	7.2	7.62	7.64			
H	x	7.2	7.57	7.58			
H	x	7.2	7.46	7.44			
H	x	7	7.27	7.23			
H		3.24	3.36	3.40			
H		3.38	3.56	3.42			
H		3.89	3.95	4.03			

Table S17. DP4+ analysis of calculated ^{13}C -NMR data of **3A** and **3B** (experimental for **3**, isomers 1–2 for **3A–3B**, respectively)

A	B	C	D	E	F	G	H
Functional	Solvent?	Basis Set		Type of Data			
B3LYP	PCM	6-31+G(d,p)		Unscaled Shifts			
		DP4+	19.02%	80.98%	-	-	-
Nuclei	sp2?	Experimental	Isomer 1	Isomer 2	Isomer 3	Isomer 4	Isomer 5
C	x	168.4	163.1	163.8			
C	x	121.9	120.4	121.1			
C	x	119.7	117.8	119.2			
C	x	160.8	157.9	156.7			
C		101.6	103.1	102.2			
C		38	40.3	41.0			
C		74.4	77.2	76.9			
C		32.1	35.2	34.1			
C		74	77.0	77.9			
C	x	164.5	161.8	162.9			
C		58.1	63.69	62.23			
C		33.8	36.87	37.66			
C		28.2	32.20	32.23			
C		17.7	20.47	21.84			
C		12.7	14.64	14.78			
C		37.6	40.16	40.41			
C	x	136.5	135.16	137.27			
C	x	130.9	127.81	127.71			
C	x	129.3	126.63	126.62			
C	x	128.1	124.11	124.28			
C	x	129.3	125.71	125.66			
C	x	130.9	126.45	127.13			
C		56.9	58.22	58.22			
C		56.1	57.18	57.09			
C		54.7	55.01	56.52			

Table S18. Calculated (calc.) and experimental (exp.) ^1H NMR chemical shift values of **3A** and **3B** at the B3LYP/6-31+G(d, p) level in methanol and total absolute deviation (TAD^a) and mean absolute error (MAE).

^1H	exp.	calc. 3A	$ \text{calc.3A}-\text{exp.} $	calc. 3B	$ \text{calc.3B}-\text{exp.} $
H-8	4.4	4.49	0.09	4.33	0.07
H-9a	2.24	2.25	0.01	1.96	0.28
H-9b	1.21	1.16	0.05	1.15	0.06
H-10	4.06	4.25	0.19	4.26	0.20
H-11a	2.08	2.52	0.44	2.03	0.05
H-11b	1.97	2.17	0.20	1.75	0.22
H-15	5.13	5.11	0.02	5.11	0.02
H-16	3.08	2.99	0.09	3.34	0.26
H-17	1.46	1.32	0.14	1.51	0.05
H-18	0.89	0.38	0.51	0.86	0.03
H-19	0.78	0.75	0.03	0.88	0.10
H-20a	3.16	3.45	0.29	3.21	0.05
H-20b	2.98	3.15	0.17	3.04	0.06
H-22	7.00	7.81	0.81	7.88	0.88
H-23	7.20	7.62	0.42	7.64	0.44
H-24	7.20	7.57	0.37	7.58	0.38
H-25	7.20	7.46	0.26	7.44	0.24
H-26	7.00	7.27	0.27	7.23	0.23
H-27	3.24	3.36	0.12	3.40	0.16
H-28	3.38	3.56	0.18	3.42	0.04
H-29	3.89	3.95	0.06	4.03	0.14
	TADc		4.72		3.96
	MAE		0.22		0.19

^aTAD = $\Sigma |\text{calc.} - \text{exp.}|$

Table S19. Calculated (calc.) and experimental (exp.) ^{13}C NMR chemical shift values of **3A** and

3B at the B3LYP/6-31+G(d, p) level in methanol and total absolute deviation (TAD^a) and mean absolute error (MAE).

¹³ C	exp.	calc. 3A	calc. 3A -exp.	calc. 3B	calc. 3B -exp.
C-1	168.5	163.07	5.43	163.75	4.75
C-3	121.9	120.37	1.53	121.14	0.76
C-4	120.0	117.78	2.22	119.23	0.77
C-6	162.8	157.85	4.95	156.73	6.07
C-8	102.7	103.13	0.43	102.22	0.48
C-9	36.5	40.32	3.82	40.98	4.48
C-10	70.6	77.18	6.58	76.86	6.26
C-11	31.8	35.2	3.4	34.12	2.32
C-12	73.1	77.04	3.94	77.90	4.8
C-13	165.1	161.84	3.26	162.88	2.22
C-15	58.2	63.69	5.49	62.23	4.03
C-16	34.0	36.87	2.87	37.66	3.66
C-17	27.8	32.2	4.4	32.23	4.43
C-18	17.6	20.47	2.87	21.84	4.24
C-19	12.8	14.64	1.84	14.78	1.98
C-20	37.6	40.16	2.56	40.41	2.81
C-21	136.5	135.16	1.34	137.27	0.77
C-22	130.9	127.81	3.09	127.71	3.19
C-23	129.3	126.63	2.67	126.62	2.68
C-24	128.1	124.11	3.99	124.28	3.82
C-25	129.3	125.71	3.59	125.66	3.64
C-26	130.9	126.45	4.45	127.13	3.77
C-27	56.5	58.22	1.72	58.22	1.72
C-28	55.8	57.18	1.38	57.09	1.29
C-29	55.0	55.01	0.01	56.52	1.52
	TADc		77.83		76.46

MAE	3.11	3.06
-----	------	------

^aTAD = $\Sigma | \text{calc.} - \text{exp.} |$

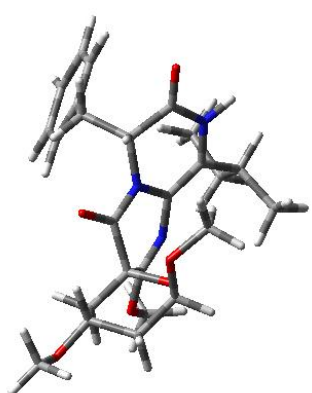
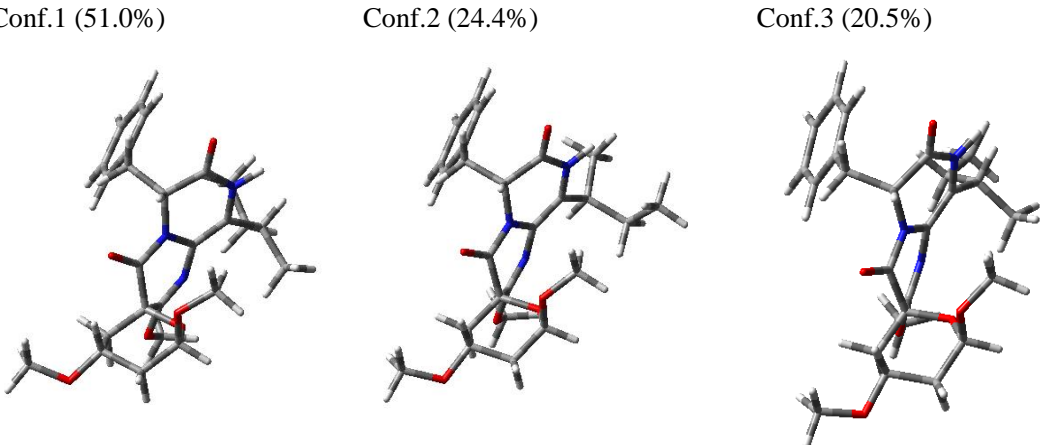
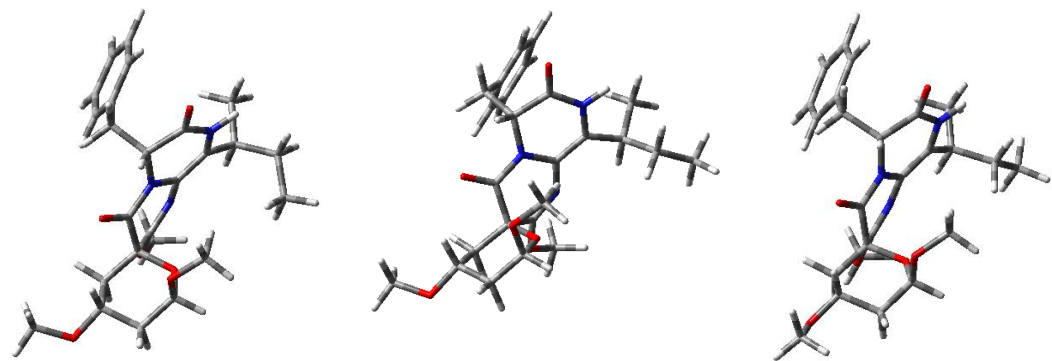
Table S20. Energies of **4** at MMFF94 force field.

Configuration	Conformer	Energy (kJ/mol)	Population (%)
(8R,10R,12R,15R,16S)- 4A	1	208.80	73.5
(8R,10R,12R,15R,16S)- 4A	2	213.74	10.0
(8R,10R,12R,15R,16S)- 4A	3	214.55	7.2
(8R,10R,12R,15R,16S)- 4A	4	218.66	1.4
(8R,10R,12R,15R,16S)- 4A	5	218.87	1.3
(8R,10R,12R,15R,16S)- 4A	6	219.23	1.1
(8R,10R,12R,15R,16S)- 4A	7	219.47	1.0
(8S,10S,12R,15R,16S)- 4B	1	211.39	72.8
(8S,10S,12R,15R,16S)- 4B	2	215.32	14.9
(8S,10S,12R,15R,16S)- 4B	3	220.02	2.2
(8S,10S,12R,15R,16S)- 4B	4	220.74	1.7
(8S,10S,12R,15R,16S)- 4B	5	220.77	1.7
(8S,10S,12R,15R,16S)- 4B	6	220.87	1.6
(8S,10S,12R,15R,16S)- 4B	7	221.54	1.2
(8S,10S,12R,15R,16S)- 4B	8	221.68	1.1

Table S21. Energies of **4** at B3LYP/6–31+G(d) level in methanol.

Configuration	Conformer	E (Hartree)	E (kcal/mol)	Population (%)
(8R,10R,12R,15R,16S)- 4A	1	-1588.1994241	-996611.020616991	51.0
(8R,10R,12R,15R,16S)- 4A	2	-1588.1987302	-996610.585187802	24.4
(8R,10R,12R,15R,16S)- 4A	3	-1588.1985668	-996610.482652668	20.5
(8R,10R,12R,15R,16S)- 4A	4	-1588.1940773	-996607.665446523	0.2
(8R,10R,12R,15R,16S)- 4A	5	-1588.1967598	-996609.348742098	3.0
(8R,10R,12R,15R,16S)- 4A	6	-1588.1953809	-996608.483468559	0.7
(8R,10R,12R,15R,16S)- 4A	7	-1588.1939739	-996607.600561989	0.2
(8S,10S,12R,15R,16S)- 4B	1	-1588.1996087	-996611.136455337	52.2
(8S,10S,12R,15R,16S)- 4B	2	-1588.1993118	-996610.950147618	38.1
(8S,10S,12R,15R,16S)- 4B	3	-1588.1944421	-996607.894362171	0.2
(8S,10S,12R,15R,16S)- 4B	4	-1588.195544	-996608.58581544	0.7
(8S,10S,12R,15R,16S)- 4B	5	-1588.1943492	-996607.836066492	0.2
(8S,10S,12R,15R,16S)- 4B	6	-1588.1972643	-996609.665320893	4.3
(8S,10S,12R,15R,16S)- 4B	7	-1588.1952788	-996608.419399788	0.5
(8S,10S,12R,15R,16S)- 4B	8	-1588.1971322	-996609.582426822	3.8

(8R,10R,12R,15R,16S)-**4A**



Conf.7 (0.2%)

(8*S*,10*S*,12*R*,15*R*,16*S*)-**4B**

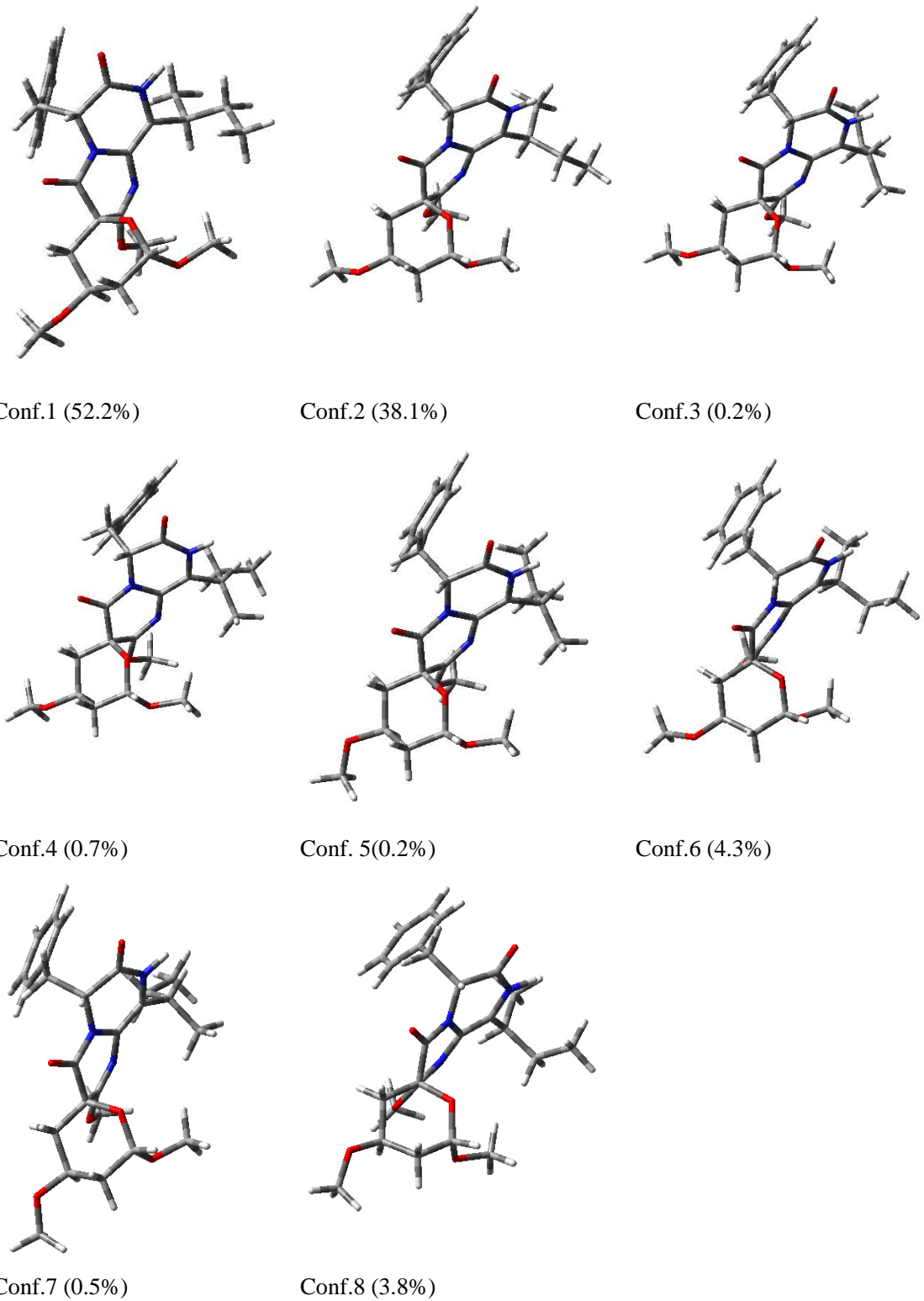


Figure S7. The optimized conformers and equilibrium populations of pyranamide D (**4**)

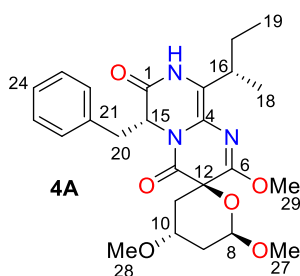
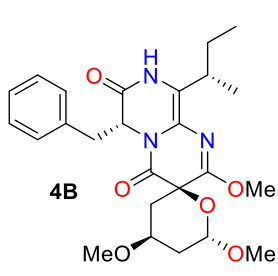
 4A	 4B
DP4+	DP4+
TAD	TAD
MAE	MAE
H	99.69%
C	85.04%
Both	99.94%
0.31%	4.59
14.96%	65.48
0.06%	70.07
4.80	2.63
2.63	2.87
0.24	0.23
2.87	2.85

Figure S8. Total absolute deviation (TAD), mean absolute error (MAE), and DP4+ probability analyses (sarotti-nmr.weebly.com) for two candidate diastereomers of **4**.

Table S22. DP4+ analysis of calculated ^1H -NMR data of **4A** and **4B** (experimental for **4**, isomers 1–2 for **4A**–**4B**, respectively)

Functional		Solvent?		Basis Set		Type of Data	
B3LYP		PCM		6-31+G(d,p)		Unscaled Shifts	
Nuclei	sp2?	Experimental	DP4+	0.31%	99.69%	–	–
H		4.8		4.8	4.9		
H		2.11		2.0	1.9		
H		1.41		1.5	1.6		
H		4.22		4.5	4.3		
H		2.08		2.2	2.4		
H		5.05		5.0	5.0		
H		3.05		2.9	3.0		
H		1.45		1.4	1.4		
H		0.88		0.4	0.4		
H		0.82		0.8	0.8		
H		3.13		3.49	3.38		
H		2.9		3.16	3.17		
H	x	6.98		7.81	7.62		
H	x	7.19		7.63	7.56		
H	x	7.19		7.59	7.56		
H	x	7.19		7.46	7.56		
H	x	6.98		7.29	7.26		
H		3.17		3.35	3.31		
H		3.37		3.60	3.60		
H		3.87		3.91	3.95		

Table S23. DP4+ analysis of calculated ^{13}C -NMR data of **4A** and **4B** (experimental for **4**, isomers 1–2 for **4A**–**4B**, respectively)

A	B	C	D	E	F	G	H
Functional		Solvent?		Basis Set		Type of Data	
B3LYP		PCM		6-31+G(d, p)		Unscaled Shifts	
	DP4+	14.96%	85.04%	-	-	-	
Nuclei	sp2?	xperimental	Isomer 1	Isomer 2	Isomer 3	Isomer 4	Isomer 5
C	x	168.5	163.6	163.0			
C	x	121.9	121.5	121.5			
C	x	120	119.3	120.3			
C	x	162.8	157.3	160.6			
C		102.7	105.6	105.6			
C		36.5	40.3	40.2			
C		70.6	73.3	73.7			
C		31.8	34.3	34.2			
C		73.1	76.8	77.0			
C	x	165.1	165.3	162.2			
C		58.2	63.14	63.74			
C		34	37.40	36.52			
C		27.8	31.85	31.55			
C		17.6	18.49	19.57			
C		12.8	14.51	14.22			
C		37.6	40.42	40.08			
C	x	136.5	136.67	136.12			
C	x	130.9	128.07	127.93			
C	x	129.3	126.72	126.26			
C	x	128.1	124.50	124.33			
C	x	129.3	125.83	126.06			
C	x	130.9	126.83	126.85			
C		56.5	57.61	57.76			
C		55.8	56.93	57.16			
C		55	56.62	55.48			

Table S24. Calculated (calc.) and experimental (exp.) ^1H NMR chemical shift values of **4A** and **4B** at the B3LYP/6-31+G(d, p) level in methanol and total absolute deviation (TAD^a) and mean absolute error (MAE).

^1H	exp.	calc. 4A	$ \text{calc.4A}-\text{exp.} $	calc. 4B	$ \text{calc.4B}-\text{exp.} $
H-8	4.80	4.81	0.01	4.89	0.09
H-9a	2.11	1.95	0.16	1.88	0.23
H-9b	1.41	1.52	0.11	1.61	0.20
H-10	4.22	4.48	0.26	4.31	0.09
H-11	2.08	2.22	0.14	2.40	0.32
H-15	5.05	4.97	0.08	5.02	0.03
H-16	3.05	2.92	0.13	3.03	0.02
H-17	1.45	1.35	0.10	1.36	0.09
H-18	0.88	0.41	0.47	0.39	0.49
H-19	0.82	0.84	0.02	0.79	0.03
H-20a	3.13	3.49	0.36	3.38	0.25

H-20b	2.90	3.16	0.26	3.17	0.27
H-22	6.98	7.81	0.83	7.62	0.64
H-23	7.19	7.63	0.44	7.56	0.37
H-24	7.19	7.59	0.40	7.56	0.37
H-25	7.19	7.46	0.27	7.56	0.37
H-26	6.98	7.29	0.31	7.26	0.28
H-27	3.17	3.35	0.18	3.31	0.14
H-28	3.37	3.6	0.23	3.6	0.23
H-29	3.87	3.91	0.04	3.95	0.08
		TADc	4.80		4.59
		MAE	0.24		0.23

^aTAD = $\Sigma | \text{calc.} - \text{exp.} |$

Table S25. Calculated (calc.) and experimental (exp.) ¹³C NMR chemical shift values of **4A** and **4B** at the B3LYP/6-31+G(d, p) level in methanol and total absolute deviation (TAD^a) and mean absolute error (MAE).

¹³ C	exp.	calc. 4A	$ \text{calc.}\mathbf{4A}-\text{exp.} $	calc. 4B	$ \text{calc.}\mathbf{4B}-\text{exp.} $
C-1	168.5	163.56	4.94	163	5.50
C-3	121.9	121.47	0.43	121.48	0.42
C-4	120	119.32	0.68	120.26	0.26
C-6	162.8	157.33	5.47	160.62	2.18
C-8	102.7	105.62	2.92	105.58	2.88
C-9	36.5	40.3	3.80	40.21	3.71
C-10	70.6	73.31	2.71	73.68	3.08
C-11	31.8	34.26	2.46	34.16	2.36
C-12	73.1	76.83	3.73	77.01	3.91
C-13	165.1	165.31	0.21	162.15	2.95
C-15	58.2	63.14	4.94	63.74	5.54
C-16	34.0	37.4	3.40	36.52	2.52
C-17	27.8	31.85	4.05	31.55	3.75

C-18	17.6	18.49	0.89	19.57	1.97
C-19	12.8	14.51	1.71	14.22	1.42
C-20	37.6	40.42	2.82	40.08	2.48
C-21	136.5	136.67	0.17	136.12	0.38
C-22	130.9	128.07	2.83	127.93	2.97
C-23	129.3	126.72	2.58	126.26	3.04
C-24	128.1	124.50	3.6	124.33	3.77
C-25	129.3	125.83	3.47	126.06	3.24
C-26	130.9	126.83	4.07	126.85	4.05
C-27	56.5	57.61	1.11	57.76	1.26
C-28	55.8	56.93	1.13	57.16	1.36
C-29	55	56.62	1.62	55.48	0.48
	TADc	65.74		65.48	
	MAE	2.63		2.62	

^aTAD = $\Sigma | \text{calc.} - \text{exp.} |$

Table S26. Energies of **6** at MMFF94 force field.

Configuration	Conformer	Energy (kJ/mol)	Population (%)
<i>R</i> - 6	1	215.33	55.7
<i>R</i> - 6	2	216.05	41.6
<i>R</i> - 6	3	225.08	1.1
<i>S</i> - 6	1	215.33	55.7
<i>S</i> - 6	2	216.05	41.6
<i>S</i> - 6	3	225.08	1.1

Table S27. Energies of **6** at B3LYP/6-31+G (d, p) level in methanol.

Configuration	Conformer	E (Hartree)	E (kcal/mol)	Population (%)
<i>R</i> - 6	1	-1241.248617	-778895.91965367	19.49
<i>R</i> - 6	2	-1241.2490723	-778896.205358973	31.59
<i>R</i> - 6	3	-1241.249485	-778896.46433235	48.92
<i>S</i> - 6	1	-1241.248617	-778895.91965367	19.49
<i>S</i> - 6	2	-1241.2490723	-778896.205358973	31.59
<i>S</i> - 6	3	-1241.249485	-778896.46433235	48.92

R-**6**

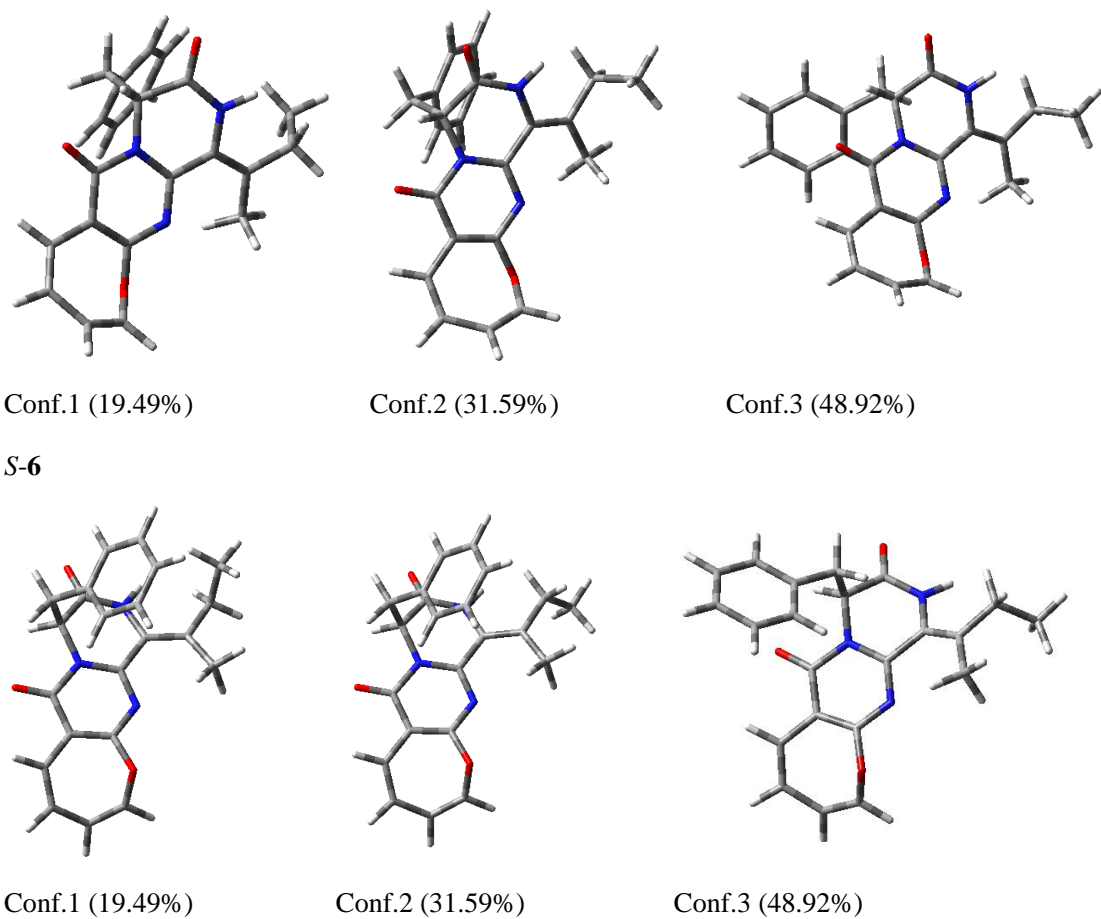


Figure S9. The optimized conformers and equilibrium populations of protuboxepin F (**6**)

Table S28. Energies of **8** at MMFF94 force field.

Configuration	Conformer	Energy (kJ/mol)	Population (%)
<i>R</i> - 8	1	195.12	57.6
<i>R</i> - 8	2	195.94	41.2
<i>R</i> - 8	3	207.15	0.4
<i>S</i> - 8	1	195.12	57.6
<i>S</i> - 8	2	195.94	41.2
<i>S</i> - 8	3	207.15	0.4

Table S29. Energies of **8** at B3LYP/6-31+G (d, p) level in methanol.

Configuration	Conformer	E (Hartree)	E (kcal/mol)	Population (%)
<i>R</i> - 8	1	-1241.3125578	-778936.043145078	9.42
<i>R</i> - 8	2	-1241.3133256	-778936.524947256	21.26
<i>R</i> - 8	3	-1241.3144405	-778937.224558155	69.32
<i>S</i> - 8	1	-1241.3125578	-778936.043145078	9.43
<i>S</i> - 8	2	-1241.313326	-778936.52519826	21.29
<i>S</i> - 8	3	-1241.3144392	-778937.223742392	69.28

R-**8**

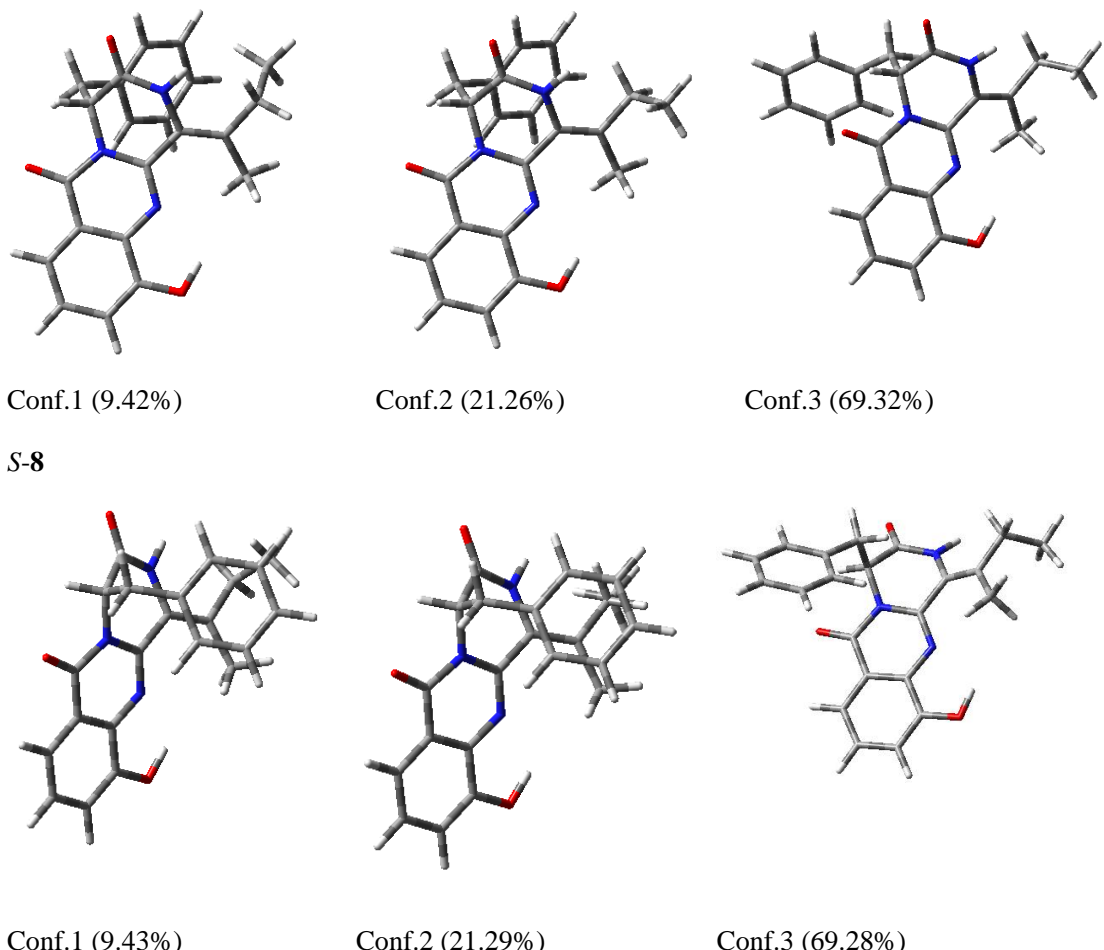


Figure S10. The optimized conformers and equilibrium populations of protuboxepin H (**8**)

Table S30. Energies of **10** at MMFF94 force field.

Configuration	Conformer	Energy (kJ/mol)	Population (%)
(3 <i>R</i> ,15 <i>R</i> ,16 <i>S</i>)- 10	1	281.92	53.0
(3 <i>R</i> ,15 <i>R</i> ,16 <i>S</i>)- 10	2	283.95	23.4
(3 <i>R</i> ,15 <i>R</i> ,16 <i>S</i>)- 10	3	284.64	17.7
(3 <i>R</i> ,15 <i>R</i> ,16 <i>S</i>)- 10	4	290.18	1.9
(3 <i>R</i> ,15 <i>R</i> ,16 <i>S</i>)- 10	5	291.27	1.2

Table S31. Energies of **10** at B3LYP/6–31+G (d, p) level in methanol.

Configuration	Conformer	E (Hartree)	E (kcal/mol)	Population (%)
(3 <i>R</i> ,15 <i>R</i> ,16 <i>S</i>)- 10	1	-1281.8330663	-804363.067433913	75.66
(3 <i>R</i> ,15 <i>R</i> ,16 <i>S</i>)- 10	2	-1281.8318655	-804362.313919905	21.18
(3 <i>R</i> ,15 <i>R</i> ,16 <i>S</i>)- 10	3	-1281.8291123	-804360.586259373	1.14
(3 <i>R</i> ,15 <i>R</i> ,16 <i>S</i>)- 10	4	-1281.8288158	-804360.400202658	0.84
(3 <i>R</i> ,15 <i>R</i> ,16 <i>S</i>)- 10	5	-1281.8291423	-804360.605084673	1.18

(3*R*,15*R*,16*S*)-**10**

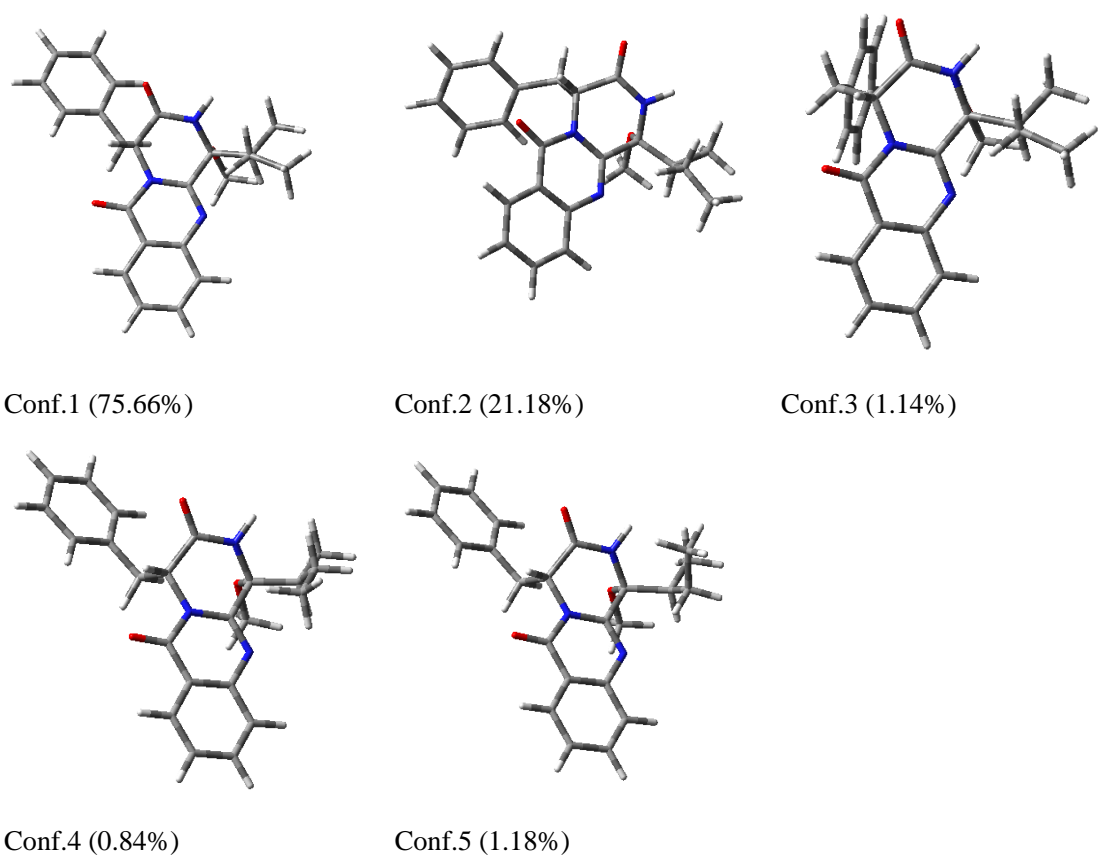


Figure S11. The optimized conformers and equilibrium populations of protuboxepin J (**10**)

3. Other Experimental Data

Table S32. ^1H and ^{13}C NMR Spectroscopic Data of **1–5** in CD_3OD (δ ppm)

no.	1		2		3		4		5	
	$\delta_{\text{C}}^{\text{a}}$	$\delta_{\text{H}}^{\text{b}}$ (J , Hz)	$\delta_{\text{C}}^{\text{a}}$	$\delta_{\text{H}}^{\text{b}}$ (J , Hz)	$\delta_{\text{C}}^{\text{a}}$	$\delta_{\text{H}}^{\text{b}}$ (J , Hz)	$\delta_{\text{C}}^{\text{c}}$	$\delta_{\text{H}}^{\text{d}}$ (J , Hz)	$\delta_{\text{C}}^{\text{a}}$	$\delta_{\text{H}}^{\text{b}}$ (J , Hz)
1	168.3		168.4		168.4		168.5		167.9	
3	115.3		115.8		121.9		121.9		120.4	
4	113.7		113.8		119.7		120.0		119.4	
6	166.4		166.9		160.8		162.8		159.8	
8	98.2	4.83, m	103.4	4.81, d (4.2)	101.6	4.40, dd (2.1, 9.8)	102.7	4.80, d (4.5)	103.7	4.50, d (5.6),
9 α	123.7	5.61, m	36.8	2.10, m,	38.0	1.21, m	36.5	2.11, m	38.2	1.92, m
9 β				1.42, m,		2.24, m		1.41, m		1.71, m
10	127.7	6.09, m	70.2	4.23, m,	74.4	4.06, m	70.6	4.22, m	75.3	3.47, m
11 α	23.8	2.87, m	31.4	2.26,dd (4.9, 13.3)	32.1	2.08, m	31.8	2.08, m	41.1	2.71, dd (8.9, 13.8)
11 β		2.32, m		1.87,dd (11.2,12.6)		1.97, m				2.13, dd (4.6, 13.8)
12	74.7		77.4		74.0		73.1		70.5	
13	167.0		168.0		164.5		165.1		167.3	
15	58.0	4.93, t (5.6)	58.0	4.94, t (5.6)	58.1	5.13, t (5.6)	58.2	5.05, t (5.6)	58.1	5.22, t (5.6)
16	33.8	2.45, m,	33.8	2.44, m	33.8	3.08, m	34.0	3.05, m	33.7	3.15, m
17	27.9	1.42, m	27.9	1.43, m	28.2	1.46, m	27.8	1.45, m	28.1	1.45, m
18	17.6	0.77, d (7.0)	17.8	0.78, d (7.0)	17.7	0.89, d (7.0)	17.6	0.88, d (7.0)	17.9	0.85, d (7.07)
19	12.5	0.89, t (7.0),	12.3	0.87, t (7.0)	12.7	0.78, t (7.0)	12.8	0.82, t (7.0)	12.6	0.83, t (7.42)
20 α	37.7	3.13, dd (5.6, 14.0)	37.6	3.12, dd (5.6, 14.0)	37.6	3.16, dd (5.6, 14.0)	37.6	3.13, dd (5.6, 14.0)	38.6	3.13, dd (4.34, 13.65)
20 β		3.05, dd (5.6, 14.0)		3.06, dd (5.6, 14.0)		2.98, dd (5.6, 14.0)		2.95, dd (5.6, 14.0)		3.01, dd (7.35, 13.65)
21	136.7		136.6		136.5		136.5		137.1	

22	130.7	7.06, o	130.7	7.07, o	130.9	7.00, o	130.9	6.98, o	130.9	7.21, o
23	129.5	7.22, o	129.5	7.23, o	129.3	7.20, o	129.3	7.19, o	129.3	7.21, o
24	128.2	7.21, o	128.2	7.21, o	128.1	7.20, o	128.1	7.19, o	128.0	7.21, o
25	129.5	7.22, o	129.5	7.23, o	129.3	7.20, o	129.3	7.19, o	129.3	7.21, o
26	130.7	7.06, o	130.7	7.07, o	130.9	7.00, o	130.9	6.98, o	130.9	7.21, o
27	56.3	3.32, s	56.4	3.23, s	56.9	3.24, s	56.5	3.17, s	53.9	3.34, s
28			55.9	3.38, s	56.1	3.38, s	55.8	3.37, s	55.8	3.20, s
29					54.7	3.89, s	55.0	3.87, s	54.2	3.85, s
30									53.7	3.36, s

^aIn 175 MHz, ^bIn 700 MHz, ^cIn 125 MHz, ^dIn 125 MHz. O: overlapped

Table S33. ¹H (700 MHz) and ¹³C (175 MHz) NMR Spectroscopic Data of **6–10** in DMSO-*d*₆ (δ ppm)

no.	6		7		8		9		10	
	δ _C	δ _H (<i>J</i> , Hz)	δ _C	δ _H (<i>J</i> , Hz)	δ _C	δ _H (<i>J</i> , Hz)	δ _C	δ _H (<i>J</i> , Hz)	δ _C	δ _H (<i>J</i> , Hz)
1	165.1		164.9		165.8		165.7		168.2	
3	119.7		120.2		120.3		121.0		88.8	
4	151.2		150.7		144.8		144.1		147.9	
6	161.5		161.7		136.1		136.4		145.7	
8	143.3	6.18, d (5.6)	143.4	6.17, d (5.6)	152.9		153.4		127.7	7.75, d (7.7)
9	117.3	5.77, t (5.6)	117.3	5.76, t (5.6)	118.7	7.25, d (7.7)	118.7	7.23, d (7.7)	134.9	7.90, m
10	127.7	6.20, t (5.6)	127.3	6.20, t (5.6)	127.5	7.34, t (7.7)	127.4	7.33, m	127.7	7.63, m
11	125.5	6.67, d (11.2)	125.5	6.67, d (11.2)	116.0	7.56, d (7.7)	115.6	7.54, o	126.7	8.19, d (7.7)
12	108.9		108.9		120.4		120.4		120.3	
13	160.0		160.1		159.6		159.8		160.0	

15	56.7	5.21, dd (4.2, 6.3)	56.7	5.22, dd (4.2, 6.3)	56.5	5.35, dd (5.6, 7.0)	56.5	5.35, dd (5.6, 7.0)	56.5	5.21, dd (4.9, 8.4)
16	137.1		137.5		134.9		134.7		37.4	2.69, m
17	27.2	2.08, m/ 1.89, m	27.8	2.53, m/ 1.83, m	26.9	2.16, m/ 2.00, m	27.	2.62, m/ 2.07, m	23.9	1.32, m/ 1.19, m
18	19.2	1.83, s	19.0	1.58, s	19.1	2.01, s	18.3	1.67, s	11.0	1.04, d (7.0)
19	11.6	0.87, t (7.7)	12.4	0.91, t (7.7)	11.7	0.96, t (7.7)	12.6	1.05, t (7.0)	12.5	0.89, t (7.0)
20 α	36.2	3.13, dd (4.2, 14.0)	36.2	3.15, dd (4.2, 14.0)	36.4	3.15, dd (7.0, 14.0)	36.5	3.16, dd (7.0, 14.0)	38.3	3.37, dd (8.4, 14.0)
20 β		3.08, dd (6.3, 14.0)		3.09, dd (6.3, 14.0)		3.11, dd (5.6, 14.0)		3.13, dd (5.6, 14.0)		3.24, dd (4.9, 14.0)
21	134.6		134.5		135.1		135.0		136.8	
22	129.3	6.91, o	129.3	6.90, o	129.2	6.93, o	129.3	6.92, o	129.5	7.18, o
23	128.4	7.21, m	128.4	7.20, m	128.3	7.18, m	128.3	7.17, m	128.2	7.24, m
24	127.2	7.18, m	127.7	7.18, m	127.0	7.16, m	127.0	7.33, m	126.2	7.20, m
25	128.4	7.21, m	128.4	7.20, m	128.3	7.18, m	128.3	7.17, m	128.2	7.24, m
26	129.3	6.90, o	129.3	6.90, o	129.2	6.93, o	129.3	6.92, o	129.5	7.18, o
27									49.8	2.97, s
2-NH		9.56, s		9.85, br s		10.00, s		9.89, br s		9.02, s

O: overlapped

Table S34. ^1H (700 MHz) and ^{13}C (175 MHz) NMR Spectroscopic Data of **1** and **4** in $\text{DMSO}-d_6$ (δ ppm)

no.	1			4		
	δ_{C}	δ_{H} (J , Hz)	HMBC	δ_{C}	δ_{H} (J , Hz)	HMBC
1	165.5			165.7		
3	113.6			120.4		
4	111.7			117.5		
6	164.2			158.7		
8	95.9	4.81, m	9, 10, 12, 27	99.7	4.30, dd (2.1, 9.8)	9, 10, 12, 27
9 α	122.5	5.55, m	8, 11	36.7	2.19, m	8, 10, 11
9 β					1.05, m	8, 10, 11
10	126.5	6.03, m	8, 11, 12	72.4	3.96, m	9, 11, 28
11 α	22.5	2.70, m	6, 8, 9, 10, 12, 13	30.7	1.94, dd (10.5, 14.0)	6, 9, 12, 13
11 β		2.17, m	6, 8, 9, 10, 12, 13		1.89, dd (5.6, 14.0)	6, 9, 12, 13
12	72.8			72.1		
13	164.3			162.1		
15	55.6	4.68, t (5.6)	1, 4, 20, 21	55.9	4.91, t (5.6)	1, 4, 13, 20, 21
16	31.7	2.60, m,	3, 4, 17, 18, 19	32.0	2.99, m	3, 4, 17, 18, 19
17	26.0	1.45, m; 1.31, m	3, 16, 18, 19	27.8	1.49, m; 1.37, m	3, 16, 18, 19
18	17.2	0.76, d (7.0)	3, 16, 17	17.3	0.86, d (7.0)	3, 16, 17
19	11.9	0.77, t (7.0),	16, 17	11.9	0.66, t (7.0)	16, 17
20 α	36.0	2.96, dd (5.6, 14.0)	1, 15, 21, 22	36.0	3.02, dd (5.6, 14.0)	1, 15, 21, 22
20 β		2.87, dd (5.6, 14.0)	1, 15, 21, 22		2.86, dd (5.6, 14.0)	1, 15, 21, 22
21	135.5			135.2		
22	129.4	7.02, o	21, 20, 24	129.5	6.96, o	21, 20, 24
23	128.1	7.19, o	21, 24	128.0	7.19, o	21, 24
24	126.7	7.19, o	22, 23	126.7	7.19, o	22, 23
25	128.1	7.19, o	21, 24	128.0	7.19, o	21, 24
26	129.4	7.02, o	21, 20, 24	129.5	6.96, o	21, 20, 24
27	54.8	3.18, s	8	56.0	3.14, s	8
28				55.1	3.27, s	10
29				54.1	3.81, s	6
2-NH		9.53, s	1, 3, 15, 16		9.76, s	1, 4, 15, 16
6-OH		10.67, s	4, 12			

O: overlapped

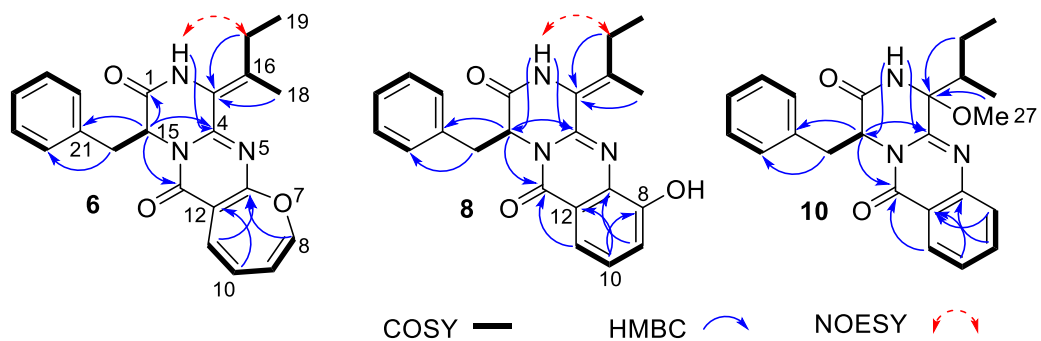


Figure S12. Key COSY, HMBC and NOESY correlations of **6**, **8** and **10**.

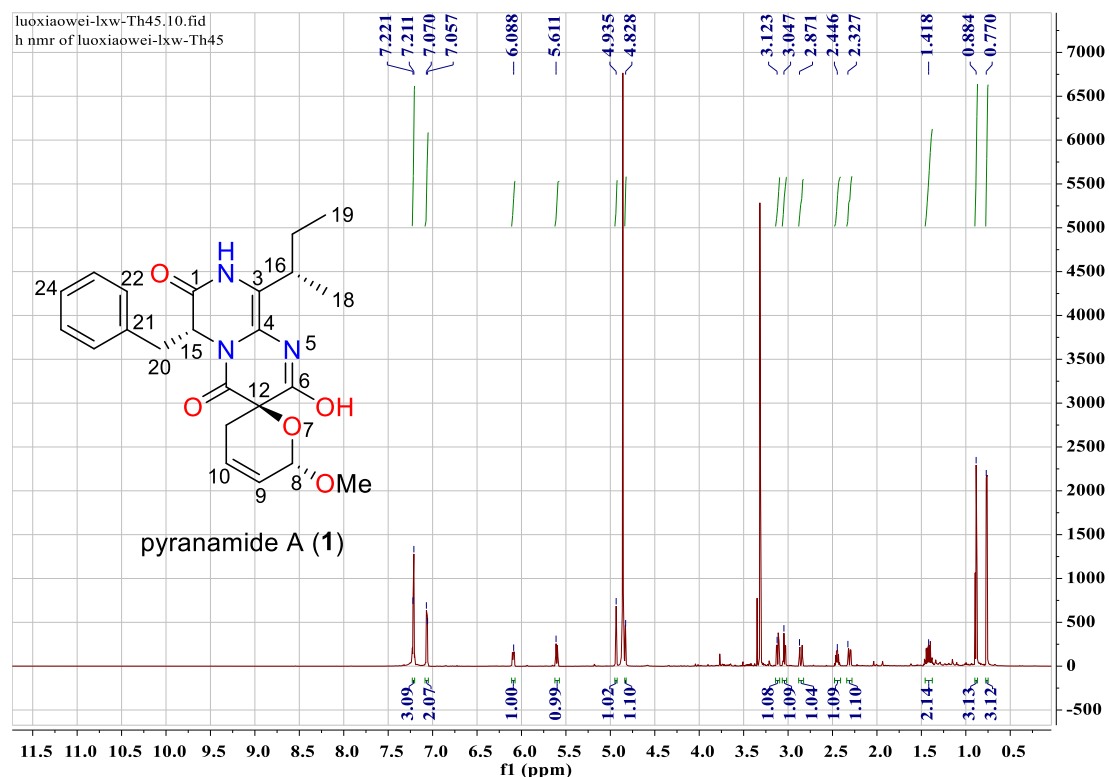


Figure S13. ¹H NMR spectrum of pyranamide A (**1**) (^{CD_3OD}, 700 MHz)

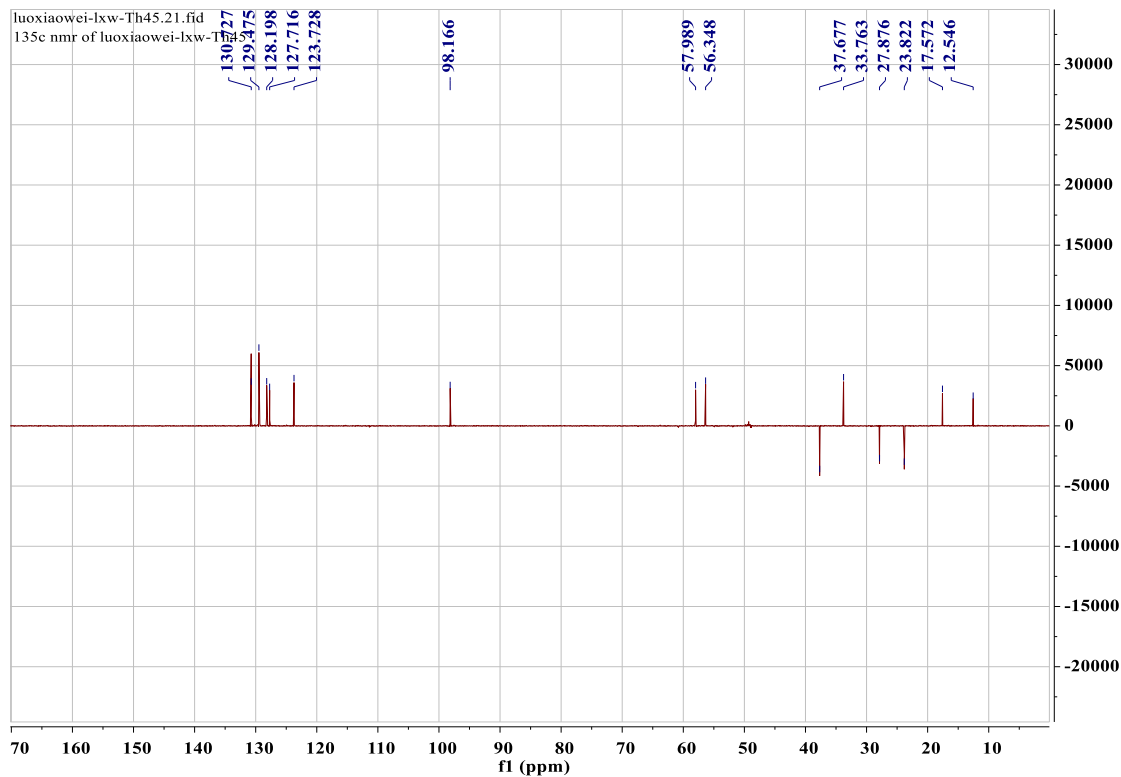
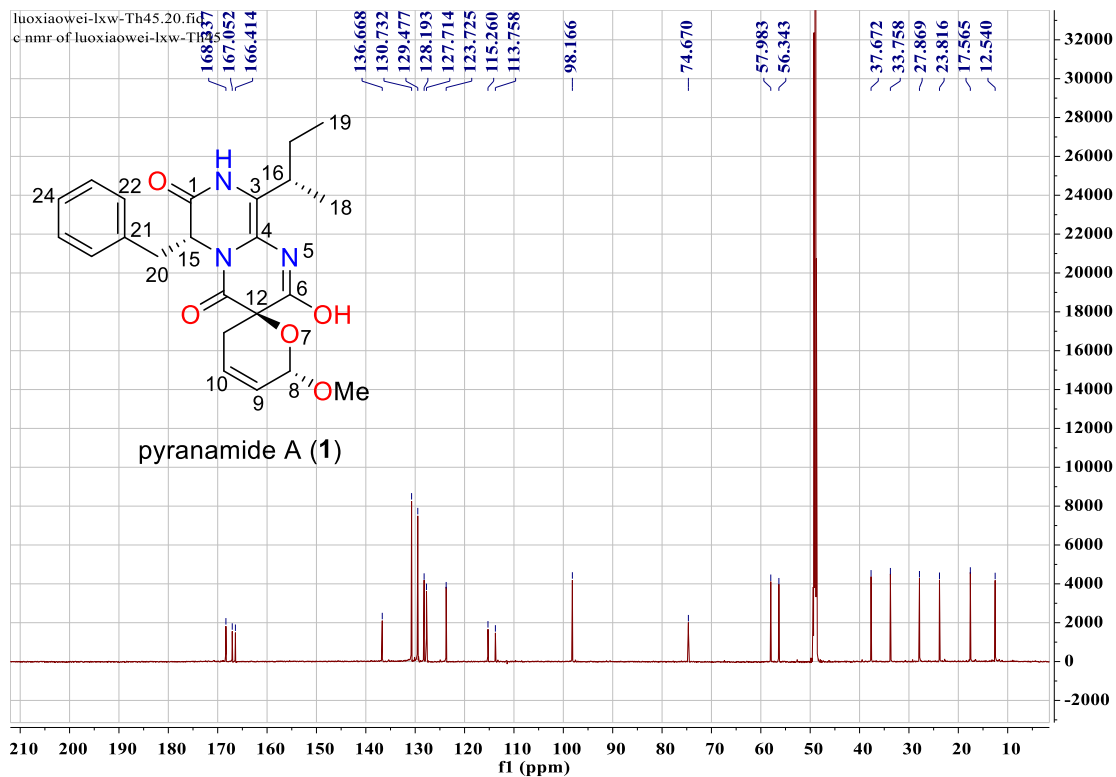


Figure S14. ^{13}C NMR and DEPT spectra of pyranamide A (**1**) (CD_3OD , 175 MHz)

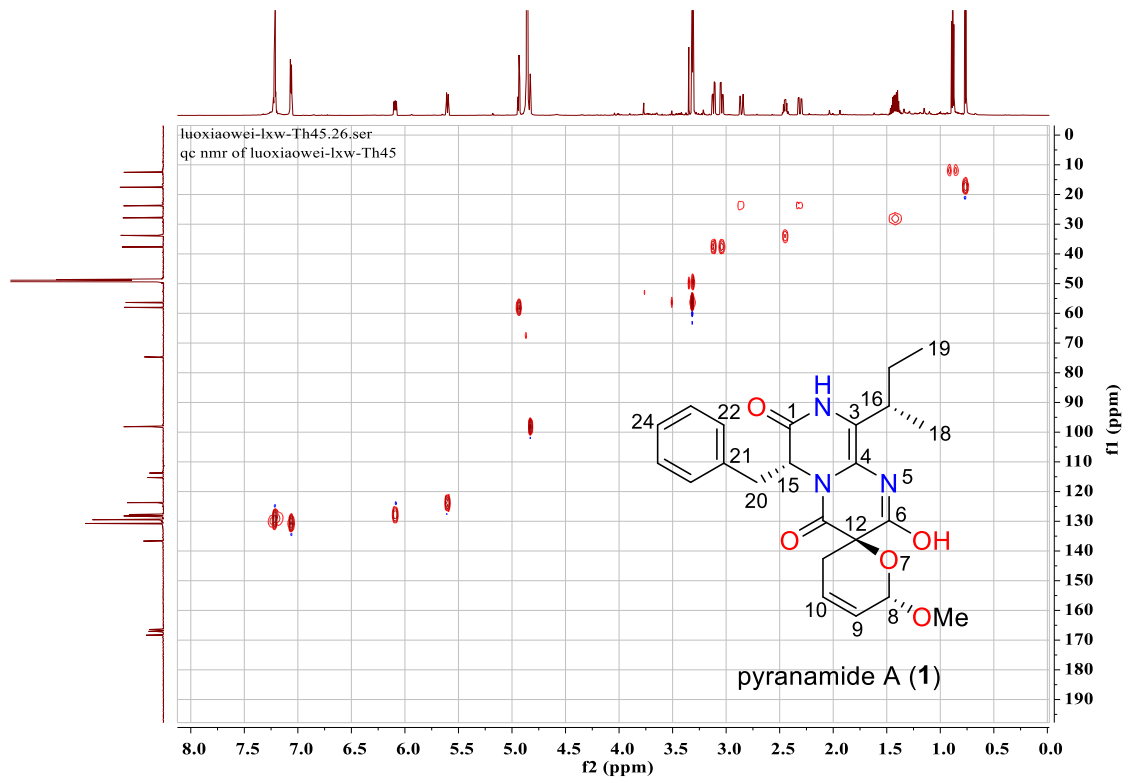


Figure S15. HSQC spectrum of pyranamide A (**1**) (CD_3OD)

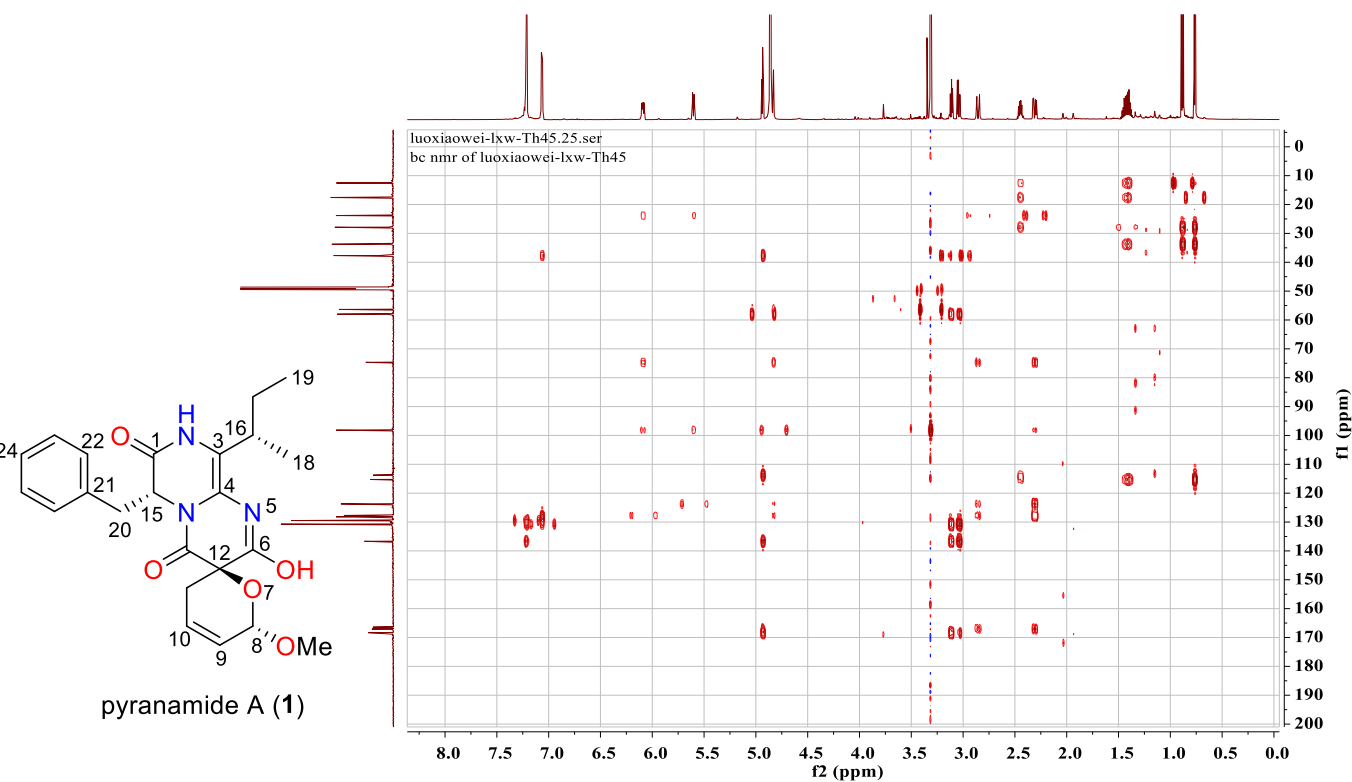


Figure S16. HMBC spectrum of pyranamide A (**1**) (CD_3OD)

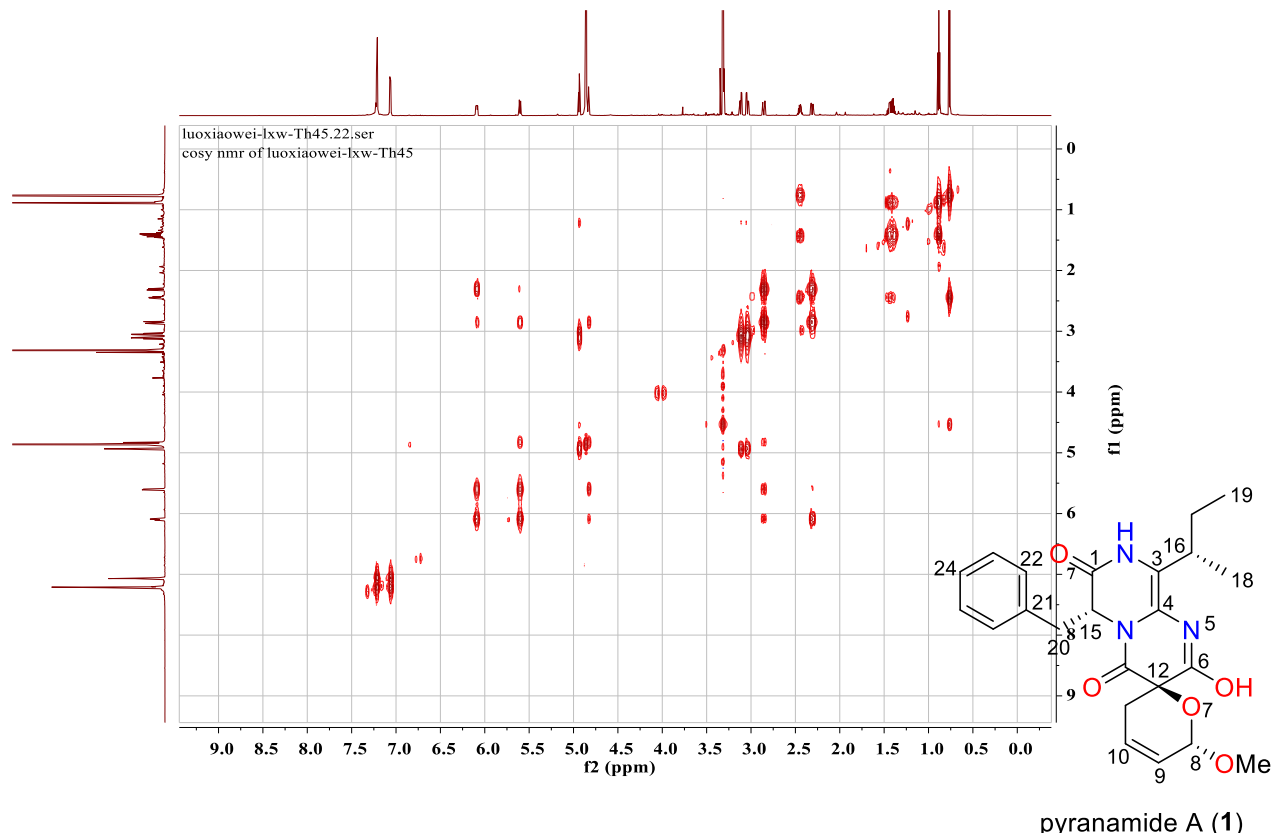


Figure S17. ^1H - ^1H COSY spectrum of pyranamide A (**1**) (CD_3OD)

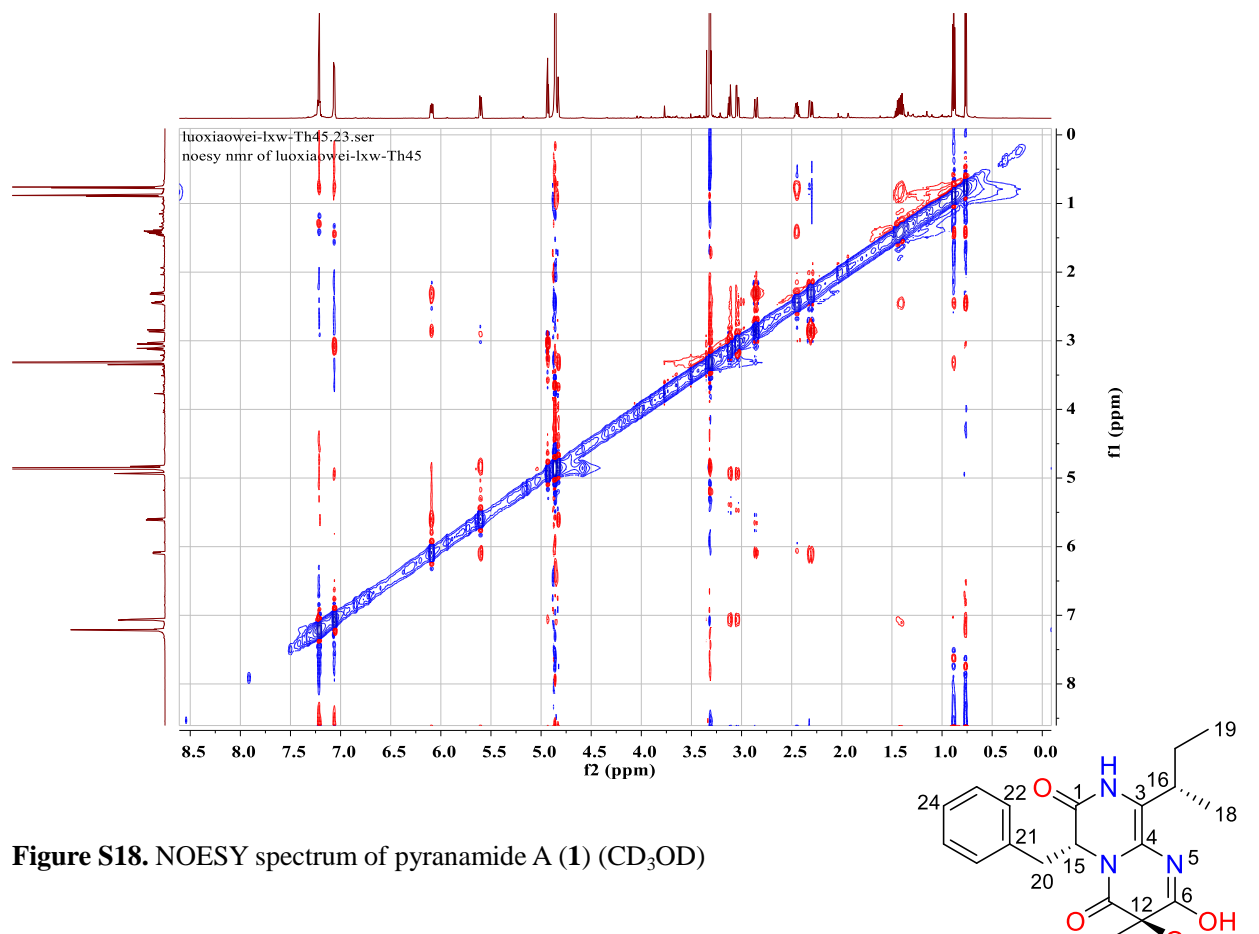


Figure S18. NOESY spectrum of pyranamide A (**1**) (CD_3OD)

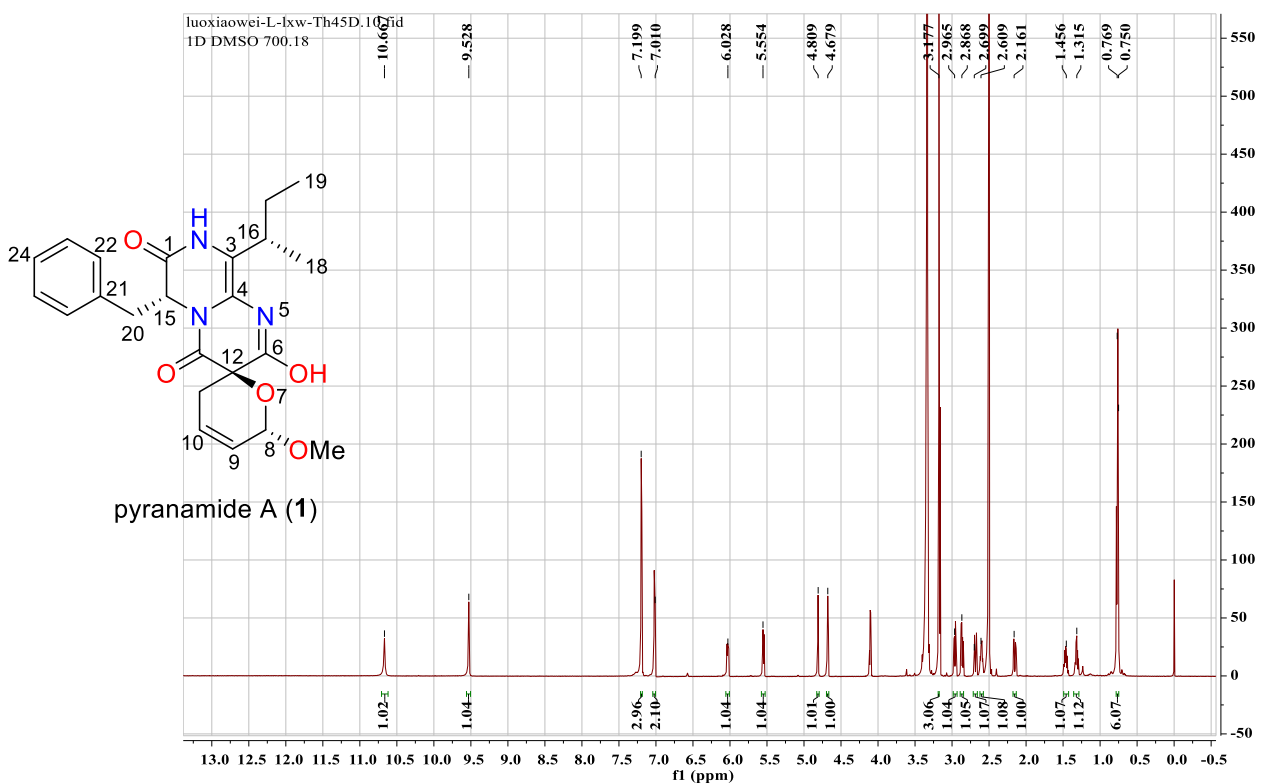
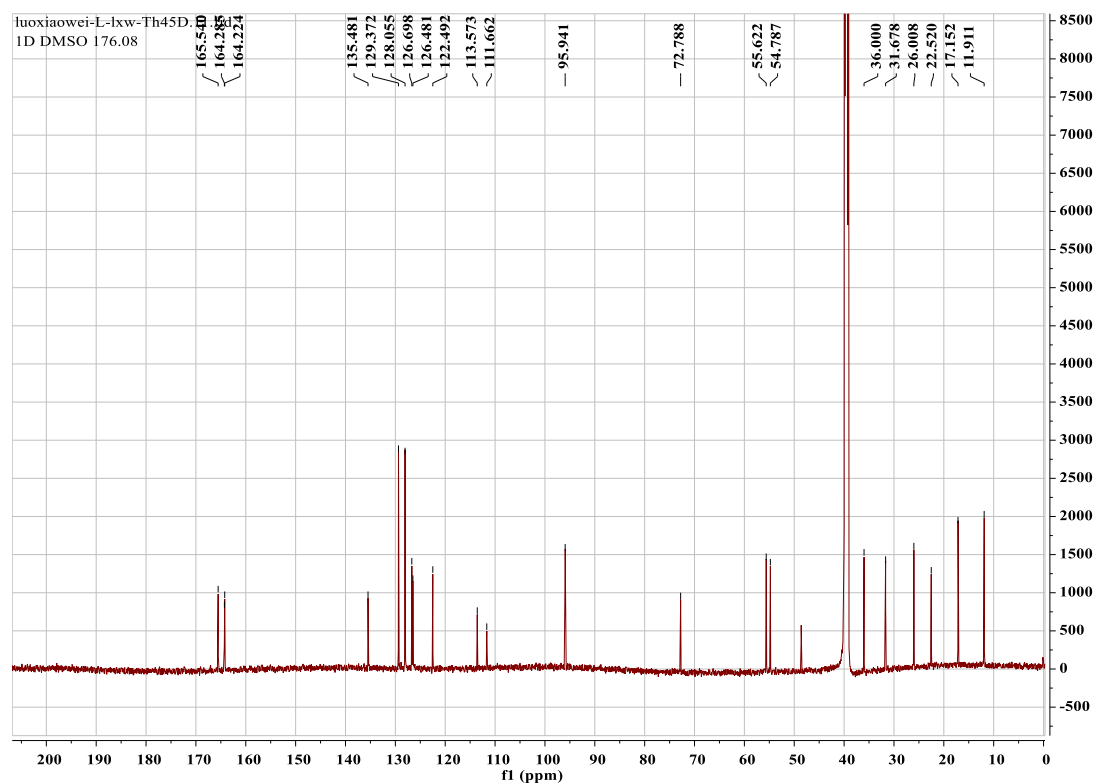


Figure S19. ^1H NMR spectrum of pyranamide A (**1**) (DMSO- d_6 , 700 MHz)



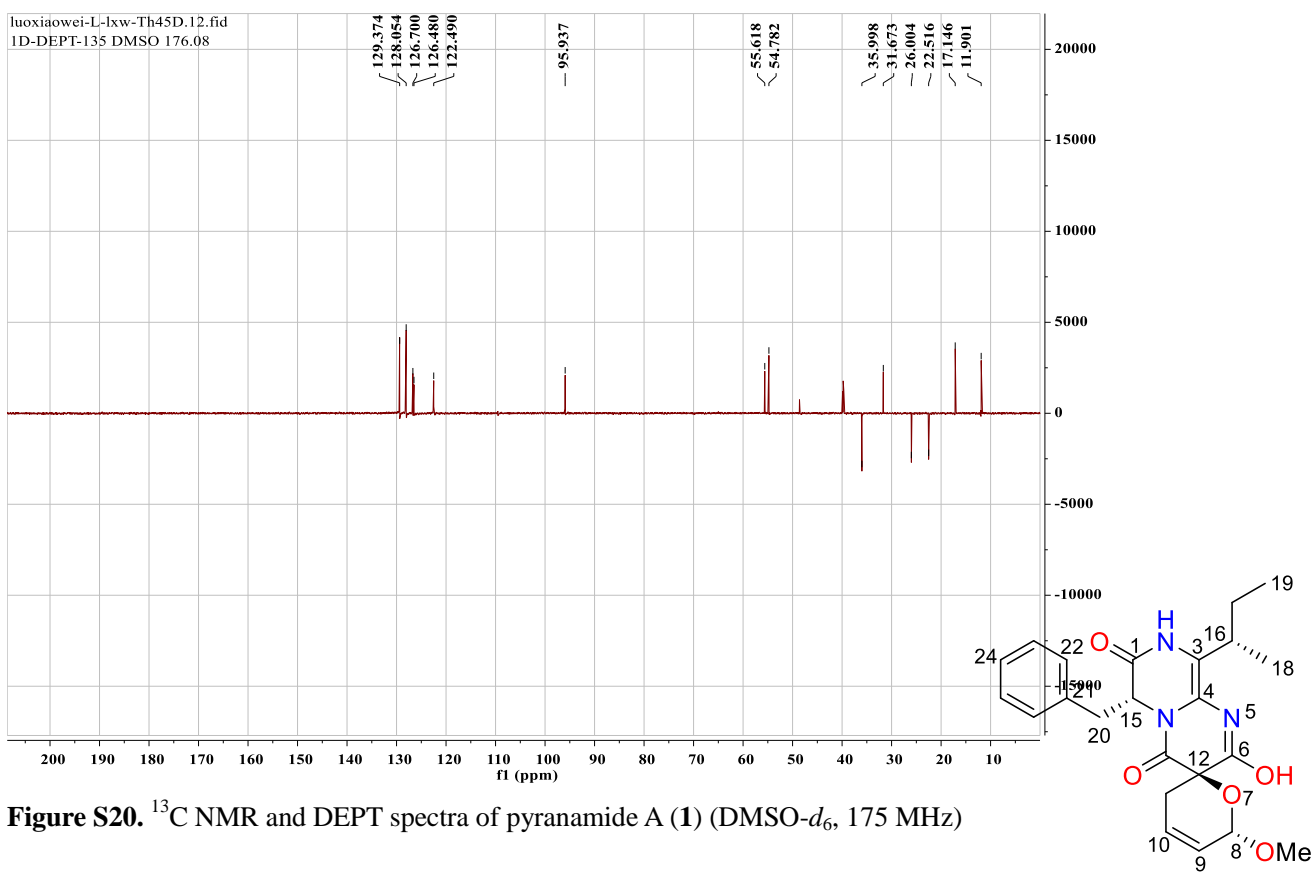


Figure S20. ^{13}C NMR and DEPT spectra of pyranamide A (**1**) (DMSO- d_6 , 175 MHz)

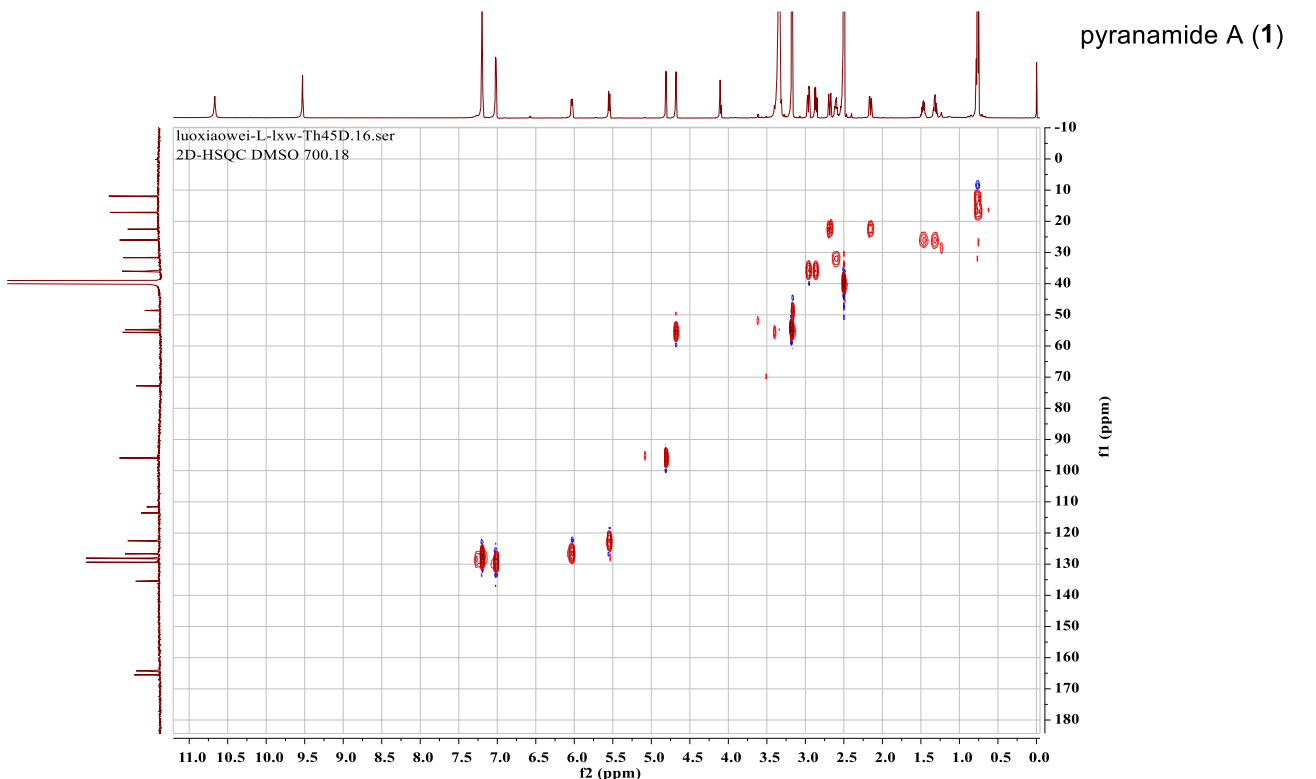


Figure S21. HSQC spectrum of pyranamide A (**1**) (DMSO- d_6)

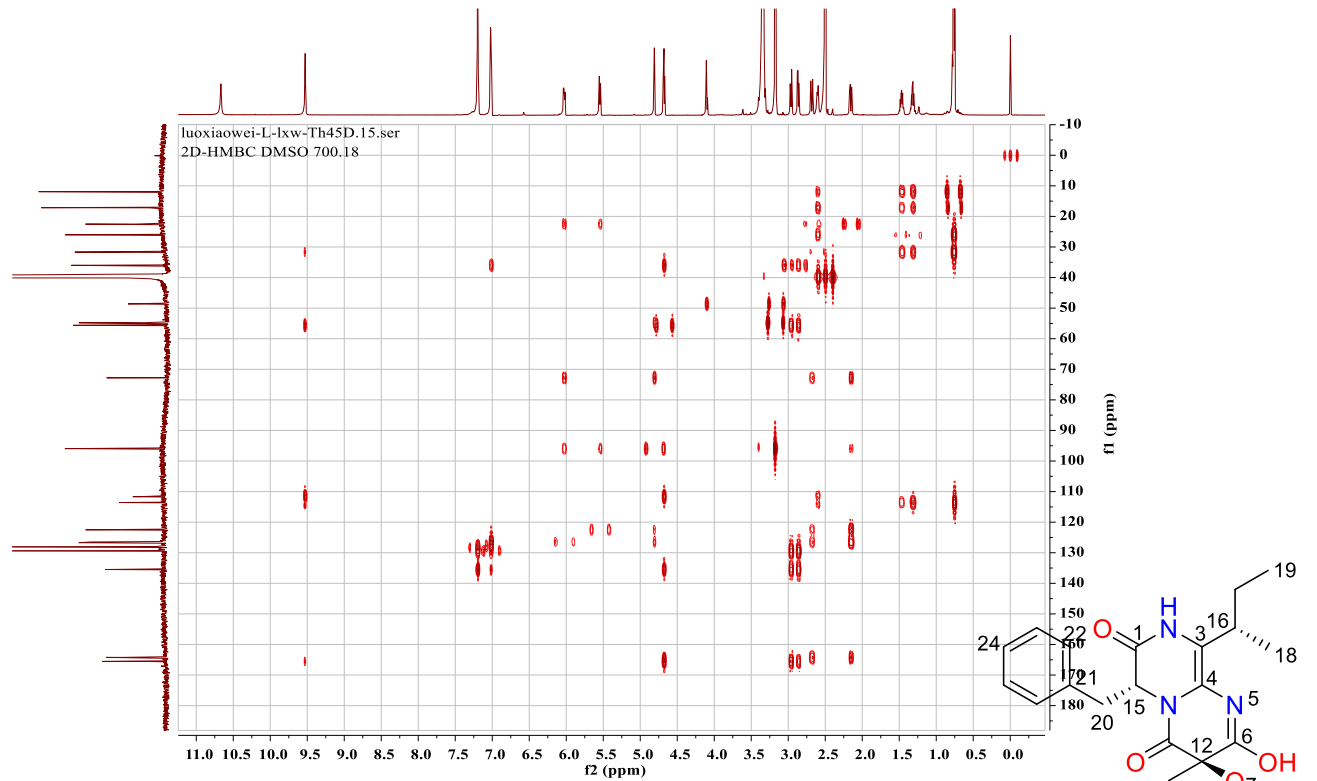


Figure S22. HMBC spectrum of pyranamide A (1) ($\text{DMSO}-d_6$)

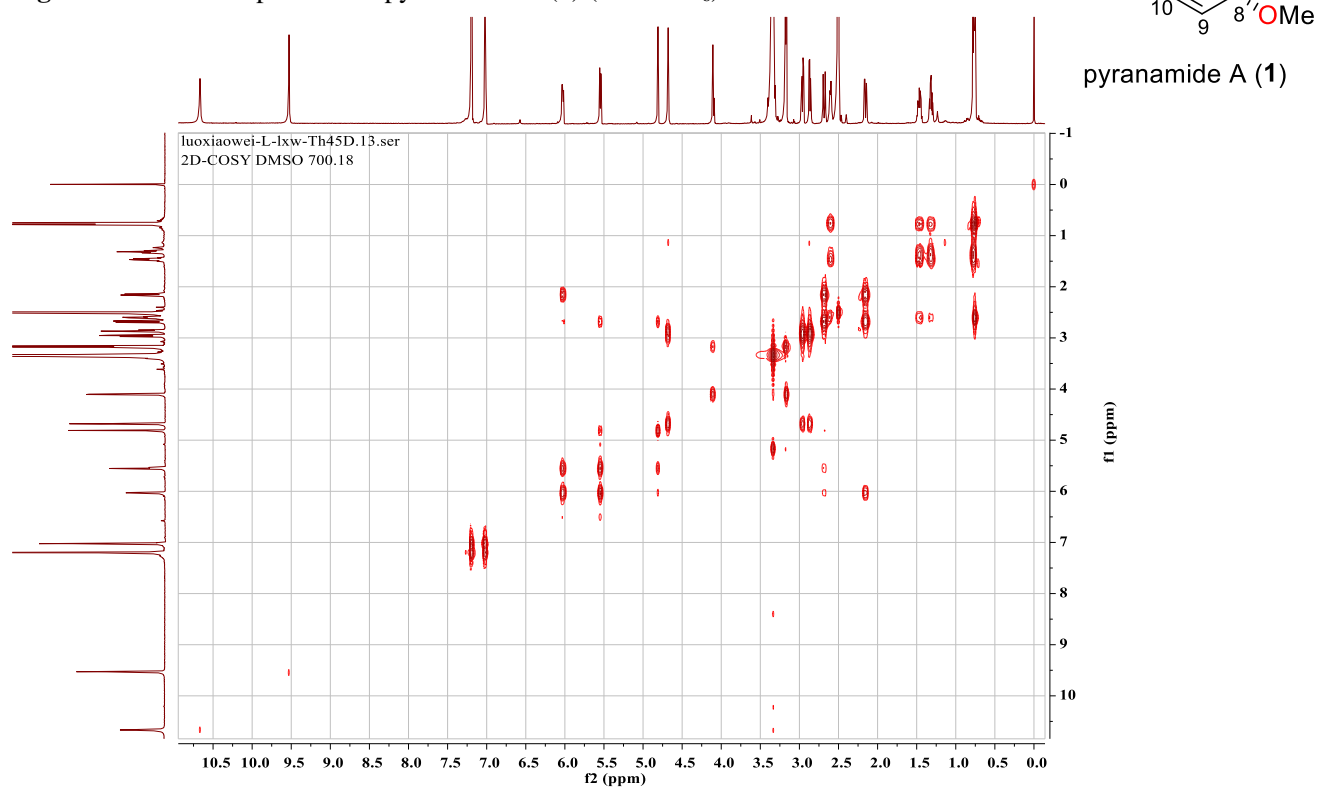


Figure S23. ^1H - ^1H COSY spectrum of pyranamide A (1) ($\text{DMSO}-d_6$)

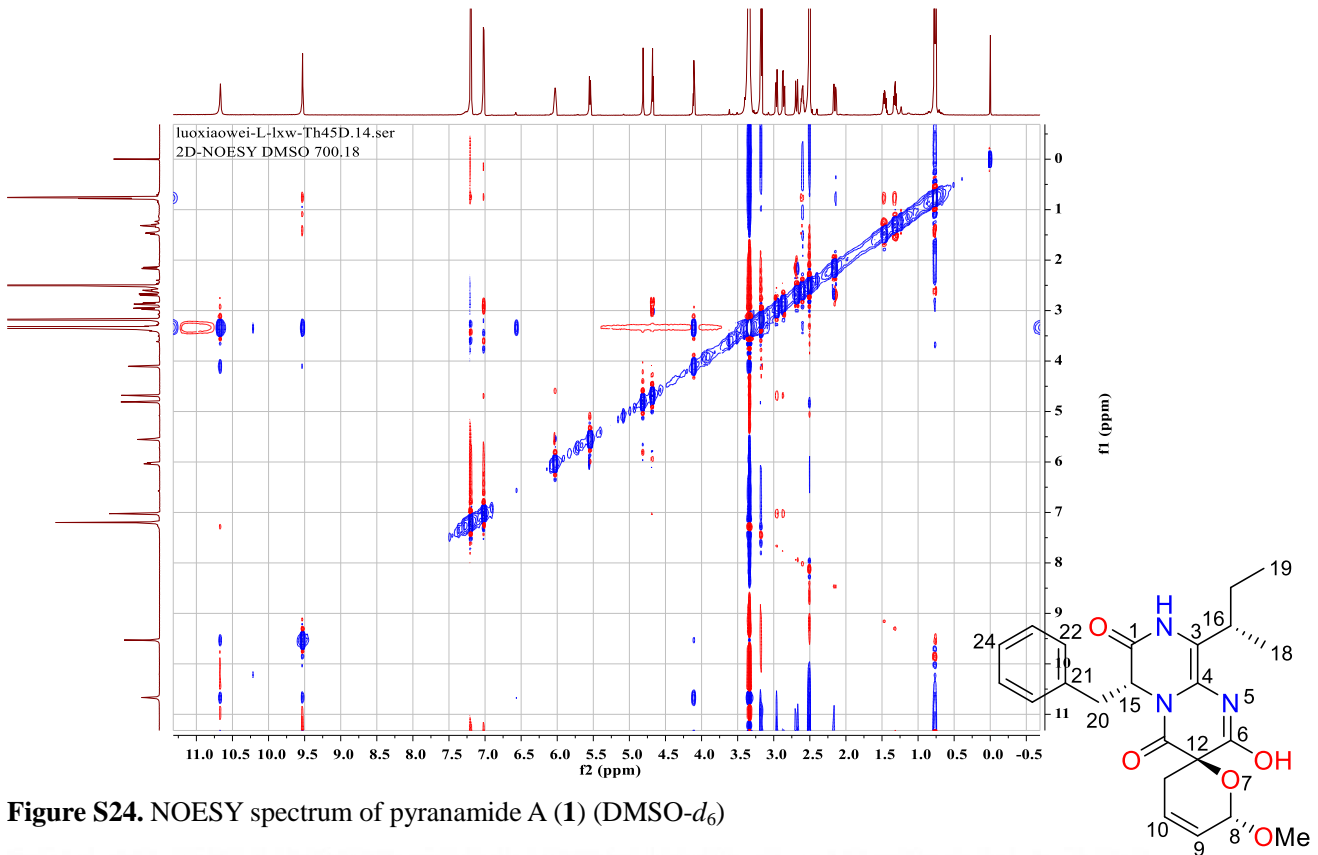


Figure S24. NOESY spectrum of pyranamide A (1) (DMSO-*d*₆)

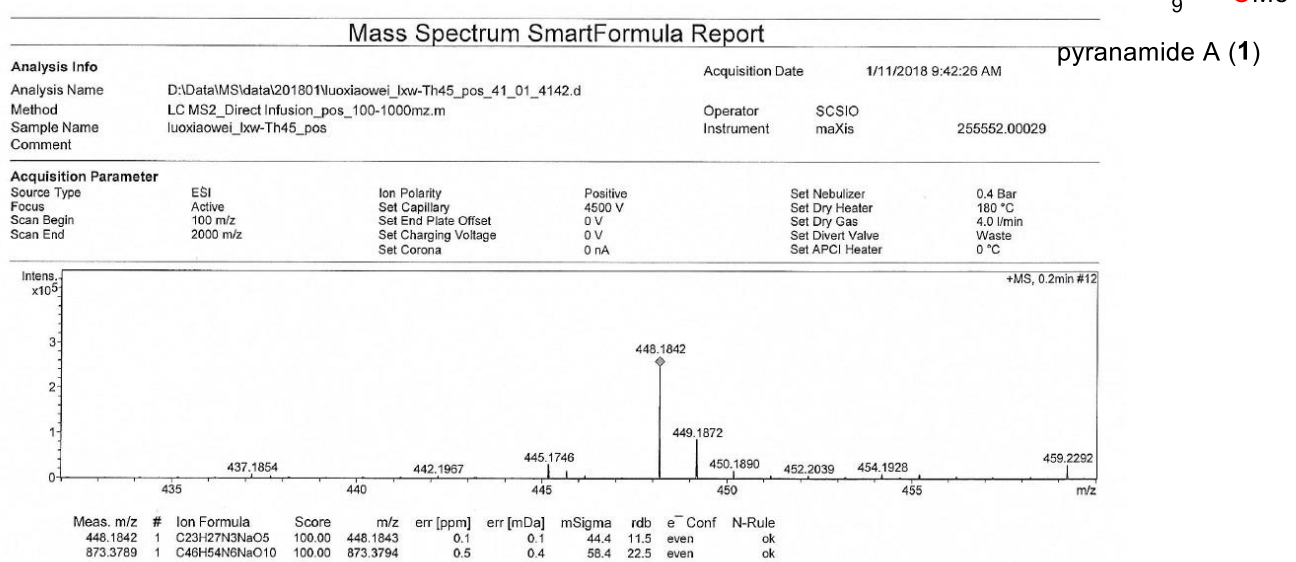


Figure S25. Positive HR-ESI-MS spectrum of pyranamide A (1)

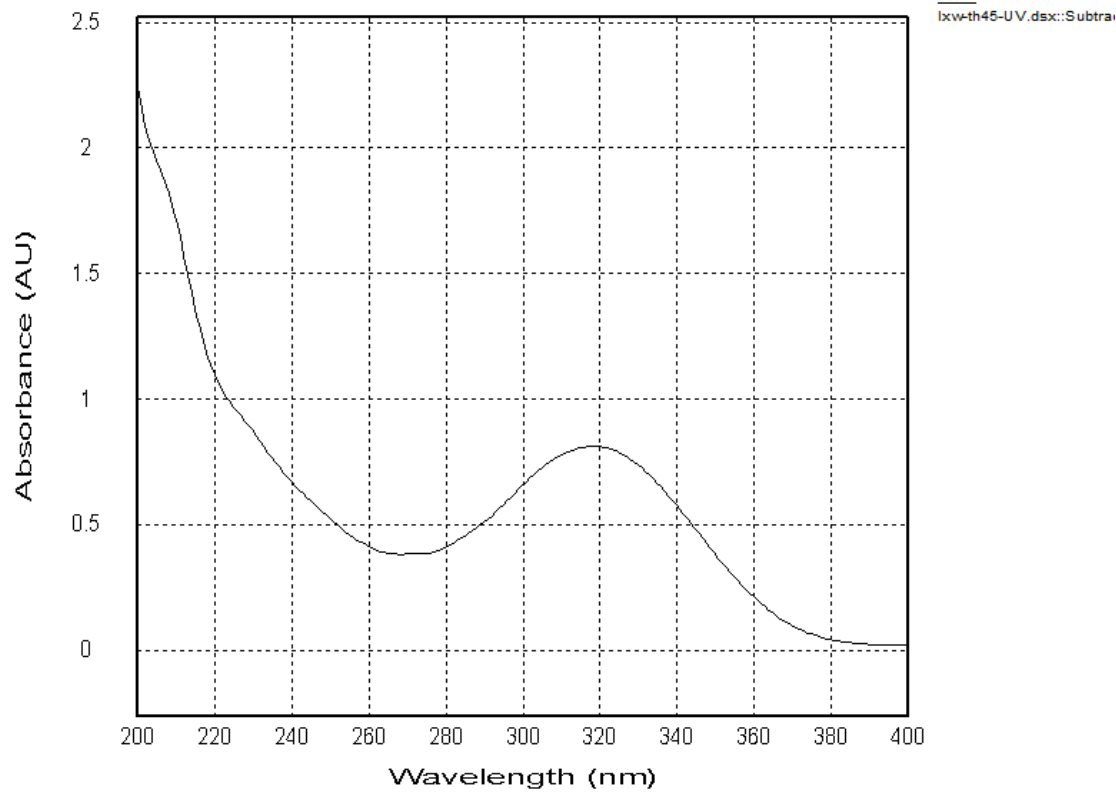


Figure S26. UV spectrum of pyranamide A (**1**)

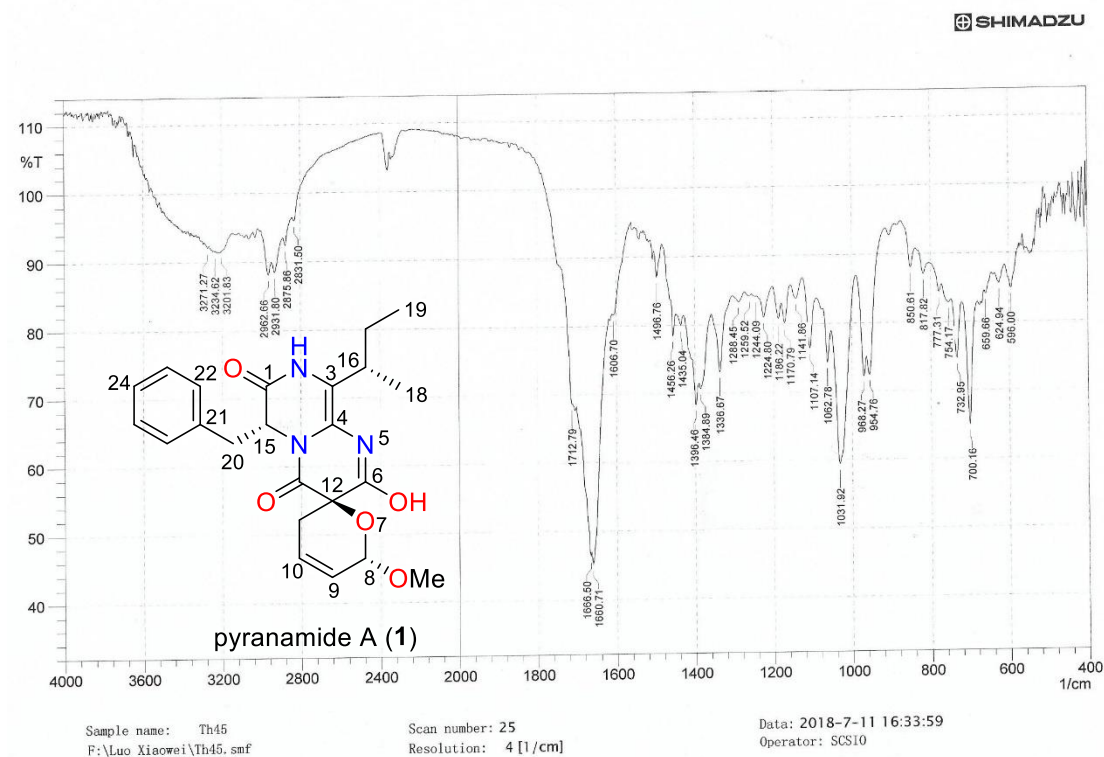


Figure S27. IR spectrum of pyranamide A (**1**)

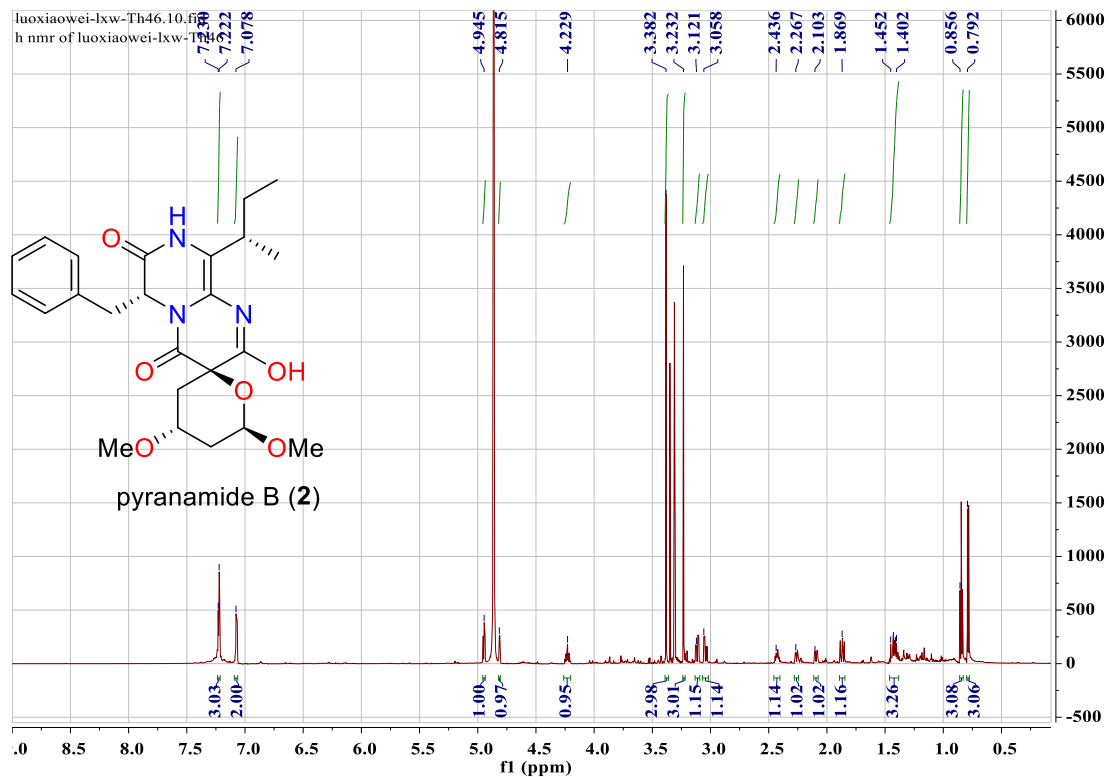
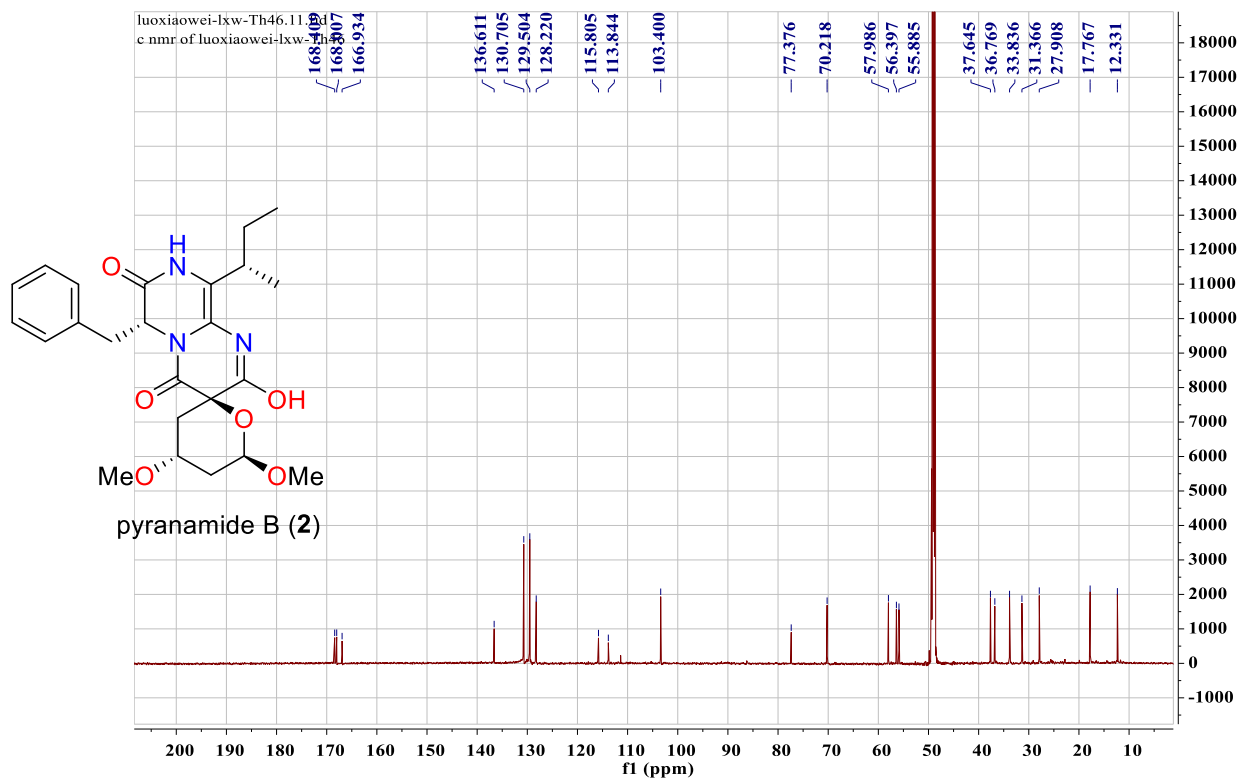


Figure S28. ¹H NMR spectrum of pyranamide B (2) (CD₃OD, 700 MHz)



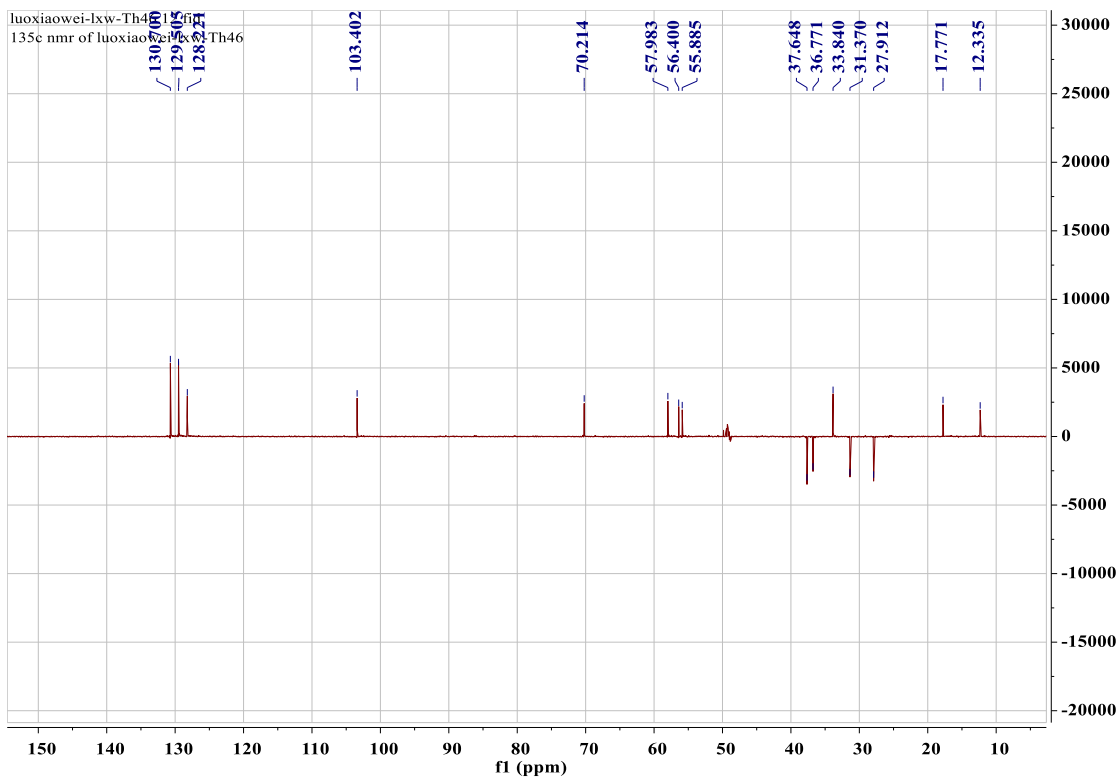


Figure S29. ^{13}C NMR and DEPT spectra of pyranamide B (2) (CD_3OD , 175 MHz)

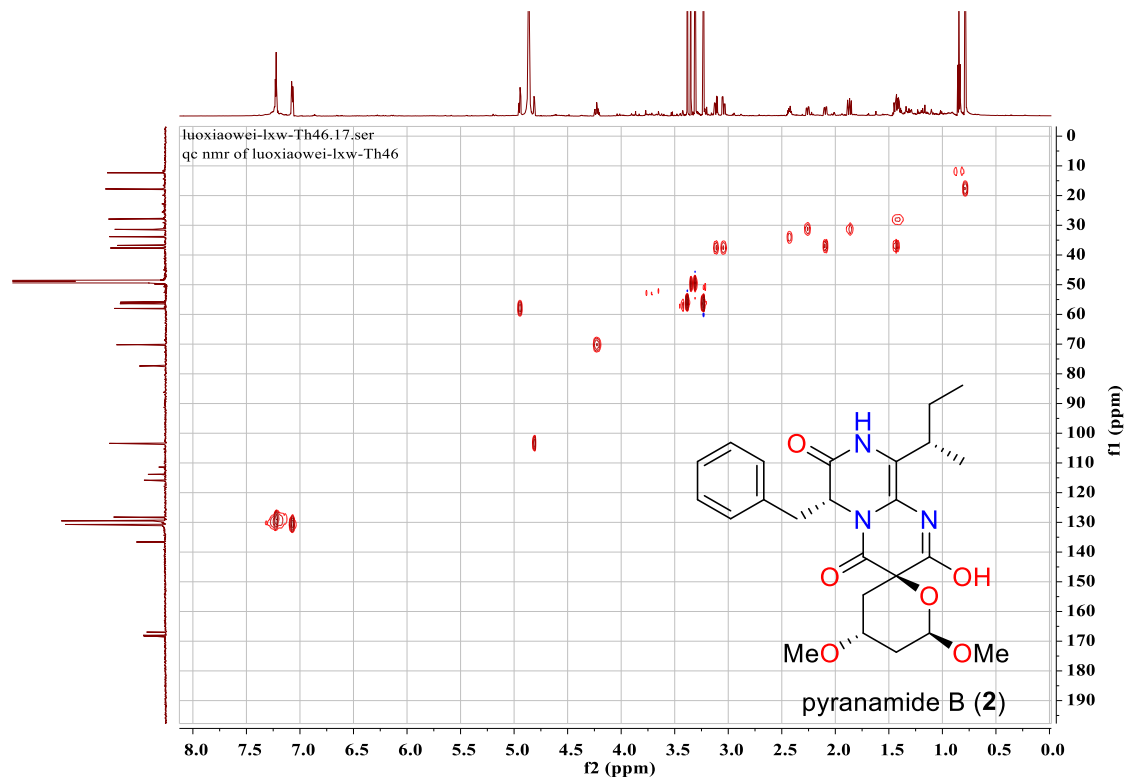


Figure S30. HSQC spectrum of pyranamide B (2) (CD_3OD)

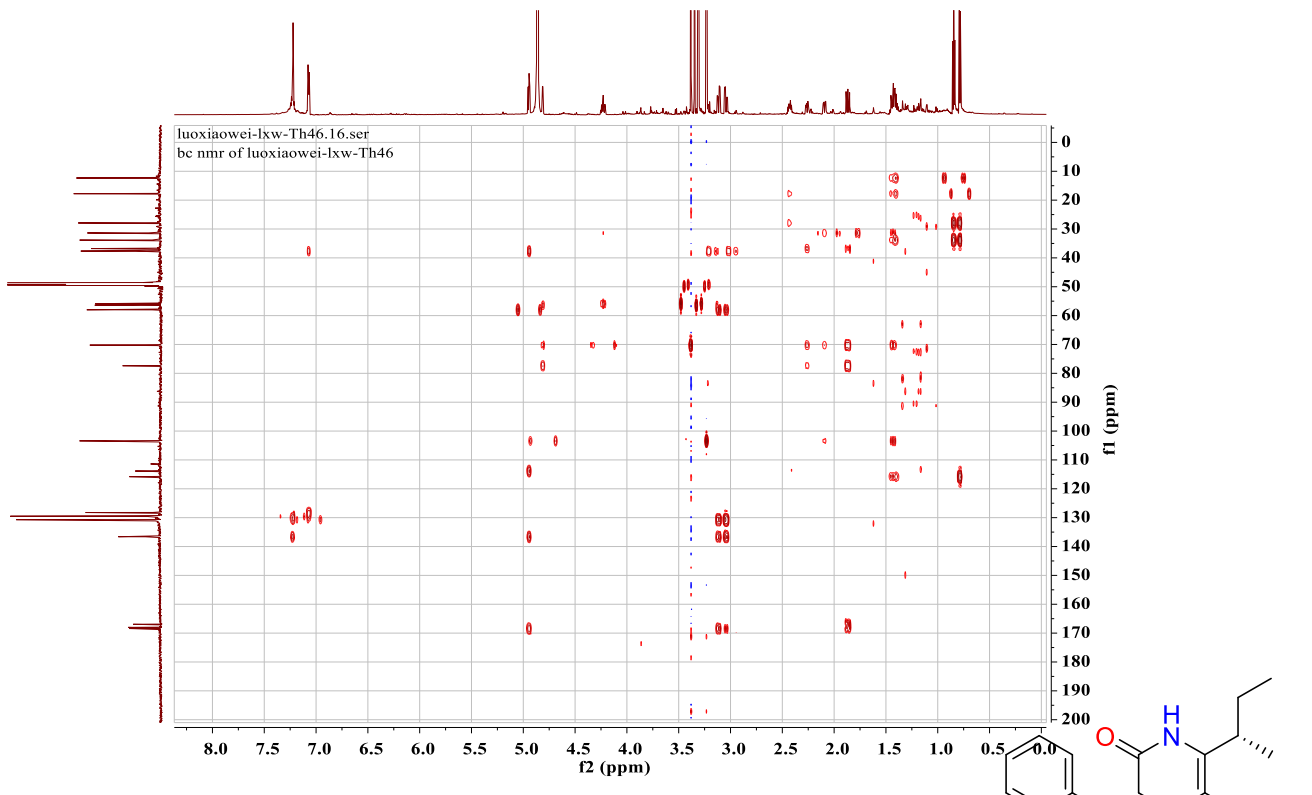


Figure S31. HMBC spectrum of pyranamide B (2) (CD_3OD)

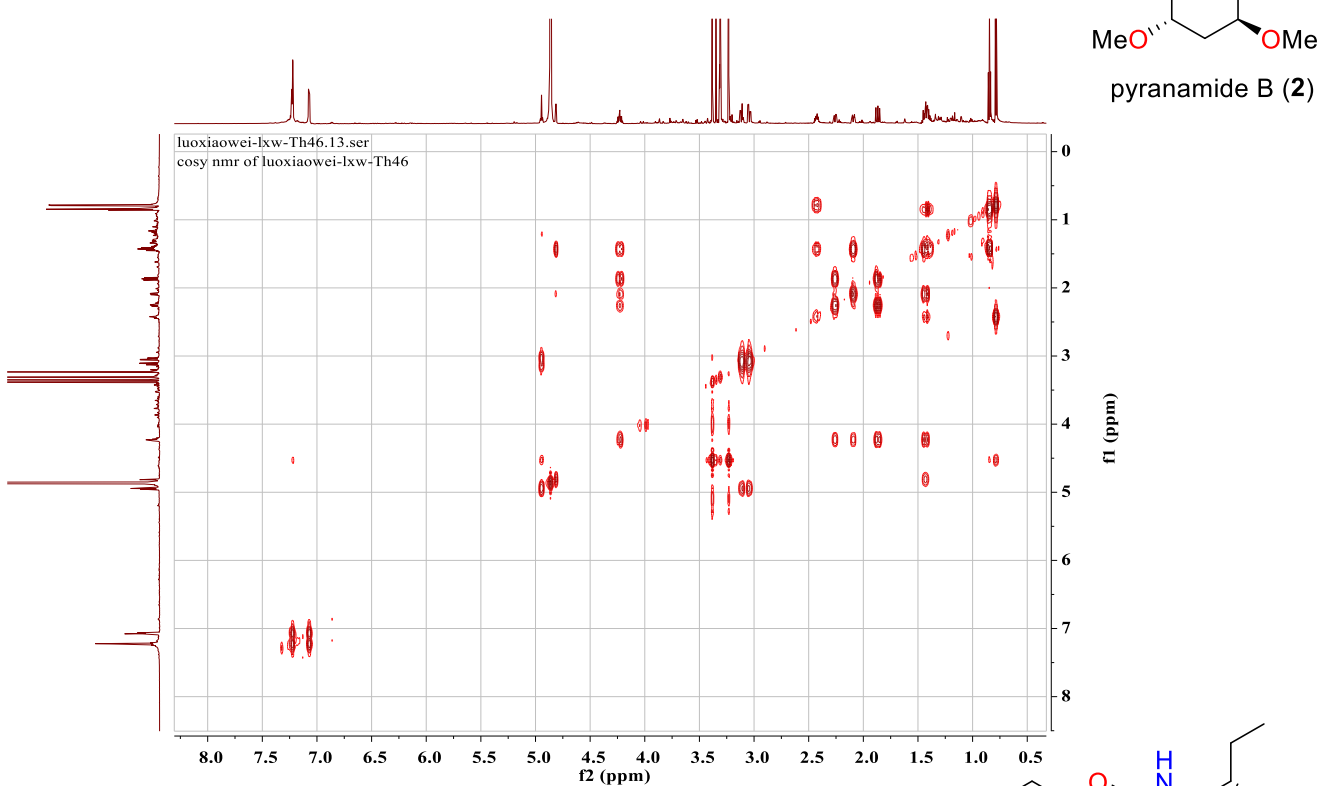


Figure S32. ^1H - ^1H COSY spectrum of pyranamide B (2) (CD_3OD)

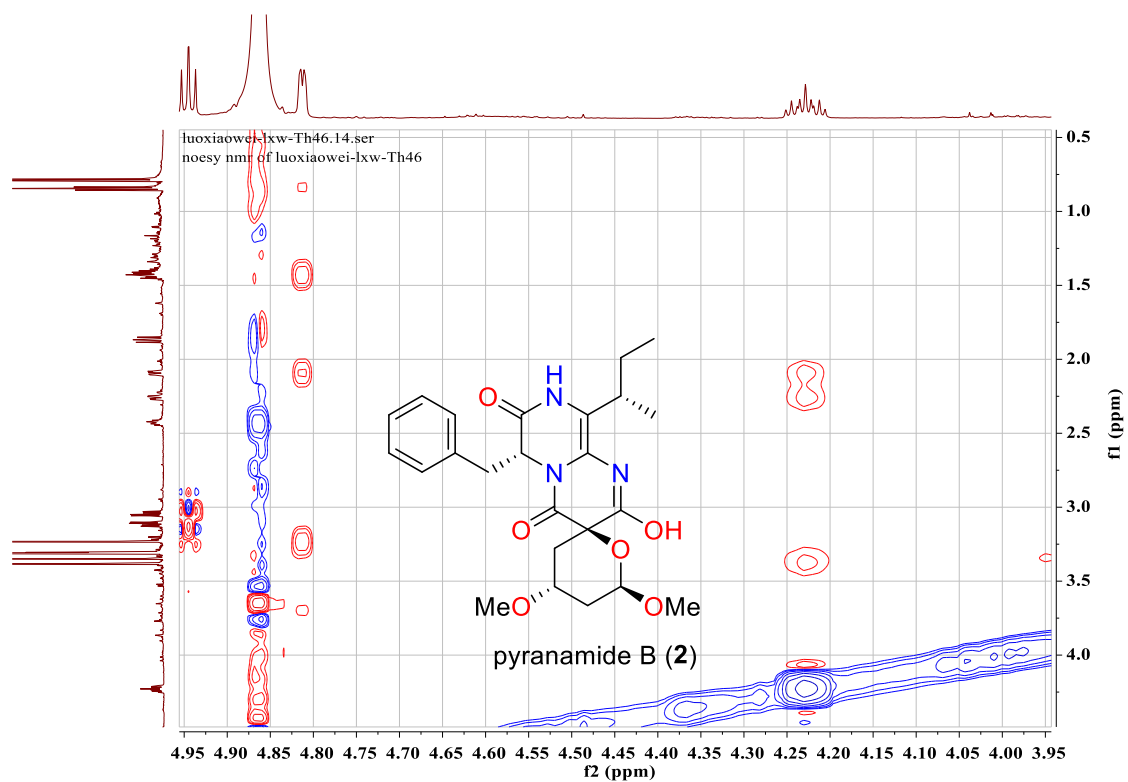
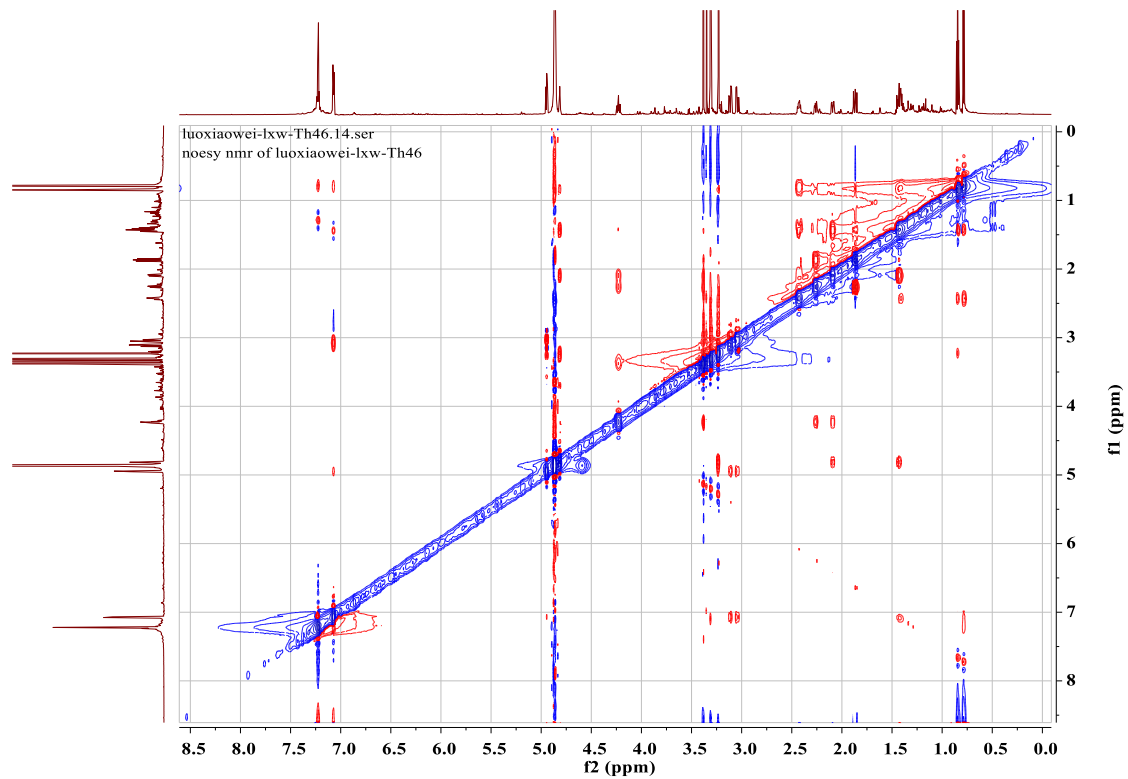


Figure S33. NOESY spectrum of pyranamide B (2) (CD_3OD)

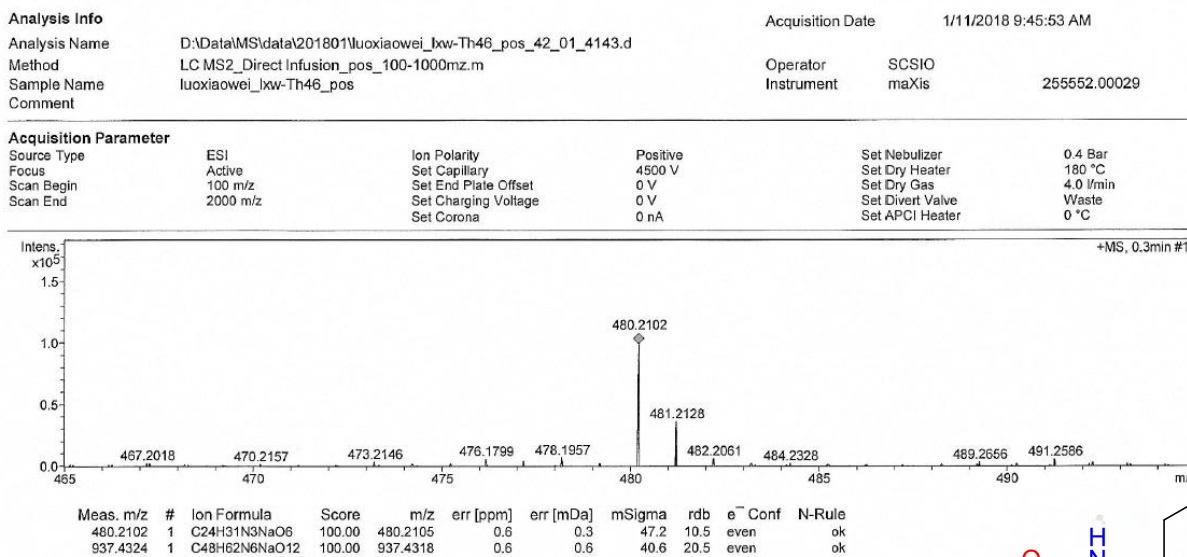


Figure S34. Positive HR-ESI-MS spectrum of pyranamide B (2)

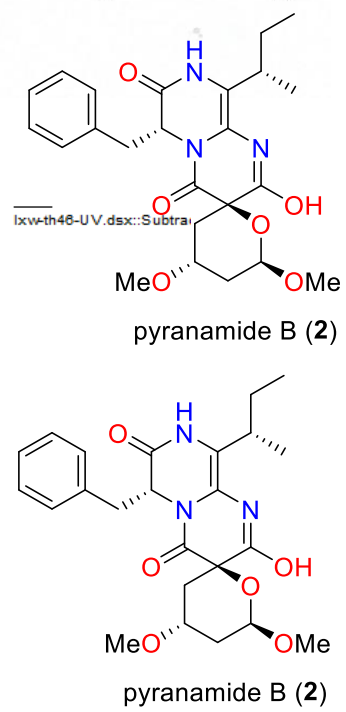
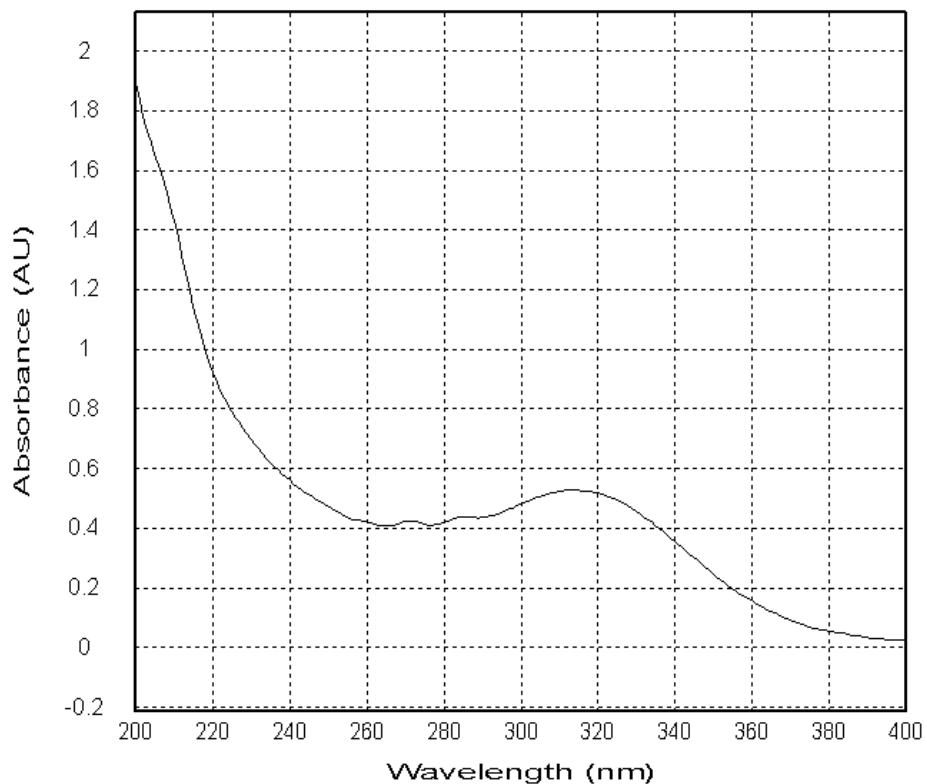


Figure S35. UV spectrum of pyranamide B (2)

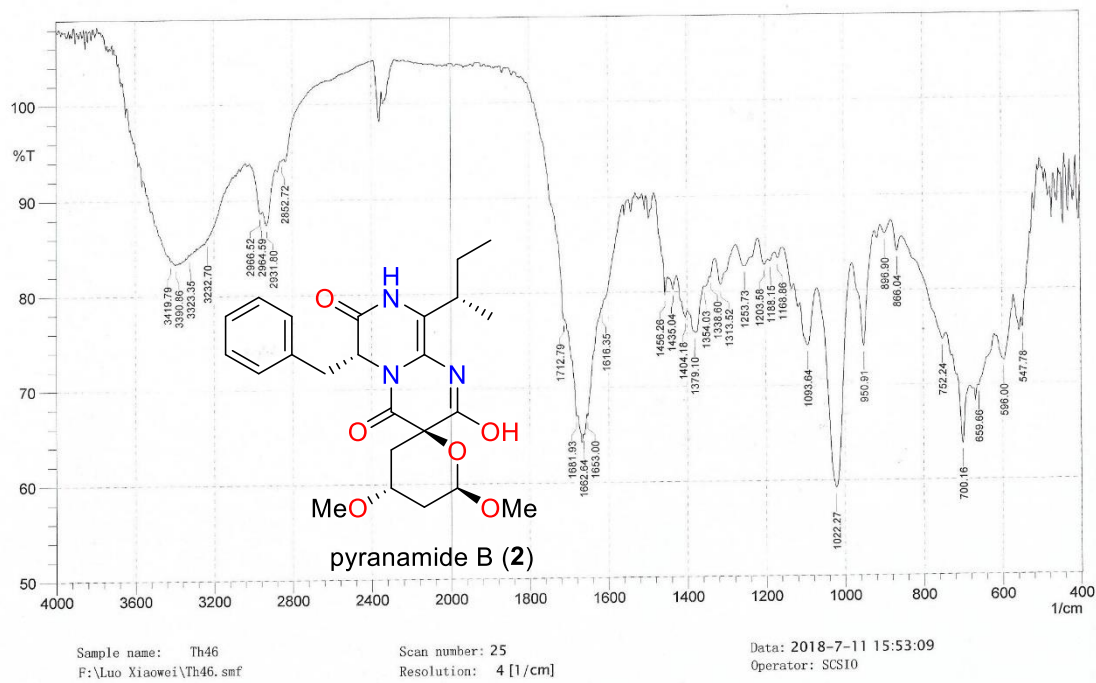


Figure S36. IR spectrum of pyranamide B (2)

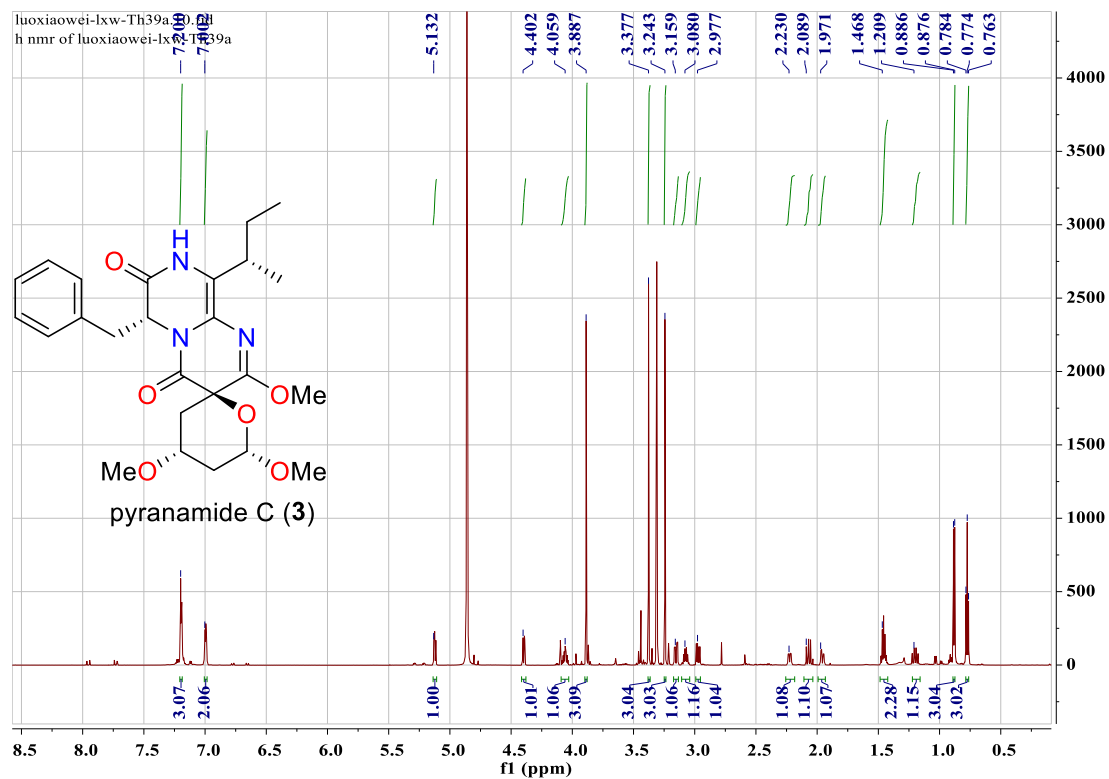


Figure S37. ¹H NMR spectrum of pyranamide C (3) (CD₃OD, 700 MHz)

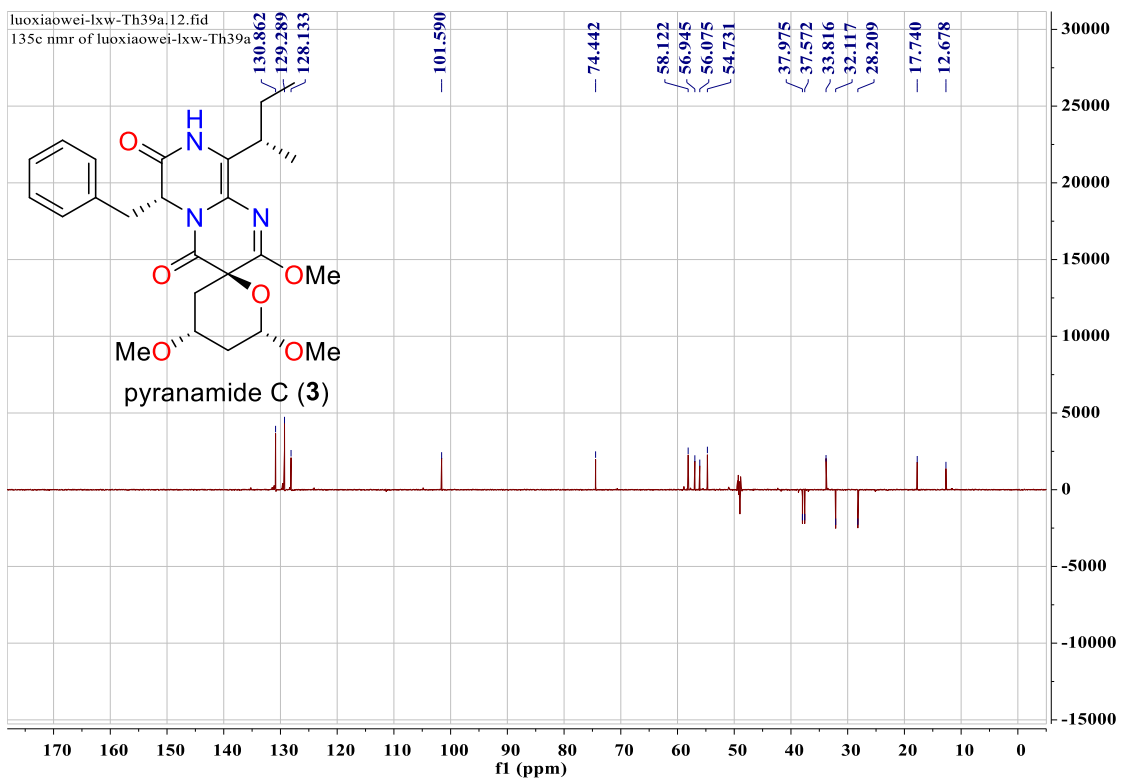
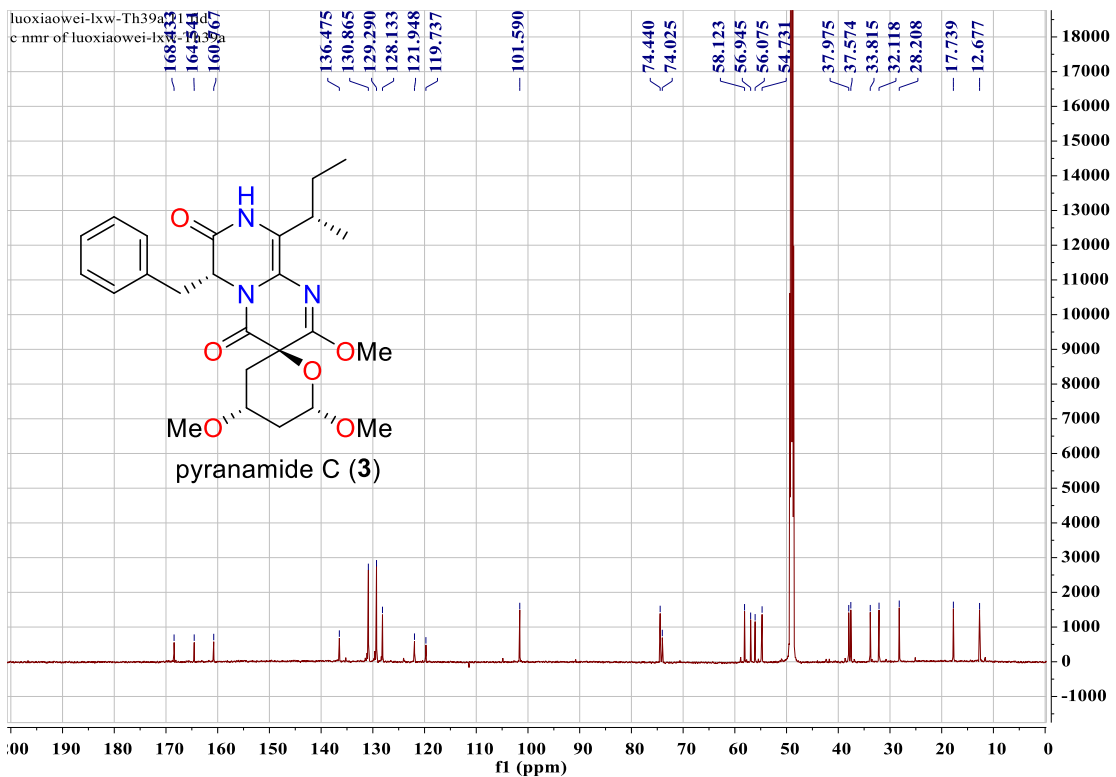


Figure S38. ^{13}C NMR and DEPT spectra of pyranamide C (3) (CD_3OD , 175 MHz)

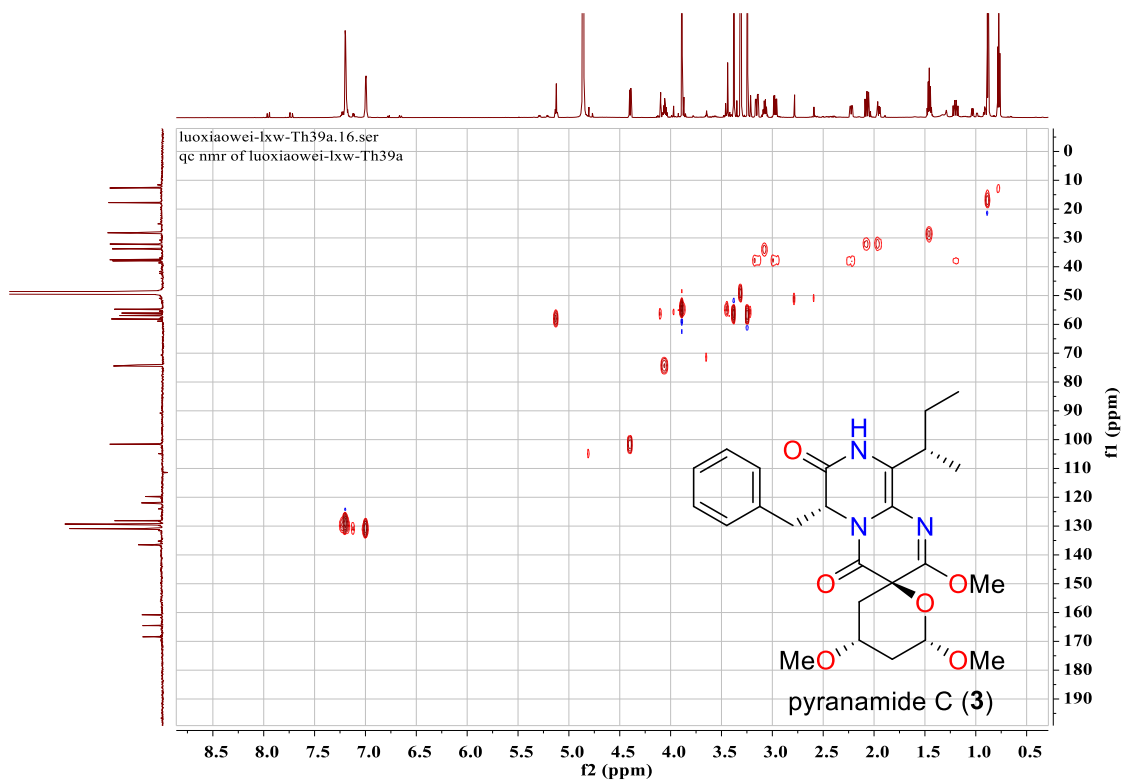


Figure S39. HSQC spectrum of pyranamide C (3) (CD_3OD)

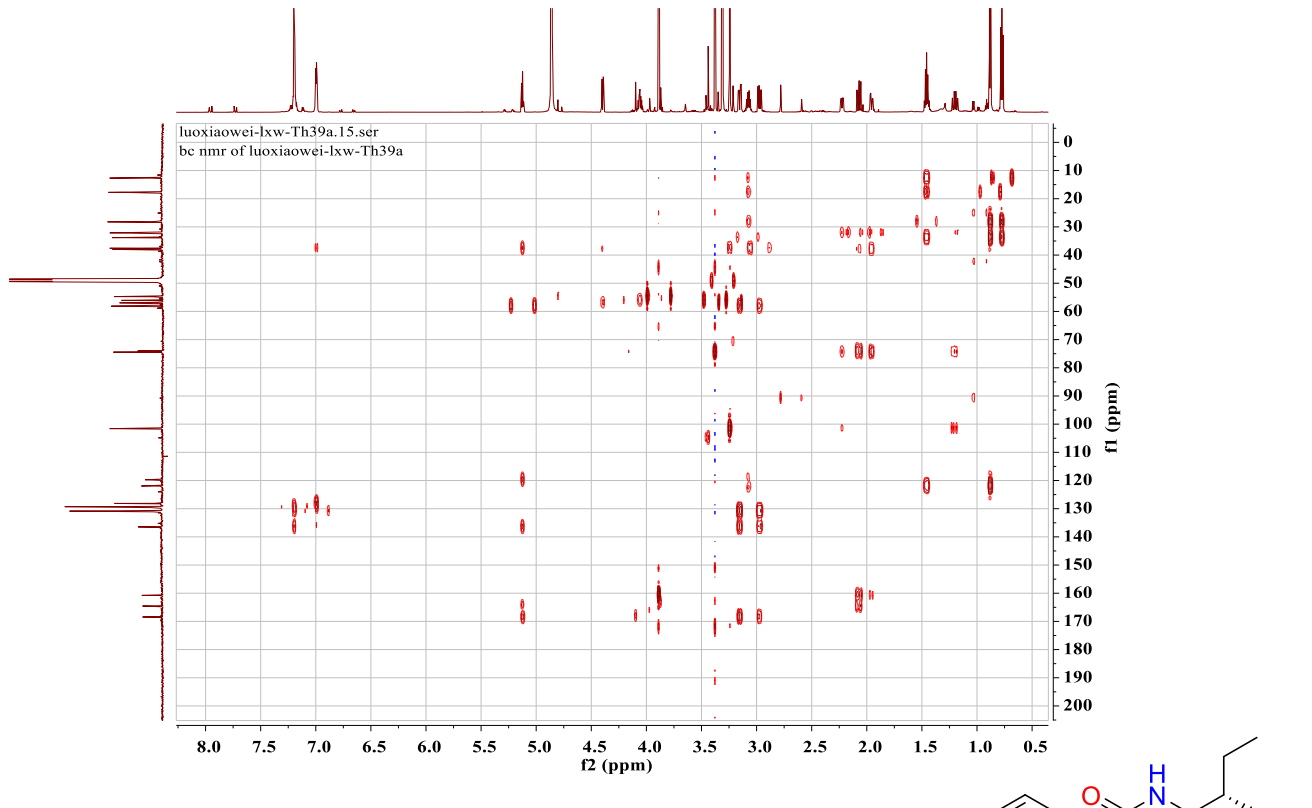
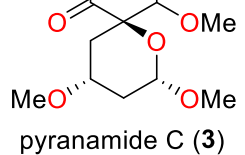


Figure S40. HMBC spectrum of pyranamide C (3) (CD_3OD)



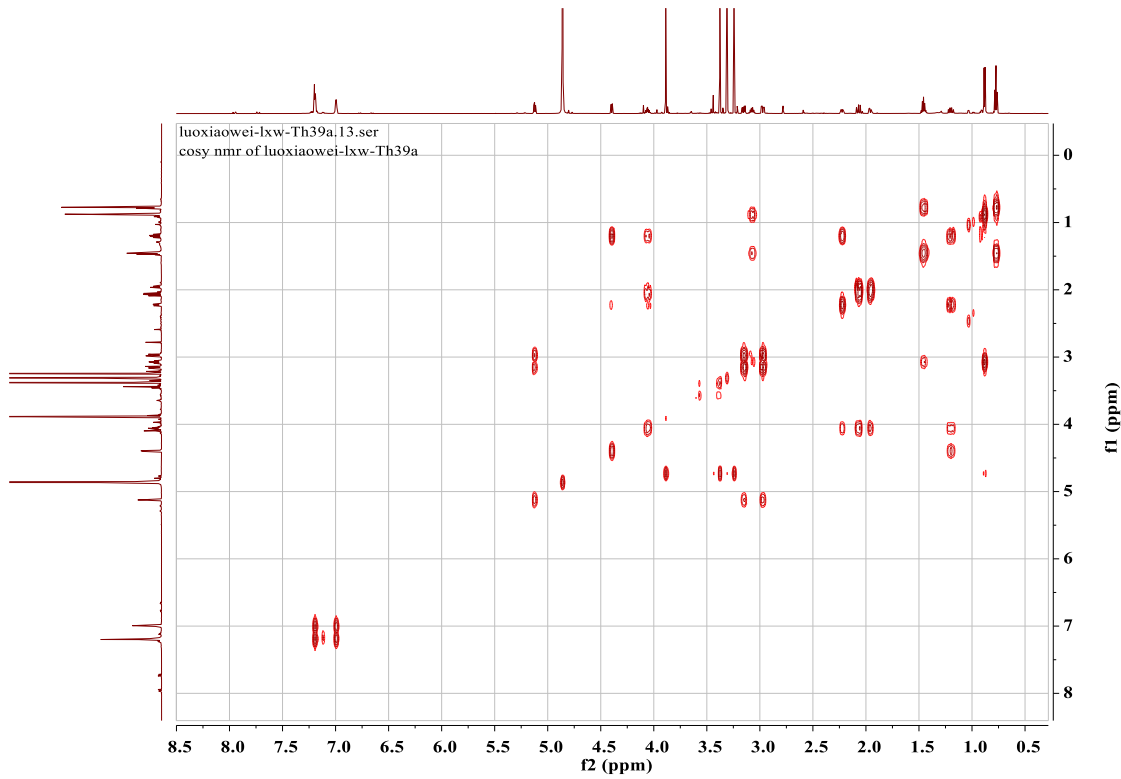
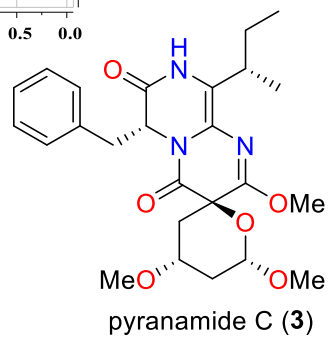
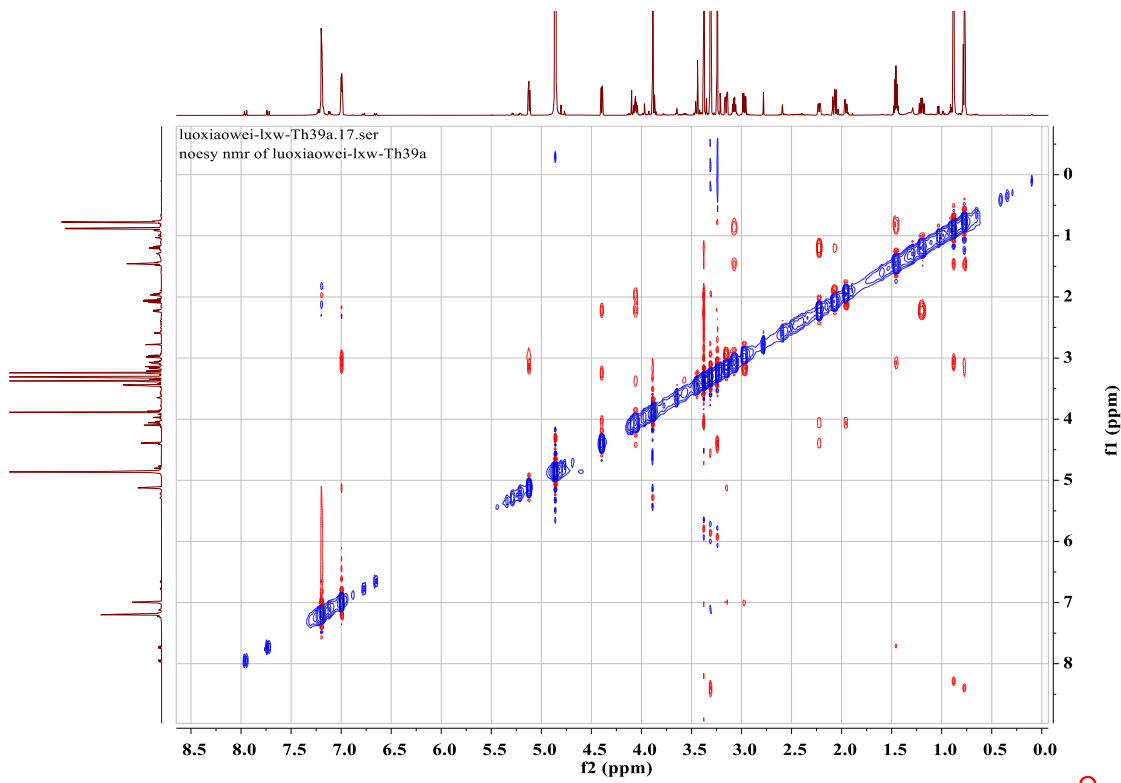


Figure S41. ^1H - ^1H COSY spectrum of pyranamide C (3) (CD_3OD)



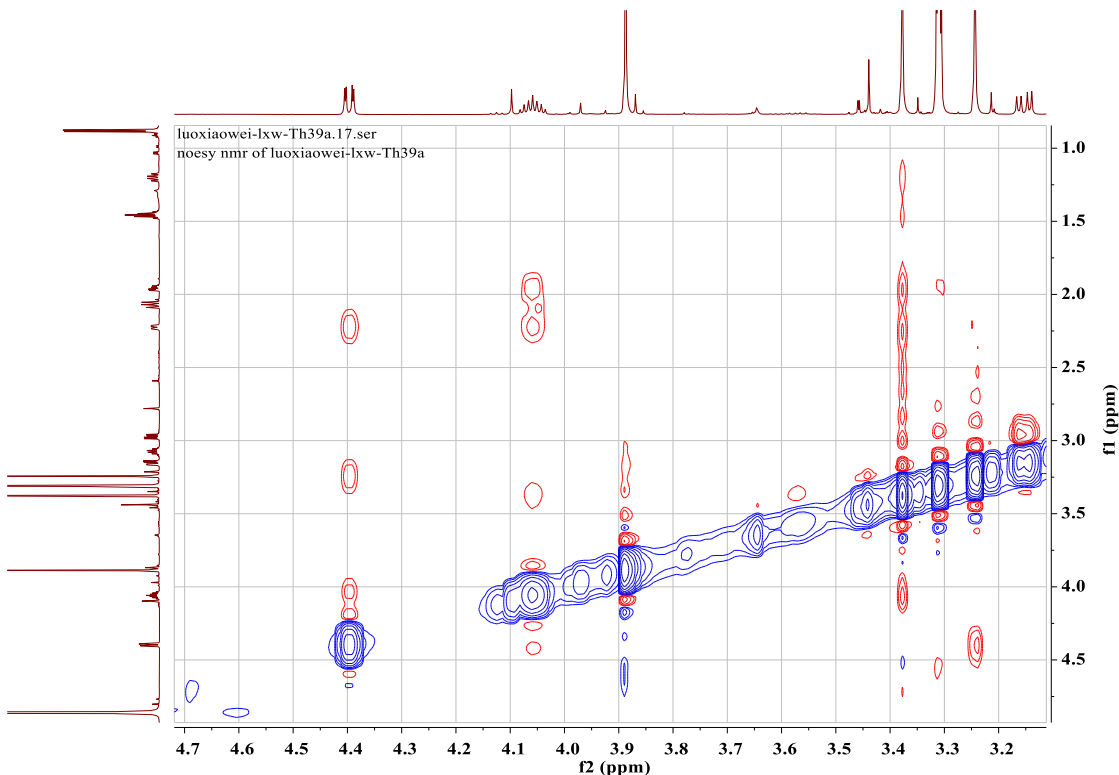


Figure S42. NOESY spectrum of pyranamide C (3) (CD_3OD)

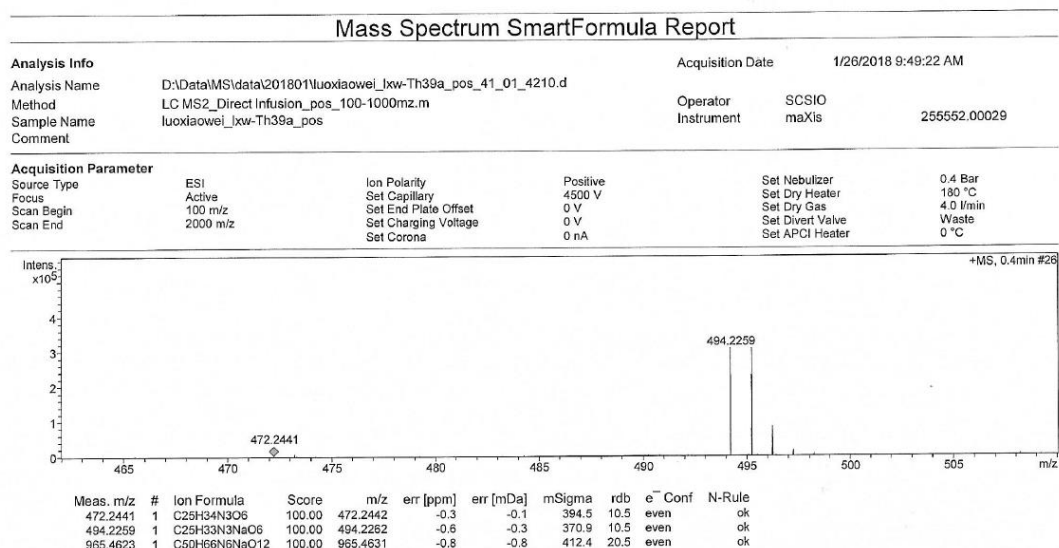
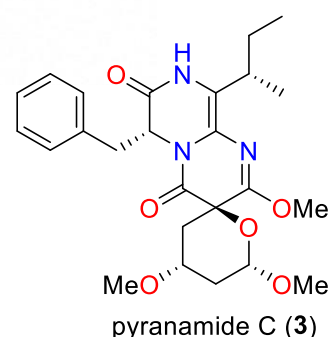


Figure S43. Positive HR-ESI-MS spectrum of pyranamide C (3)



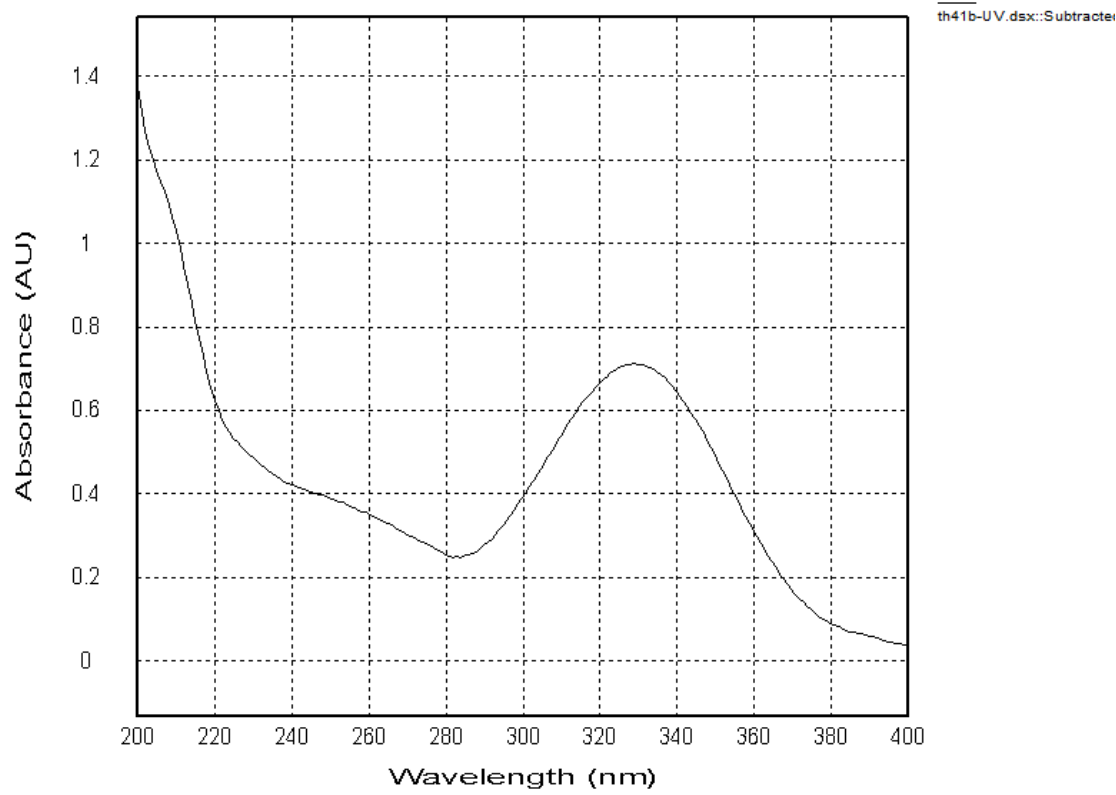


Figure S44. UV spectrum of pyranamide C (3)

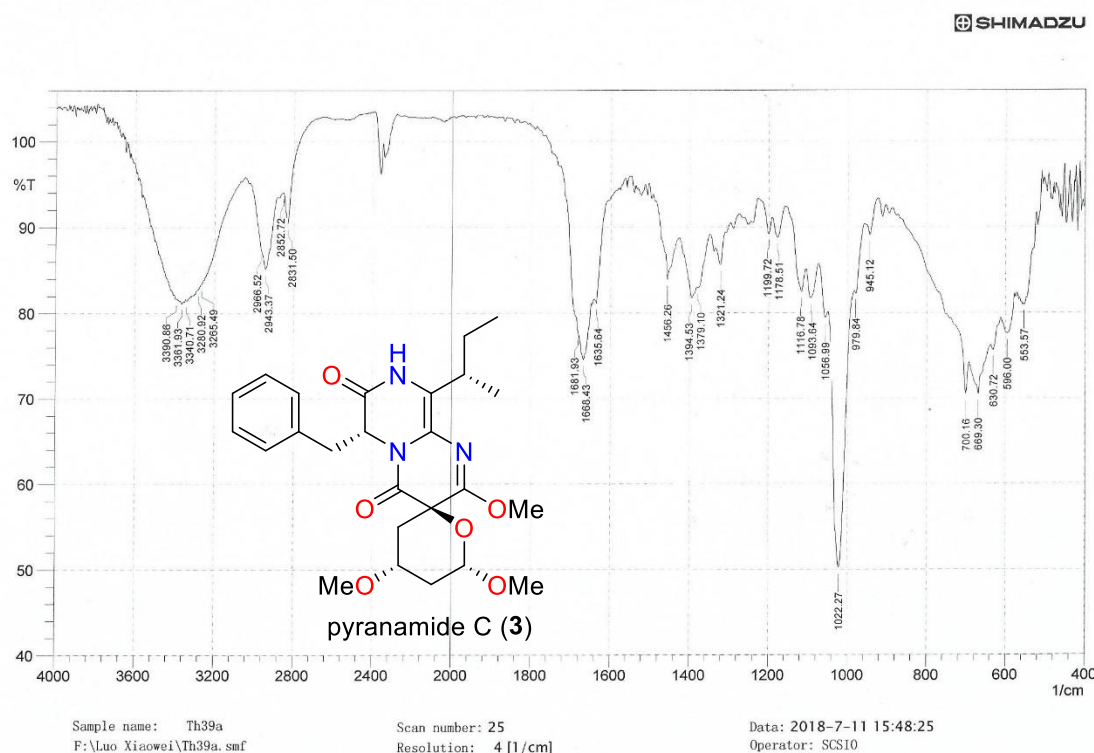


Figure S45. IR spectrum of pyranamide C (3)

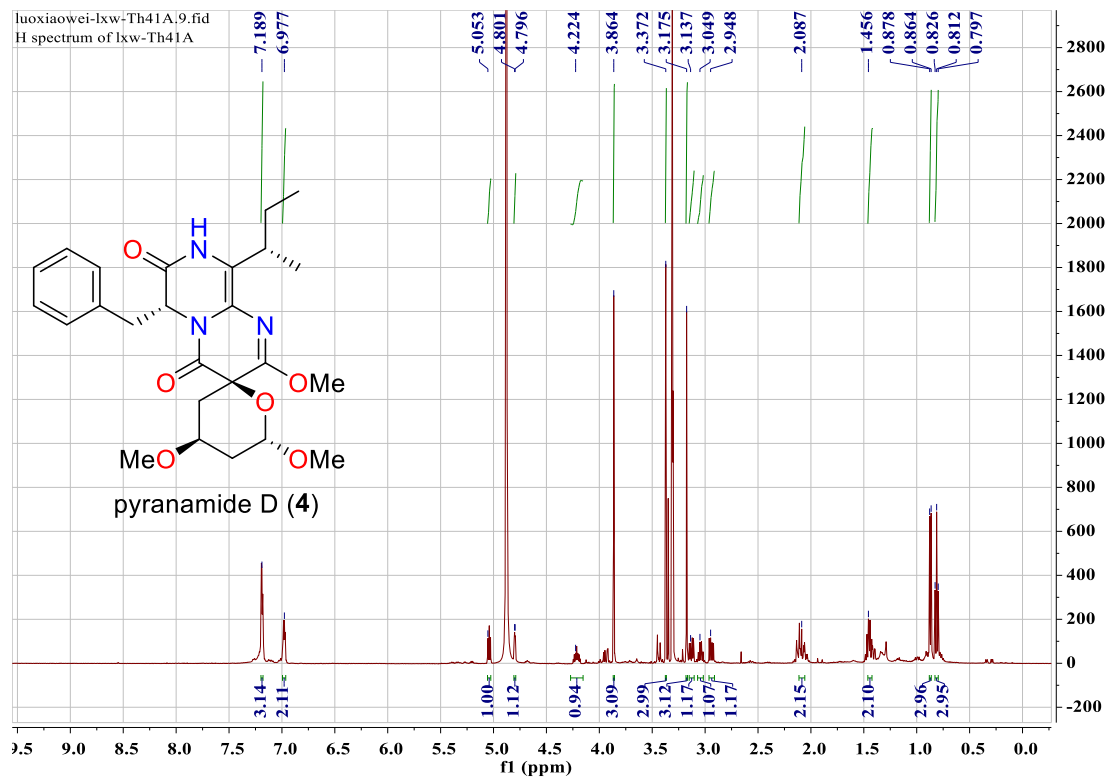
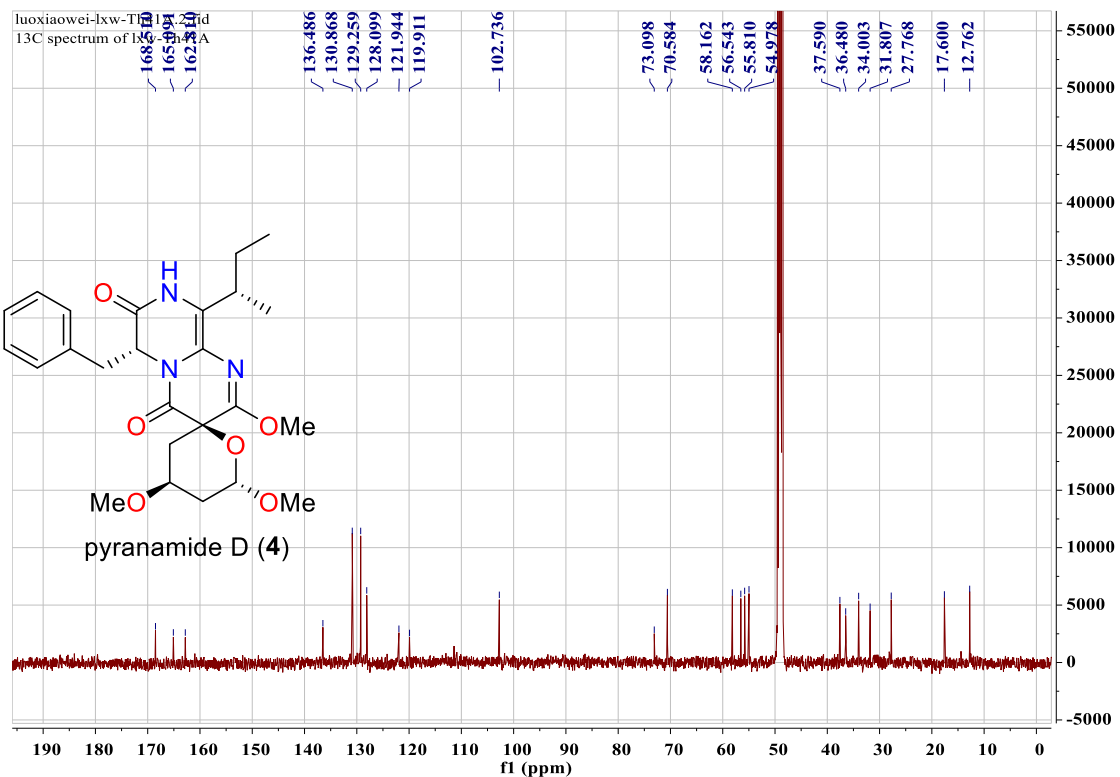


Figure S46. ¹H NMR spectrum of pyranamide D (4) (CD₃OD, 500 MHz)



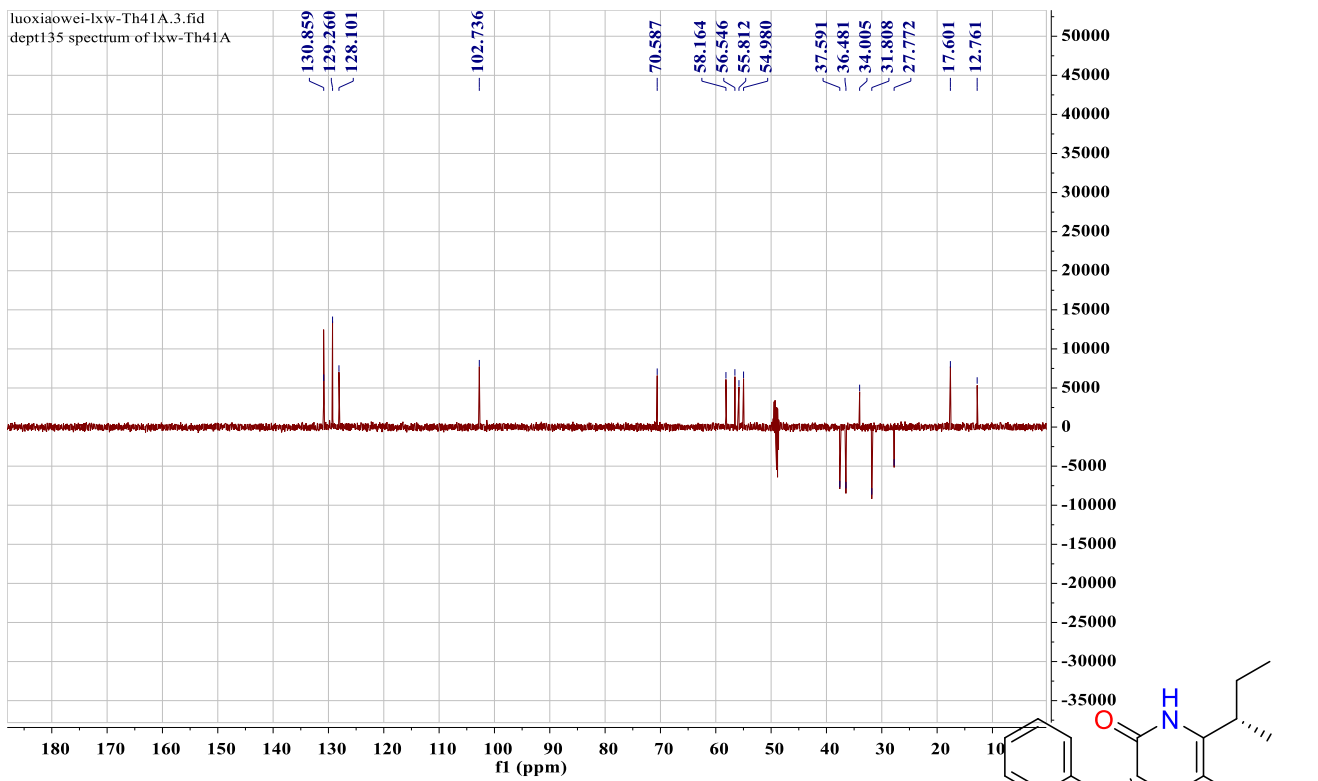


Figure S47. ^{13}C NMR and DEPT spectra of pyranamide D (**4**) (CD_3OD , 125 MHz)

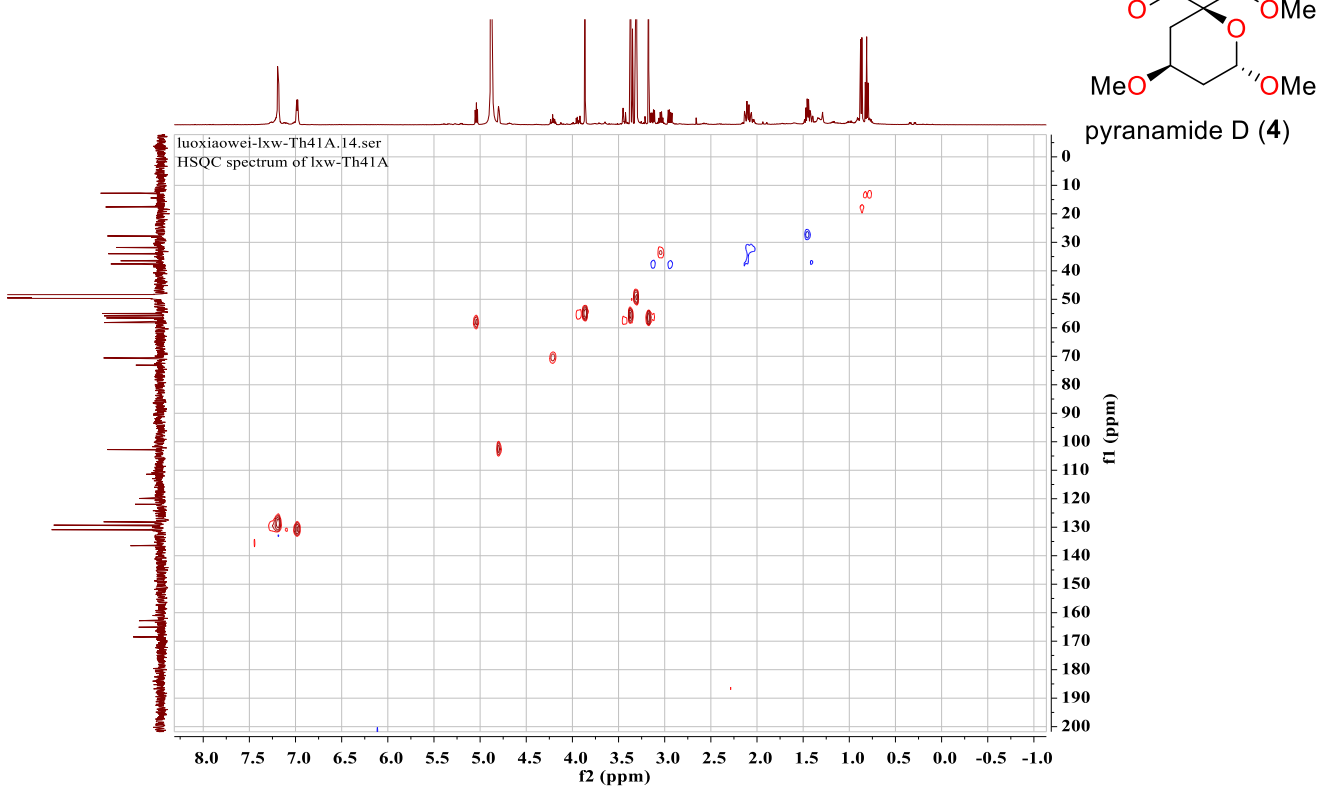


Figure S48. HSQC spectrum of pyranamide D (**4**) (CD_3OD)

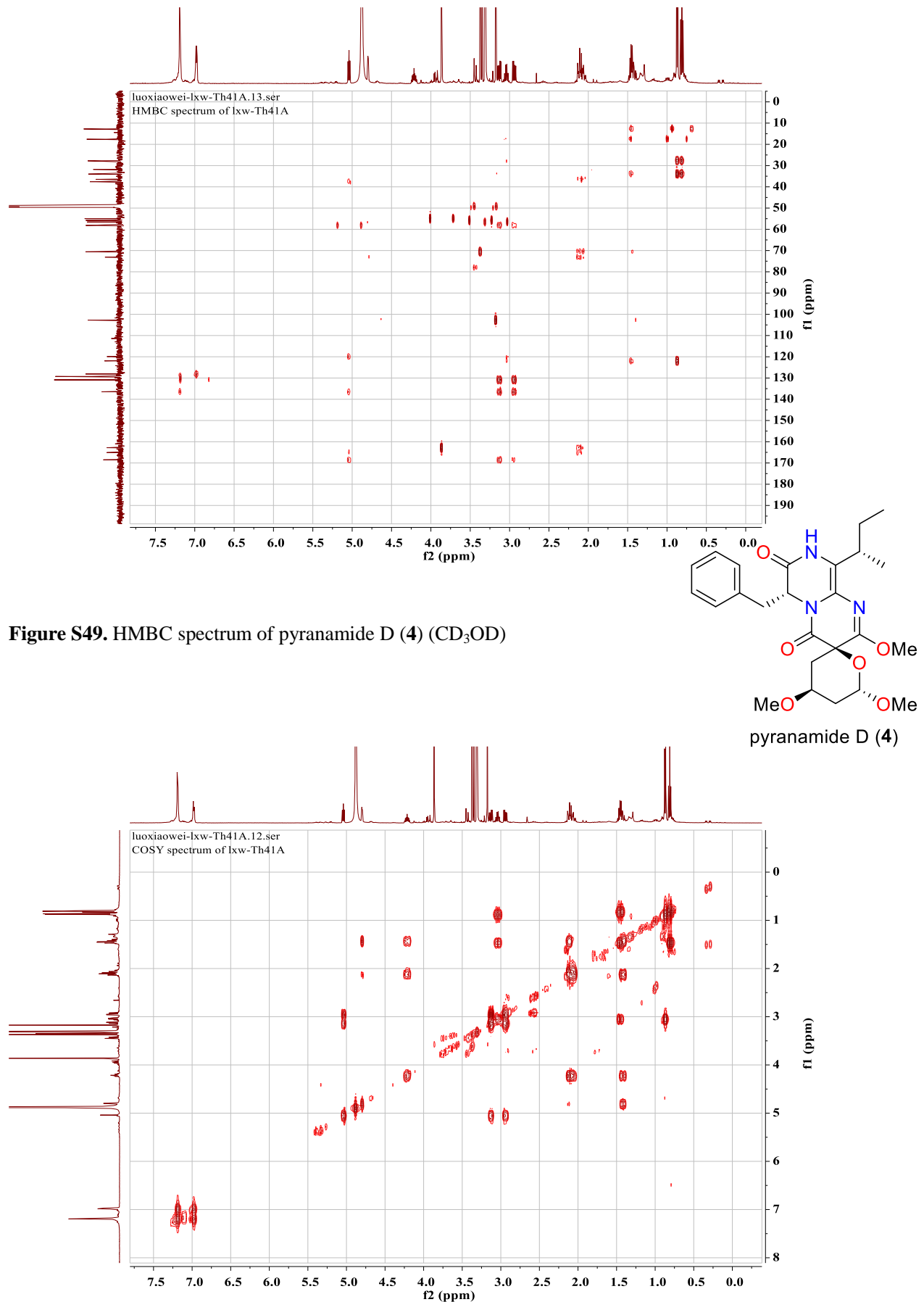


Figure S49. HMBC spectrum of pyranamide D (**4**) (CD_3OD)

Figure S50. ^1H - ^1H COSY spectrum of pyranamide D (**4**) (CD_3OD)

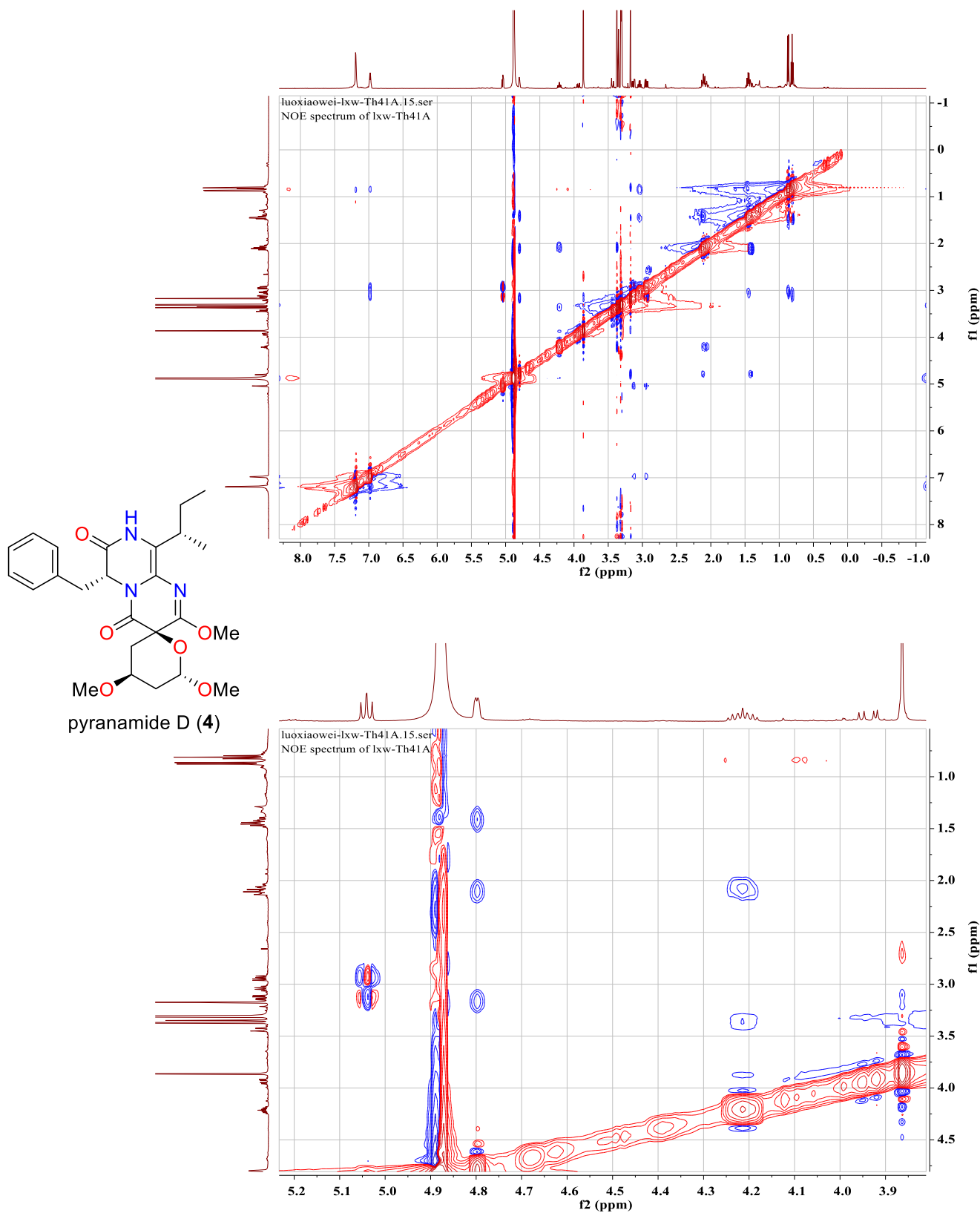


Figure S51. NOESY spectrum of pyranamide D (**4**) (CD_3OD)

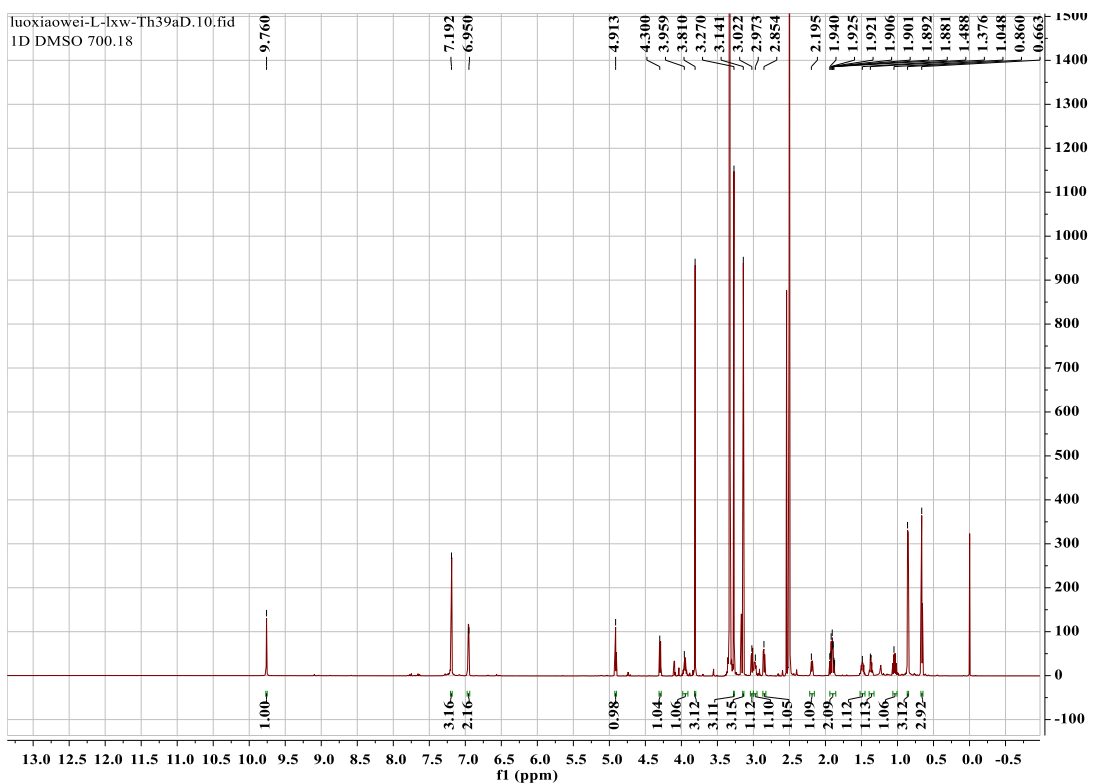
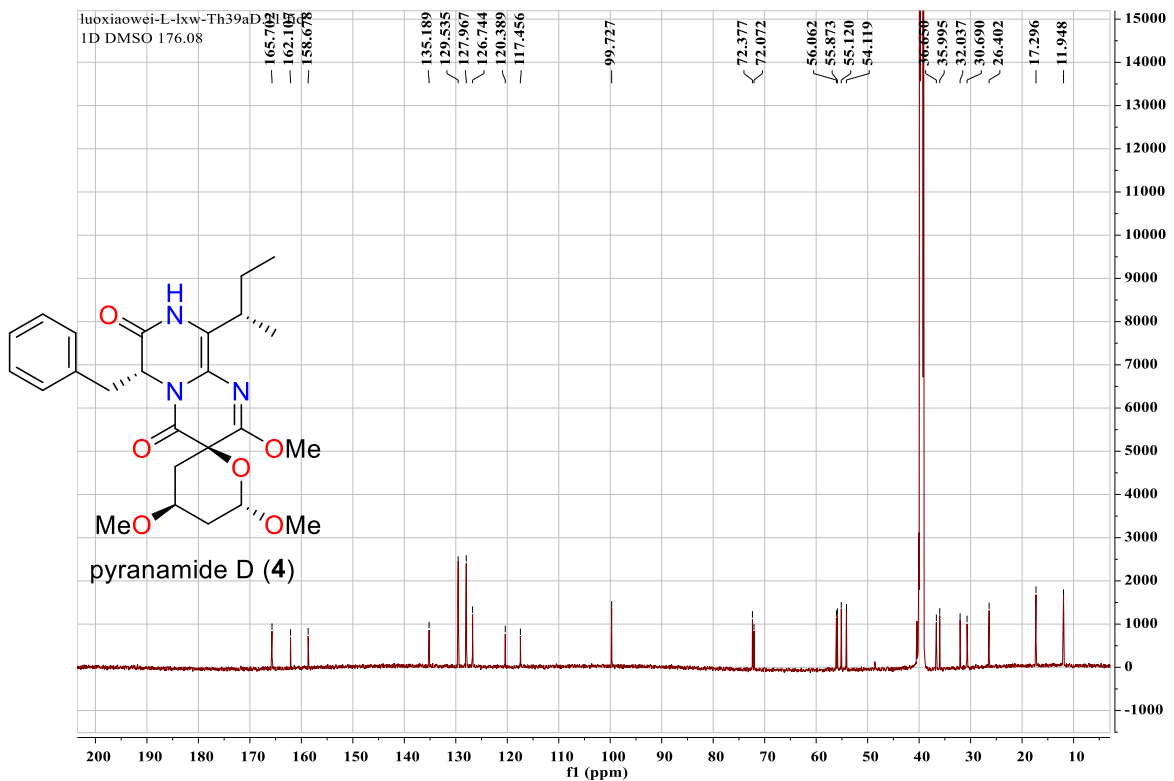


Figure S52. ^1H NMR spectrum of pyranamide D (**4**) (DMSO- d_6 , 700 MHz)



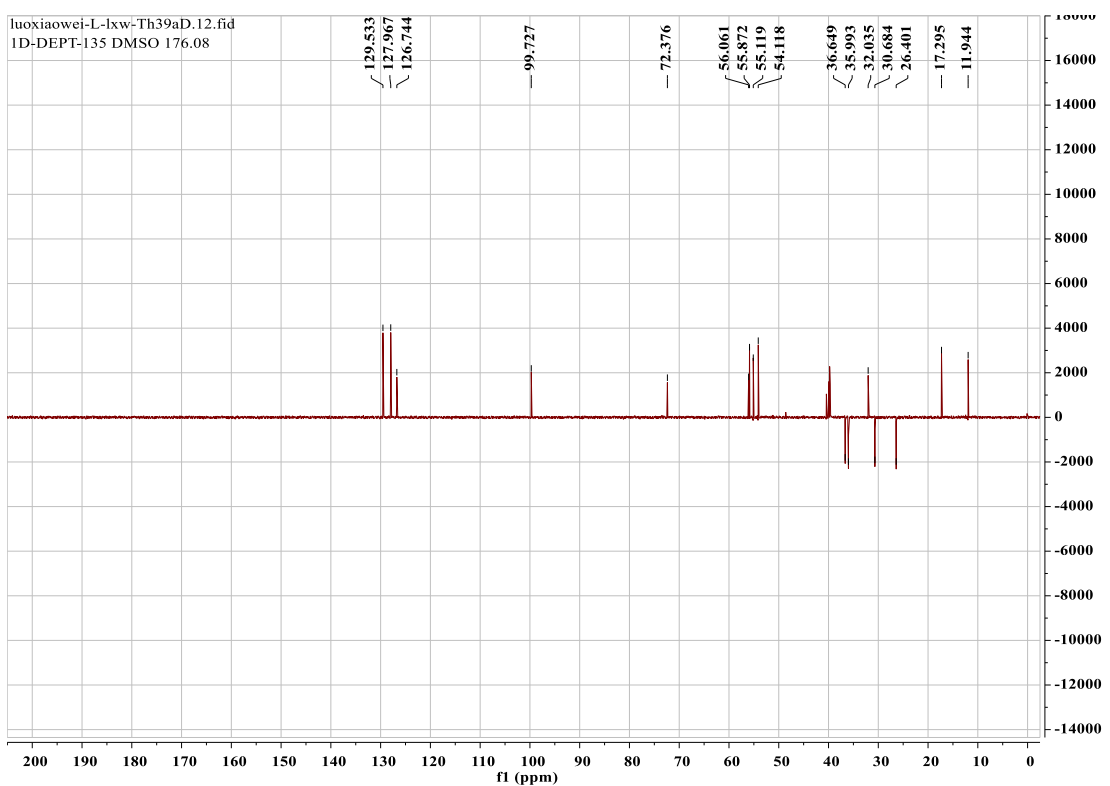


Figure S53. ^{13}C NMR and DEPT spectra of pyranamide D (**4**) (DMSO- d_6 , 175 MHz)

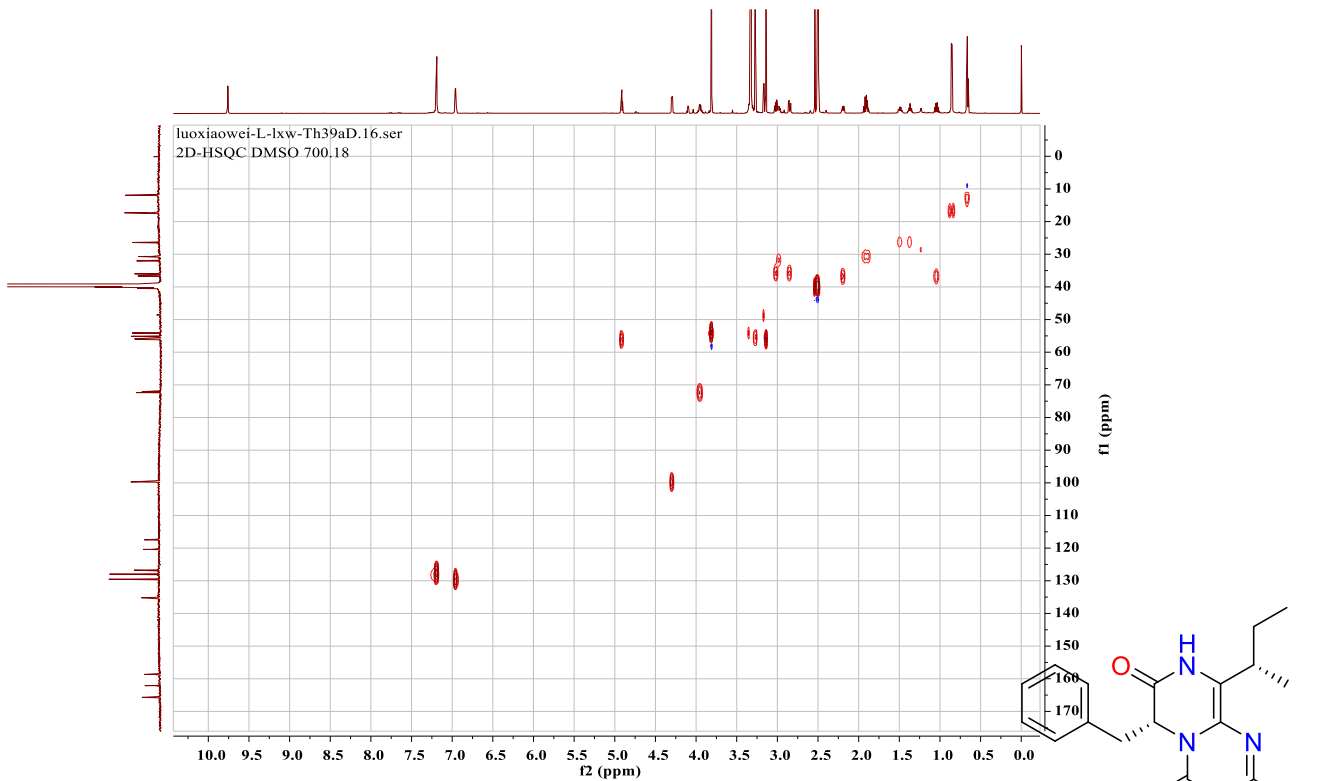


Figure S54. HSQC spectrum of pyranamide D (**4**) (DMSO- d_6)

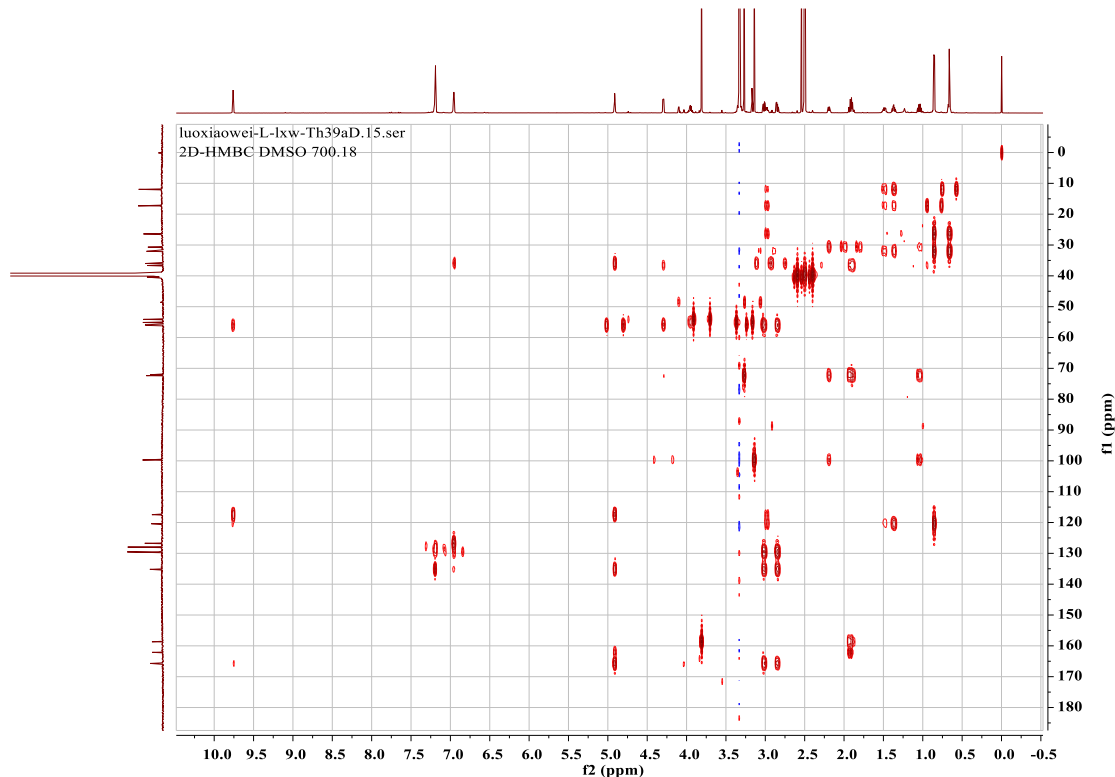


Figure S55. HMBC spectrum of pyranamide D (**4**) (DMSO-*d*₆)

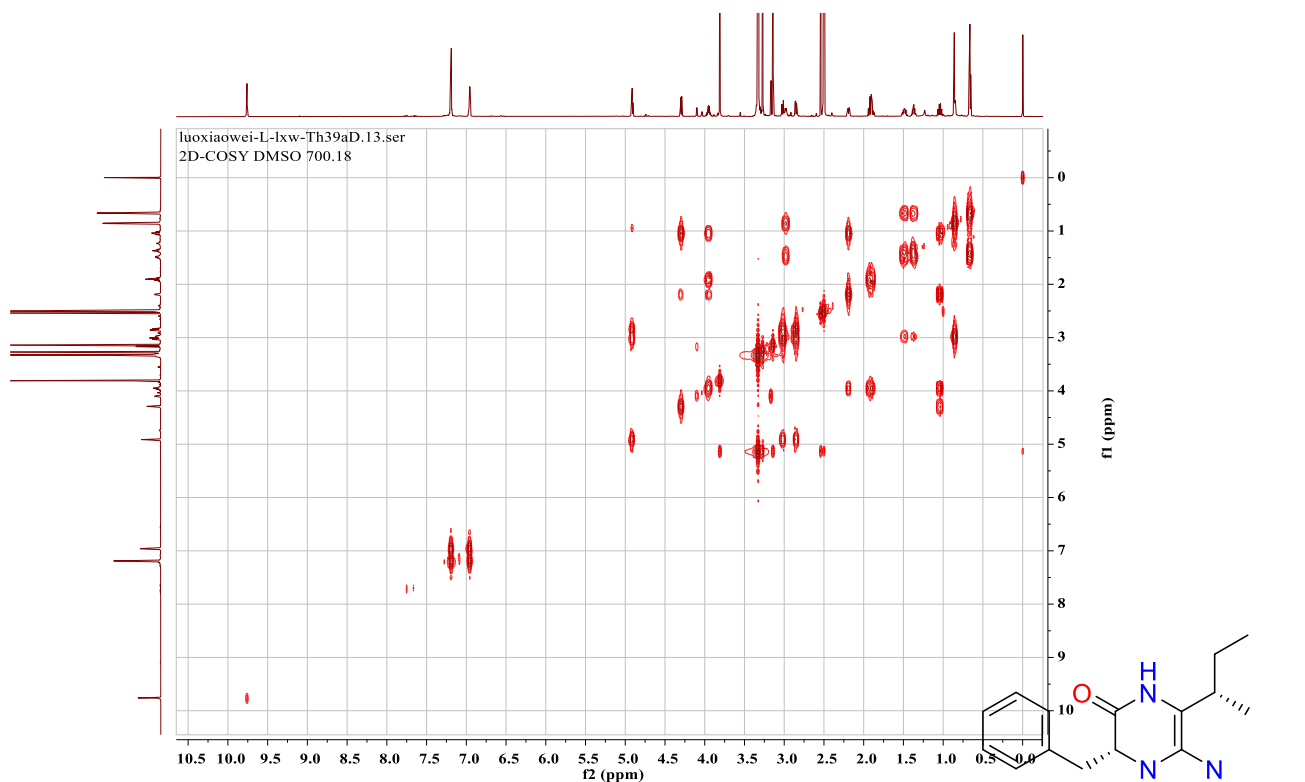
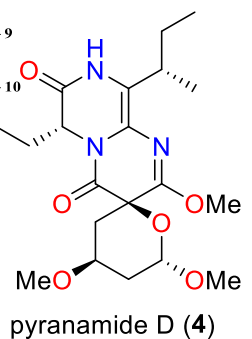


Figure S56. ^1H - ^1H COSY spectrum of pyranamide D (**4**) (DMSO- d_6)



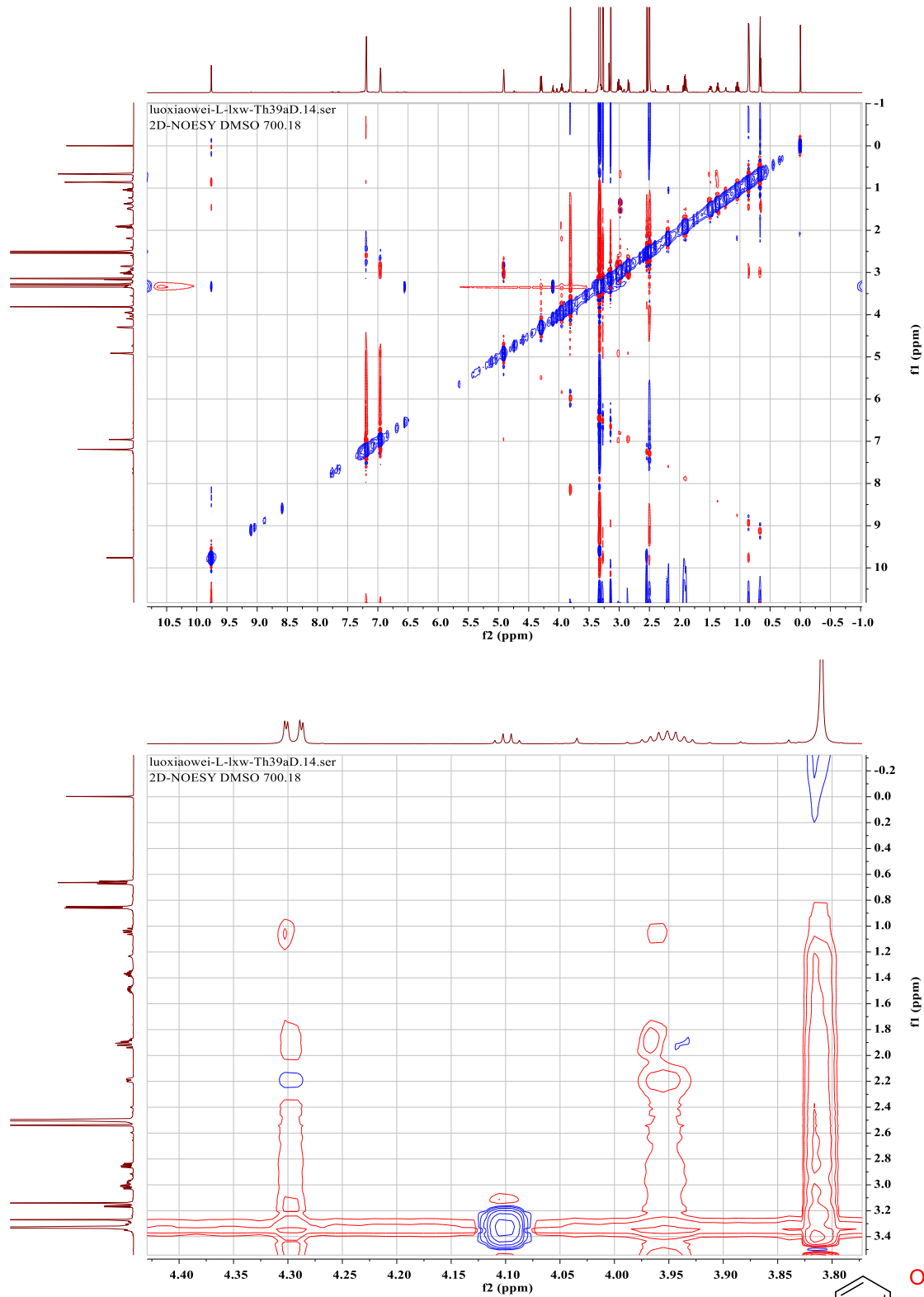
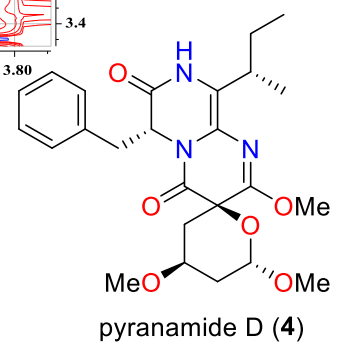


Figure S57. NOESY spectrum of pyranamide D (**4**) (DMSO-*d*₆)



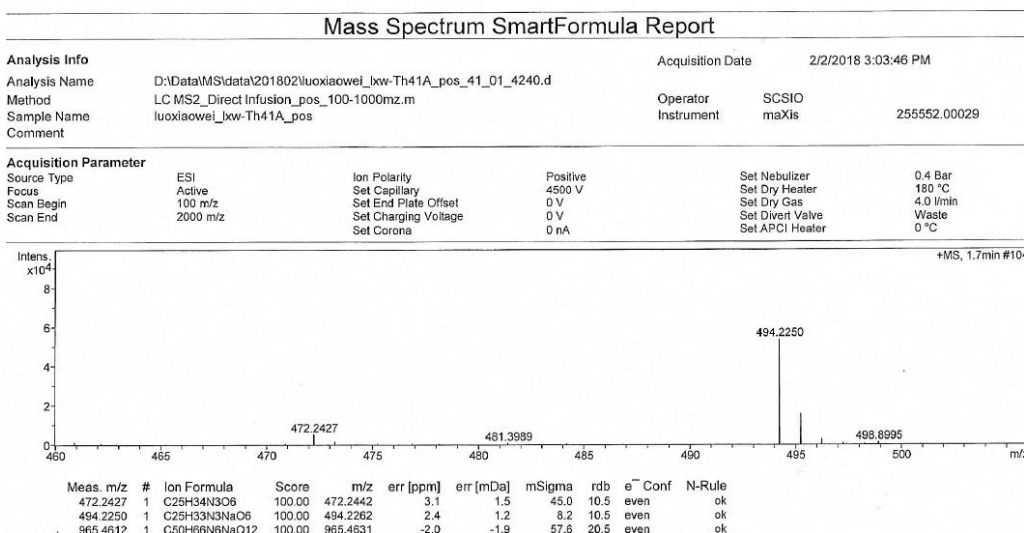


Figure S58. Positive HR-ESI-MS spectrum of pyranamide D (**4**)

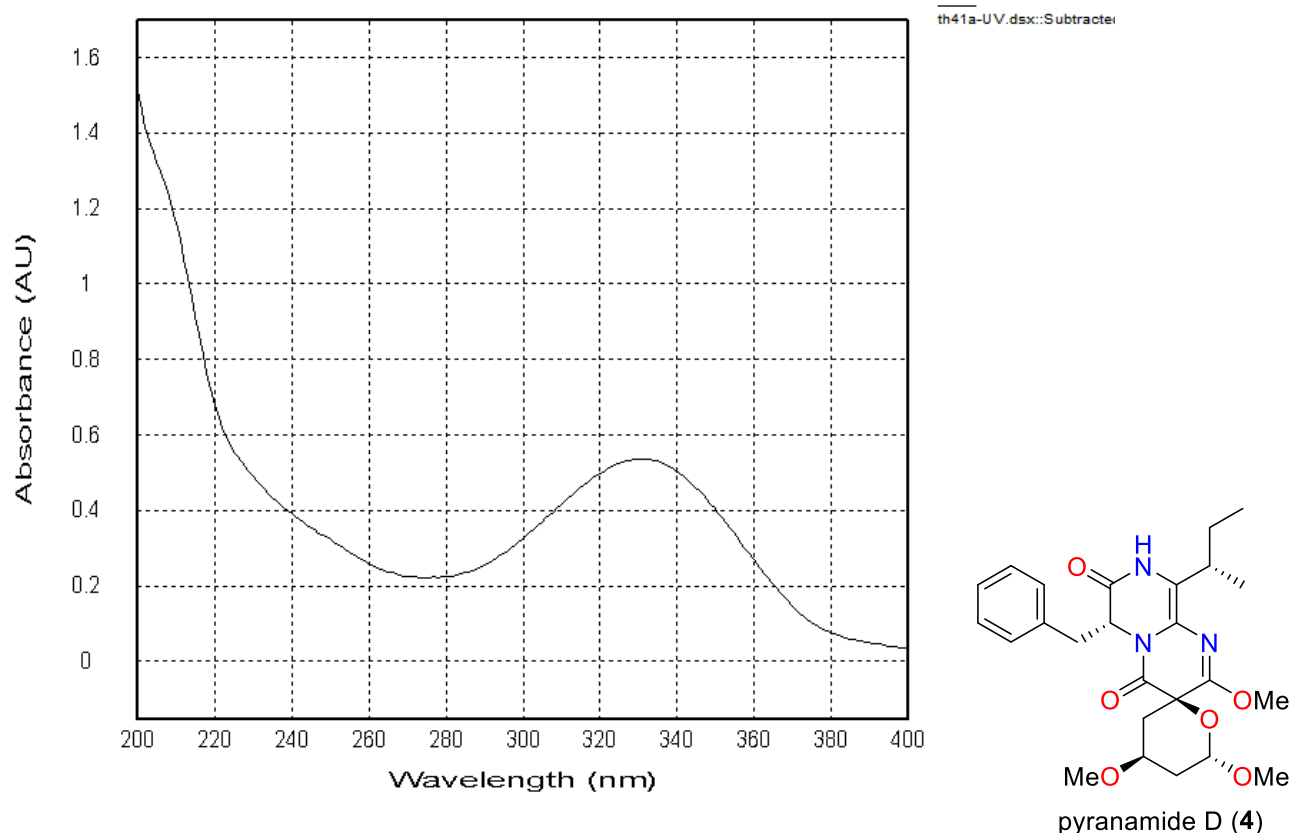


Figure S59. UV spectrum of pyranamide D (**4**)

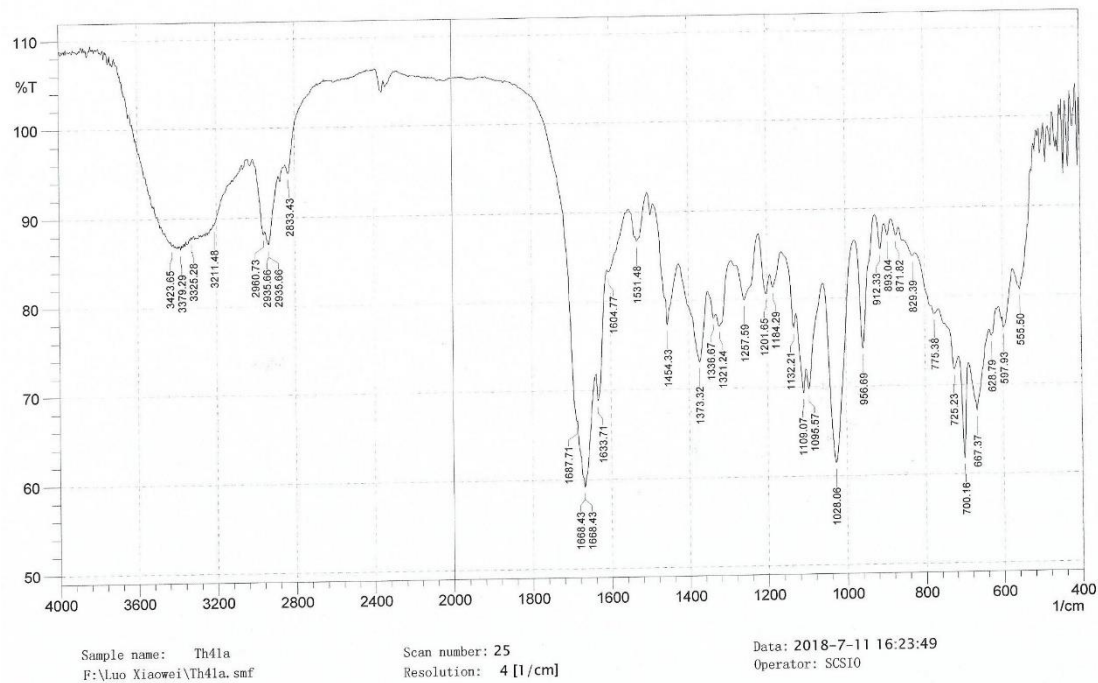


Figure S60. IR spectrum of pyranamide D (**4**)

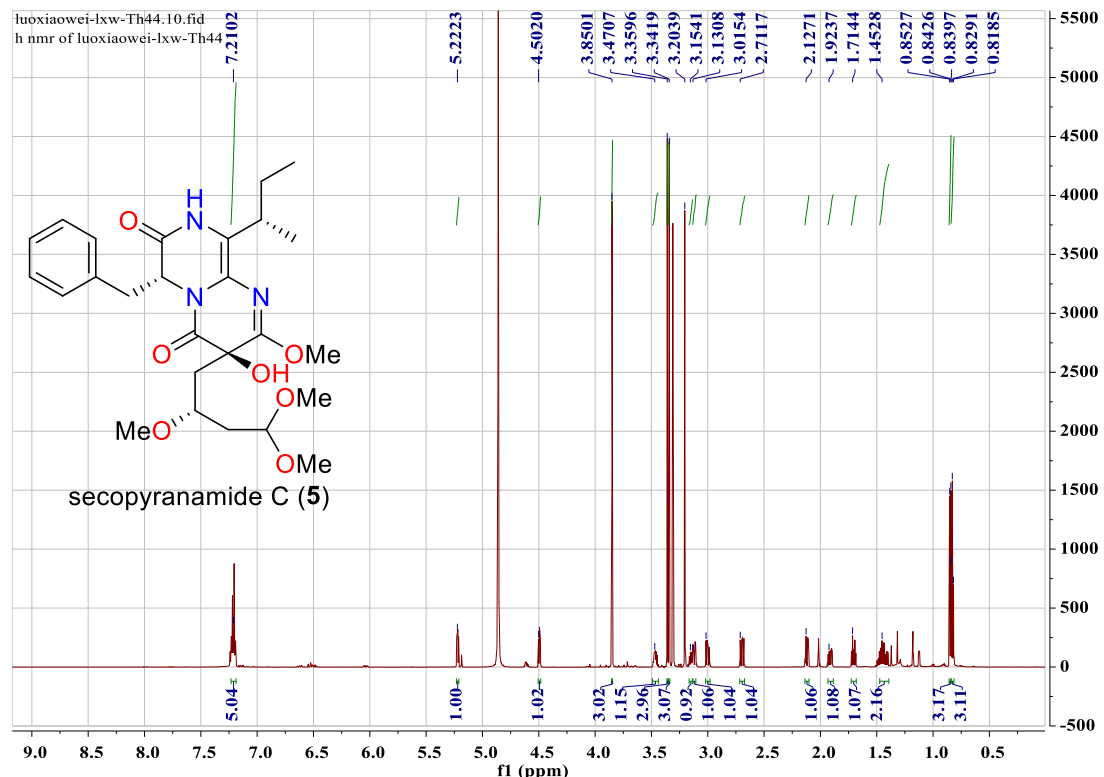


Figure S61. ^1H NMR spectrum of secopyranamide C (**5**) (CD_3OD , 700 MHz)

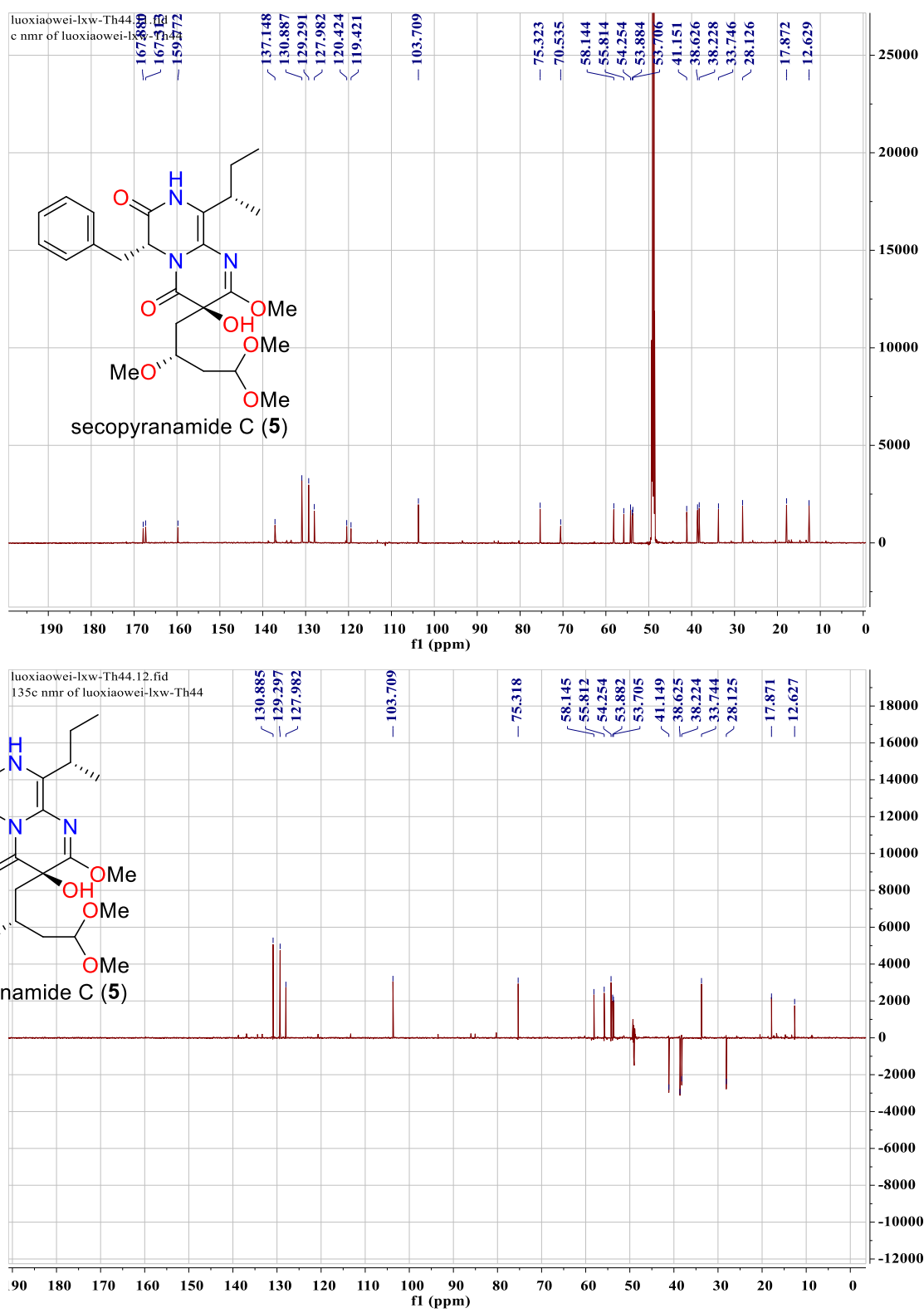


Figure S62. ^{13}C NMR and DEPT spectra of secopyranamide C (**5**) (CD_3OD , 175 MHz)

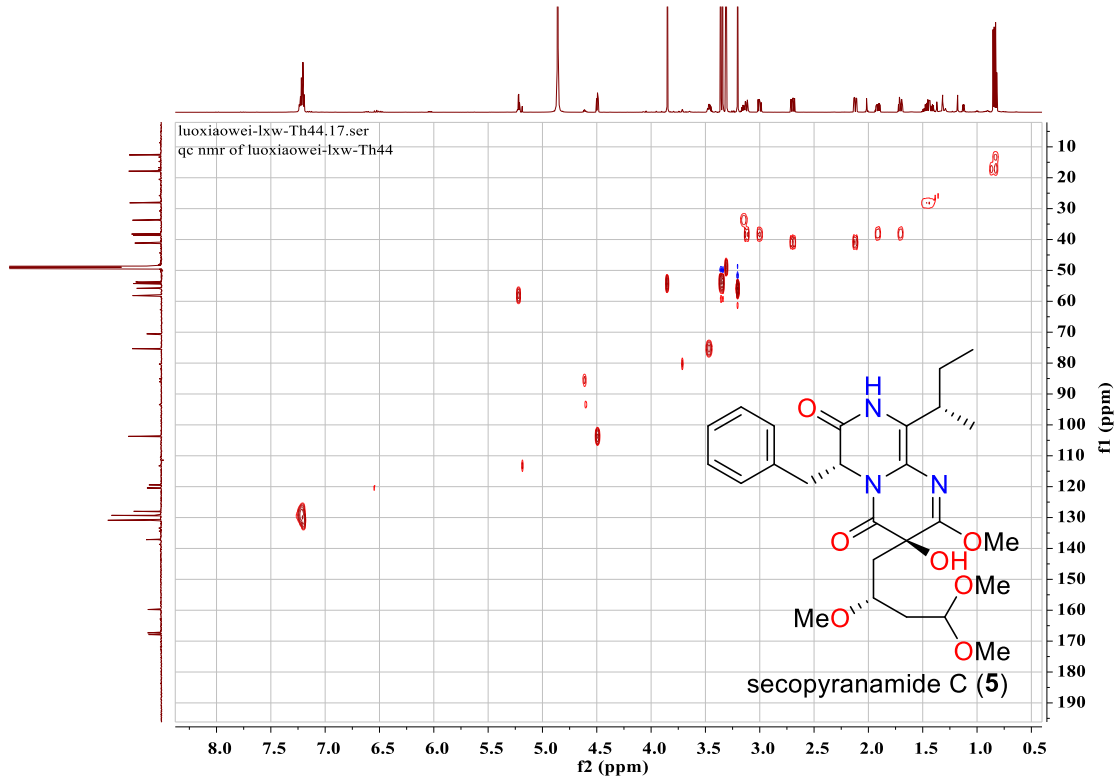


Figure S63. HSQC spectrum of secopyranamide C (5) (CD_3OD)

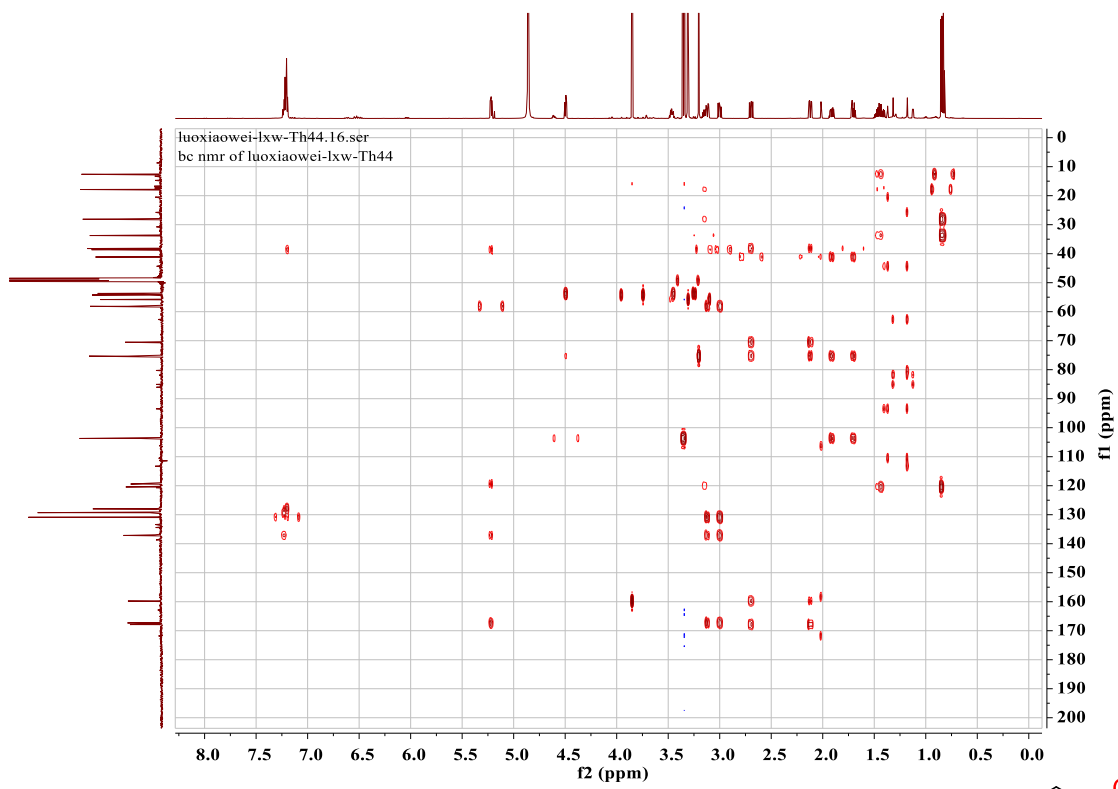
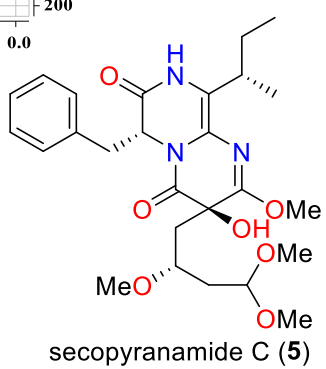


Figure S64. HMBC spectrum of secopyranamide C (5) (CD_3OD)



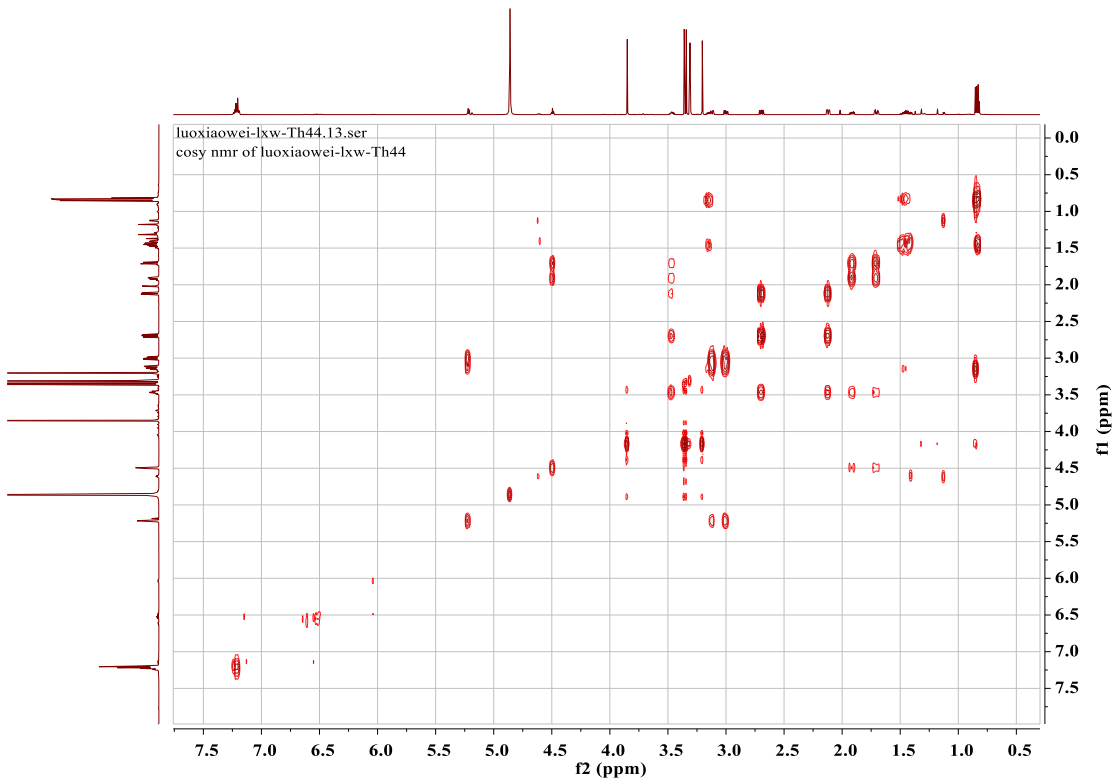


Figure S65. ^1H - ^1H COSY spectrum of secopyranamide C (**5**) (CD_3OD)

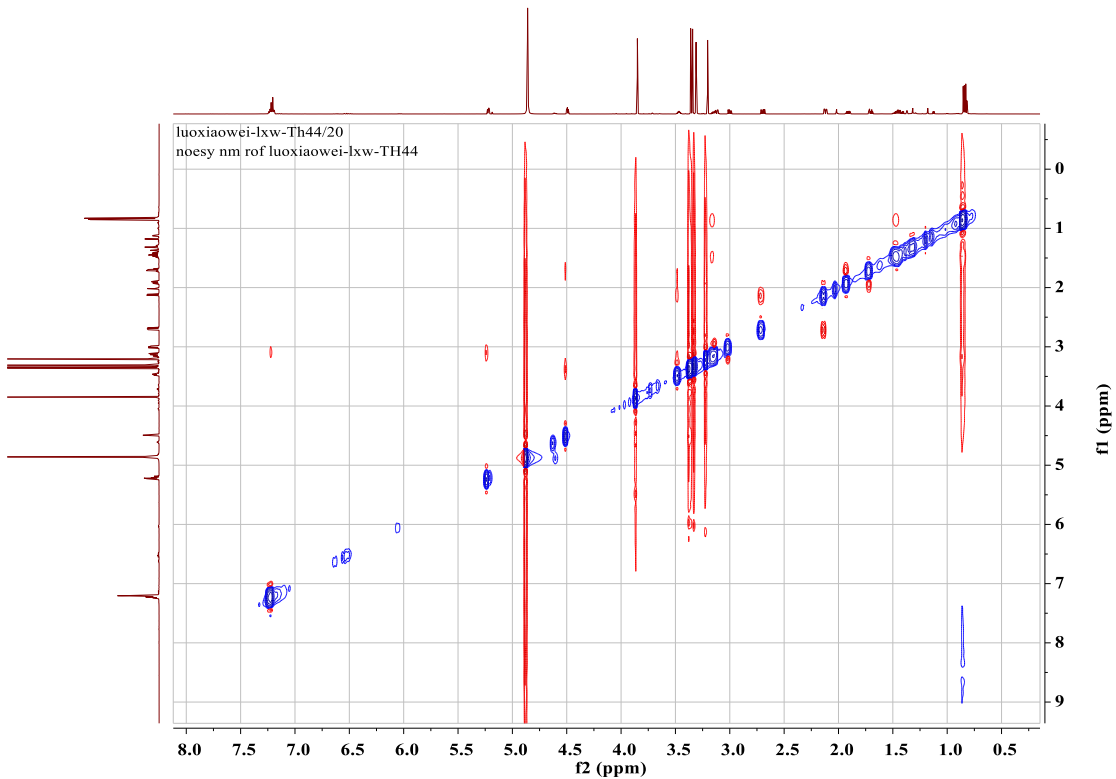
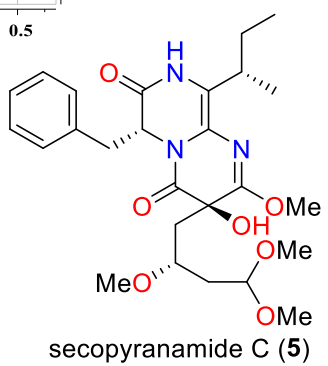


Figure S66. NOESY spectrum of secopyranamide C (**5**) (CD_3OD)



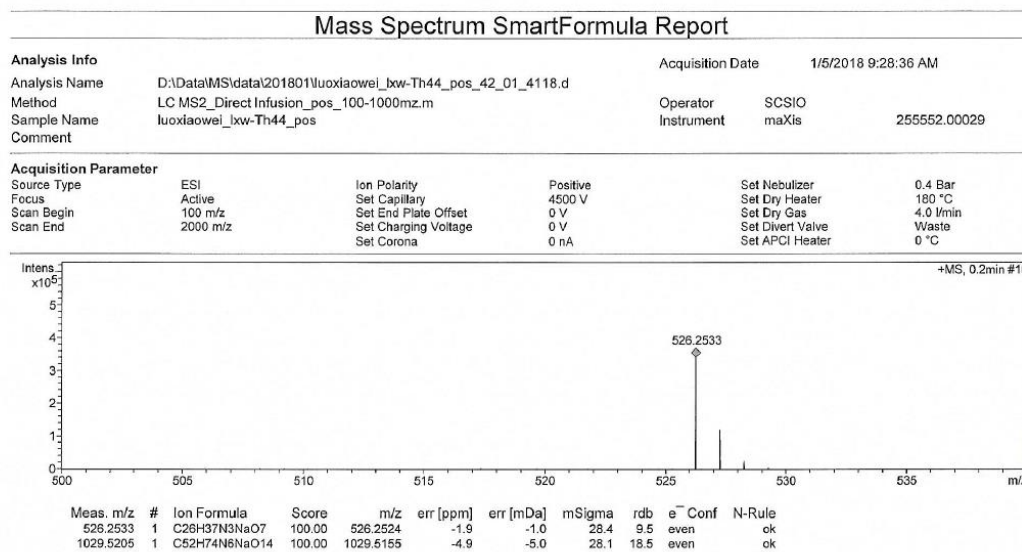


Figure S67. Positive HR-ESI-MS spectrum of secopyranamide C (**5**)

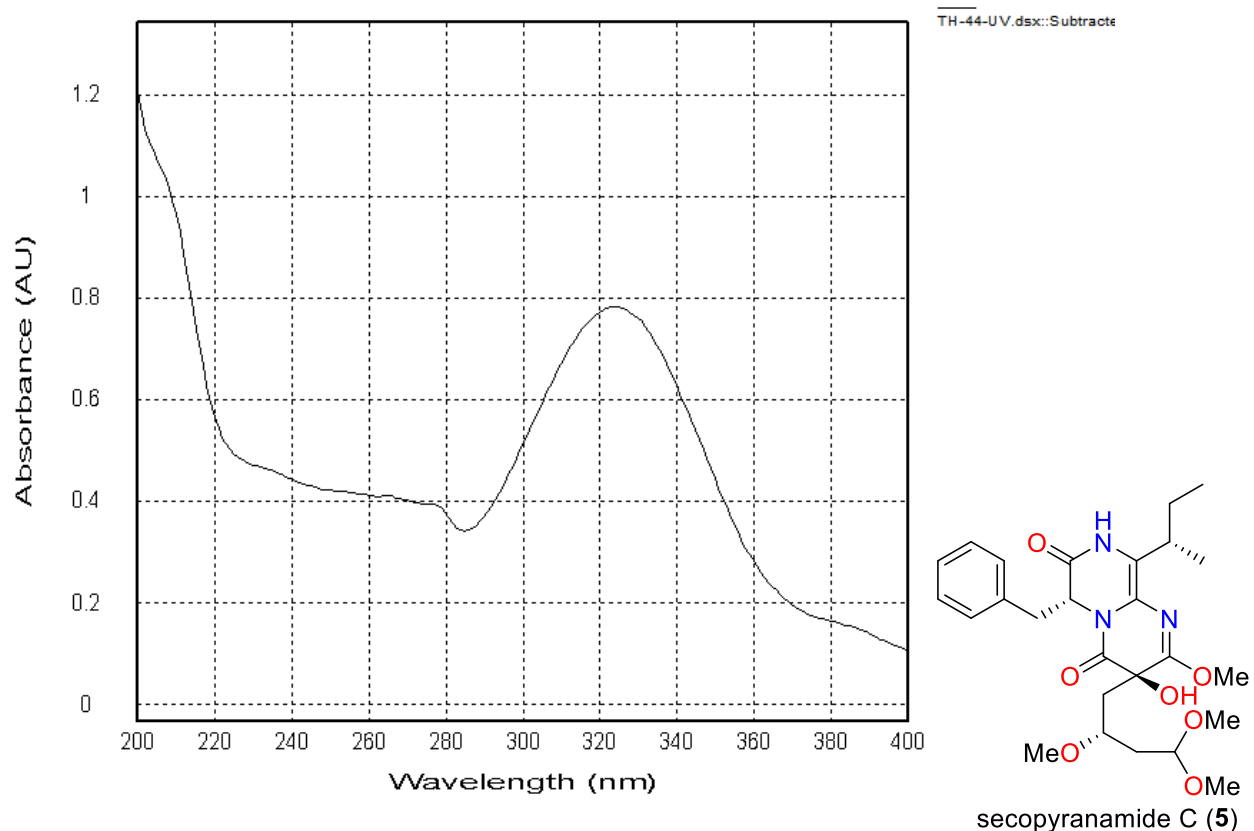


Figure S68. UV spectrum of secopyranamide C (**5**)

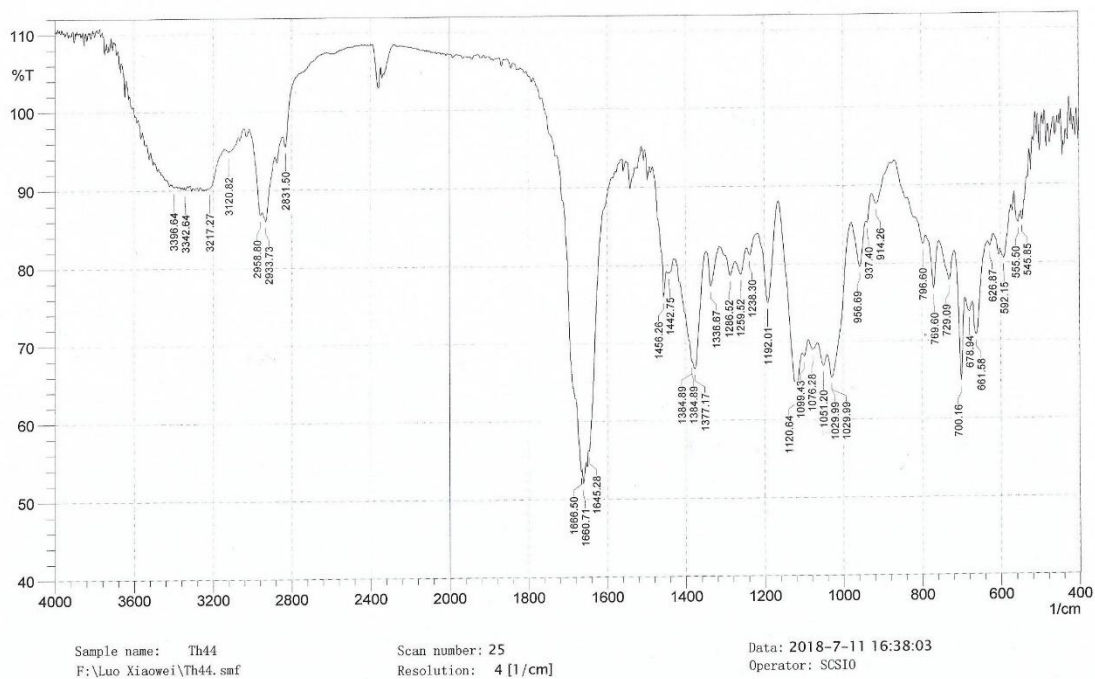


Figure S69. IR spectrum of secopyranamide C (5)

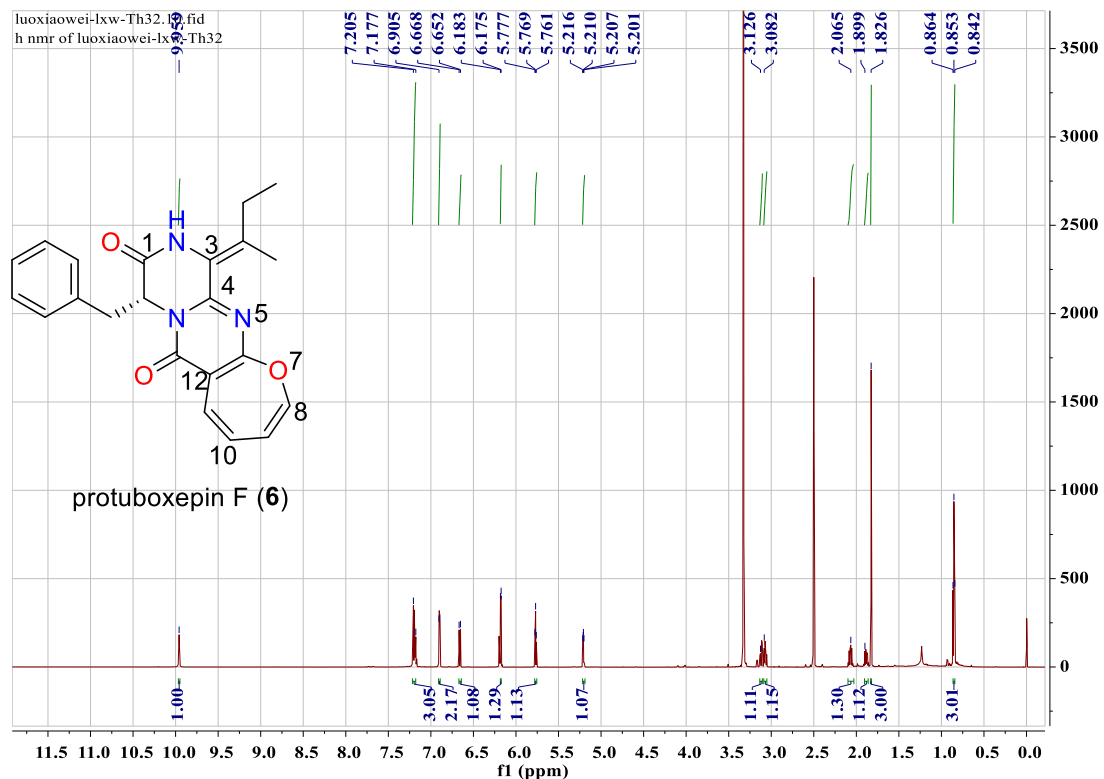


Figure S70. ^1H NMR spectrum of protuboxepin F (6) ($\text{DMSO}-d_6$, 700 MHz)

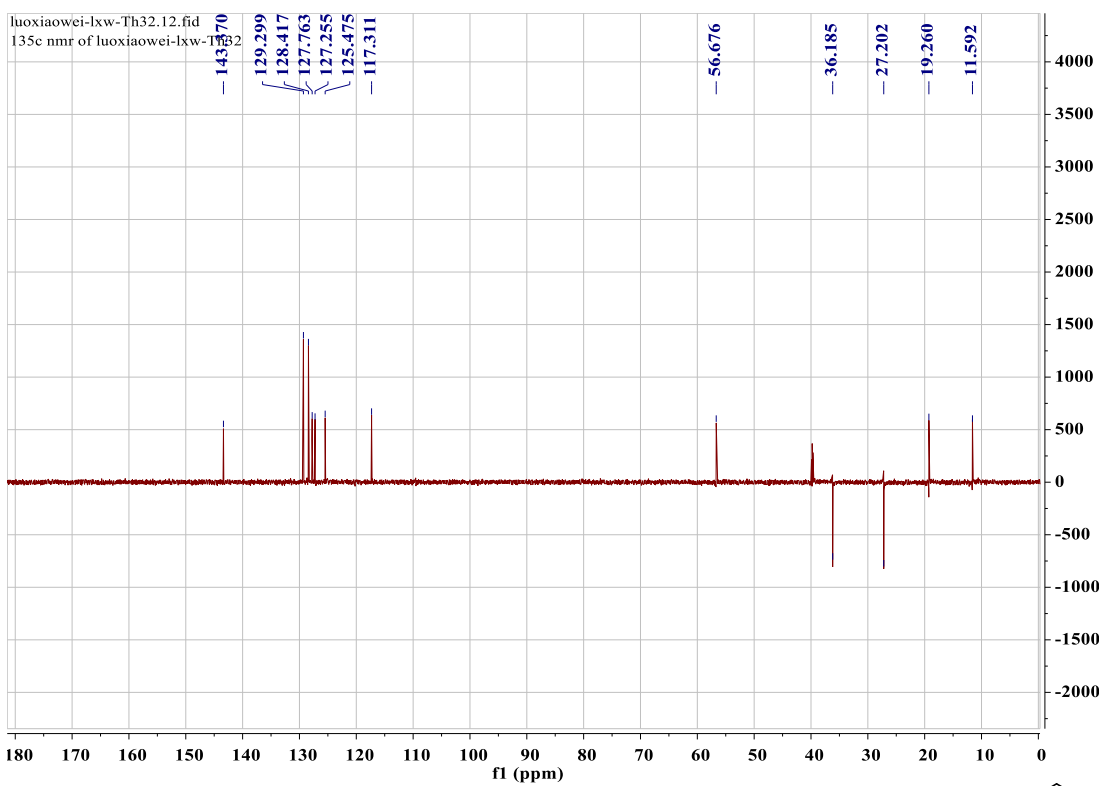
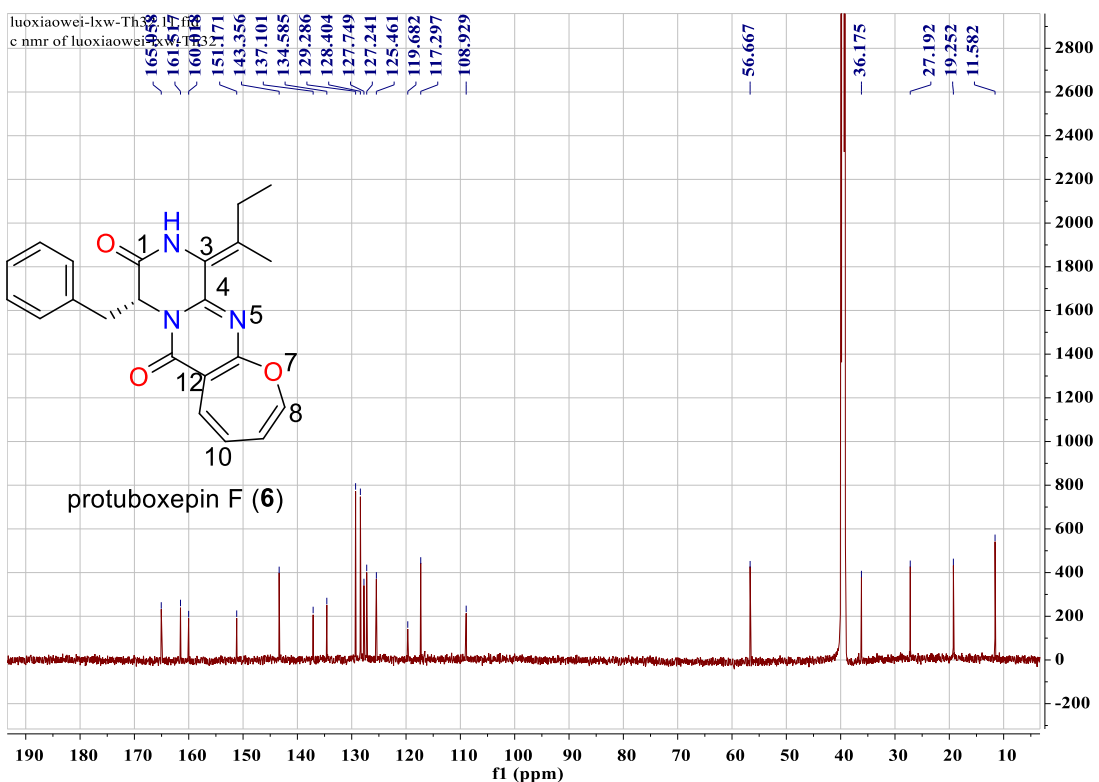
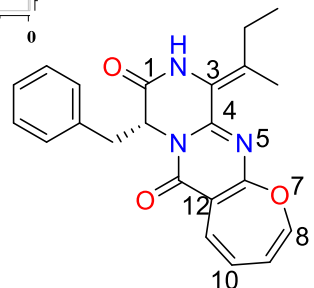


Figure S71. ^{13}C NMR and DEPT spectra of protuboxepin F (6) (DMSO- d_6 , 175 MHz)



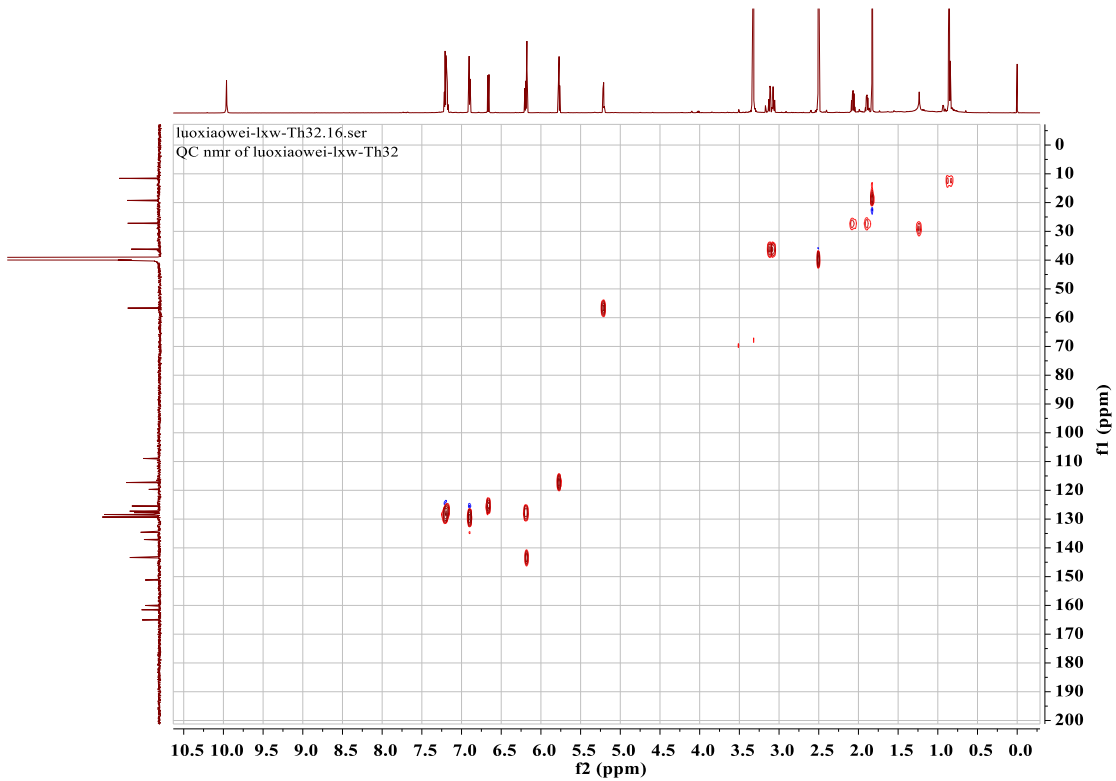


Figure S72. HSQC spectrum of protuboxepin F (**6**) (DMSO-*d*₆)

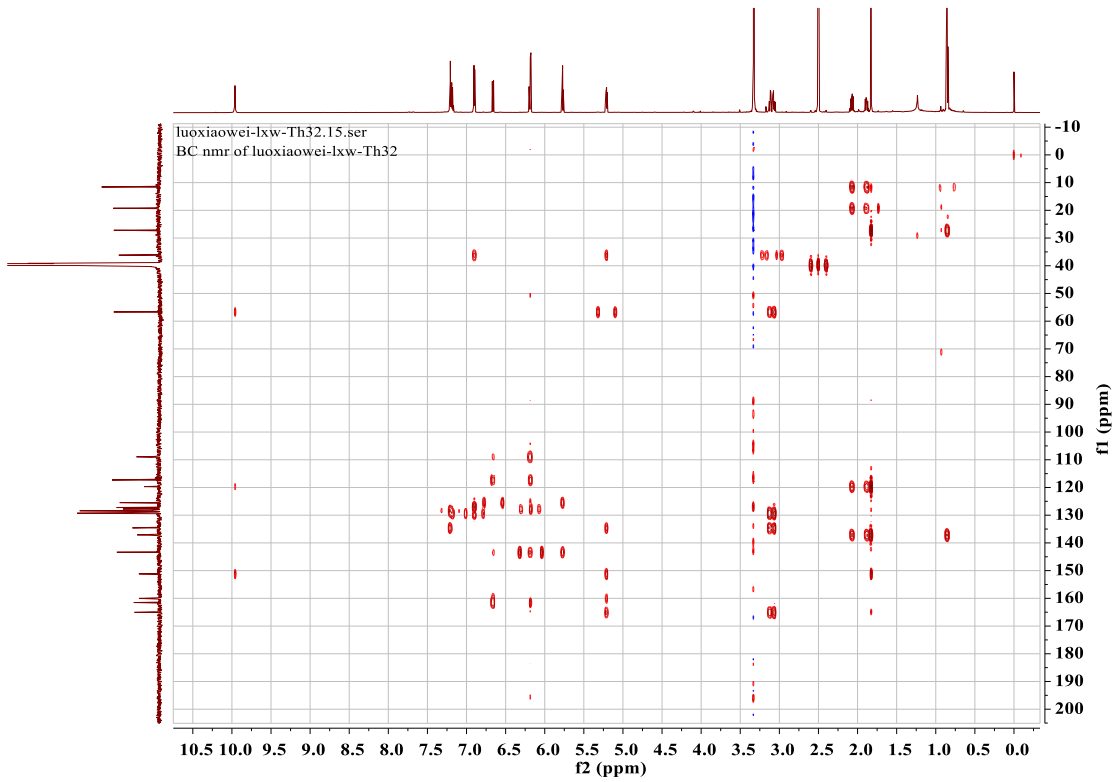
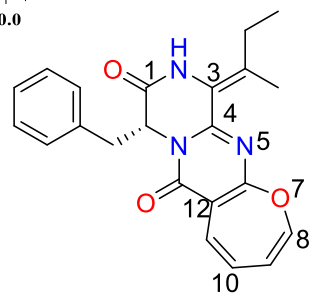


Figure S73. HMBC spectrum of protuboxepin F (**6**) (DMSO-*d*₆)



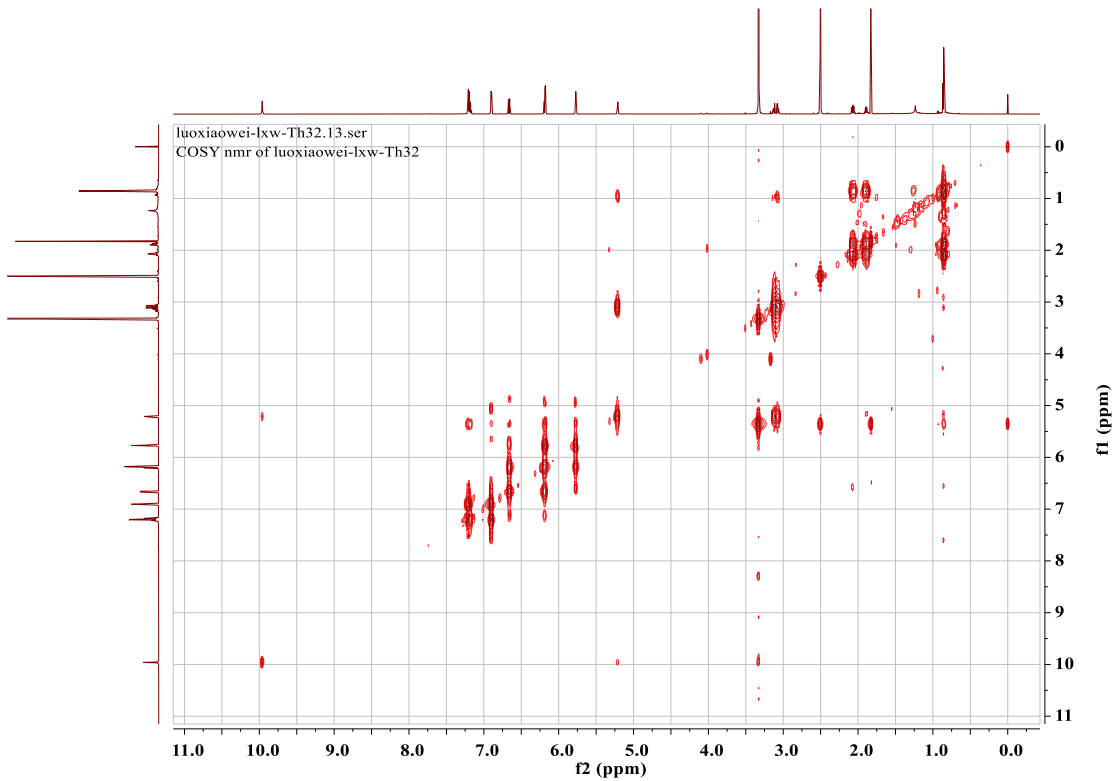
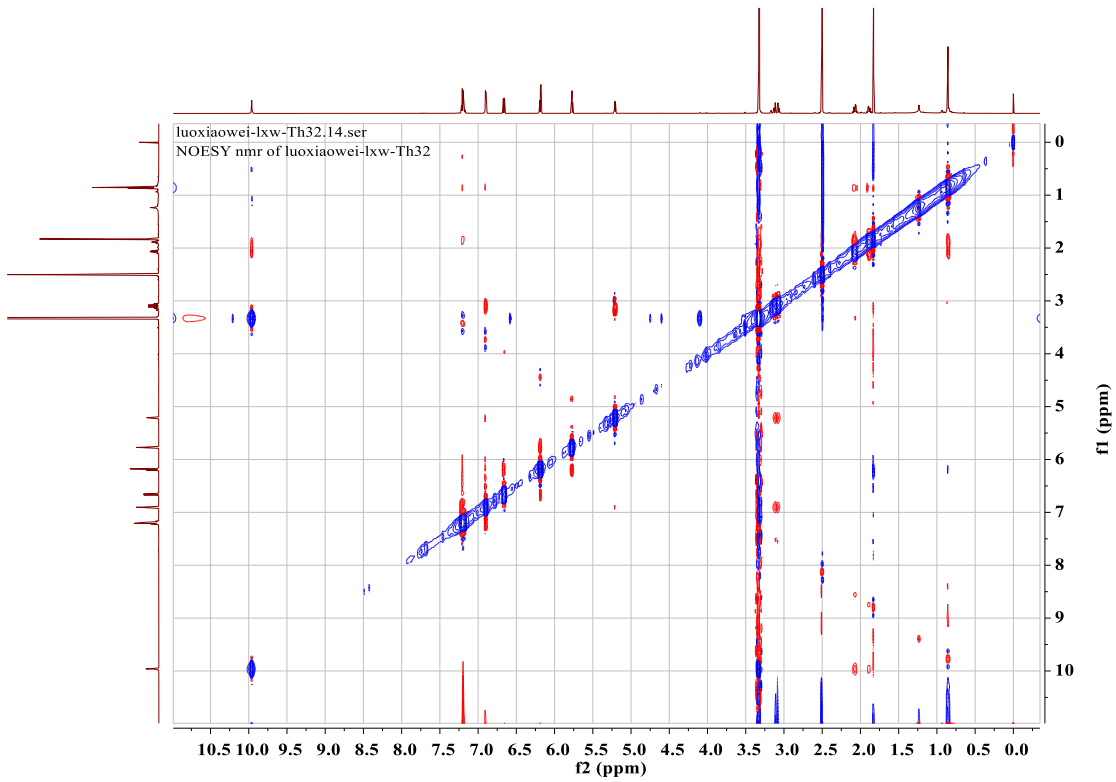


Figure S74. ^1H - ^1H COSY spectrum of protuboxepin F (**6**) (DMSO- d_6)



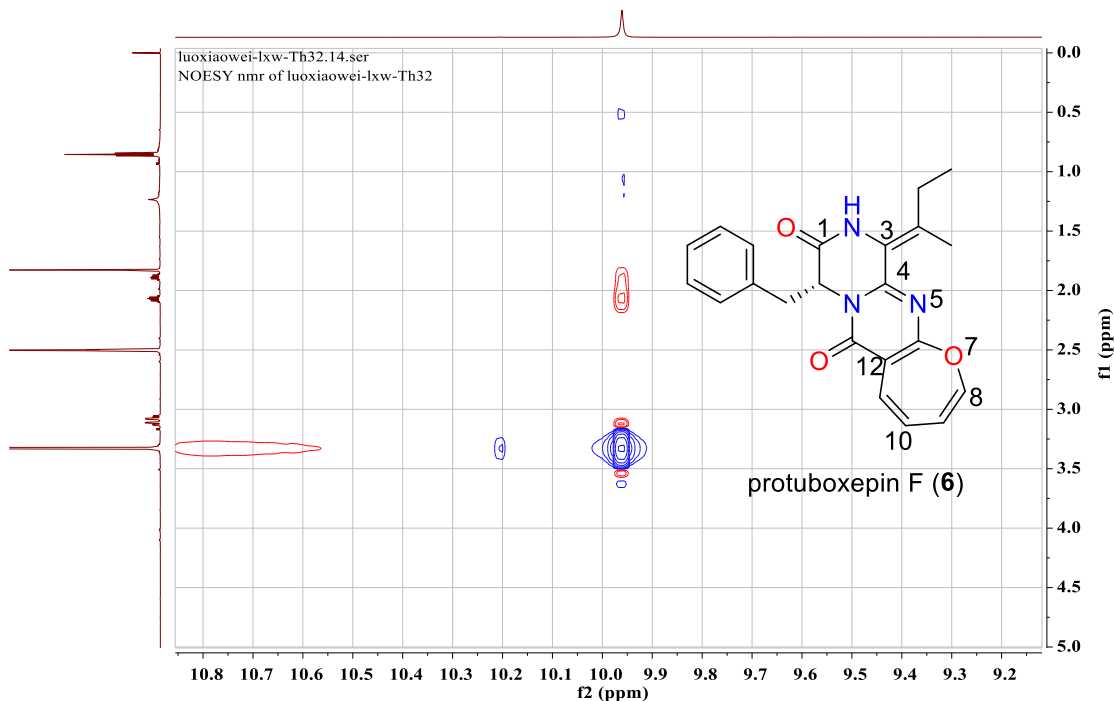


Figure S75. NOESY spectrum of protuboxepin F (**6**) (DMSO-*d*₆)

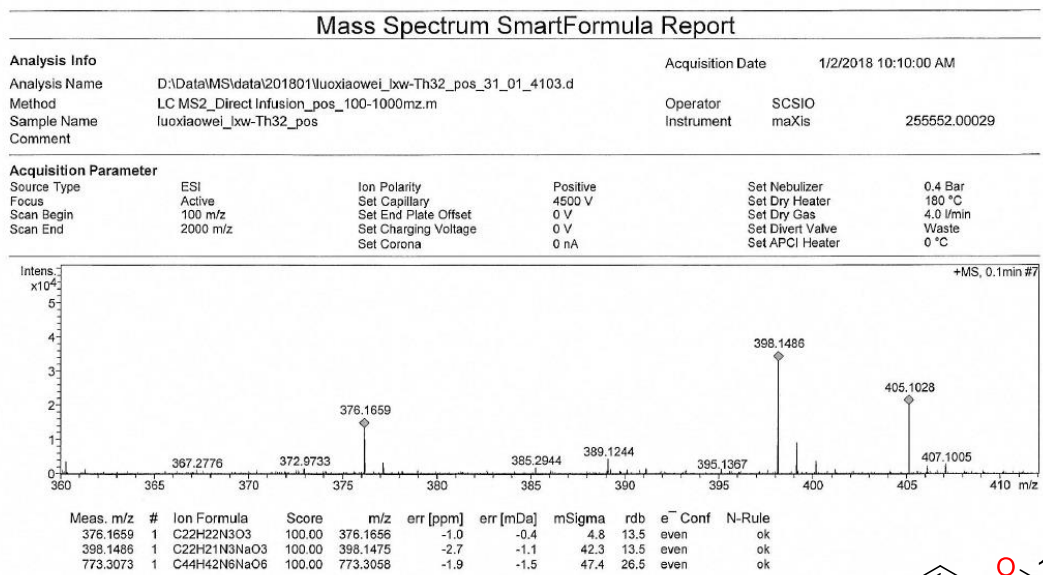
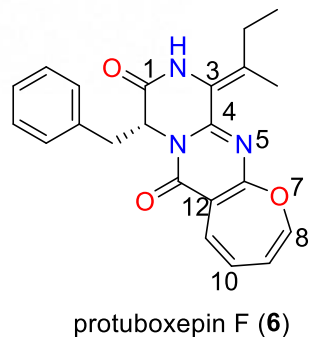


Figure S76. Positive HR-ESI-MS spectrum of protuboxepin F (**6**)



protuboxepin F (**6**)

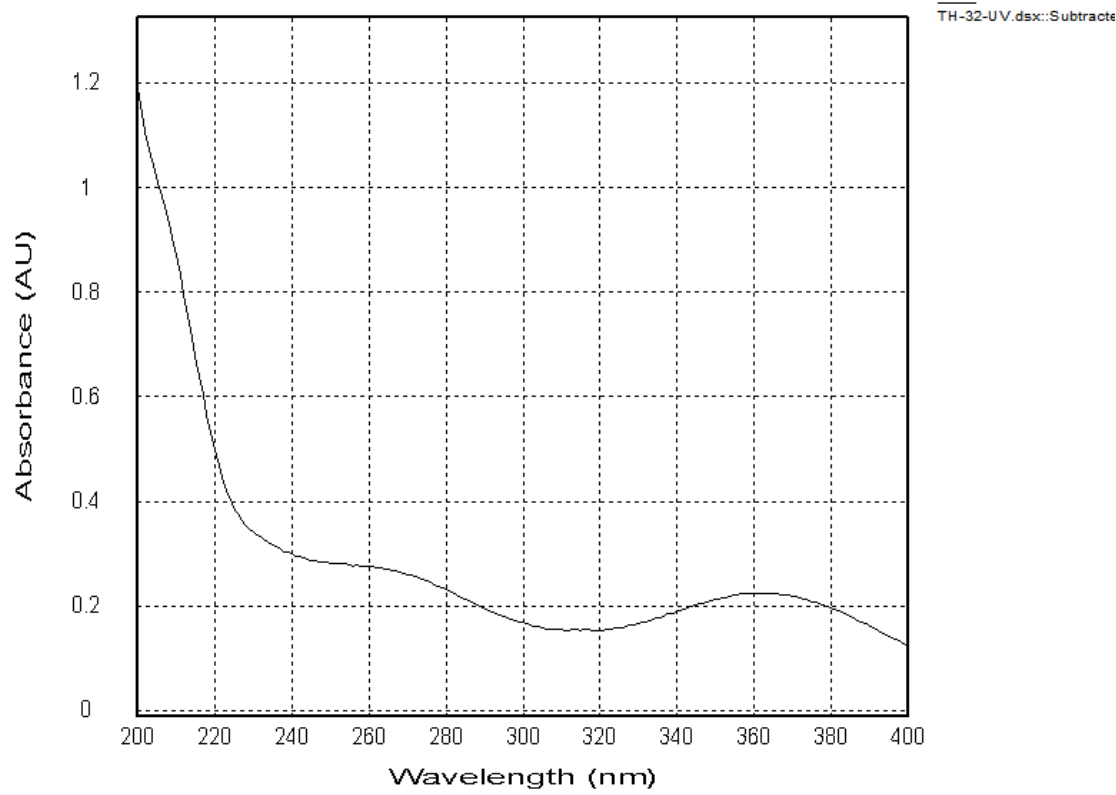


Figure S77. UV spectrum of protuboxepin F (**6**)

SHIMADZU

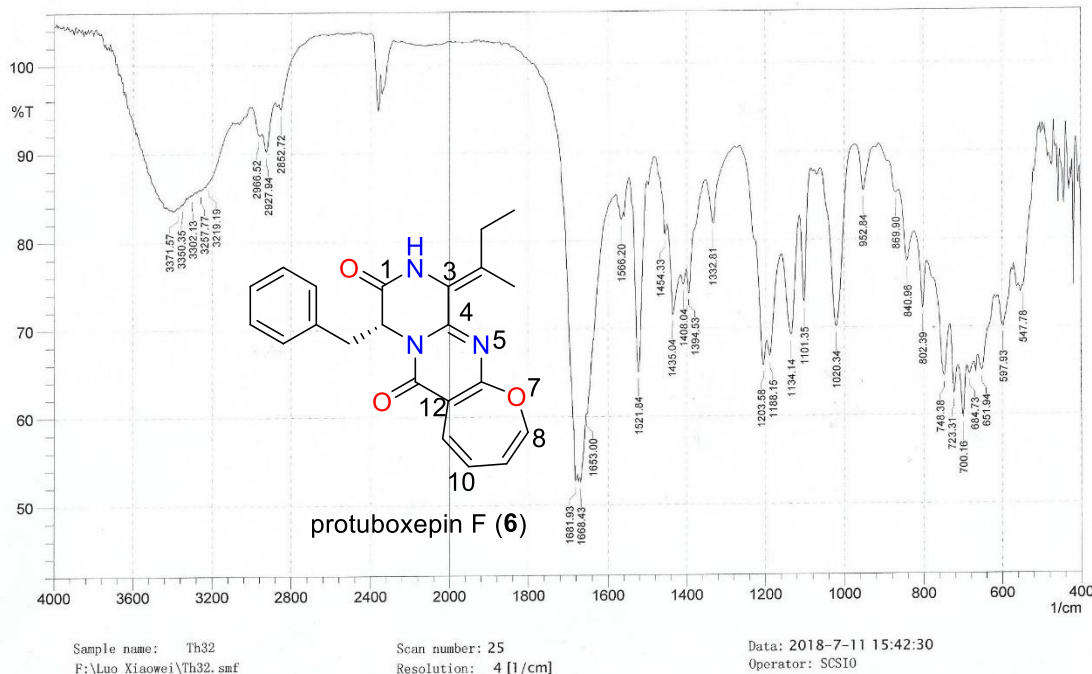


Figure S78. IR spectrum of protuboxepin F (**6**)

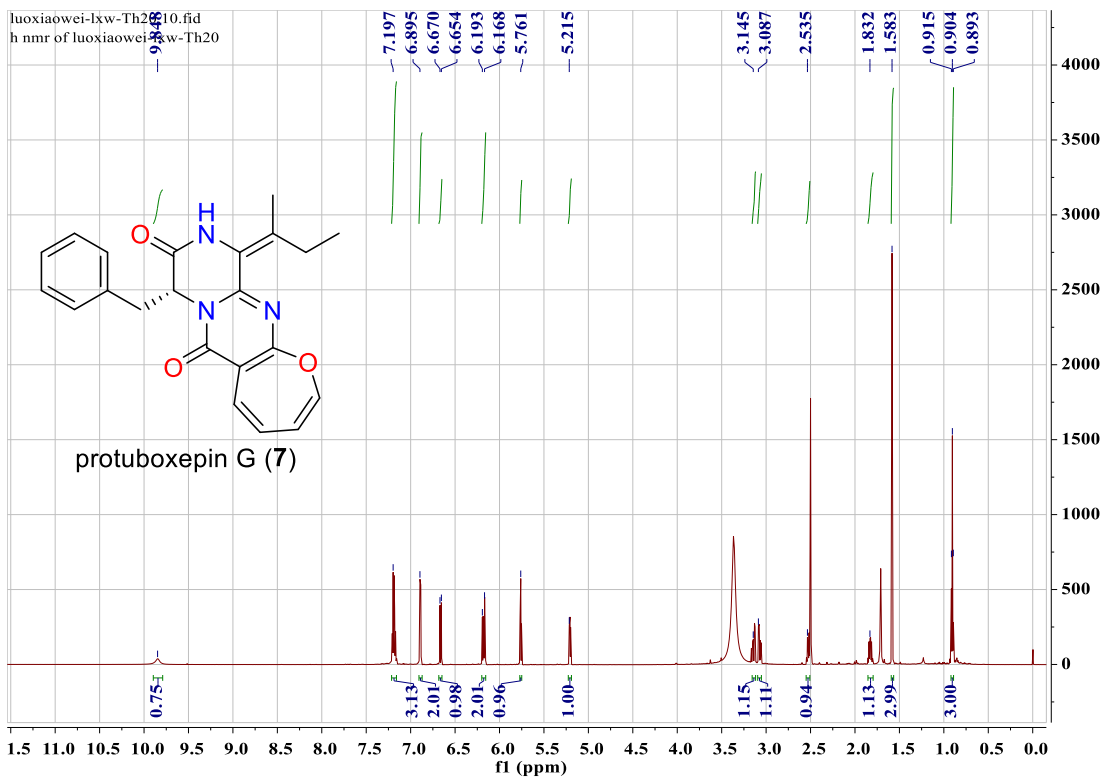
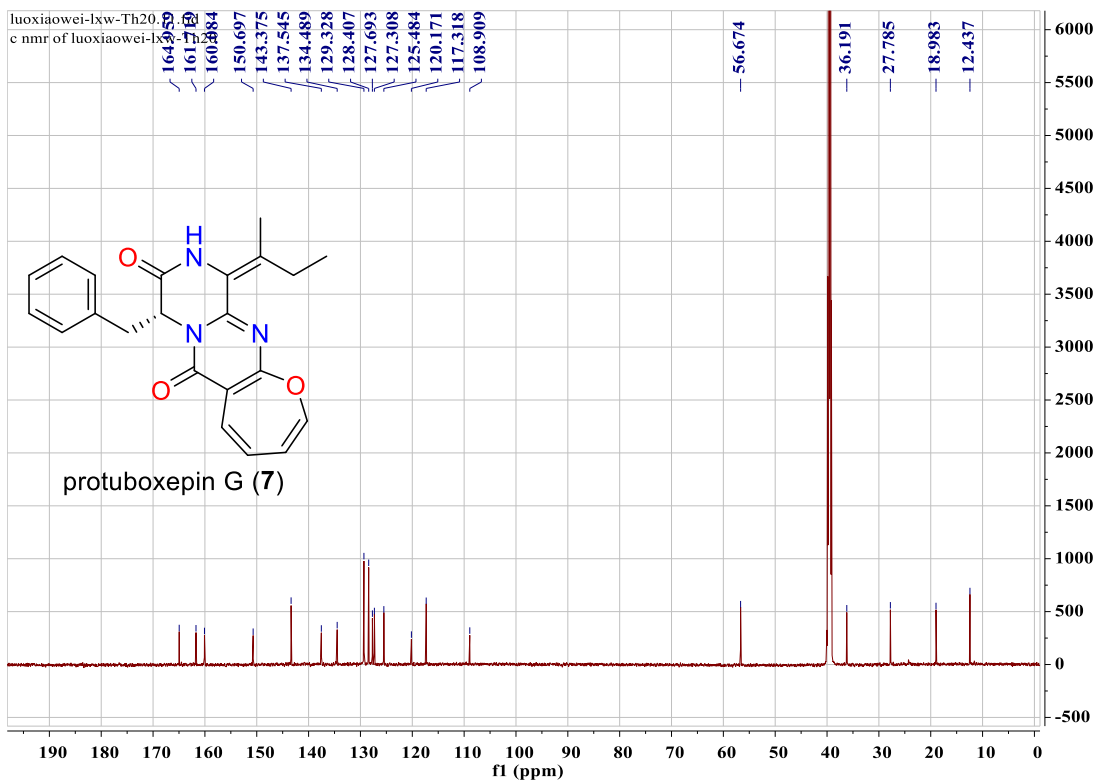


Figure S79. ¹H NMR spectrum of protuboxepin G (7) (DMSO-*d*₆, 700 MHz)



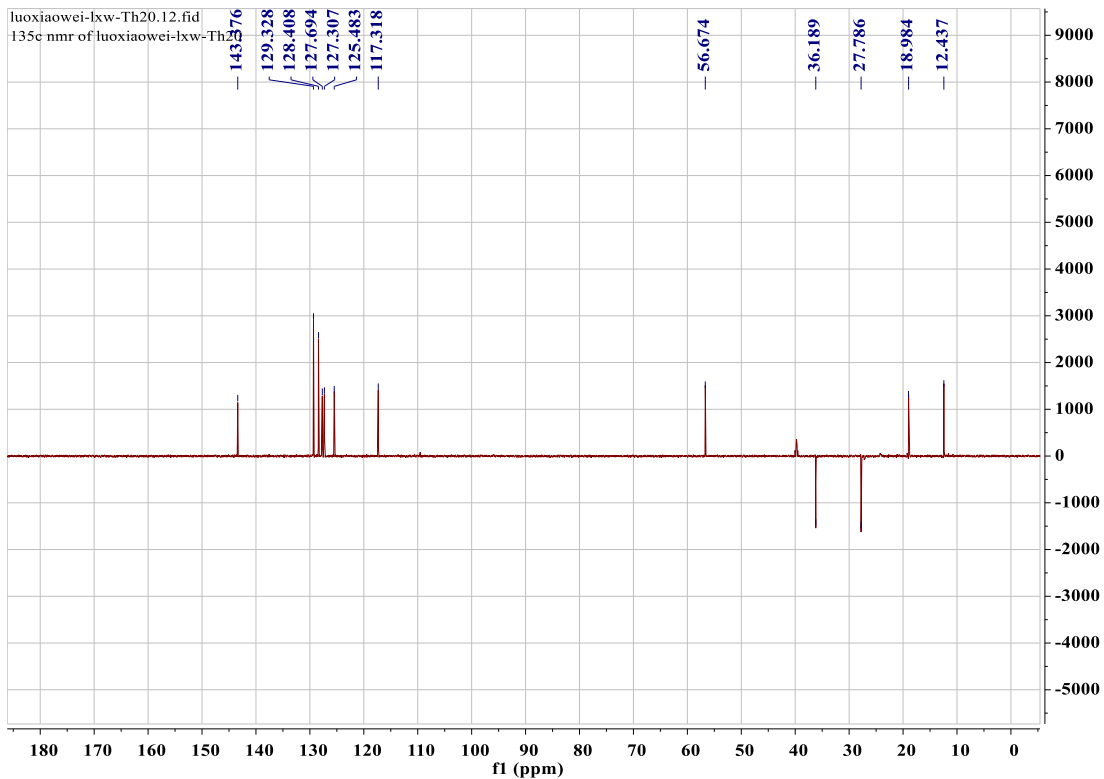


Figure S80. ¹³C NMR and DEPT spectra of protuboxepin G (7) (DMSO-*d*₆, 175 MHz)

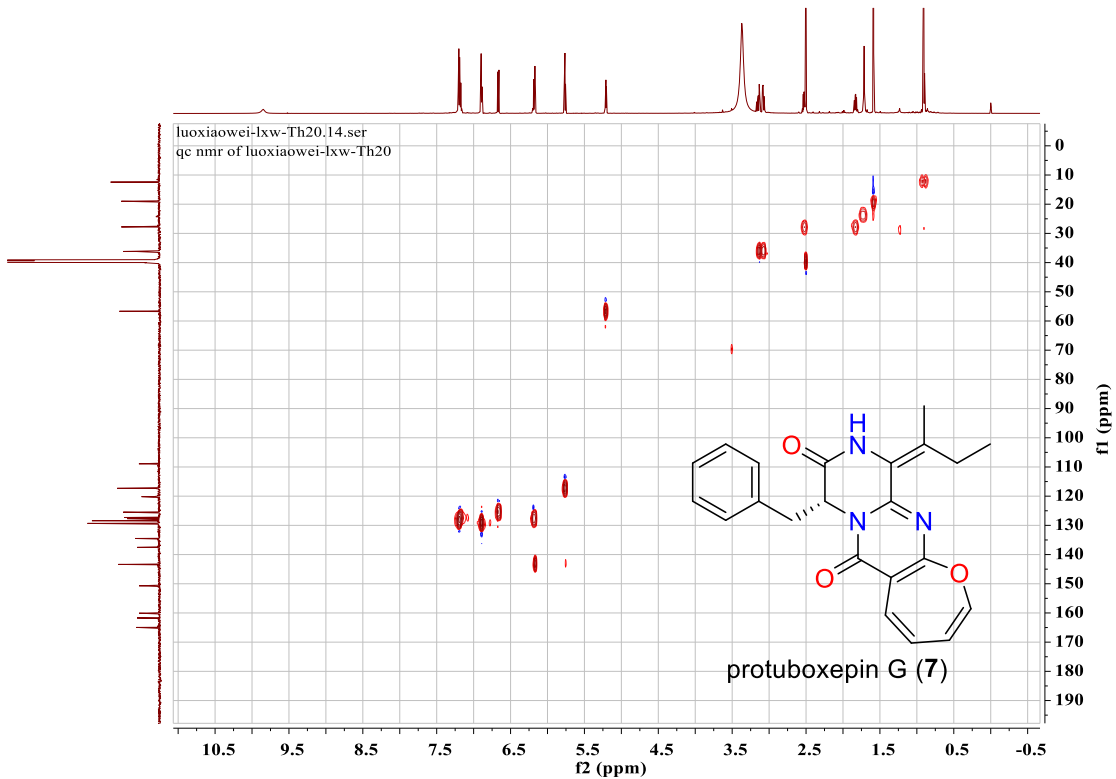


Figure S81. HSQC spectrum of protuboxepin G (7) (DMSO-*d*₆)

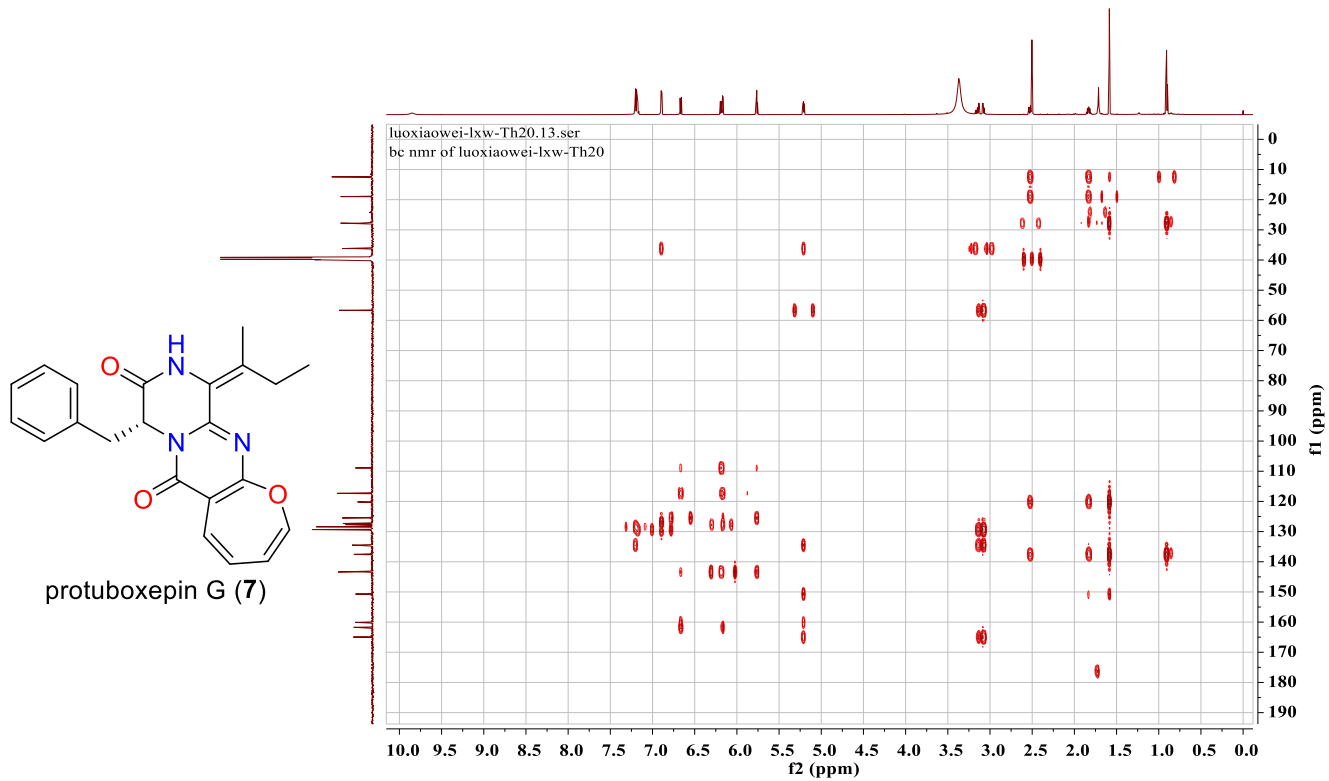


Figure S82. HMBC spectrum of protuboxepin G (7) (DMSO- d_6)

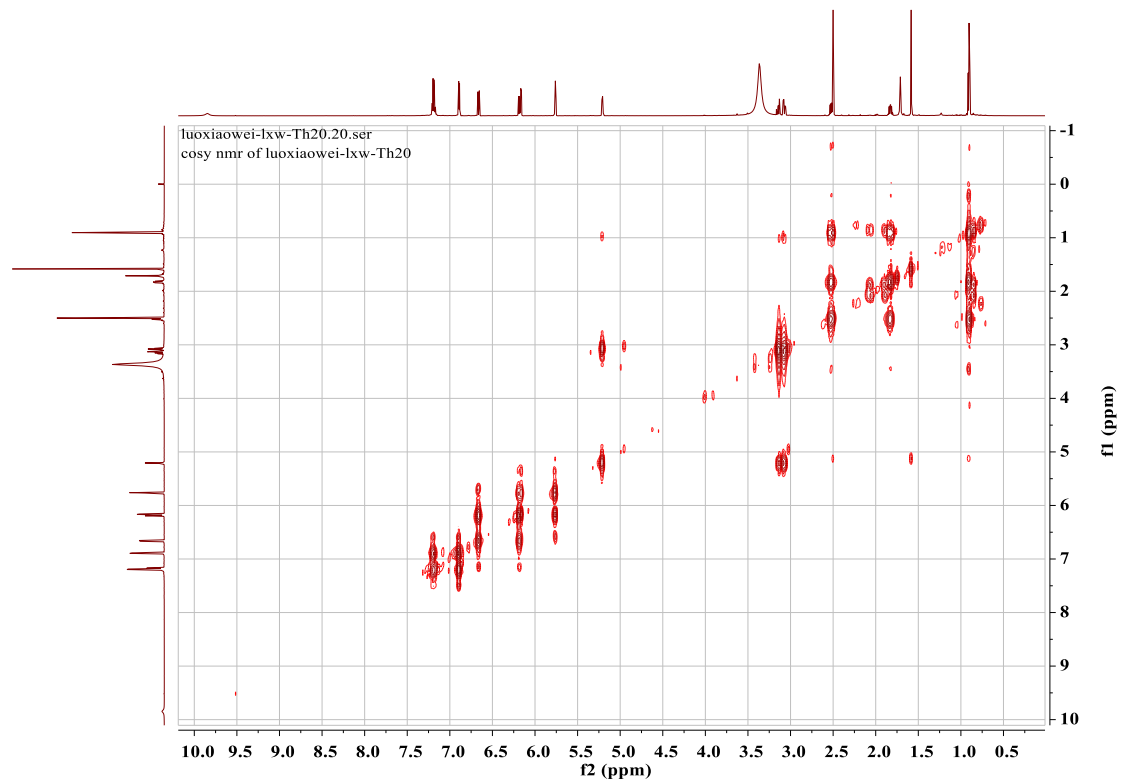
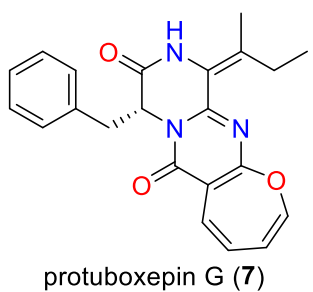


Figure S83. ^1H - ^1H COSY spectrum of protuboxepin G (7) (DMSO- d_6)



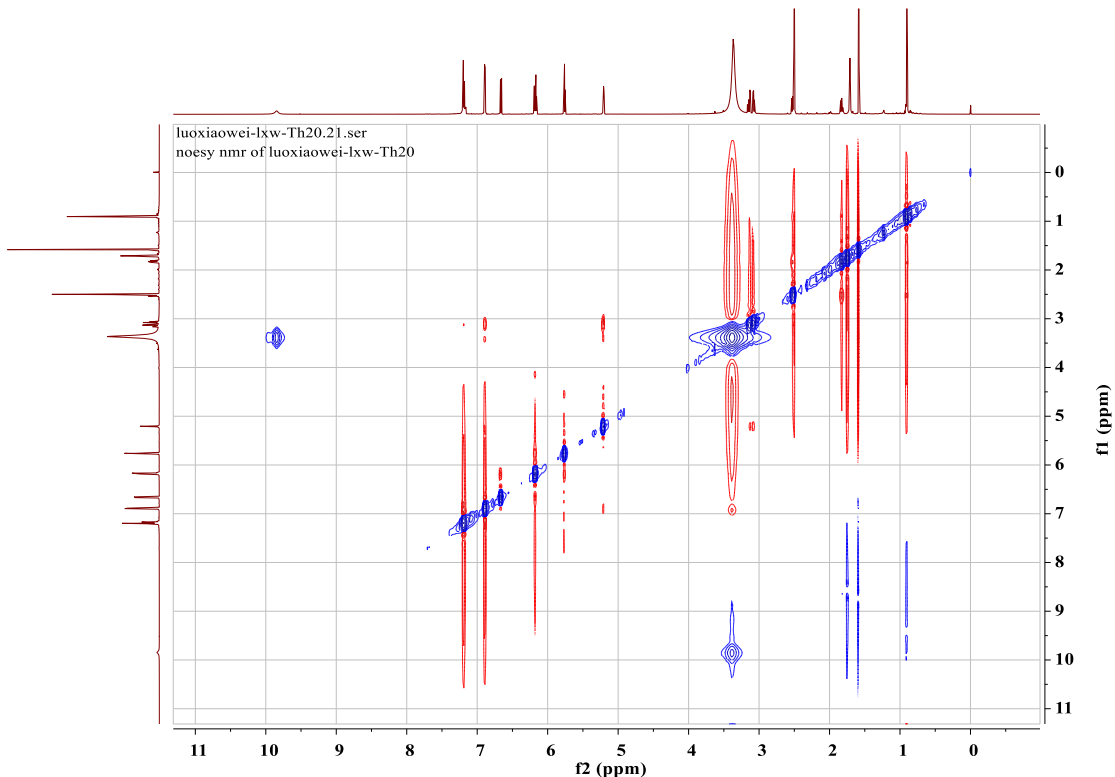


Figure S84. NOESY spectrum of protuboxepin G (7) ($\text{DMSO}-d_6$)

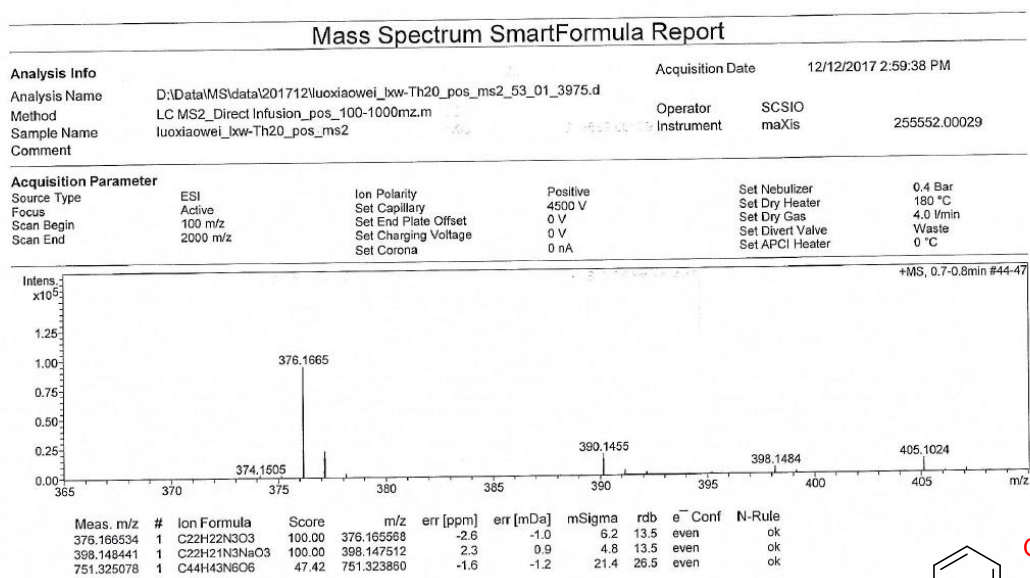
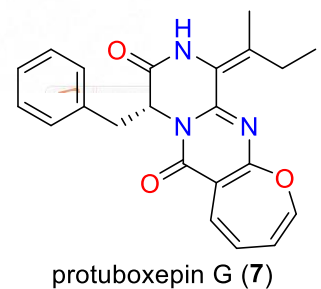


Figure S85. Positive HR-ESI-MS spectrum of protuboxepin G (7)



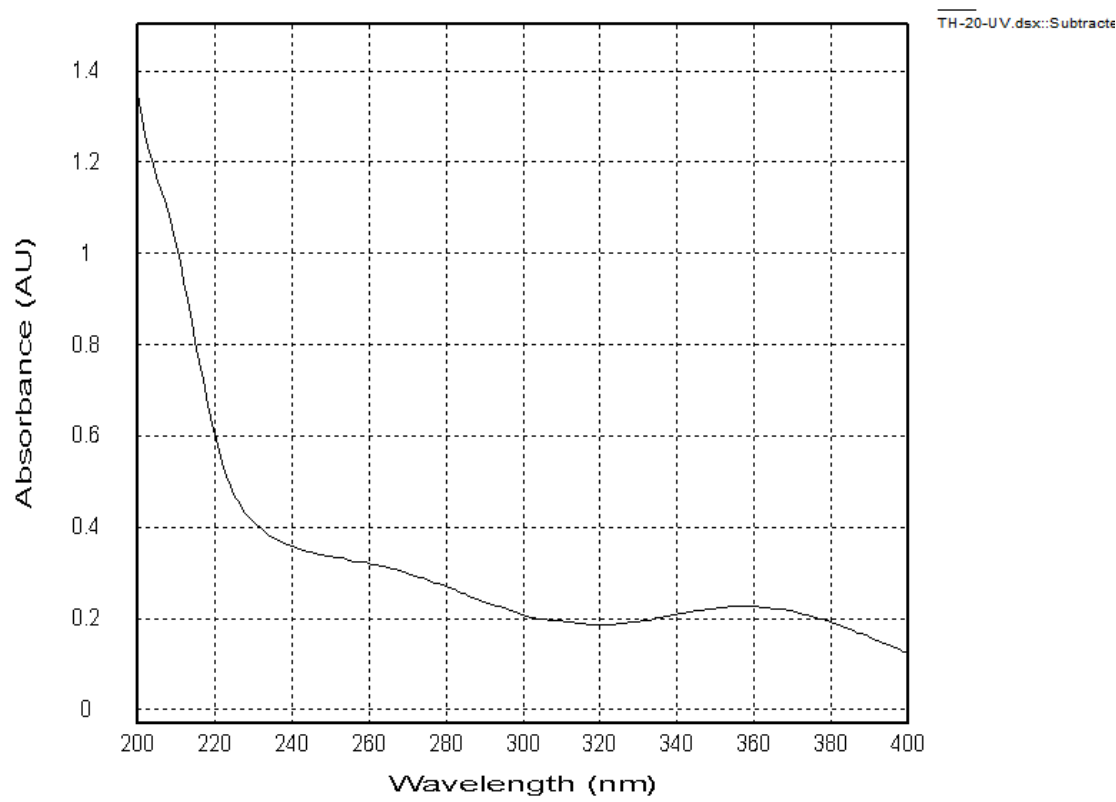


Figure S86. UV spectrum of protuboxepin G (7)

SHIMADZU

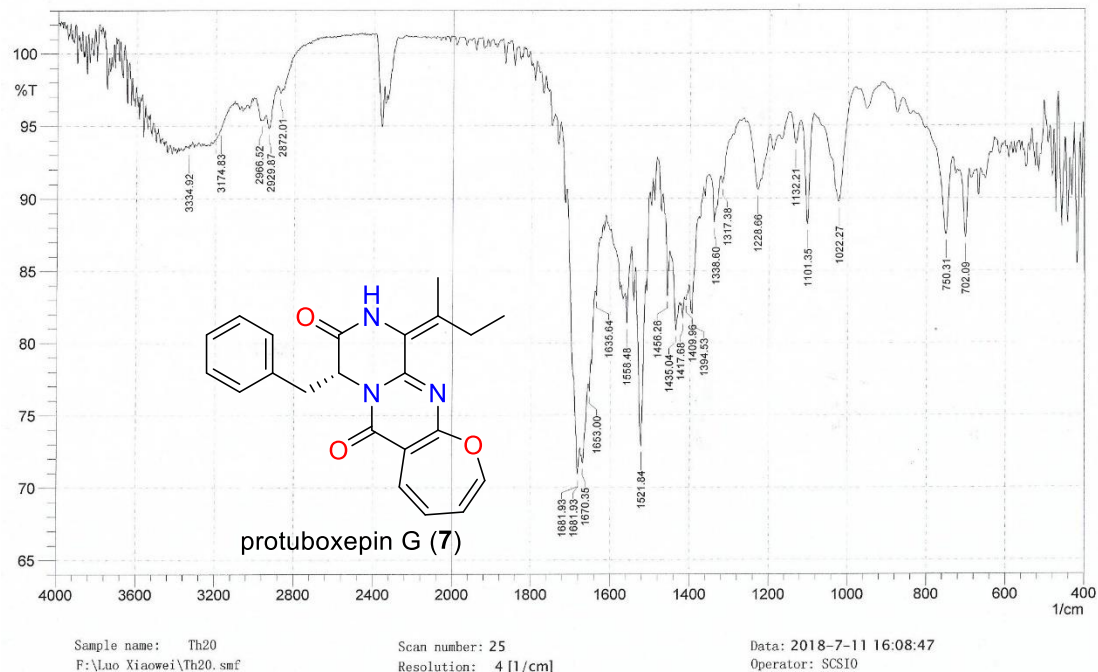


Figure S87. IR spectrum of protuboxepin G (7)

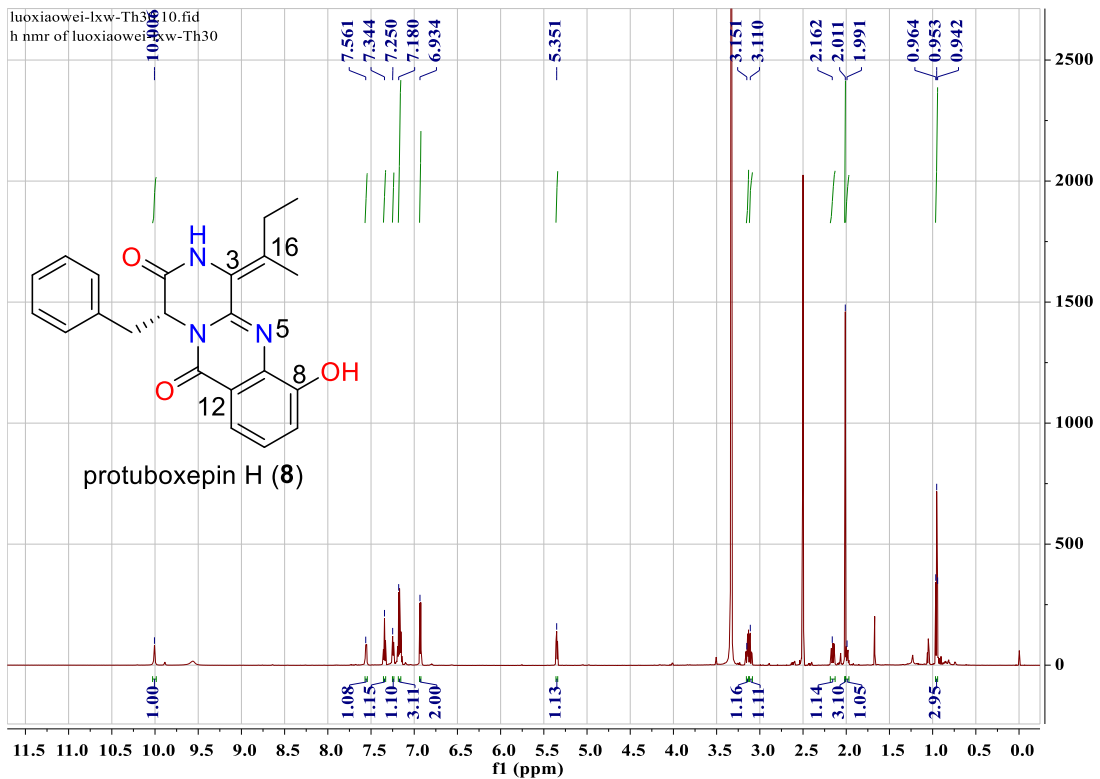
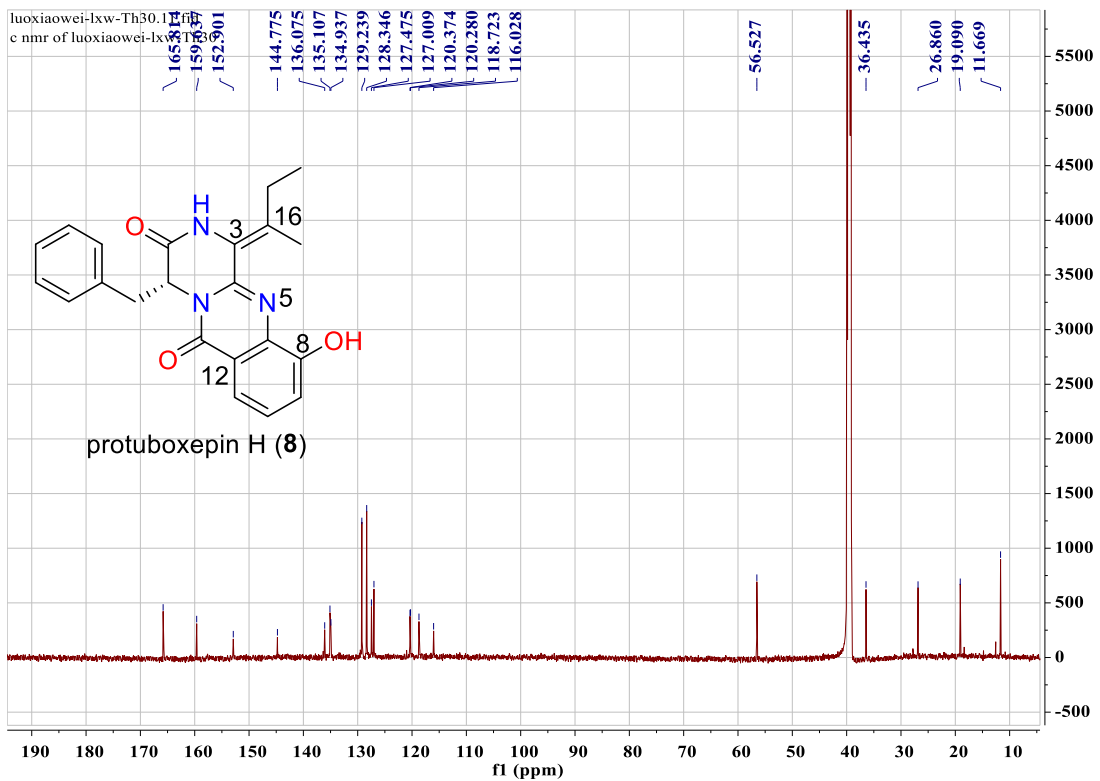


Figure S88. ^1H NMR spectrum of protuboxepin H (8) (DMSO- d_6 , 700 MHz)



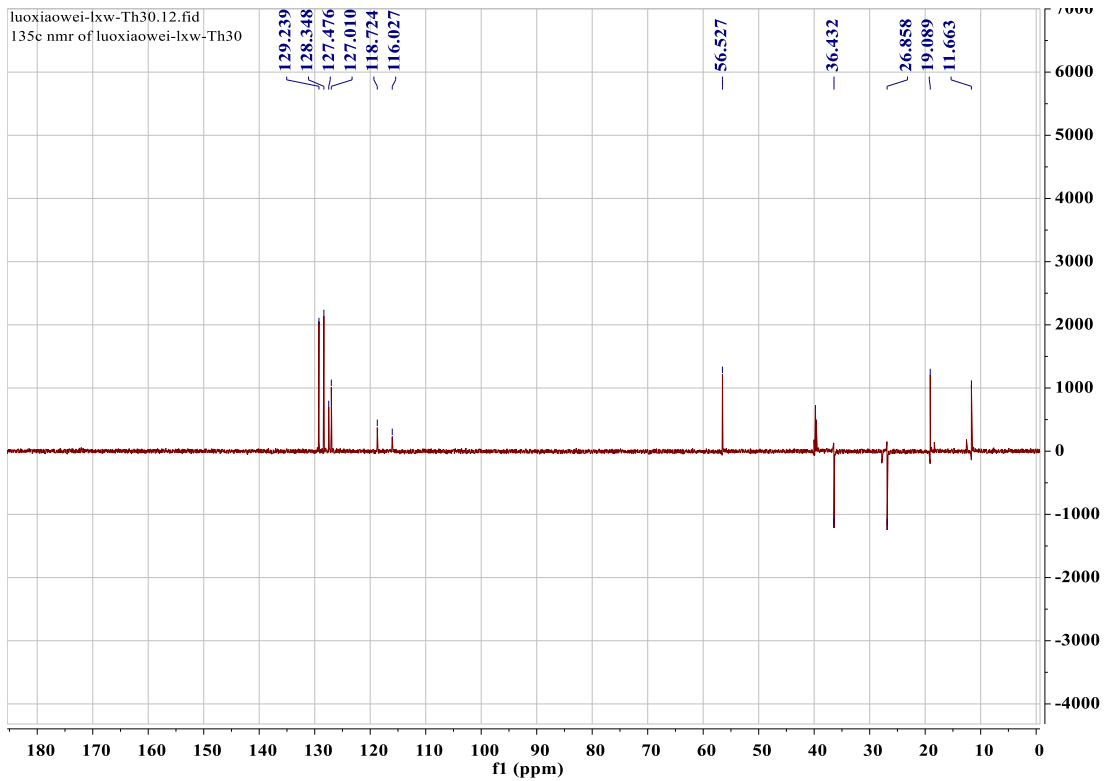


Figure S89. ^{13}C NMR and DEPT spectra of protuboxepin H (8) (DMSO- d_6 , 175 MHz)

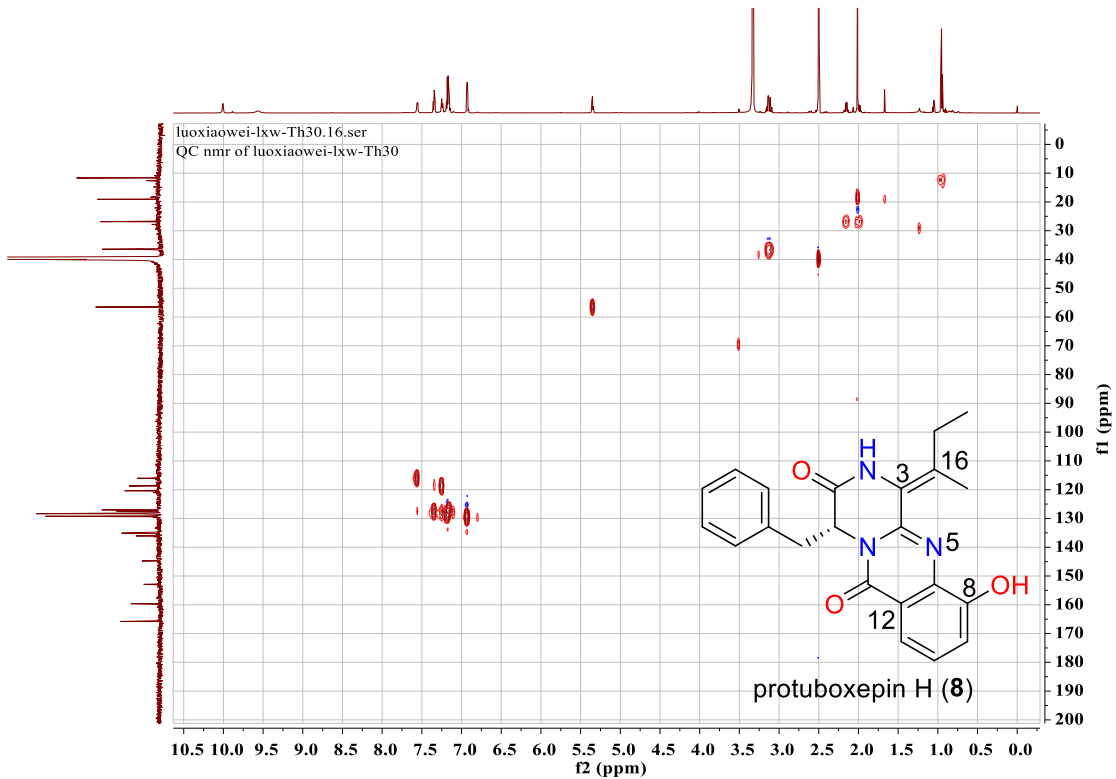


Figure S90. HSQC spectrum of protuboxepin H (8) (DMSO- d_6)

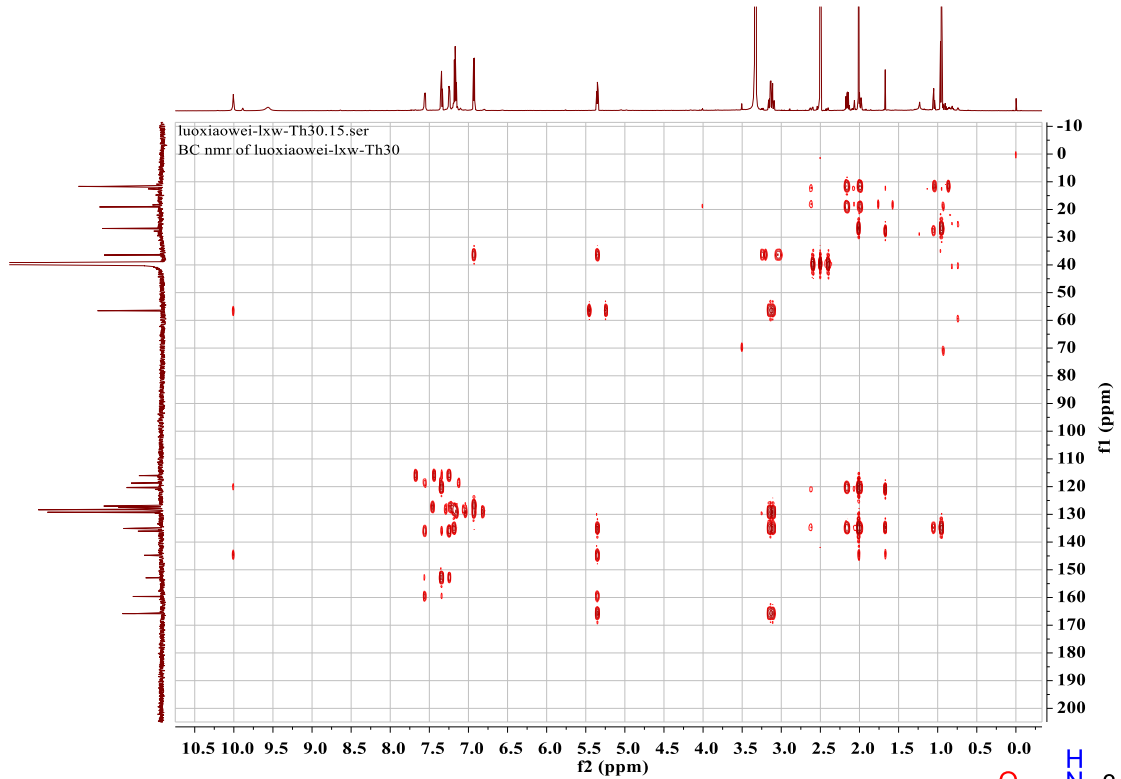


Figure S91. HMBC spectrum of protuboxepin H (8) (DMSO-*d*₆)

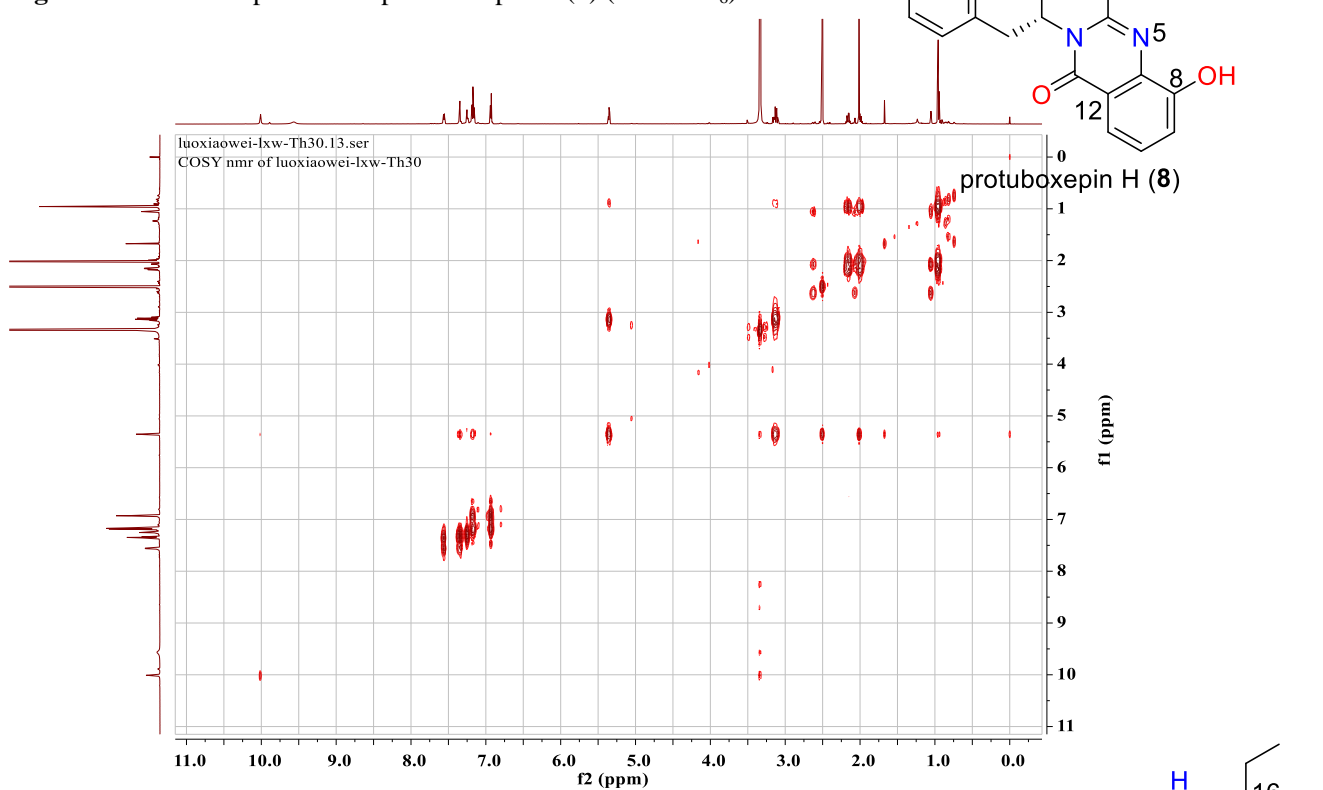
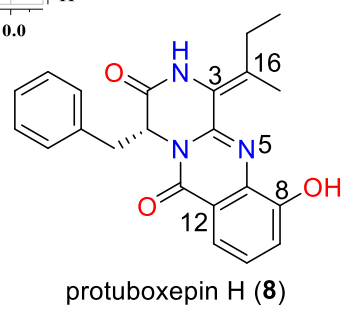


Figure S92. ¹H-¹H COSY spectrum of protuboxepin H (8) (DMSO-*d*₆)



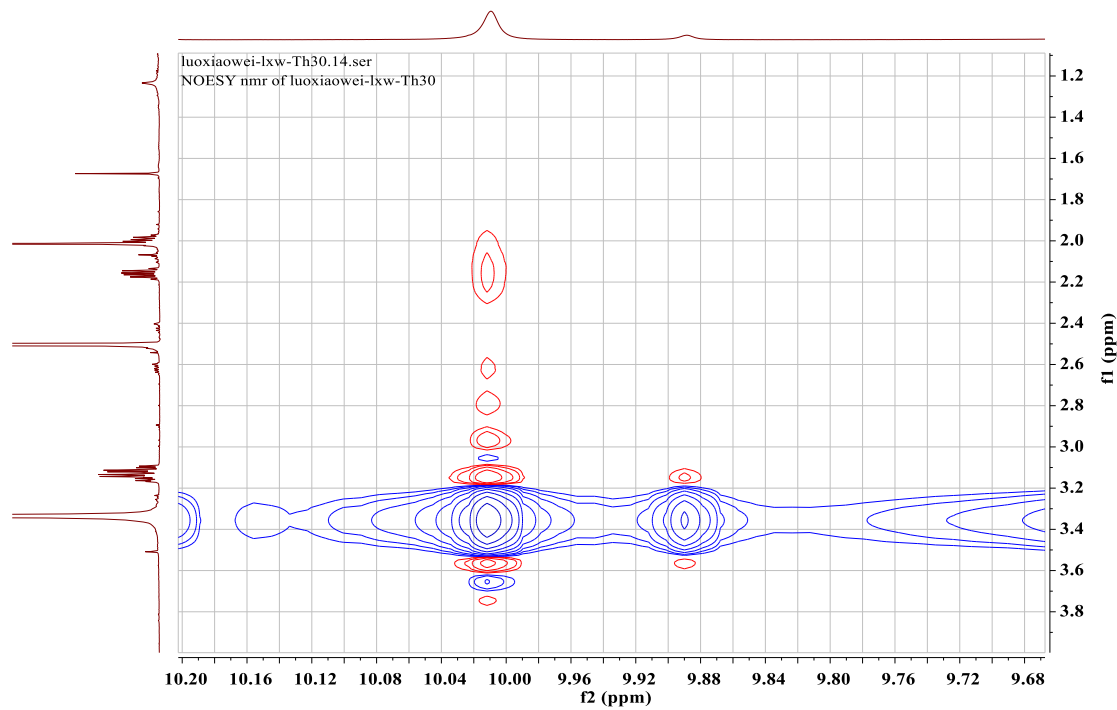
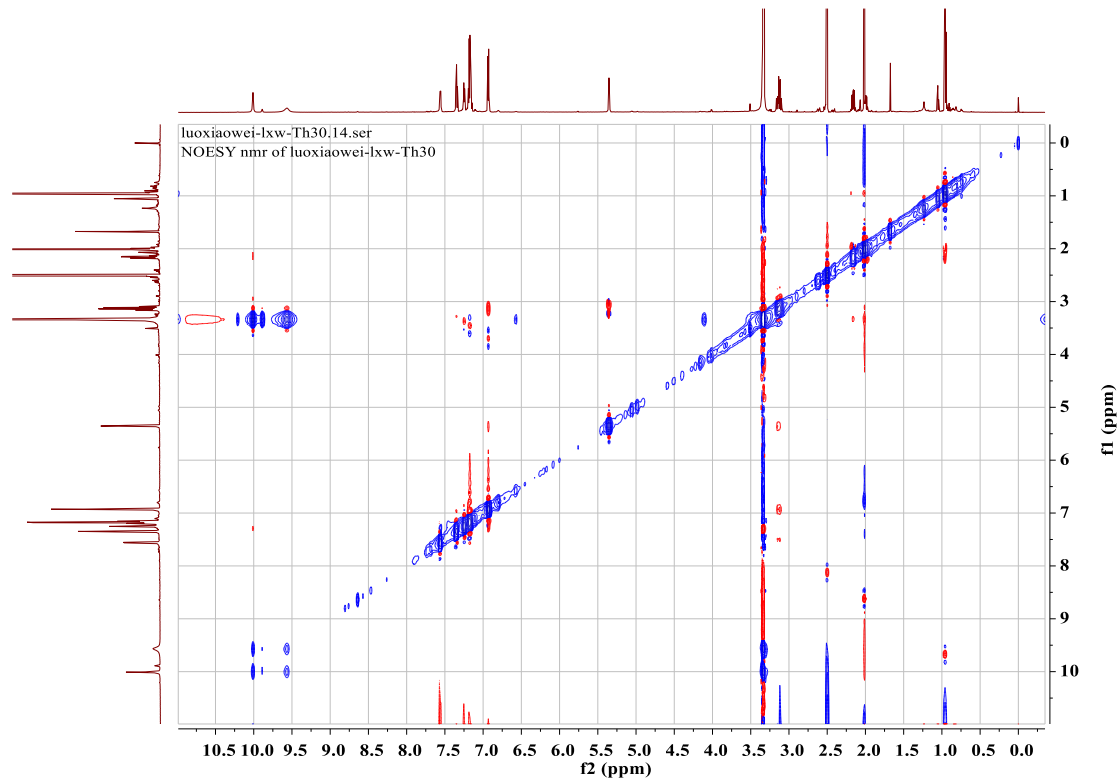
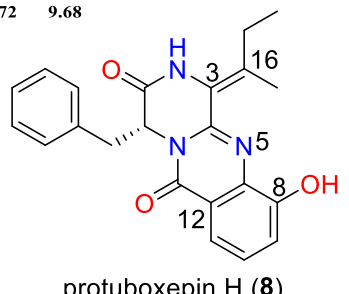


Figure S93. NOESY spectrum of protuboxepin H (**8**) (DMSO-*d*₆)



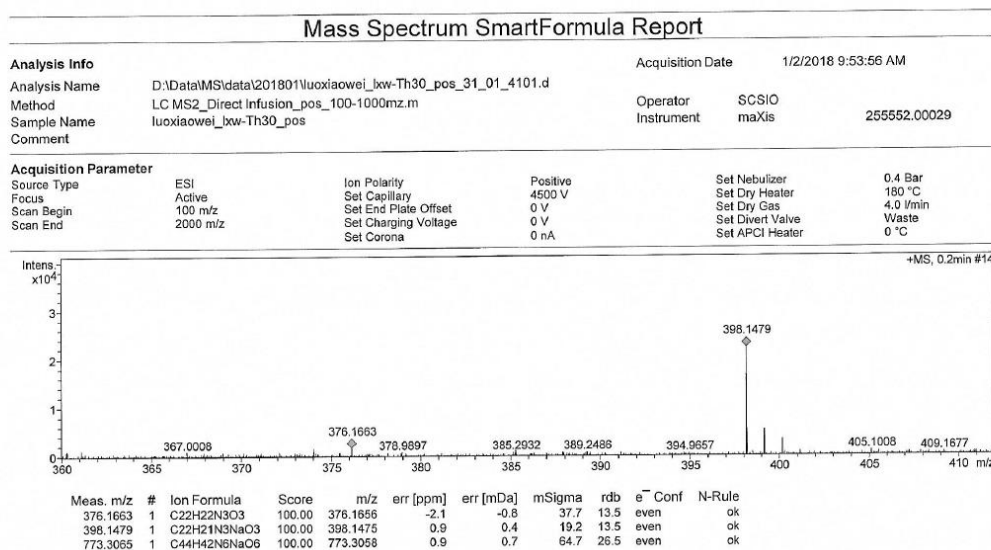


Figure S94. Positive HR-ESI-MS spectrum of protuboxepin H (**8**)

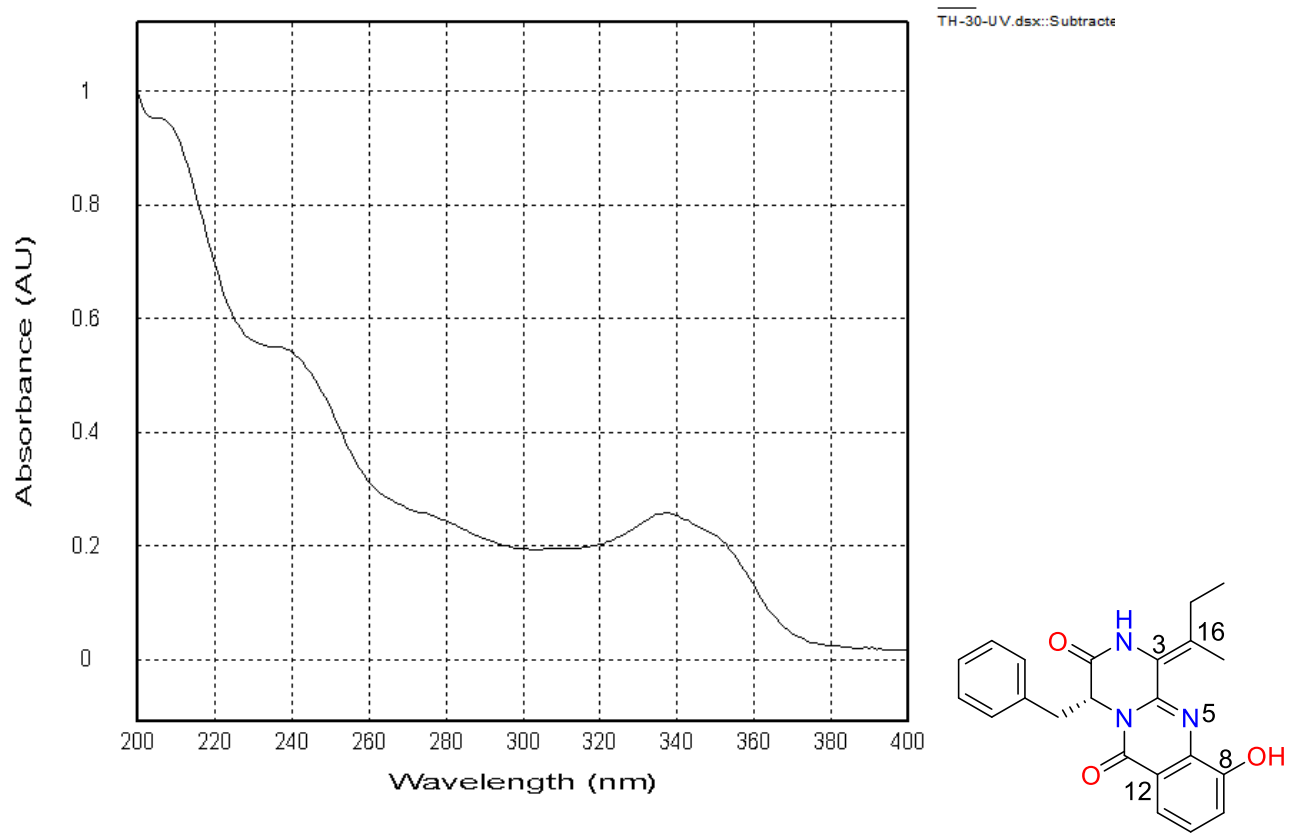
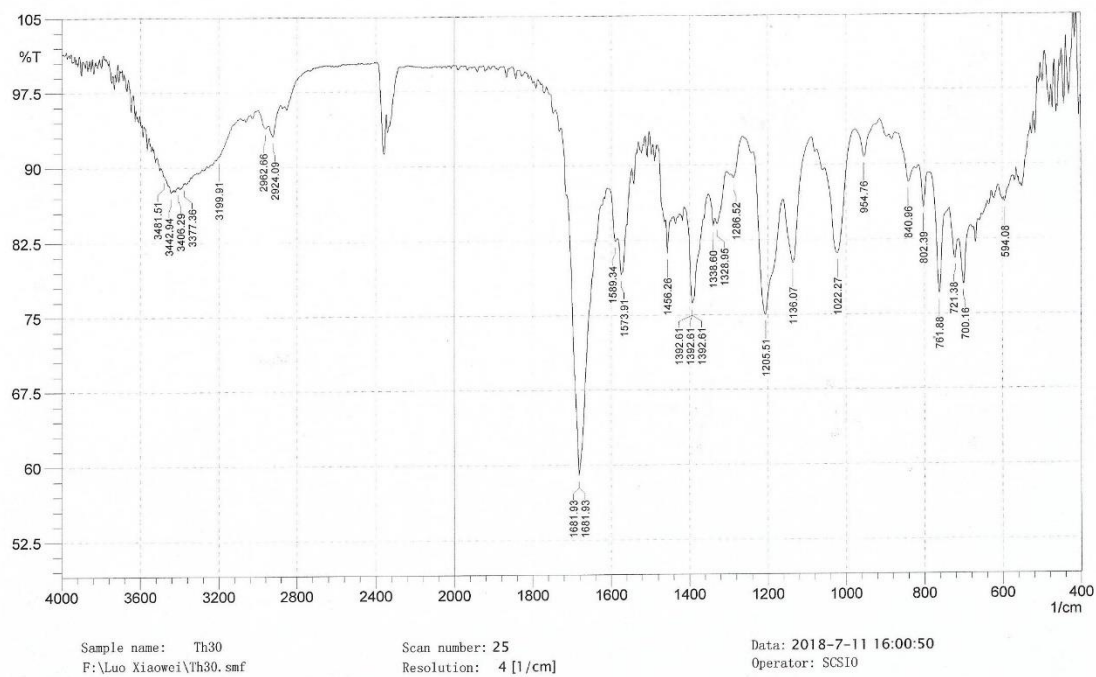
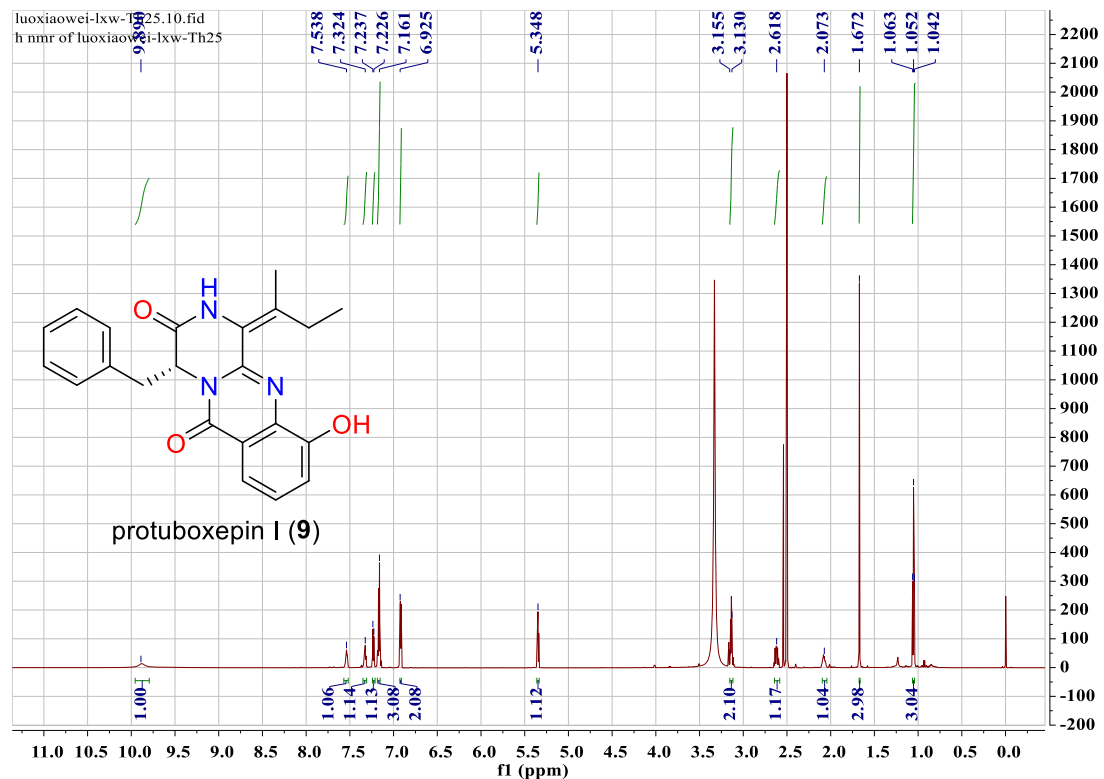


Figure S95. UV spectrum of protuboxepin H (**8**)

**Figure S96.** IR spectrum of protuboxepin H (8)**Figure S97.** ^1H NMR spectrum of protuboxepin I (9) (DMSO- d_6 , 700 MHz)

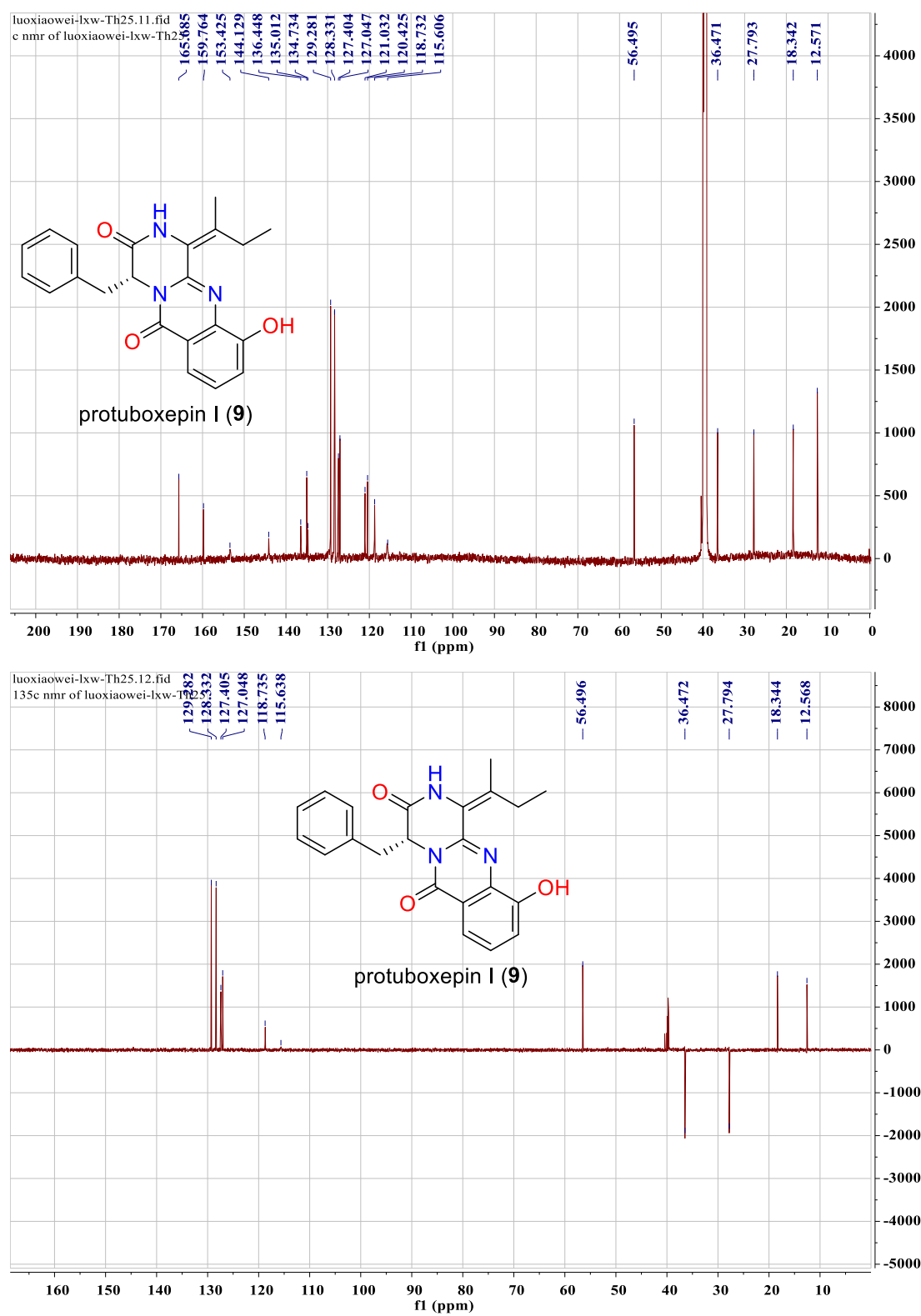


Figure S98. ^{13}C NMR and DEPT spectra of protuboxepin I (9) ($\text{DMSO}-d_6$, 175 MHz)

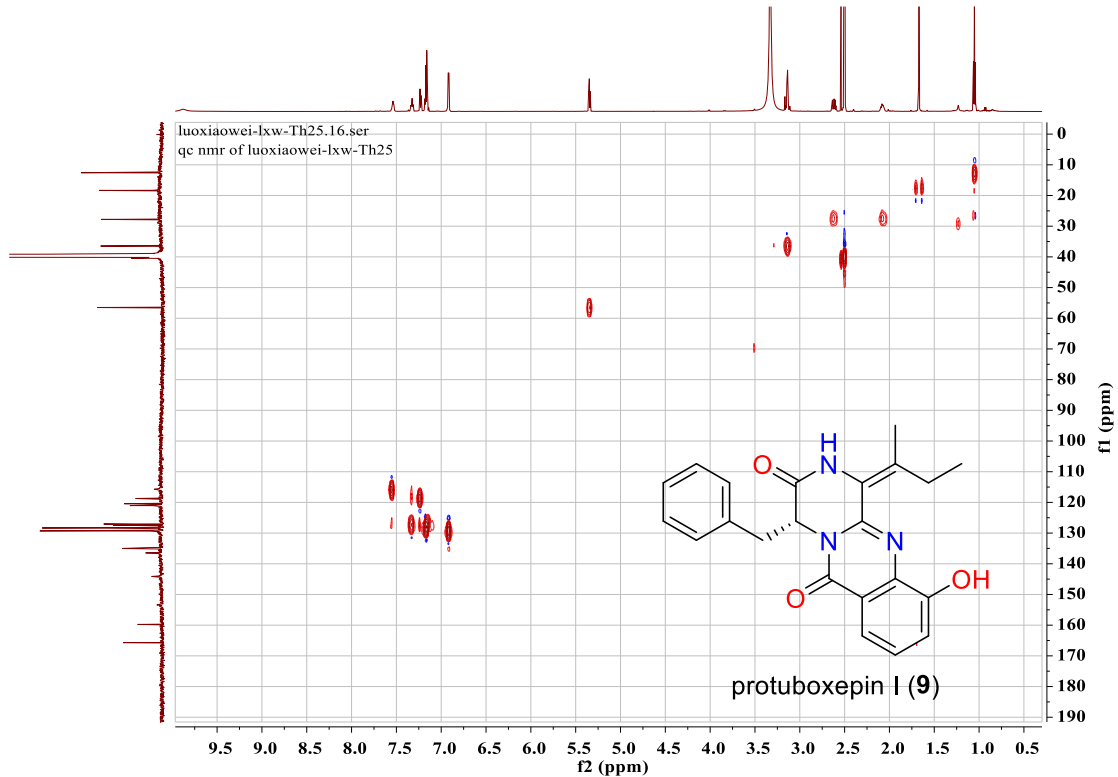


Figure S99. HSQC spectrum of protuboxepin I (9) (DMSO-*d*₆)

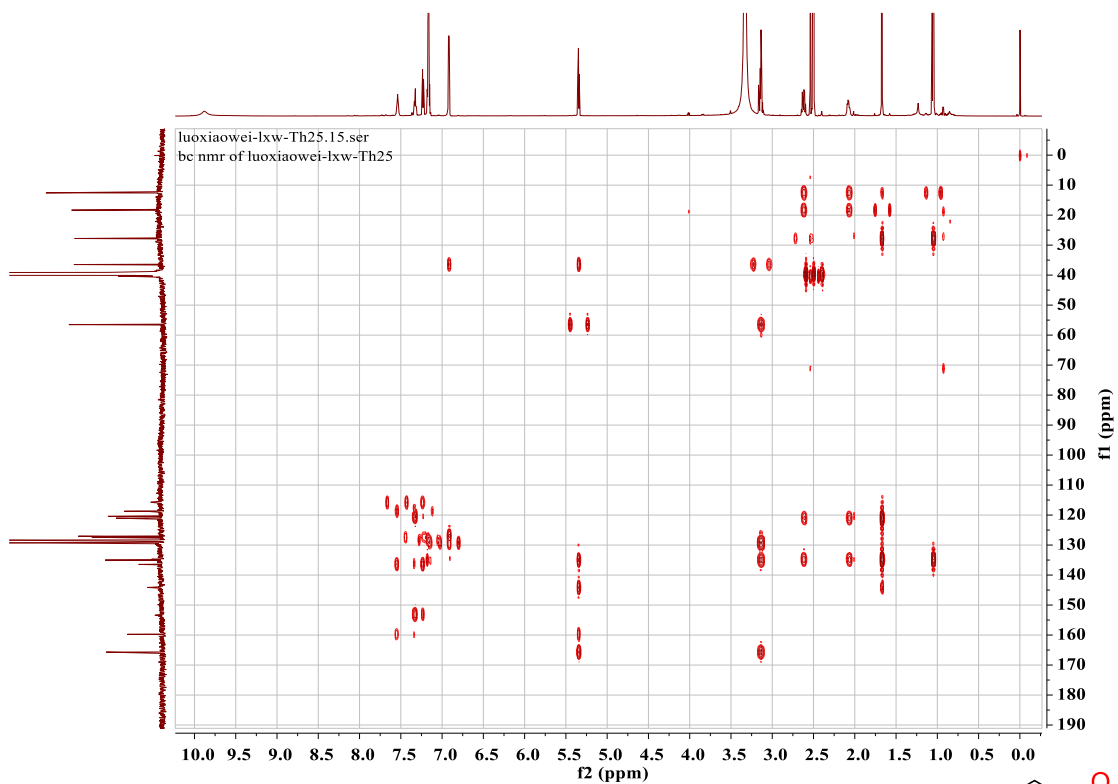
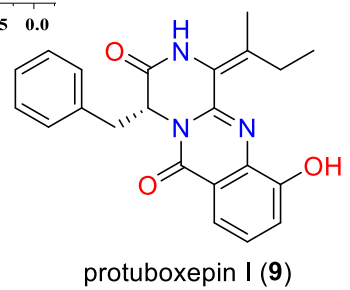


Figure S100. HMBC spectrum of protuboxepin I (9) (DMSO-*d*₆)



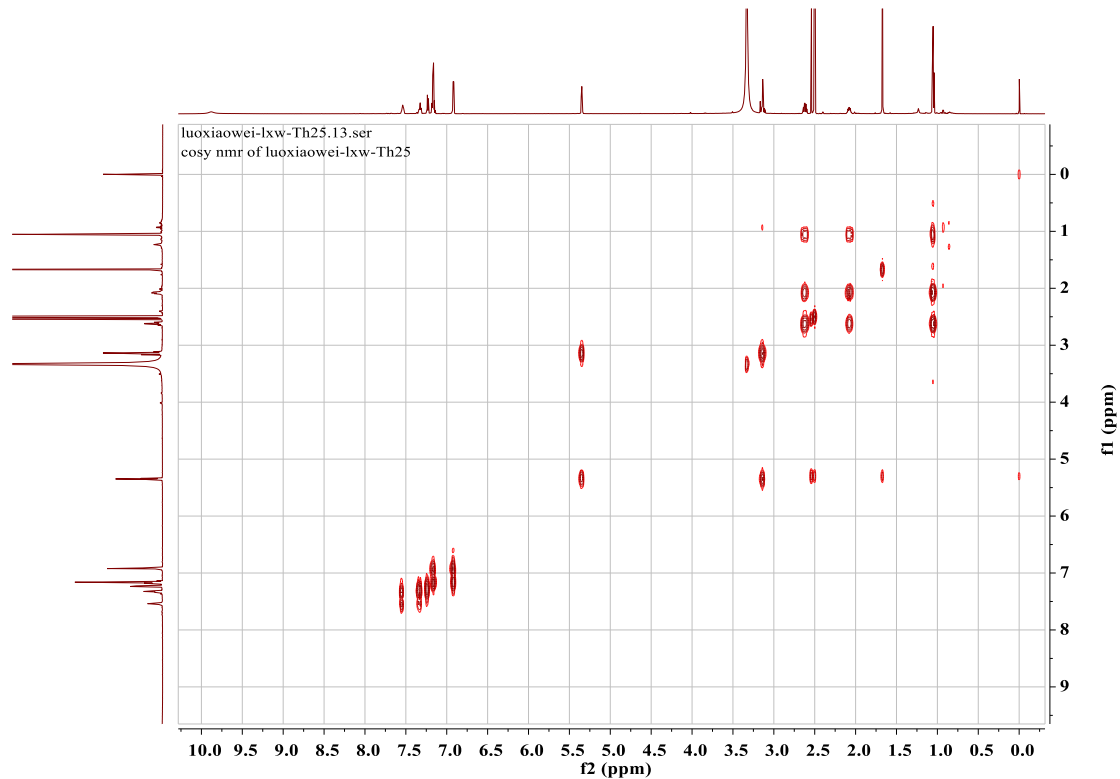


Figure S101. ¹H-¹H COSY spectrum of protuboxepin I (**9**) (DMSO-*d*₆)

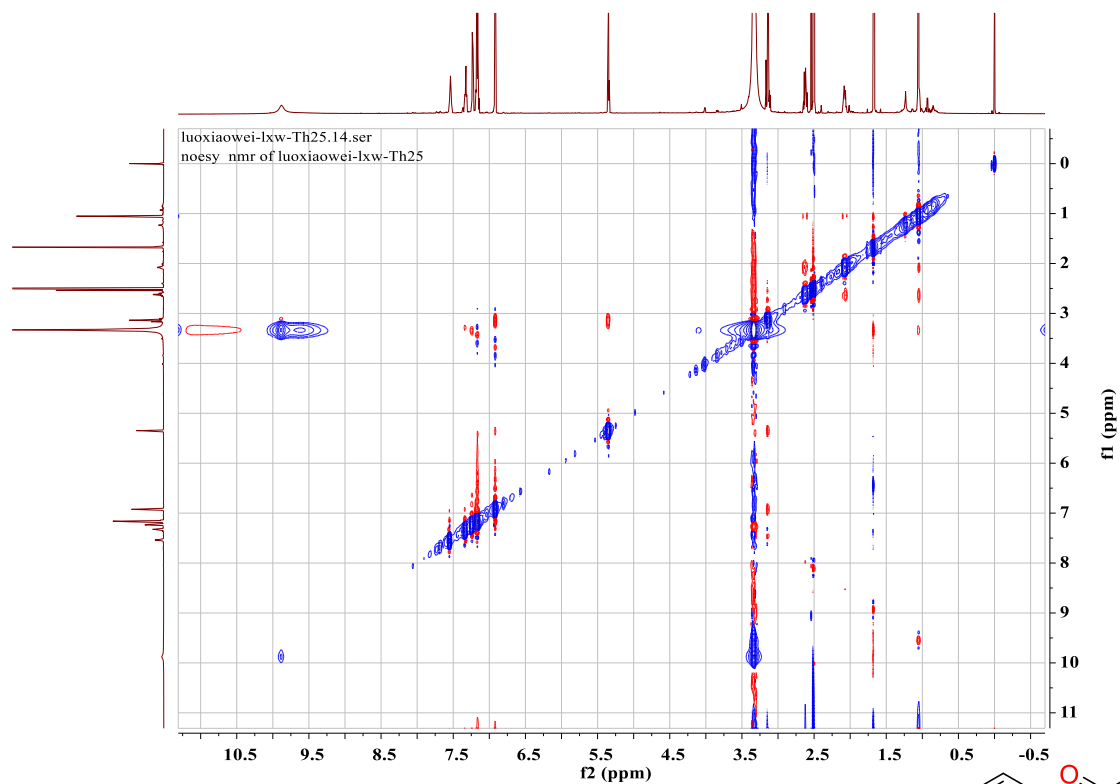
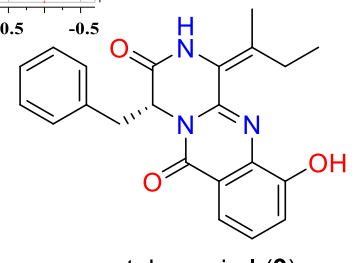


Figure S102. NOESY spectrum of protuboxepin I (**9**) (DMSO-*d*₆)



Mass Spectrum SmartFormula Report

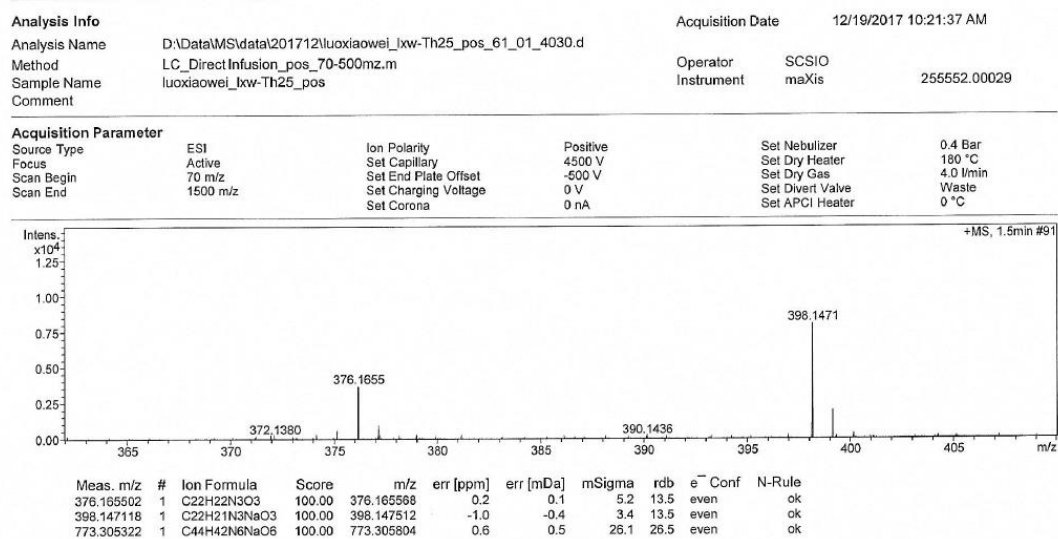


Figure S103. Positive HR-ESI-MS spectrum of protuboxepin I (**9**)

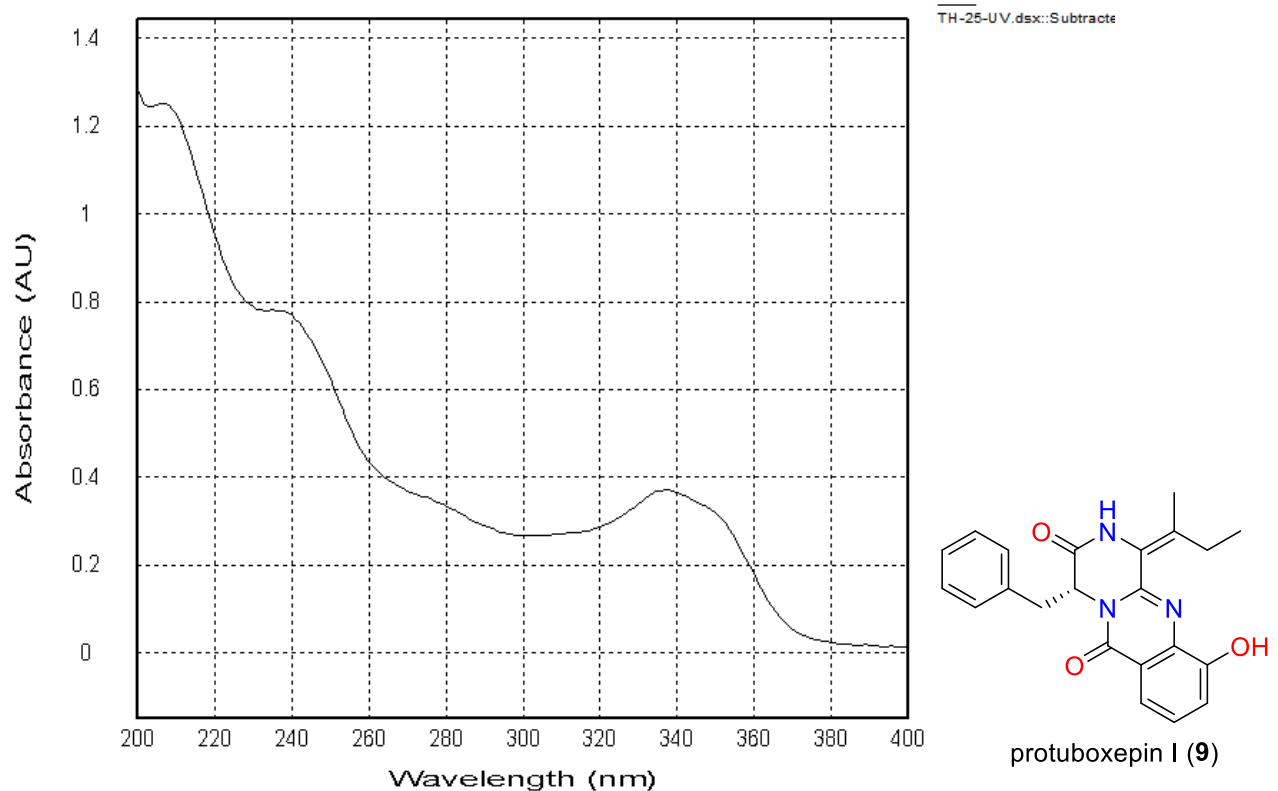


Figure S104. UV spectrum of protuboxepin I (**9**)

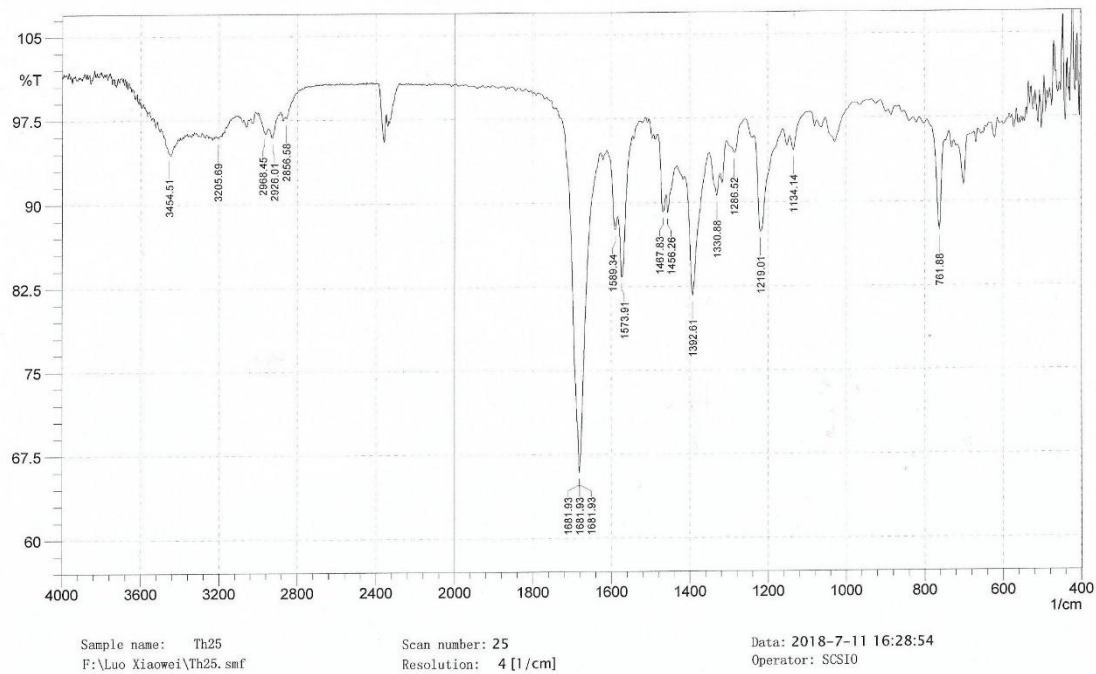


Figure S105. IR spectrum of protuboxepin I (**9**)

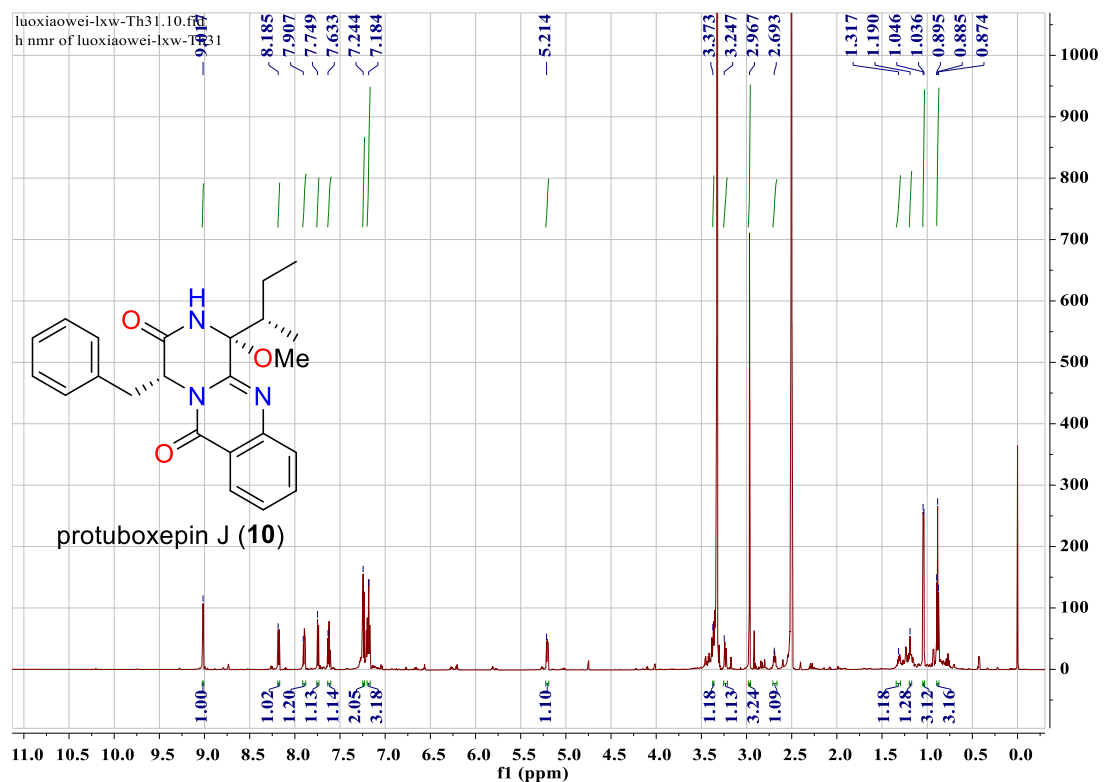


Figure S106. ^1H NMR spectrum of protuboxepin J (**10**) (DMSO- d_6 , 700 MHz)

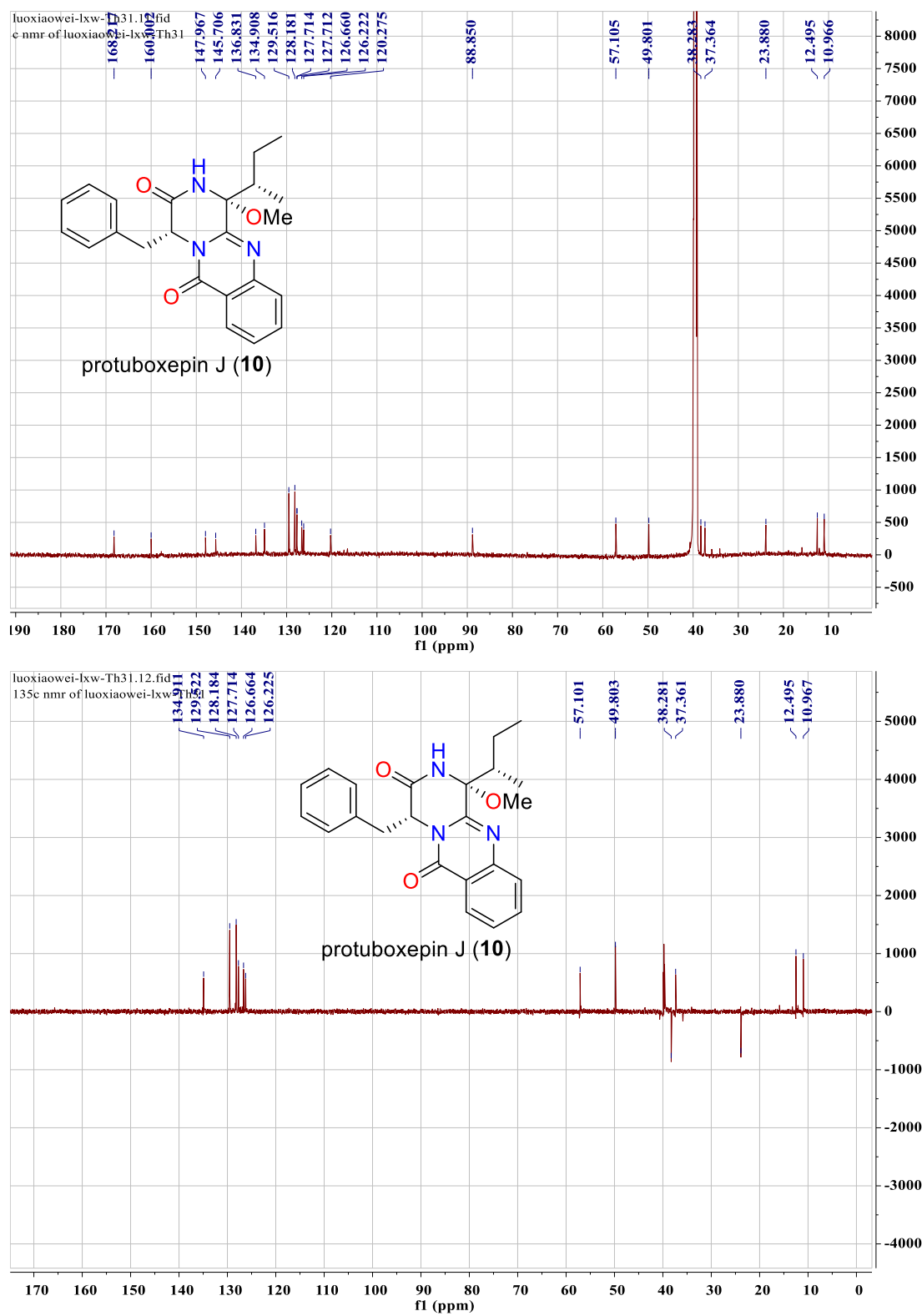


Figure S107. ^{13}C NMR and DEPT spectra of protuboxepin J (**10**) (DMSO- d_6 , 175 MHz)

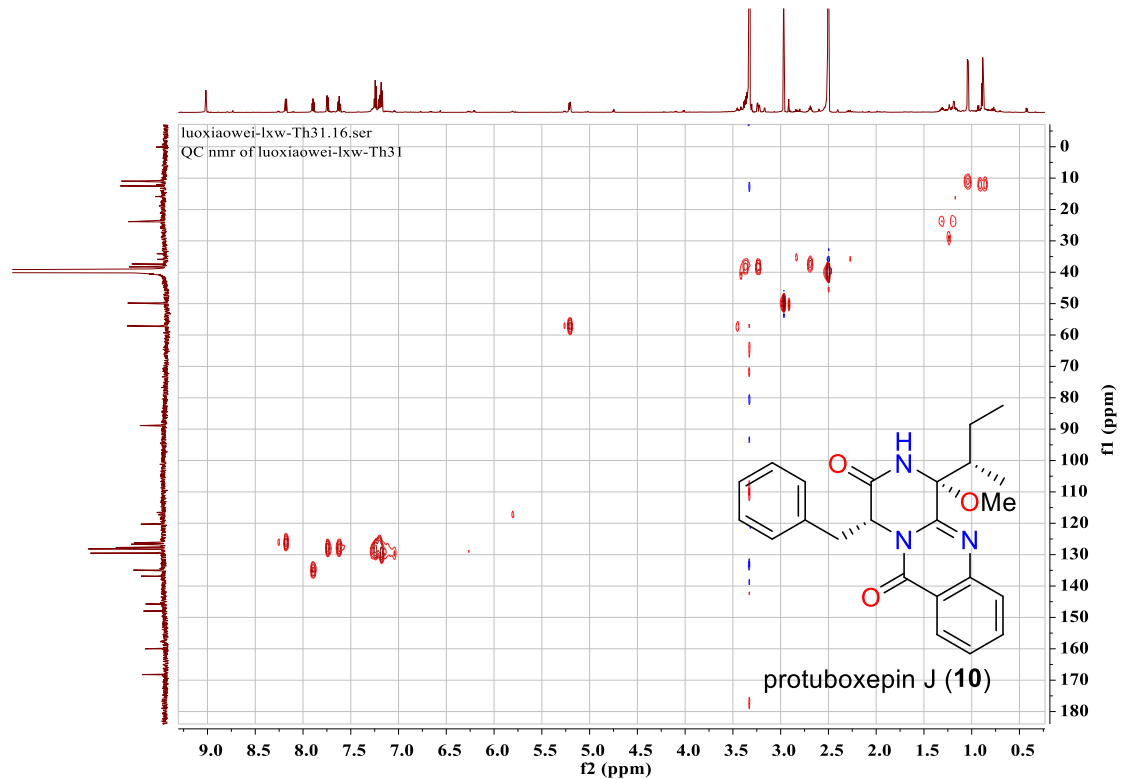


Figure S108. HSQC spectrum of protuboxepin J (**10**) (DMSO-*d*₆)

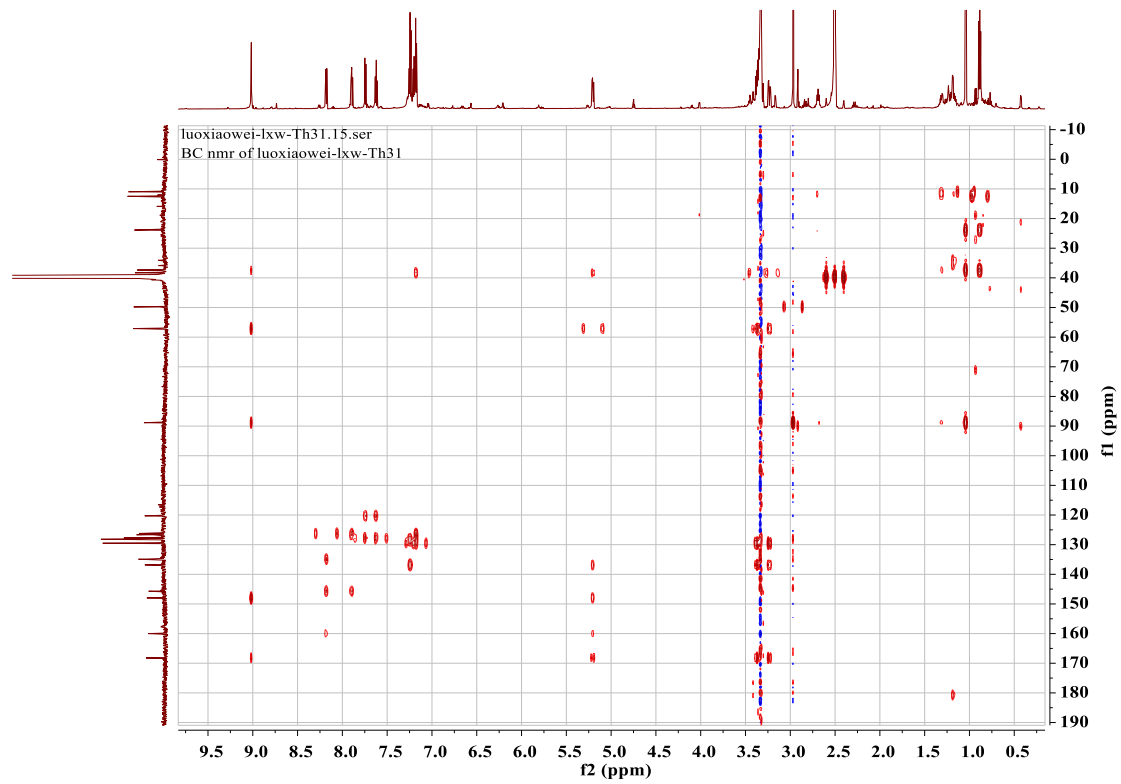
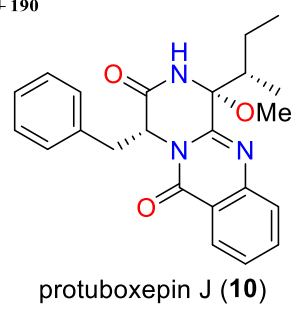


Figure S109. HMBC spectrum of protuboxepin J (**10**) (DMSO-*d*₆)



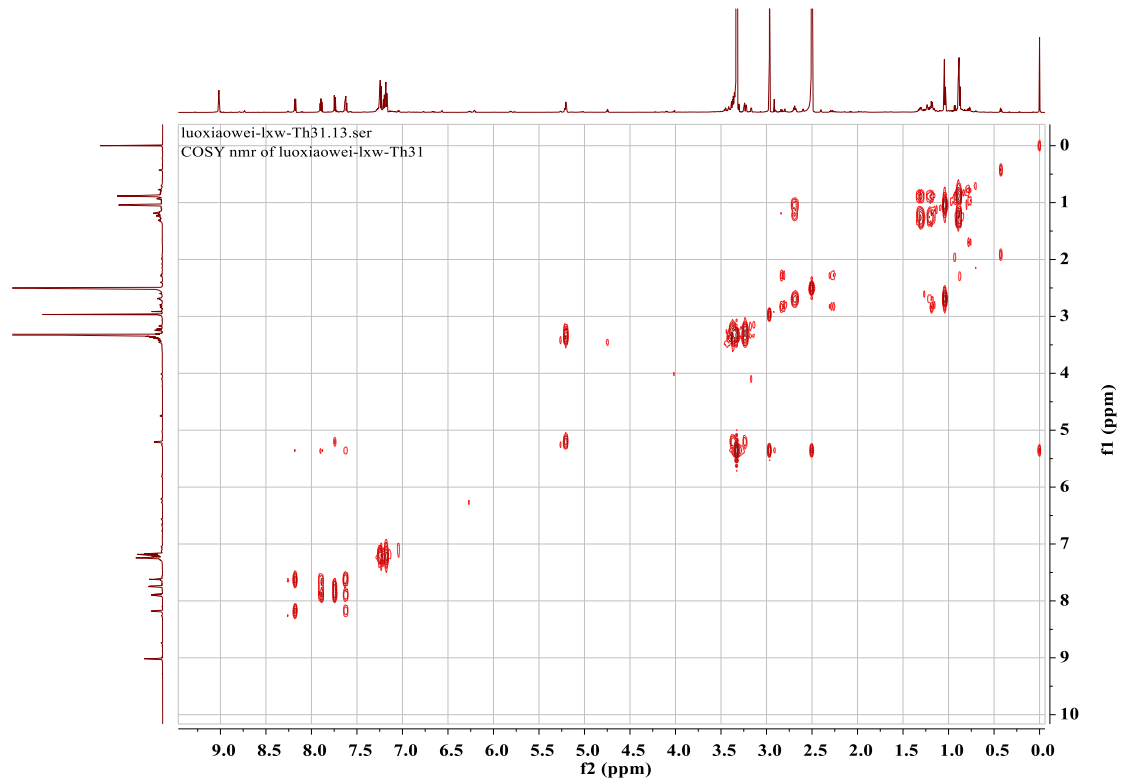


Figure S110. ^1H - ^1H COSY spectrum of protuboxepin J (**10**) (DMSO- d_6)

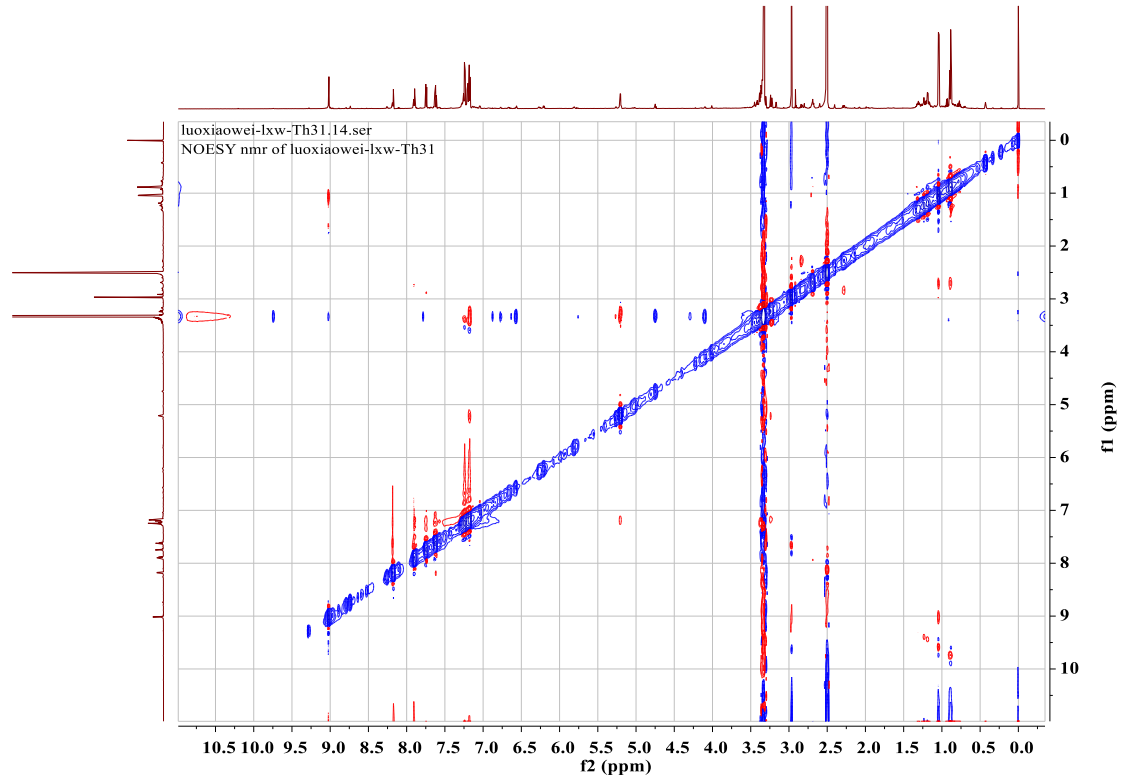
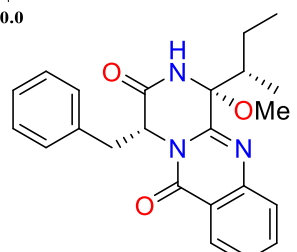


Figure S111. NOESY spectrum of protuboxepin J (**10**) (DMSO- d_6)



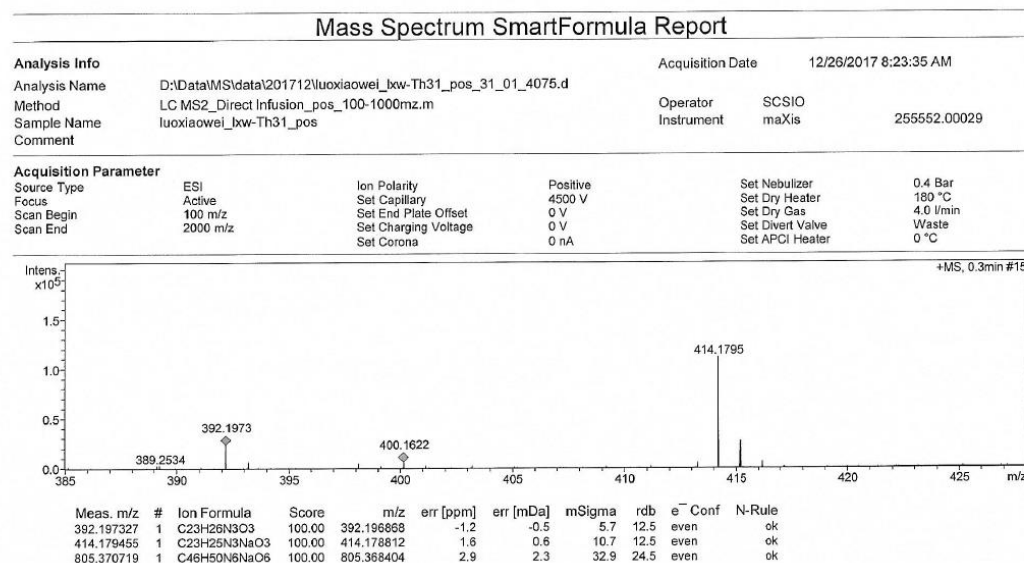


Figure S112. Positive HR-ESI-MS spectrum of protuboxepin J (**10**)

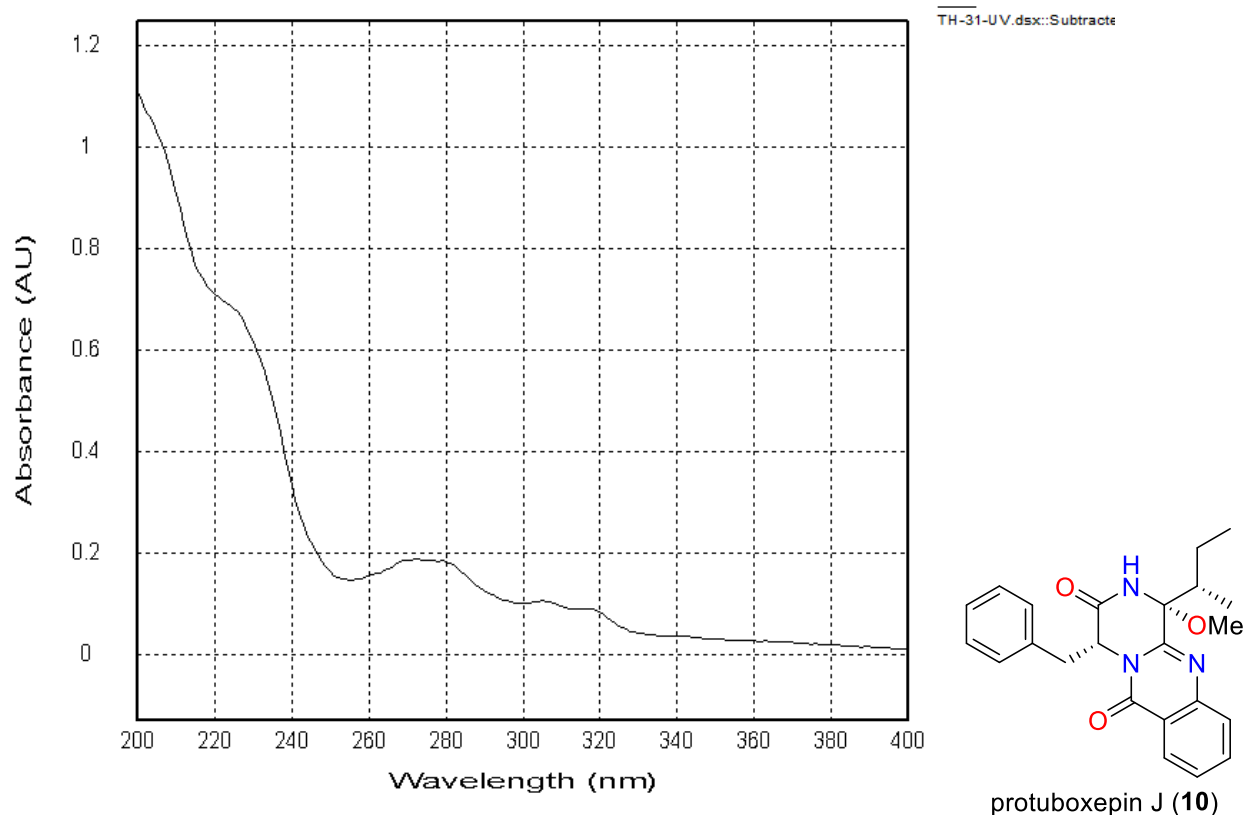


Figure S113. UV spectrum of protuboxepin J (**10**)

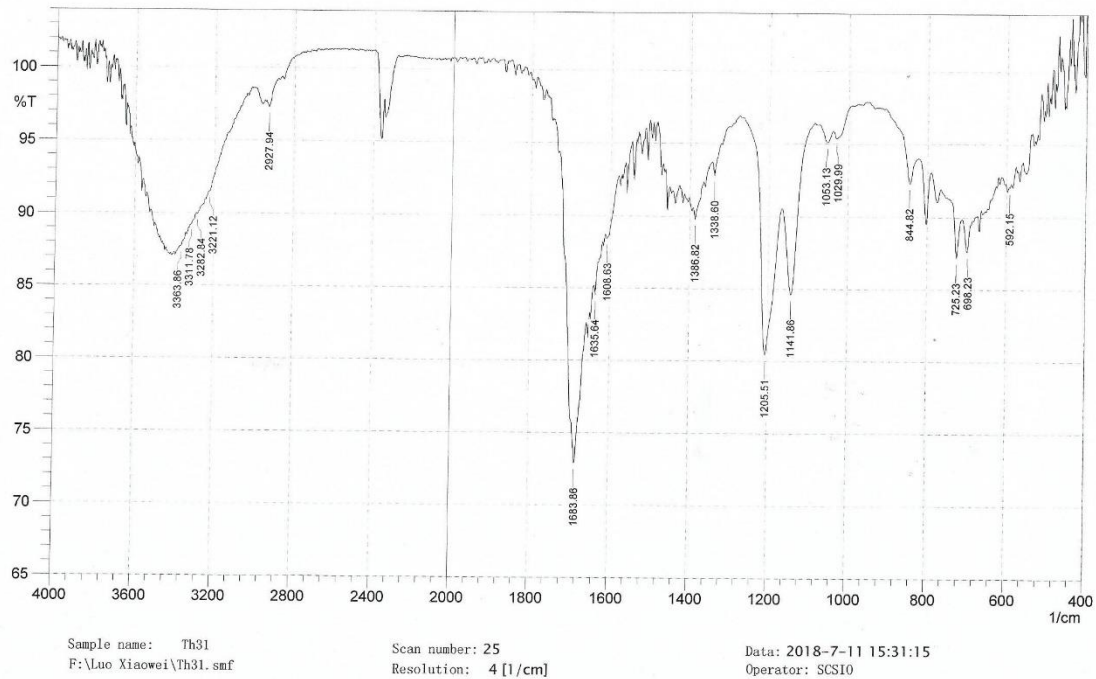


Figure S114. IR spectrum of protuboxepin J (**10**)

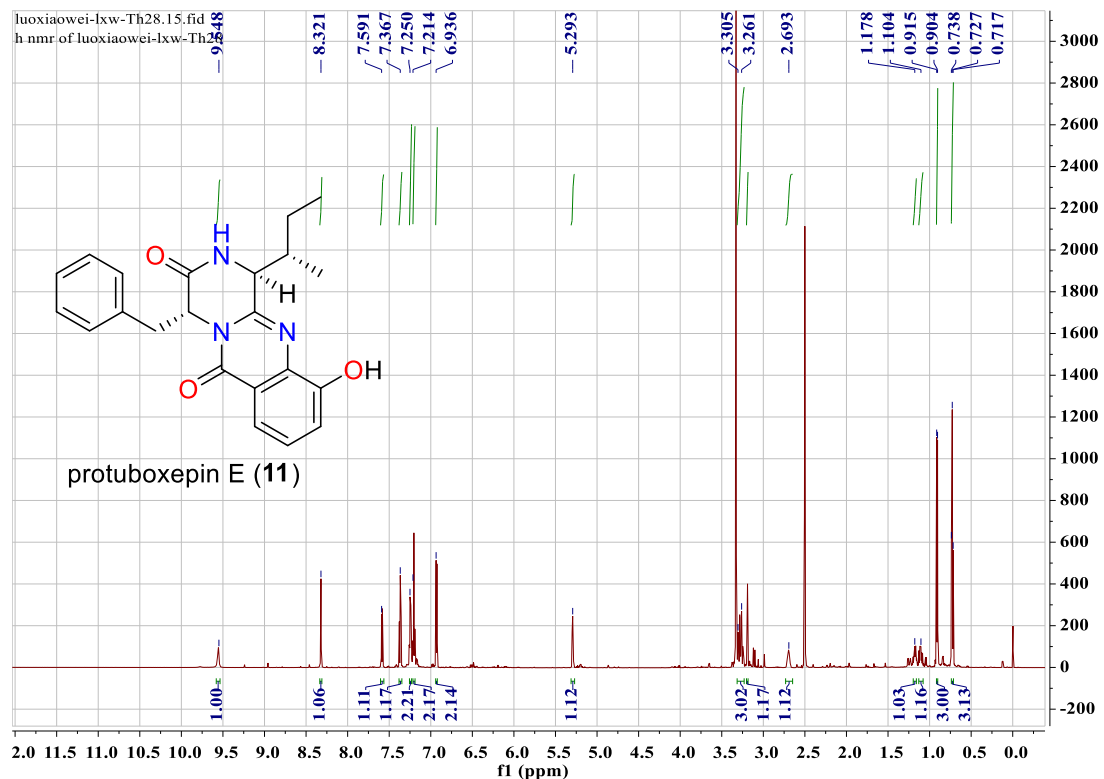


Figure S115. ¹H NMR spectrum of protuboxepin E (**11**) (DMSO-*d*₆, 700 MHz)

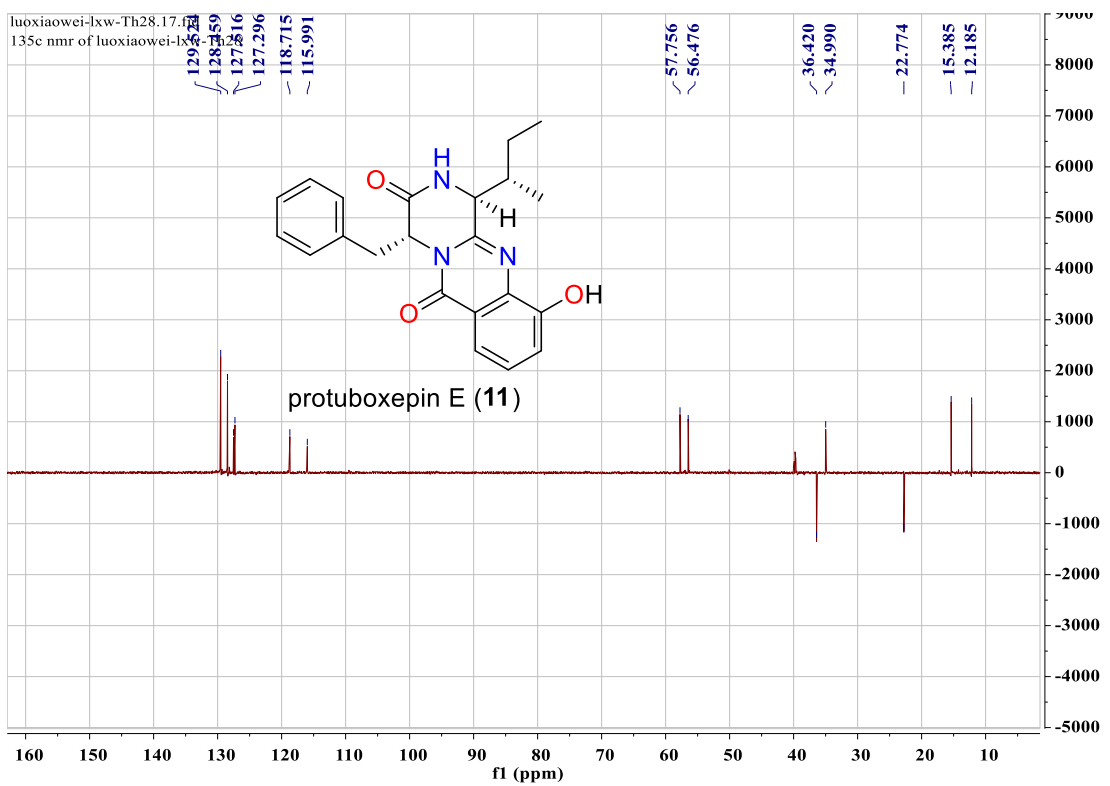
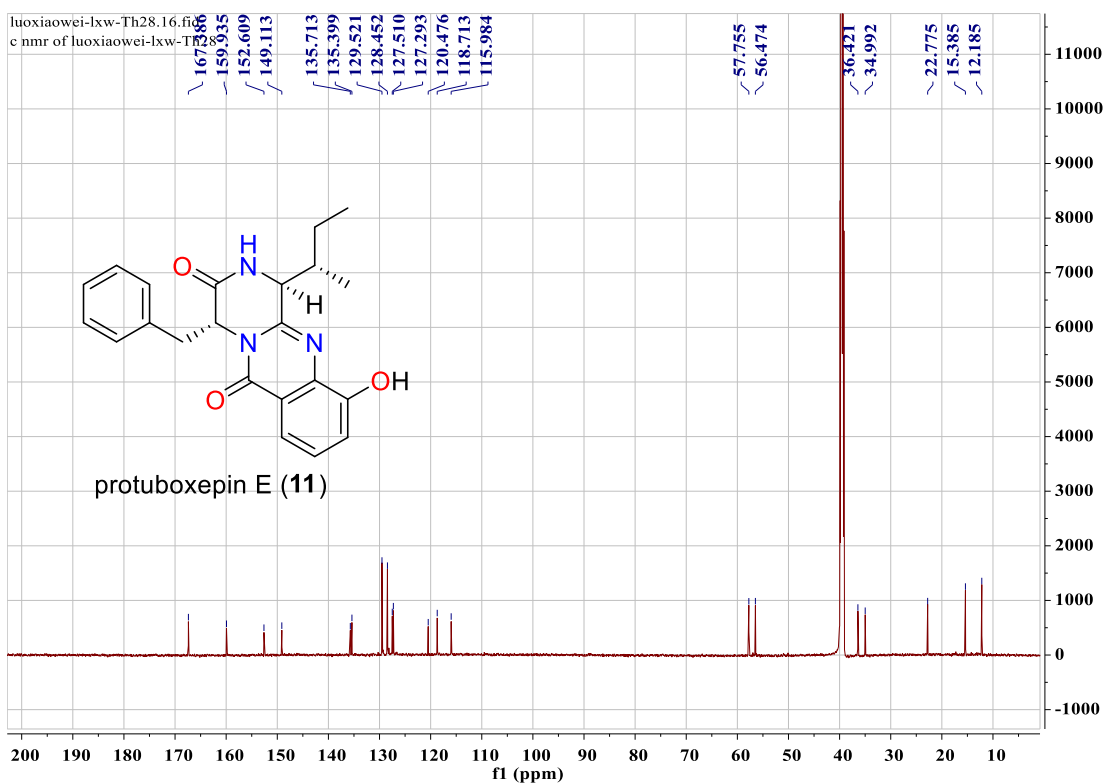


Figure S116. ^{13}C NMR and DEPT spectra of protuboxepin E (11) (DMSO- d_6 , 175 MHz)

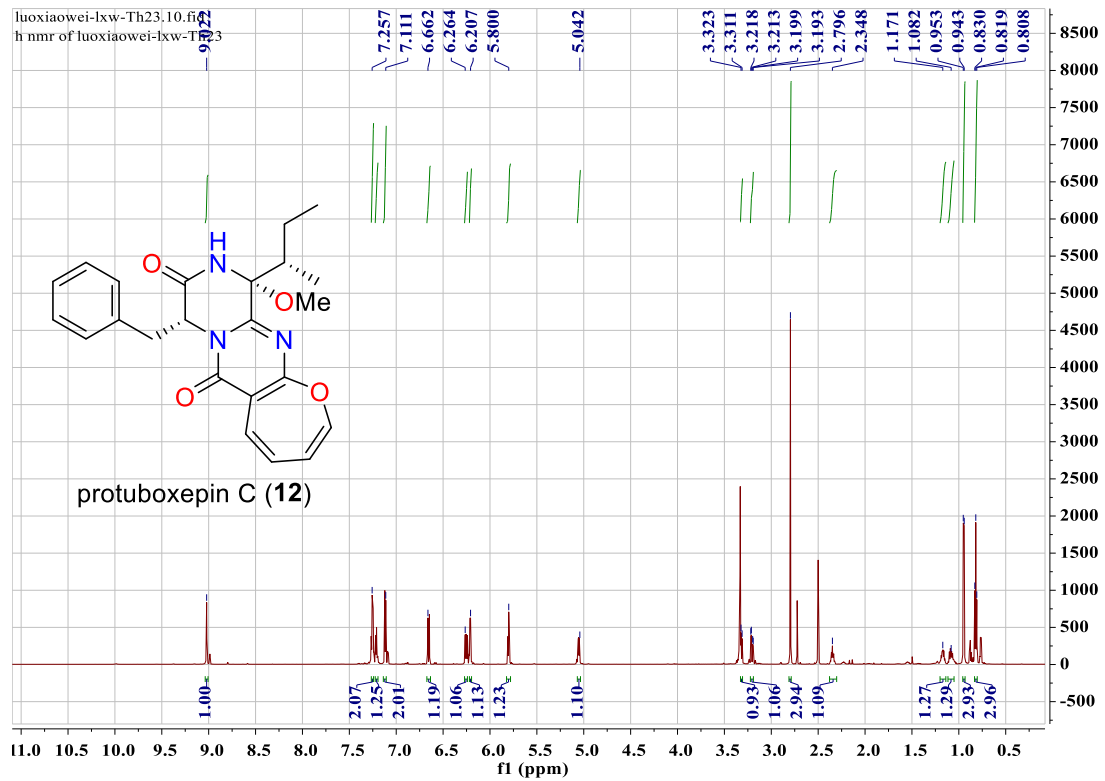
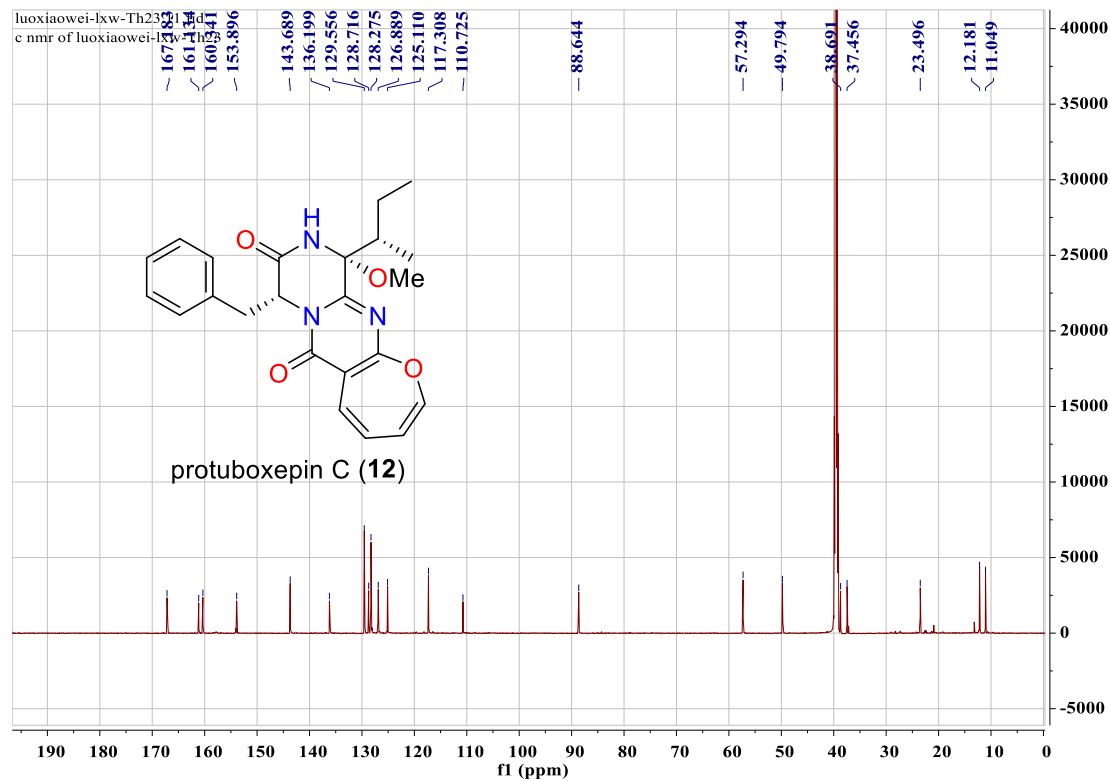


Figure S117. ^1H NMR spectrum of protuboxepin C (12) (DMSO- d_6 , 700 MHz)



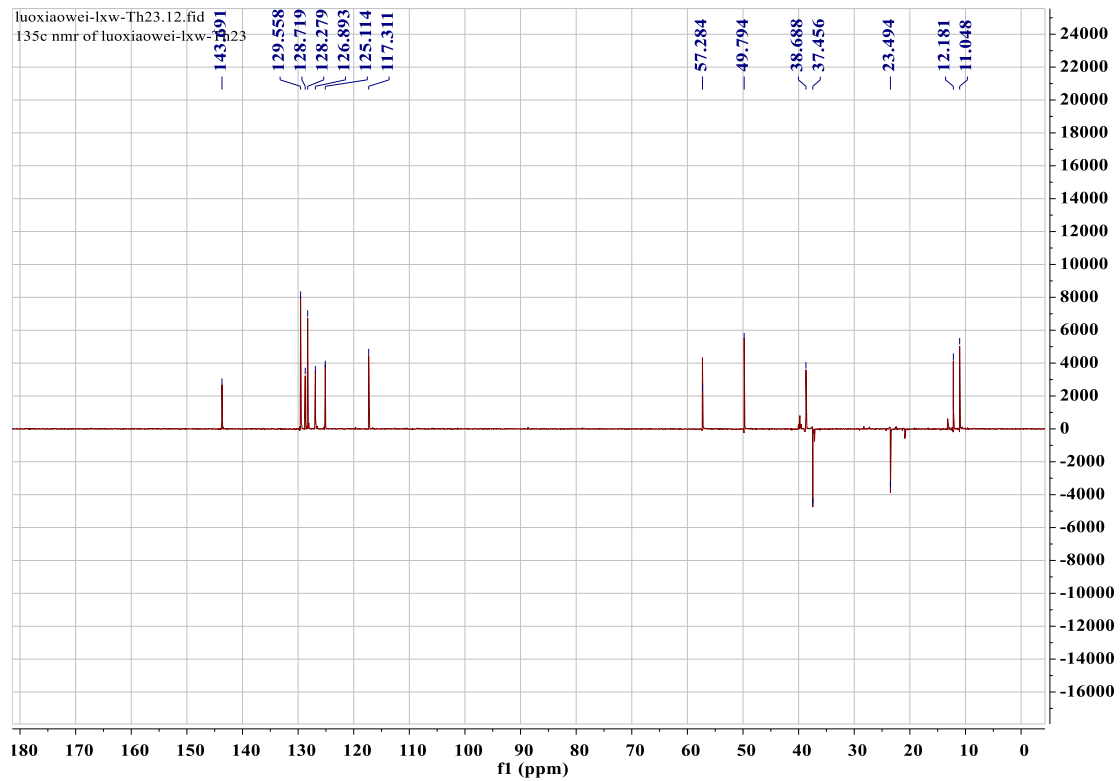


Figure S118. ¹³C NMR and DEPT spectra of protuboxepin C (**12**) (DMSO-*d*₆, 175 MHz)

4. References

- (1) Luo, X. W.; Lin, X. P.; Tao, H. M.; Wang, J. F.; Li, J. Y.; Yang, B.; Zhou, X. F.; Liu, Y. H. *J. Nat. Prod.* **2018**, *81*, 934-941.
- (2) Frisch, M. J.; Trucks, G. W.; Schlegel, H. B.; Scuseria, G. E.; Robb, M. A.; Cheeseman, J. R.; Scalmani, G.; Barone, V.; Mennucci, B.; Petersson, G. A.; Nakatsuji, H.; Caricato, M.; Li, X.; Hratchian, H. P.; Izmaylov, A. F.; Bloino, J.; Zheng, G.; Sonnenberg, J. L.; Hada, M.; Ehara, M.; Toyota, K.; Fukuda, R.; Hasegawa, J.; Ishida, M.; Nakajima, T.; Honda, Y.; Kitao, O.; Nakai, H.; Vreven, T.; Montgomery, J. A., Jr.; Peralta, J. E.; Ogliaro, F.; Bearpark, M.; Heyd, J. J.; Brothers, E.; Kudin, K. N.; Staroverov, V. N.; Kobayashi, R.; Normand, J.; Raghavachari, K.; Rendell, A.; Burant, J. C.; Iyengar, S. S.; Tomasi, J.; Cossi, M.; Rega, N.; Millam, J. M.; Klene, M.; Knox, J. E.; Cross, J. B.; Bakken, V.; Adamo, C.; Jaramillo, J.; Gomperts, R.; Stratmann, R. E.; Yazyev, O.; Austin, A. J.; Cammi, R.; Pomelli, C.; Ochterski, J. W.; Martin, R. L.; Morokuma, K.; Zakrzewski, V. G.; Voth, G. A.; Salvador, P.; Dannenberg, J. J.; Dapprich, S.; Daniels, A. D.; Farkas, Ö.; Foresman, J. B.; Ortiz, J. V.; Cioslowski, J.; Fox, D. J. *Gaussian 09*; Gaussian, Inc.: Wallingford, CT, 2009.